ICEIT

ICT inspired

PROCEEDINGS

ICEIT Conference on Advances in Mobile Communications, Networking and Computing – MCNC 2017

February 16-17, 2017, New Delhi

Editors:
H M Gupta
Y N Singh

Institution of Communication Engineers and Information Technologists (ICEIT)
www.iceit.org.in
www.iceit.org.in

Collaborating Partner:
Indian Institute of Information Technology and Management (IIITM), Gwalior

Centre for Development of Advanced Computing (CDAC), Noida

Organizing Partner:
CDT Foundation, New Delhi

ICEIT Conference on

Advances in Mobile Communications, Networking and Computing-MCNC-2017

16-17 February, 2017

ACKNOWLEDGEMENTS

Institution of Communication Engineers & Information Technologists (ICEIT) gratefully acknowledges collaborative/financial support from

- **Indian Institute of Information Technology and Management, Gwalior**
- **Centre for Development of Advanced Computing, Noida**
- **Association for Security of Information Systems**
- **Indira Gandhi Delhi Technical University for Women, Delhi**
- **Centre for Development of Technology (CDT) Foundation, Delhi**

About the Conference

Perhaps, the combination Mobility, Communication Techniques and Computing is most potent in the recent time. It is manifested in many diverse areas such as banking systems, educational content development and delivery, entertainment etc. Two broad aims have been maximum data transfer and computation on the move. Engineers and technologists are constantly devising techniques and systems to meet these goals. But the goal posts have been shifting – we always need higher than the present data rates and increased connectivity. Add to these reliability and security and the challenges becomes huge. We need to understand the mobile channels in greater details and in-depth manner. The trouble is that such channels have no unique characterization leading to a vast array of system design constraints. We also need to be integrating latest developments in form of newer and more efficient devices in pursuit of our goals. For example, recent thrust in Free-Space Optical (FSO) systems is one such big effort. It opens up path for high data rates comparable to fiber-optic systems. Similarly peer-to-peer computing is a new regime to address connectivity, efficiency and reliability.

The contributions in the Conference discuss mobile communication techniques, mobile channel characterization, sensor networks, peer- to - peer computing, mobile applications and optical systems. These are in form of analysis, modeling, simulations, algorithms, overall system design and implementation. The material contained in these papers and presentations and discussions in the Conference will stimulate further research in the broad area of the Conference.

H M Gupta
General Chair

ICEIT Conference on

Advances in Mobile Communications, Networking and Computing- MCNC-2017

16-17 February 2017

General Chair____ ***Prof H M Gupta, President, ICEIT***

Advisory Committee _____

Padma Shree Dr Utpal K Banerjee ***(Chair)***
Prof S G Deshmukh, *Director, IIITM, Gwalior*
Prof Nupur Prakash*, Vice Chancellor, IGDTUW, Delhi*
Prof S Sancheti, President *Manipal Univ, Jaipur*
Prof Karmeshu, *JNU, Delhi*
Lt Gen Ashok Agarwal, *PVSM (Retd), Former DG, Quality Assurance, MoD, Govt. of India*
Maj Gen Yashwant Deva*, AVSM (Retd), Past President IETE*
Mr K N Gupta, *Former Executive Director, C-DoT*
Prof R P Singh, *Former Director, MANIT, Bhopal*
Mr J P Garg, *Former Senior Advisor, Nokia-Siemens*
Mrs Smriti Dagur*, Past President IETE*
Mr V K Sharma*, Executive Director, CDAC, Noida*

Organizing Committee _____

Brig S V S Chowdhry (Retd)*, Past President CSI and IETE* ***(Chair)***
Dr (Mrs) Sneh Mohan, *ED, CDT Foundation*
Prof Ramesh Garg*, IIT, Ropar*
Prof K K Tripathi*, AKGEC, Ghaziabad*
Prof Nar Singh*, Allahabad University, Allahabad*
Dr SRN Reddy, *IGDTUW, Delhi*
Mr Prem Tandon*, ICEIT, Delhi*
Mr R K Bhatia*, IT Consultant, Delhi*
Mr S K Sud, *ICEIT, Delhi*
Prof A S Tavildar*, VIIT, Pune*
Mr Vivek Pal, *UtamedSpectrum, Helsinki, Finland*

Technical Programme Committee _____

Prof Y N Singh, *IIT, Kanpur* ***(Chair)***
Prof M Salim Beg, *AMU, Aligarh*
Prof P Mohana Shankar*, Drexel University, USA*
Prof Sanjay Tanwani*, DAVV, Indore*
Dr Rajeev Agrawal, *GLBITM, Greater Noida*
Prof S D Joshi*, IIT, Delhi*
Prof Vikas Kumar*, Sharda University, Noida*
Dr Swades De*, IIT, Delhi*
Prof D K Mehra*, ICEIT, Delhi*
Prof Aditya Trivedi, *IIITM, Gwalior*
Prof Sunil Joshi*, MPUAT, Udaipur*
Prof Parul Garg*, NSIT, Delhi*
Dr S Bhattacharya*, University of Leeds, U K*

ICEIT Conference on
Advances in Mobile Communications, Networking and Computing
16 – 17 February, 2017
India International Centre (Annexe), New Delhi

Contents

- **Mr Suraj Suman and Prof Swades De**
  Indian Institute of Technology, Delhi
  Dimensioning of Solar Enabled Base Stations: An Utility Maximization Approach

- **Mr Anshul Thakur and Prof Swades De**
  Indian Institute of Technology, Delhi
  Impact of Co-Channel and Adjacent Channel Transmissions on DVB-T2 Broadcast

- **Ms Kamna Sharma, Ms Mona Aggarwal and Dr Swaran Ahuja**
  The NorthCap University, Gurgaon
  A Brief Survey on Femtocells and Interference Management Techniques

- **Mr Akhil Rana and Prof Aditya Trivedi**
  Indian Institute of Information Technology & Management, Gwalior
  Towards Depth Prediction in Indoor Scenes

- **Ms P Sai Sheela, Ms Rashika Joshi, Ms Jasleen Kaur and Dr S R N Reddy**
  Indira Gandhi Delhi Technical University for Women, Delhi
  A Survey on Smart Learning Platforms for Kids

- **Ms Nisha Sharma, Ms Zeenat Shareef and Dr S R N Reddy**
  Indira Gandhi Delhi Technical University for Women, Delhi
  Wearable Healthcare Technologies in India: Review and Survey

- **Renuka Lakhanpal and Rishibha Yadav**
  Indira Gandhi Delhi Technical University for Women, Delhi
  Speech to Text application based smart notice board

- **Ms Manasi Mishra, Rachit Thukral and Dr S R N Reddy**
  Indira Gandhi Delhi Technical University for Women, Delhi
  Design and Development of 8051 Based Embedded Trainer Kit for Teaching and Project Development Purpose

- **Md Arquam and Dr Anurag Singh**
  National Institute of Technology, Delhi
  Masquerade Detection Technique based on User Profiling

- **Ms Nonita Sharma and Dr Ajay K Sharma**
  National Institute of Technology, Delhi
  A Pareto-optimal solution for Data Aggregation in WSN using Fuzzy Logic and Genetic Algorithm

- **Prof H M Gupta**
  ICEIT, Delhi
  Some Remarks on QoS in WLANs

- **Ms Sunita Prasad**
  Centre for Development of Advanced Computing, Noida
  Pareto optimal solution for joint optimization of power assignment and delay in wireless ad hoc networks

- **Megha Goyal, Ridhi, Shivangi Jha, Tanvi Surana and Vivekanand Jha**
  Indira Gandhi Delhi Technical University for Women, Delhi
  Energy Efficient Approach for a Wireless Sensor Networks using Matrix Completion

- **Ms Ayushi Jha, Ms Khushboo Goel, Ms Megha Agarwal, Ms Vidhi Jindal and Mr Vivekanand Jha**
  Indira Gandhi Delhi Technical University for Women, Delhi
  Avoiding Coverage Holes and Energy Holes using Mobile Sink in Wireless Sensor Network

- **Mr P K Mishra, Mr Rameshwar Nath Tripathi and Prof Y N Singh**
  Indian Institute of Technology, Kanpur
  QoS Analysis in Data Network: Stability,Reliability, QoS Invoke Rate Perspectives

- **Mr Sateesh Kumar Awasthi and Prof Y N Singh**
  Indian Institute of Technology, Kanpur
  Reputation System and Incentive Mechanism to Handle the Malicious Peers and Free-riders in Peer-to-Peer Networks

- **Mr Anupam Soni and Prof Y N Singh**
  Indian Institute of Technology, Kanpur
  Configuration of Offset time in Optical Burst Switching networks for delay sensitive traffic

- **Prof Parul Garg (Invited)**
  NSIT, Delhi
  Wireless Systems with Optical and RF Signals

- **Ms Kamna Sharma, Anshul Vats and Ms Mona Aggarwal**
  The NorthCap University, Gurgaon
  Outage Analysis of Variable-Gain Amplify and Forward Relayed Hybrid FSO/VLCCommunication System

- **Mr Gaurav Pandey, Ms Mona Aggarwal and Dr Swaran Ahuja**
  The NorthCap University, Gurgaon
  A Brief Survey on Underwater Wireless Optical Communication System

- **Ms Pallavi Athe and and Prof Y N Singh**
  Indian Institute of Technology, Kanpur
  Impact Zone Analysis of P-cycles

- **Mr Akash Gupta, Dr Parul Garg, Mr Shashikant**
  Netaji Subas Institute of Technology,Dwarka
  Mobilty Management for Indoor VLC System

- **Ms Varsha Lohani and Prof Yatindra Nath Singh**
  Indian Institute of Technology, Kanpur
  Migration to Next Generation Elastic Optical Network

Higher Channel Capacity using Massive MIMO in 5G

Shriya Narayanan and P C Jain
Shiv Nadar University
Sn761@snu.edu.in, premchand.jain@snu.edu.in

The next major phase of mobile communications standards providing data rate of greater than1Gbps is the 5th generation (5G) cellular technology. Massive MIMO (Multiple input multiple output) is an emerging technology that can be utilized to address the capacity requirement that 5G demands. In massive MIMO system, the base station is equipped with hundreds or thousands of antennas while the mobile station have around tens of antennas. Massive MIMO offers several advantages over other technologies such as increased channel capacity up to ten times, reduction of latency, etc. Massive MIMO relies on spatial multiplexing in which the data is divided into different parts and then transmitted. This provides an increase in data rate and additional channel capacity. In this paper, massive MIMO for different number of antennas at the downlink for a single cell multi-user system has been simulated using MATLAB. In this simulation, two pre-coding schemes –zero forcing (ZF) and maximum ratio combining (MRC) have been applied at the downlink. A comparison of the two schemes in terms of better capacity has also been carried out. Spatial diversity and spatial multiplexing, two categories of multiple antenna techniques has also been dealt with.
Keywords: Alamouti codes, Zero Forcing, Maximum Ratio Combining, Channel estimation,
Spatial Multiplexing.

1. Introduction

Mobile Communication has revolutionized the way people communicate. The world has witnessed tremendous growth in the mobile and wireless devices over the last years. New generations have appeared in consecutive successions over the past three decades, since the advent of an analog (1G) to digital (2G) network. This was followed by the (3G) multimedia support, spread spectrum transmission, and (4G) Long term Evolution (LTE) for mobile devices. The 5G network technology opens a new era in mobile communication technology. The 5G mobile phones will have access to different wireless technologies at the same time and the it should be able to combine different flows from different technologies. A 5G network will be able to handle 10,000 times more calls and data traffic than the current 4G network. Research suggests that 5G networks will run on mm-wave band like 15 GHz, 27 GHz or even 60 GHz. These bands offer far broader bandwidth than the 700 MHz, 800 MHz or 1800 MHz frequencies used for 4G, and hence can carry a lot more data at super speeds.

Massive MIMO, a candidate for 5G technologies, promises significant gains in wireless data rates and link reliability by using large numbers of antennas (more than 64) at the base transceiver station (BTS) and mobile receiver end. Compared to multi-antenna aided systems, such as LTE based fourth generation (4G) mobile communication system which allows for up to eight antenna elements at the base station (BS), the Massive MIMO system entails an unprecedented number of antennas at the BS. The huge leap in the number of BS antennas opens the door to a new research field in communication theory, radio wave propagation, and electronics. In this system the number of MS antennas are much less than the number of BS antennas. These extra antennas at the transmitter side help in focusing energy into smaller regions of space (beam forming) thereby improving radiated energy efficiency and throughput. In the air interface, there is a significant reduction of latency. As the system deals with large number of antennas and beam forming, fading no longer limits the latency. With OFDM, each subcarrier in a massive MIMO system will have substantially the same channel gain. Each terminal can be given the whole bandwidth, which renders most of the physical layer control signaling redundant[1]. Massive MIMO relies on spatial multiplexing, which in turn relies on the base station having good enough channel knowledge, on both the uplink and the downlink. For next-generation wireless data networks, it promises significant gains that offer the ability to accommodate more

users at higher data rates with better reliability while consuming less power. The technology offers huge advantages in terms of energy efficiency, spectral efficiency, robustness, and reliability. This paper discusses massive MIMO challenges in section 2 while section 3 provides MIMO simulations using MATLAB and results obtained. Section 4 concludes the paper.

2. Multi-Input Multi-Output Antenna System

MIMO technologies can be divided into two main categories: diversity and spatial multiplexing with respect to how data is transmitted across the given channel? The diversity techniques employ multiple antennas that are physically separated from one another. In this case, the same data is sent across different propagation paths, thereby improving the transmission reliability. This technique also prevents fading. In spatial multiplexing, different portions of the data are transmitted simultaneously on different independent paths, hence improving the data rate. Massive MIMO relies on spatial multiplexing. One of the key advantages of utilizing it is that it is able to provide additional data capacity[2].
With so many antennas and its elements, massive MIMO has several system challenges not encountered in today's networks. For example, today's advanced data networks based on LTE or LTE-Advanced require pilot overhead proportional to the number of antennas. Massive MIMO manages overhead for a large number of antennas using time division duplex (TDD) between uplink and downlink assuming channel reciprocity. Channel reciprocity allows channel state information obtained from uplink pilots to be used in the downlink pre-coder. Additional challenges in realizing massive MIMO include scaling data buses and interfaces by an order of magnitude or more and distributed synchronization amongst a large number of independent RF transceivers[3]. Another challenge lies in making many low cost low-precision components of antennas that work effectively together. The sheer size of a massive MIMO system brings in the requirement of synchronization for newly joined terminals and the exploitation of extra degrees of freedom that the excess of service antennas provide. Channel characterization is an integral component of massive MIMO. In order to assess a realistic performance assessment of the system, it is necessary to have channel models that reflect the true behavior of the radio channel. These models may not necessarily be accurate but they provide information regarding the behavior of the channel. The problem of pilot contamination has received widespread attention within the ongoing study of massive MIMO. Theoretical analysis has identified pilot contamination as the fundamental limit on the throughput of massive MIMO systems [4]. The effect of reusing pilots from one cell to another and the associated negative consequences is termed pilot contamination. When the service array correlates its received pilot signal with the pilot sequence associated with a particular terminal, it obtains a channel estimate that is contaminated by a linear combination of channels with other terminals that share the same pilot sequence. This results in interference at the uplink and downlink. This interference grows with the number of service antennas at the same rate as the desired signal [5]. There are several concerns with respect to deploying new wireless standards for massive MIMO systems. One possibility lies in introducing dedicated applications of massive MIMO technology that do not require backward compatibility [6].

2.1 Space Time Block Codes

It is necessary to add coding to the different channels so that the receiver can detect the correct data. There are various forms of terminology used including Space-Time Block Code (STBC), MIMO pre-coding, MIMO coding, and Alamouti codes. The Alamouti codes achieve spatial diversity with 2 transmit antennas that requires no channel knowledge. It is a rate-1 code as it takes two time slots to transmit two symbols. It is the only STBC that achieves its full diversity gain without sacrificing on data rate [7].

2.2 Pre Coding Schemes

Pre-coding is a preprocessing technique that exploits Channel-state information at the transmitter (CSIT) to match the transmission to the instantaneous channel conditions Linear pre-coding provides a simple and efficient method to utilize CSIT. Linear pre-coding has been shown to be optimal in certain situations involving partial CSIT. However, in much instances the main motivation of linear pre-coders is to simplify the MIMO receiver. Linear pre-coders include zero-forcing (ZF), maximal ratio combining (MRC), Matched filtering (MF), Wiener filtering, and regularized zero-forcing (RZF)[8]. The ZF pre-coding schemes were extensively studied in multiuser systems as the ZF decouples the multiuser channel into independent single-user channels. It often involves channel inversion, using the pseudo-inverse of the channel or other generalized inverses. In Maximum Ratio Combining technique, the received signals are adjusted both in magnitude and phase by the weights in the combining filter to maximize the Signal-to-Noise -Ratio (SNR) at the output of the combiner. The weighting applied to each diversity branch is adjusted independently from other branches according to the SNR at that branch. In Maximum Ratio combining each signal branch is multiplied by a weight factor that is proportional to the signal amplitude, that is, it branches with strong signal are further amplified, while weak signals are attenuated [9].

3. Simulations and Results

MATLAB Matrix laboratory is a multi-paradigm numerical computing environment and interactive program for data visualization. A proprietary programming language developed by MathWorks (MATLAB) allows matrix manipulations, plotting of functions and data, implementation of algorithms, creation of user interfaces [10]. Fig.1 shows the Channel capacity for different number of antennas. It can be observed from the graph that as the number of antennas are increased, its channel capacity increases. This is the basic premise for the development of massive MIMO systems. At higher SNR the capacity of the channel scales as logSNR bits/s/Hz which is a degree of freedom of gain whereas at lower SNR, the capacity scales as SNR log2e bits/s/Hz which is the receive beam forming gain.

Fig.2 shows performance of Alamouti Codes. In this system, we assume two transmit antennas and one receive antenna. At the transmitter end the data of a two consecutive slots will be considered. In the odd time slots, the first antenna transmit symbol 1 (s1) and the second ones will transmit symbol 2 (s2) simultaneously. At the even time slots the -s2* and s1* will be transmitted from the first and second antenna respectively (* represents Consecutive of..). As seen from the second plot in Fig. 2, the error rate is significantly reduced when Alamouti codes are used. It provides full diversity at full data rate (1 symbol/time slot) for two transmit antennas.

Fig.3 shows comparison of zero forcing (ZF) and maximum ratio combining (MRC) for 4*4 MIMO system. In the plot the number of receiving antennas is equal to the transmitting antennas. When the SNR is less than 0 dB, the output SINR for MRC is less than that of ZF. However, when the SNR is larger than 0 dB, the SINR of MRC is more than that of ZF. This indicates that MRC pre-coding method has larger interference characteristics at higher SNR. Therefore, ZF is preferred over MRC at higher SNR and vice versa at low SNR. Fig.4 and Fig.5 shows comparison of ZF and MRC for 125X8 and 256X16 antenna system. From the graphs it can be seen that at lower SNR, MRC has a lesser value of SINR and is therefore, better than ZF whereas at higher SNR, ZF is more suitable. Also, SINR values are more in comparison to MIMO antenna system(4*4) for the individual pre-coding schemes, thereby indicating higher capacity, which can be computed from the Ergodic capacity formula: $C=\log_2(1+SINR)$.

From the above simulations, we observe the following:

1. As the ratio of the number of transmit antennas/receive antennas increases, the channel capacity increases. This is one of the governing principles behind massive MIMO due to which it is currently being exploited. This is the reason massive MIMO offers high channel capacity. It is due to the fact that as the number of

antennas increase, more number of channels is introduced, that automatically increases the capacity of the entire system.
2. As the SNR is increased, zero forcing is more suitable than maximum ratio combining. However, if the SNR value is fixed and we increase the number of antennas, then maximum ratio combining is more suited. This is due to the computational simplicity and independent functioning at each antenna by MRC.

4. Conclusions

The evolution from MIMO to massive MIMO in the form of spatial diversity to spatial multiplexing has been simulated. From results we observed that spatial diversity is a reliable option for information transmission while spatial multiplexing utilizes full channel capacity. The
Alamouti space-time block coding was simulated to illustrate spatial diversity and it reduced the Bit error rate (BER) of a system at a specific SNR without any loss on the data rate. It has also been demonstrated through the simulation that massive MIMO systems can significantly improve the channel capacity. At the downlink of the system, two pre-coding - Zero forcing and Maximum Ratio Combining schemes were simulated for reduction of interference. From the results and simulations we observe that MRC works well for Massive MIMO systems while ZF is suited for conventional or moderately sized MIMO (<64) systems. Thus the independent functioning at each antenna unit makes MRC the better choice for pre-coding.
The spectrum crunch is a global phenomenon, where wireless networks constrained by scarce spectrum resource cannot keep pace with the explosion in mobile broadband use, particularly at a time when smart phones and tablets are becoming even more prevalent and heavily used. Future direction will be the measurement of massive MIMO in high speed trains (HST), M2M and mm-Wave communication, which are key technologies in 5G wireless networks. Massive MIMO can improve the performance of these systems.

Acknowledgment
The authors are grateful to Prof. Dinkar Prasad, Head, EE Dept., and Associate Director, School of Engg., Shiv Nadar University, G. Noida (UP), India for providing his encouragement, and permission to publish this paper.

References

[1] Erik G Larsson, Ove Edfors, Fredrik Tufvesson, T.L.Marzetta, Massive MIMO for Next Generation Wireless Systems, IEEE Communication Magazine, vol.52, no.2, pp 186-195, 2014
[2] G. J. Foschini, “Layered space-time architecture for wireless communication in a fading environment when using multi-element antennas,” Bell Labs Tech. J., vol. 1, no. 2, pp. 41–59, 1996369–363, Oct., 2006.
[3]National Instruments, "5G Massive MIMO Testbed: From Theory to Reality-every thing RF", http://www.ni.com/white-paper/52382/en/#t0c1
[4] T. L. Marzetta, “How much training is required for multiuser MIMO” in Proc. IEEE Asilomar Conf. Signals, Systems, and Computers (ACSSC'06), Pacific Grove, CA, USA, pp.359-363, Oct., 2006
[5] T. L. Marzetta, “Non-cooperative Cellular Wireless with Unlimited Numbers of Base Station Antennas,” IEEE Trans. Wireless Commun., vol. 9, no. 11, pp. 3590–600,Nov. 2010.
[6] Institute for Digital Communication, "Massive MIMO Systems", http://www.idc.lnt.de/en/forschung/massive-mimosystems/
[7] Nutaq Innovations, "Alamouti Space-time block coding", http://www.nutaq.com/blog/alamouti-space-time-block-coding
[8] G. Caire and S. Shamai, “On the capacity of some channels with channel state information,” IEEE Trans. on Information Theory, vol.45, no. 6, pp 2007-2019, Sept., 1999.
[9] Ahmed Hesham, Mehana, and Aria Nosratinia, "Diversity of MIMO Linear Pre-coding", IEEE Transactions of Information Theory, vol.60, no. 2, pp 1019-1038, Feb 2014

[10] Mathworks, http://in.mathworks.com/products/matlab/

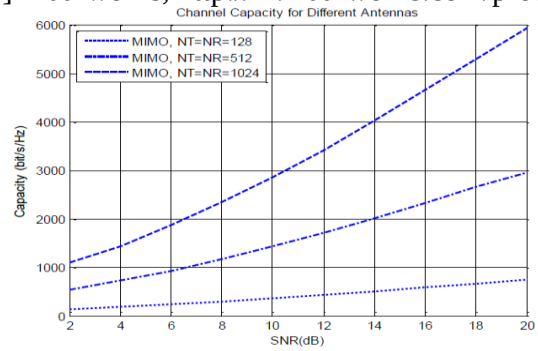

Fig. 1: Channel capacity for different number of antennas

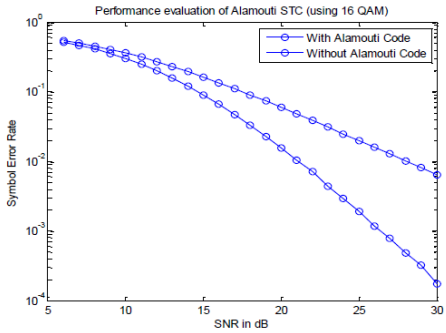

Fig.2: Performance of Alamouti Codes

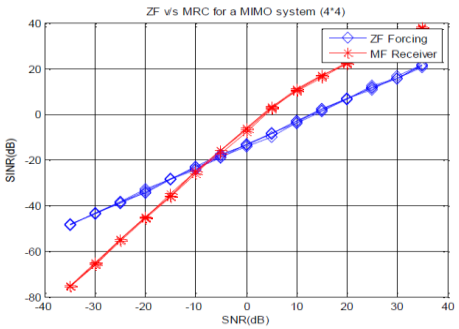

Fig.3: Comparison of zero forcing and maximum ratio combining for 4*4 system

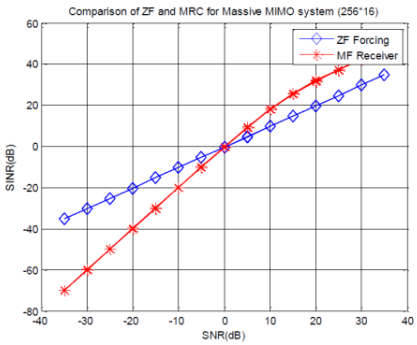

Fig.5: Comparison of ZF and MRC for 256*16 system

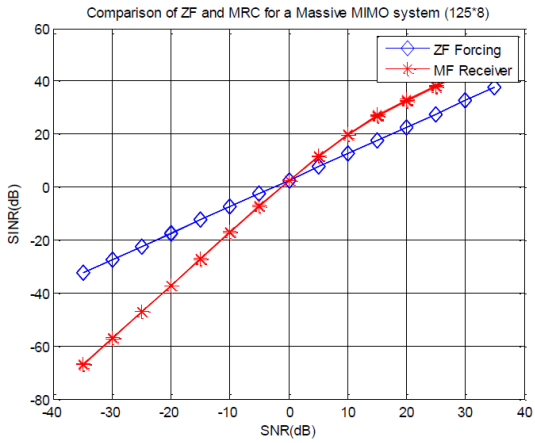

Fig.4: Comparison of ZF and MRC for 125*8 system

On the RF Energy Harvesting Networks

Swades De
Indian Institute of Technology, Delhi
swadesd@ee.iitd.ac.in

End nodes in Wireless networks are characterized by limited energy resources. Although the interests in wireless connectivity is ever-increasing and the needs for automated remote access, monitoring, and control are well-appreciated, widespread adoption of networked wireless devices is largely constrained by their affordable deployment and maintenance costs and convenience of their long-term usage. To this end, while energy efficient protocol design is a key for long-lasting network operation, energy harvesting aware solutions are becoming widely popular as green and affordable approaches towards timeless network operation. In this presentation, we will discuss radio frequency (RF) energy-harvesting aware network protocols for energy-constrained wireless devices. From our research experiences, we will take a few example cases of state-of-the-art research solutions on RF energy harvesting towards sustainable network communications.

A Dual Band Circularly Polarized High Gain Metal Plate Sector Antenna Design For 2.4/5GHz WLAN Bands

Varun Jain*, Shreyas Joshi[#], Priyanka Kumawat*, Pranay Joshi*, Sunil Joshi*
* Department of Electronics & Communication Engineering, MPUAT, Udaipur
[#] Institute of Technology, Nirma University, Ahmedabad
priyanka.kumawat2@gmail.com

Abstract*—This paper presents a novel dual-band metal plate dipole antenna for 2.4/5 GHz WLAN bands. Further, using this antenna, two sector antennas are designed. The dual-band functionality of metal plate antenna is achieved by designing two parallel dipole arms. The two dipole arms are derived by cutting two L-shaped slits in each radiating arm of the metal plate. The designed antenna elements are then strategically placed in front of a corner reflector and a back reflector to create two high gain WLAN sector antennas. Maximum vertical height of configure antenna is 131.5mm with very low vertical beamwidth and peak gain of ~13.56dBi. This facilitates vertical placement of multiple sector antenna units to be incorporated as MIMO sector antenna.

Keywords—WLAN, Sector antenna, Reflector, Dipole.

I. INTRODUCTION

WLAN is used to provide wireless data coverage to a number of users within a limited area. There are certain situations when there is need to provide data coverage within a large area viz. hotel lobbies, airports etc. Such situations demand either a distributed repeater network with several antennas or a high gain antenna which can cover the entire area. Mostly sector antennas are used when the requirement is to cover a large region. Metal plate antennas can be a suitable choice to design a high gain sector antenna for this purpose.

This paper presents design and development of sector antennas to meet requirements of dual band WLAN applications at 2.4/5 GHz. The IEEE 802.11n standard states that the maximum speed for WLAN can be upto 600 Mbps. It also specifies the use of MIMO technology to increase the data transmission speed [1]. Keeping this fact in mind, the proposed antenna is designed with low vertical beamwidth so that multiple antennas could be accommodated into a single radome, thereby forming a MIMO antenna system.

There are a number of antenna designs available for WLAN applications [2–7]. However; most of these antennas are printed antennas with low antenna gain. The antenna designed in [8] is a metal plate antenna with reasonable characteristics, but the drawback is that the feeding cable has to lie over the antenna body and the feed points are directly soldered over the antenna body. Absence of balun and feeding port may cause instability in the operation and may result in high reflective power thereby increasing VSWR. The antenna in [9] is also a metal plate antenna but the impedance band-width is 470 MHz in upper band which does not cover the entire WLAN band.

For the rest of this paper, the dual band metal plate dipole antenna is referred to as elementary antenna for convenience. Rest of this paper is divided into 4 sections. Section 2 covers designing of the elementary antenna along with its simulation and measurement results. Section 3 explains sector antenna designs and strategy involved in the process. Section 4 contains results and discussion about sector antenna testing. Section 5 concludes the paper.

II. ELEMENTARY ANTENNA

A. Antenna Design

The elementary antenna is designed using a copper strip having dimensions 37.3 mm(length) × 11 mm(width) × 0.3 mm(thickness) as shown in Figure 1. Two L- slots are cut into the strip at both sides to create two radiating dipole arms. A narrow T-slot is cut into the center of strip to achieve the symmetry. The perimeter of the dipole arm should

be multiples of half or quarter times the operating wavelength. To increase the frequency band, the width of the dipole arm is increased. Increasing the width will result in larger frequency bands but will reduce the gain due to spreading of current in a larger area. A trade-off must be maintained between the two parameters to achieve a specific band of frequency. Dimensions of the smaller dipole arms are adjusted to 9 mm(length) x 2.75 mm(width). The dimensions for larger dipole arms are kept 11.85 mm(length) x 4 mm(width) for optimal performance. The feed points are at the upper corner of T-slot as shown in Figure 1(a). The antenna is fed using a SMA connector connected to a 50Ω coaxial cable. Since the structure is symmetrical, the positive and negative feed can be interchanged. Figure 1(b) shows the fabricated dual-band metal plate antenna.

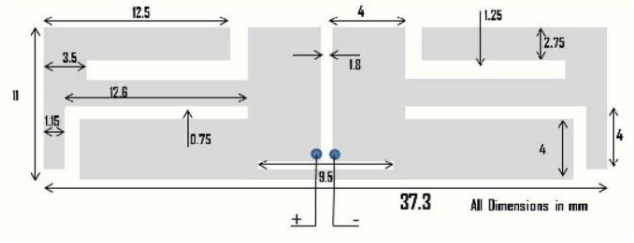

(a)

(b)

Fig.1: The elementary antenna (a) Design (b) Fabricated.

B. Elementary Antenna Testing and Results

The antenna design is simulated on EMSS FEKOv6.1 and obtained results are verified through the fabricated antenna. Figure 2 shows the return loss curve for the elementary antenna. The return loss for elementary antenna is greater than 10dB for the entire WLAN frequency band i.e. from 2400 MHz-2488 MHz and 5185 MHz-5875 MHz. The measured results agree with the simulation results.

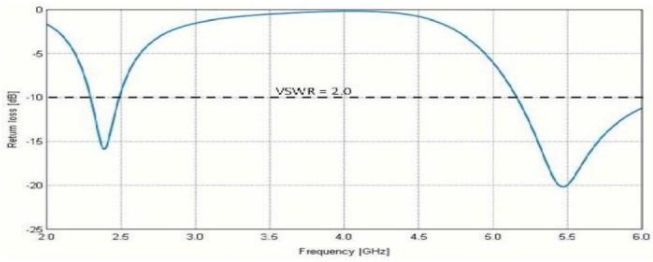

Fig. 2: Return loss curve for the elementary antenna.

The radiation pattern of the elementary antenna is similar to the dipole antenna patterns. Figure 3 shows the radiation pattern of the elementary antenna for 2.45 GHz and 5.5 GHz.

Figure 3(a) shows the doughnut shaped radiation pattern for the elementary antenna which is exactly similar to radiation pattern of a wire dipole antenna. However Figure 3(b) shows that as we move towards the upper band, the radiations are somewhat inclined.

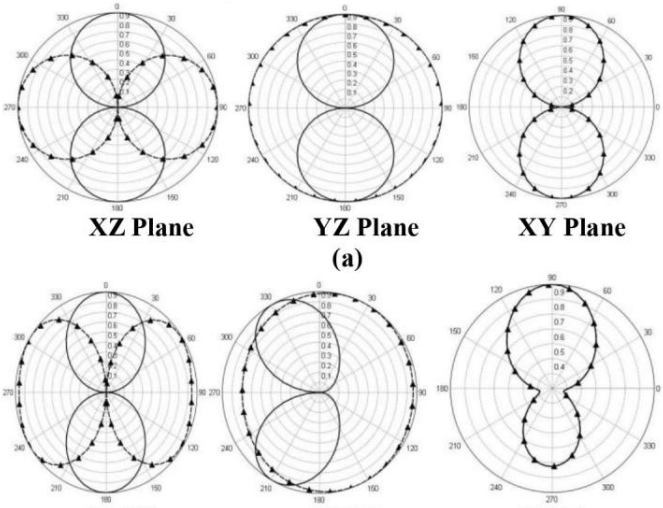

Fig. 3: Radiation pattern of the elementary antenna at (a) 2.45 GHz (b)5.5 GHz.

The reason for this inclination may be attributed to the larger dipole which is designed for the lower frequency band, but when excited with upper frequency, it distorts the radiation pattern by interfering with the radiations of smaller dipole. Figure 4 shows the antenna gain plot. Gain is nearly consistent for lower band, i.e. approximately 2 dBi. For upper band, the gain varies from 2.3 dBi to 2.7 dBi.

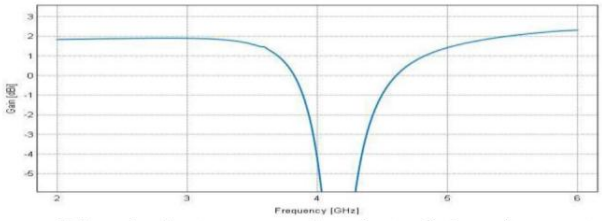

Fig. 4: Antenna gain plot of the elementary antenna

The above mentioned results assure successful working of elementary antenna and thus pave the way for designing sector antennas.

III. SECTOR ANTENNA DESIGN

To design the required sector antenna, two types of reflectors are used. Firstly a V-reflector or corner reflector and secondly a rectangular back reflector is used.

A. Corner Reflector base Sector Antenna (CRSA)

To design the CRSA, a V-shaped Aluminum sheet of thickness 0.5 mm is placed at the back side of elementary antennas as shown in Figure 5. In view of designing this sector antenna as a part of MIMO sector antenna, the vertical beamwidth was decided to be kept as low as possible. To minimize the vertical beamwidth, two elementary antenna elements are placed in front of the reflector. The optimum position for the elementary antennas placement in front of the reflector is deter- mined by considering various crucial parameters viz. return loss, horizontal beamwidth and front to back ratio. The return loss of the antenna depends on many factors which include distance between the elementary antennas and distance of reflector from the elementary antennas. The distance between the elementary antennas determine the vertical beamwidth and the distance between reflector and elementary antenna is a key factor in determining the horizontal beamwidth. If the elementary antennas are placed too close to each other, it will result in a very low vertical beamwidth but the return loss will decrease considerably. To restrict the return loss and the beamwidth at same time, a trade- off must be made between the two parameters. Table 1 shows the variation of return loss and vertical beamwidth with the distance between elementary antennas. The distance between the elementary antennas is kept 6 mm to achieve satisfactory return loss as well as vertical beamwidth.

Table 1:Variation of return loss and vertical beamwidth with the distance between elementary antennas.

Distance between Elementary antenna	ReturnLoss@2.45 GHz	Vertical beamwidth @2.45GHz
8mm	9.7dB	32.47
6mm	8.3dB	27.88
4mm	6.4dB	23.41

The dimensions of the reflector sheet are decided only after spacing between the antenna elements is fixed. The reflector should be large enough to reflect all the radiated waves from the antenna. Therefore, the dimensions of each arm of corner reflector are kept 170 mm (length) x 120 mm (width).The distance between reflector and the antenna elements depends on the operating wavelength of the antenna. It is generally kept as a multiple of half wavelength. However, determining the optimum distance for dual-band antenna is a tedious task. To do this, firstly we place the antenna at distances that are multiples of half wavelengths corresponding to center frequencies of both bands. Then the minimum distance for which the return loss is within the reasonable limits is selected. After that, trial and error method is used to obtain the optimum distance. In the present case, this distance is found to be 98.25 mm from the center of the reflector.

The Return loss is satisfactory; however the radiation patterns are not. Multiple beams are obtained after re- flection from the corner reflector. To converge the beam, the antenna elements are shifted sideways from the center of the reflector. Again this shifting is based on trial and error. As the antennas are moved sideways, a con- verged radiated beam is obtained but at the same time, return loss is degraded. So a trade-off should be maintained between return loss and radiation pattern. The optimum position, at which return loss and radiation patterns are satisfactory, is 18 mm from the center for top antenna element and 16 mm from the center for bottom antenna element. This way, the complete sec- tor antenna structure is

formed. The dimensions of this sector antenna are 170 mm x 170 mm x 120 mm.

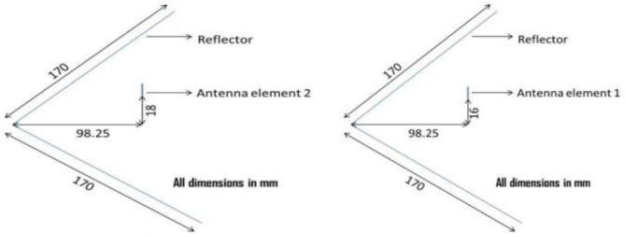

(a) (b)

Fig.5: The CRSA (a) Top View (b)Bottom View.

B. Back Reflector based Sector Antenna (BRSA)

The BRSA is designed by using a rectangular sheet of Aluminum with thickness of 0.5 mm. Here again, the distance between back reflector and elementary antennas is found out using the same approach. In this case, the optimum distance is found to be 21.5 mm. The gap between the elementary antennas is 30 mm in this sec- tor antenna. The reason of such large distance between elementary antennas is that there is no optimum point less than this distance where both the parameters viz. return loss and vertical beamwidth are at a satisfactory value. This fact has been verified by simulations. Due to this gap, there exist multiple beams in the radiation patterns of this antenna. Figure 6(a) shows the BRSA design. The dimensions of this antenna are 100 mm x 21.5 mm x 131.5 mm.

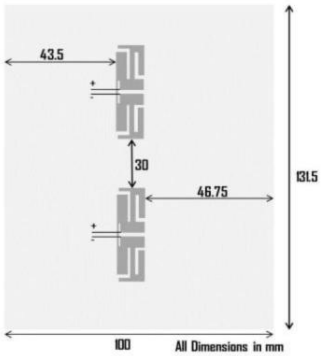

Fig. 6: The BRSA Antenna

IV. RESULTS AND DISCUSSION

The return loss curve for CRSA is shown in Figure 7. It reveals that for lower band, the VSWR is less than 3.1 and for upper band, the VSWR is less than 2.0. The inferior performance in lower band can be attributed to the trade-off made to improve vertical beamwidth. Measured results agree closely with the simulated results. The minor variation between the two may be attributed to manufacturing inaccuracies and environmental conditions.

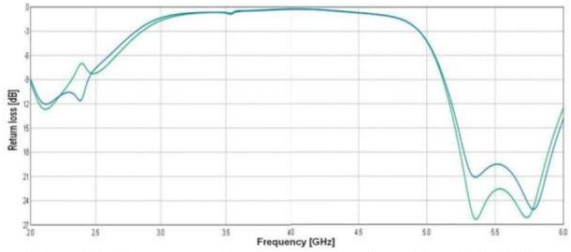

Fig. 7: Return loss curve for the CRSA.

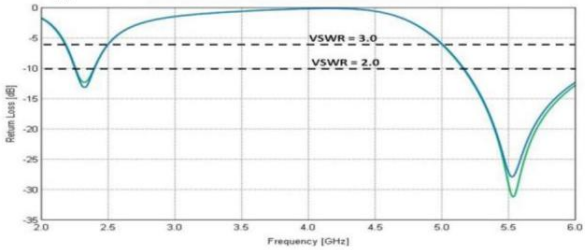

Fig. 8: Return loss curve for the BRSA.

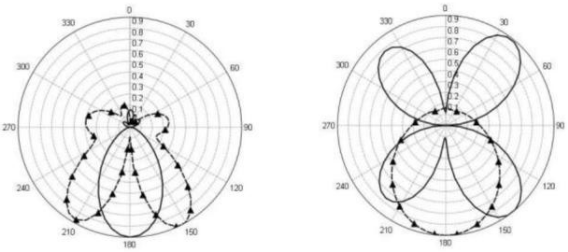

(a) (b)

Fig.9:Radiation pattern of BRSA(a)XZ-plane(b)YZ-plane.

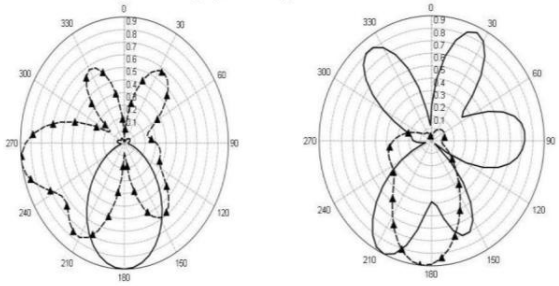

(a) (b)

Fig.10:Radiation pattern of BRSA(a)XZ-plane(b)YZ-plane.

Table 2 reveals that the horizontal beamwidth of the BRSA is nearly 80^{o}in lower band and nearly 120^{o}in upper band. The vertical beamwidth is varying almost similar to the CRSA. The horizontal beamwidth in up- per band is much larger for BRSA as compared to the CRSA, this variation is because of the fact that corner reflector confines the

radiations within a sector of 60°while in case of back reflector, there is no physical obstacle in path of radiations which allows them to expand when they get reflected by the back reflector. The same factor is responsible for higher gain of CRSA, since the radiations are confined; the gain is higher in case of CRSA.

Table 2: Beamwidth of BRSA and CRSA.

Frequency(MHz)	Horizontal Beamwidth		Vertical Beamwidth	
	CRSA	BRSA	CRS	BRSA
2400	56.42◦	80.03◦	29.15	30.11◦
2450	54.74◦	78.62◦	27.88	29.21◦
2488	53.41◦	77.14◦	26.13	28.84◦
5185	51.77◦	118.74◦	15.12	12.71◦
5500	51.22◦	118.15◦	14.19	11.47◦
5875	50.75◦	117.79◦	13.77	10.42◦

Fig. 11 shows the curve between gain and frequency for both type of sector antenna. It shows that for CRSA, the gain in lower band is nearly 10 dBiover the entire band, while in the upper band; it varies from 7.21 dBi to 13.56 dBi. The reason for this variation is due to variation of current distribution along the surface of dipole arm. The elements are designed to optimize the center frequency i.e. 5.5.GHz, therefore current flow in the smaller dipole is maximum at center frequency which leads to higher gain. As we shift to either sides of center frequency, the current gradually decreases and so does gain. For BRSA, gain in lower band is between 8.27 dBi to 9.45 dBi, while in the upper band, it varies from 7.61 dBi to 4.28 dBi.

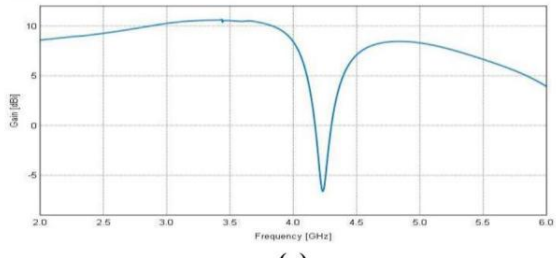

(a)

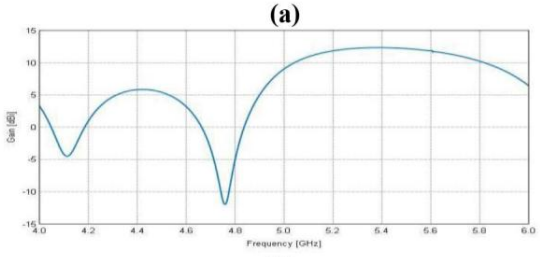

(b)

Fig. 11: Antenna Gain plot of (a) BRSA and (b) CRSA.

V. CONCLUSION

A novel dual-band metal plate antenna is designed using only a single metal plate. Using this elementary antenna, two sector antennas are designed with a corner reflector and a back reflector referred to as CRSA and BRSA respectively. The VSWR for elementary antenna is below 2.0 for entire frequency band. The return loss for both the sector antennas is less than 3.0 for lower band and less than 2.0 for upper band. The CRSA has consistent horizontal beamwidth which makes it suitable to be used as a 60°sector antenna while the back reflector based sector antenna has horizontal beamwidth in the range of 90°and 120°sector antenna in lower band and up- per band respectively. The vertical beamwidth of both types of sector antennas is considerably low. Owing to the small size, these sector antennas can be placed vertically to create multi-port MIMO sector antennas inside a single radome structure.

REFERENCES

[1] IEEE-SA-IEEE Get 802 Program-802.11: Wireless LANs http://standards.ieee.org/about/get/802/802.11.html.

[2] C. Y. Huang, and E. Z. Yu, "A slot-monopole antenna for dual-band WLAN applications," in IEEE antenna and wireless prop. letters, 2011, Vol. 10, pp. 500-502.

[3] Y. S. Wang, M. C. Lee, and S. J. Chung, "Two PIFA-Related Miniaturized Dual-Band Antennas," in IEEE trans. on antennas and prop., Mar. 2007, Vol. 55, pp. 805-811.

[4] W. S. Chen, and S. H. Cheng, "Design of a Dual-Band Planar Dipole Antenna for WLAN Applications," in Microwave Journal, Jul. 2009.

[5] S. H. Hwang, J. I. Moon, W. I. Kwak, S.O. Park, in "Printed compact dual band antenna for 2.4 and 5 GHz ISM band applications," in Electronics letters, Dec. 2004, Vol. 40.

[6] G. Y. Chen, and J. S. Sun,"Design of the Dual Band Dipole Antenna Serve WLAN and DSRC for its Application" in Proc. ISAP2005, pp. 129-132.

[7] T. H. Kimand D. C. Park, "Compact dual-band antenna with double l-slits for WLAN operations," in IEEE antenna and wireless prop. letters, 2005, Vol. 4, pp. 249-253.

[8] S. He, and J. Xie, "Analysis and design of a novel dual-band array antenna with a low profile for 2400/5800-MHz WLAN systems," in IEEE trans. on antennas and prop., Feb 2010, Vol. 58, pp. 391-396.

[9] S. W. Su, and J. H. Chou, "Low cost flat metal-plate dipole antenna for 2.4/5 GHz WLAN operation, "in Microwave and optical tech. letters, June 2008, Vol. 50, pp. 1686-1687.

[10] Y. T. Liu, J. H. Chou, and S. W. Su, "A one-piece flat-plate dipole antenna for dual band WLAN Operation," in Microwave and optical tech. letters, Mar 2008, Vol. 50, pp. 678-680.

Power Efficient Analog Multiplexer For Pulse Processing ASIC

Vatsala Sharma*, Shreyas Joshi[#], Pranay Joshi*, Kamal Nayanam[$], Sunil Joshi[*]

**Department of Electronics & Communication Engineering, MPUAT, Udaipur, India.*

#Institute of Technology, Nirma University, Ahmedabad, India.

$Arya college of engineering & IT, Jaipur, India

***Abstract*— A low power, fast analog multiplexer (AnaMux) for pulse processing ASIC is designed in 0.35 µm CMOS AMS technology. The design optimization is carried out via layout results without compromising power consumption. The methodology of design included circuit design, layout design and their optimization. The design has been carried out in public domain CAD tool. This find application in readout electronics of radiation detectors chip.**

***Keywords*— AnaMux, Pulse processing channel, ASIC, CMOS, AMS, CAD tool.**

I. INTRODUCTION

In high energy physics experiments that results in harmful radiations, there is a need to capture the amount of radiations present in the working environment. In such situations radiations are converted to electrical pulses which are digitized using pulse processing ASIC. A huge number of electrical pulses require many pulse processing channels to be placed in a small volume. A low power, fast analog multiplexer is designed to meet the design considerations of pulse processing ASIC. The work presented in this paper is concerned with the design and optimization of track & hold and analog multiplexer. It includes both front-end and back-end design.

II. DESIGN METHODOLOGY

The methodology used while carrying out the proposed work is based on the standard ASIC design flow as shown in figure 1. Definition of the design is the beginning and most important step towards designing a chip as the features and functionalities of the chip are defined. Speed, size & power consumption are among the consideration

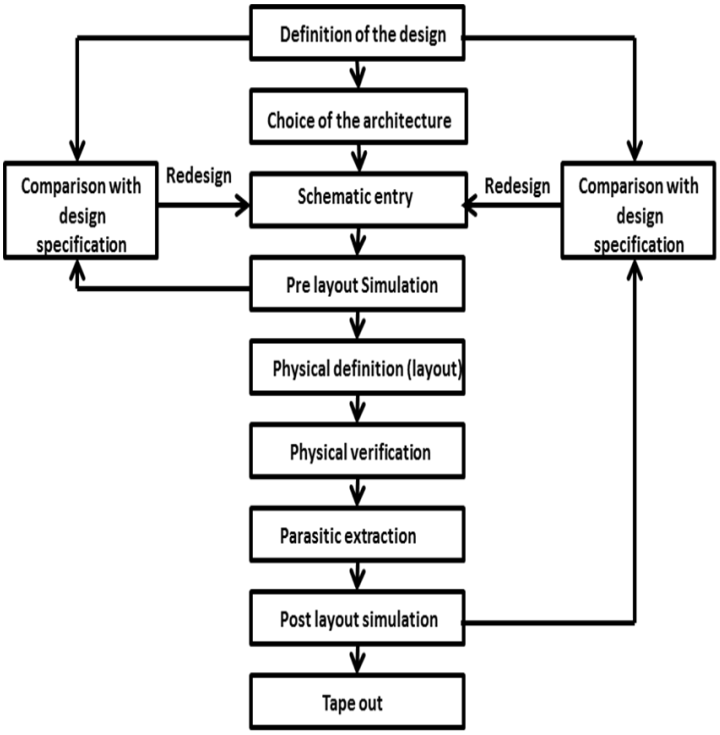

Figure 1: ASIC Design Flow

on which the accepted range of values is specified. Choice of architecture includes selecting the appropriate design that satisfies the target specifications. Schematic entry is the most common method of design entry for ASICs and is likely to be useful in one form or another for some time. The schematic shows how all the components are connected together, the connectivity of an ASIC. For pre-layout simulation, we must build up a circuit schematic to include all elements of the simulation. The main purpose of pre-layout simulation is to develop design constraints. Once the pre layout simulation is done, the layout of the schematic design is carried out. This is known as

back-end design or the physical definition of the design. Physical verification step is done prior to ensure proper functionality of the circuits implemented. After the layout is complete, silicon extracted parasitics are generated using RC extraction tool. Post-layout simulation involves extraction of physical information from the routed board. When the design passed the logic verification check, it is now ready for fabrication.

III. Architecture of Analog Multiplexer

The architecture include track & hold circuit which provide input to the analog multiplexer and D flip flop provides the control signal to analog multiplexer for time division multiplexing.

A. Track & Hold

As the name indicates it tracks the input signal from the semi Gaussian pulse shaper which is an analog signal & hold its peak amplitude value for a period. Therefore the output signal can be stored for measurement & analysis.

It consists of a CMOS switch followed by amplifier. The switch is accompanied with a dummy device. This dummy device can reduce the charge injection and clock feedthrough. The primary advantage of CMOS switch over the single channel MOS switch is that the dynamic analog-signal range in ON state is greatly increased. Capacitor is used for the charge storage as shown in figure 2 [2].

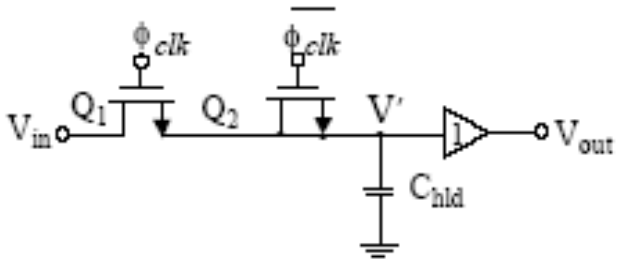

Figure 2: Track & Hold circuit [2]

B. Analog Multiplexer

Analog multiplexer is simply a selection switch which selects the track & hold outputs to be multiplexed. Its control logic comes from D flip-flop. Multiplexer has more than one inputs and one output. All the track & hold output signals are time multiplexed among which the multiplexer selects the one for which the control signal is high and produce it as the output at that particular instance of time. The design of analog multiplexer is shown in figure 3.

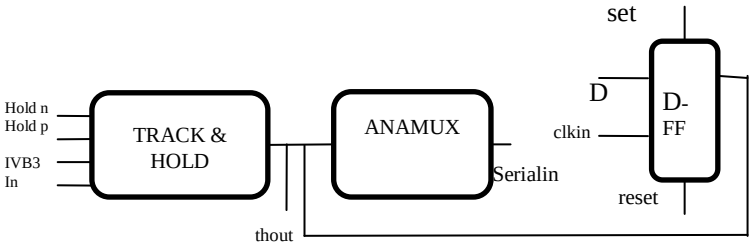

Figure 3: Design of Analog Multiplexer

IV. Technology Implemented

The design has been carried out in commercially available 0.35µ CMOS process technology. Basically it is a 3 metal 1 poly 3.3 volt N-well P-substrate CMOS process. Beside that it provides a high resistive poly resistor layer, a thin top metal layer (metal 4) and poly to poly capacitor layer. This process also supports 5 volt MOS transistor model. 0.35µ CMOS process has been utilized to develop photodiode and the readout electronics on the same wafer. The wafer cross section of this process has been shown in figure 4 [4].

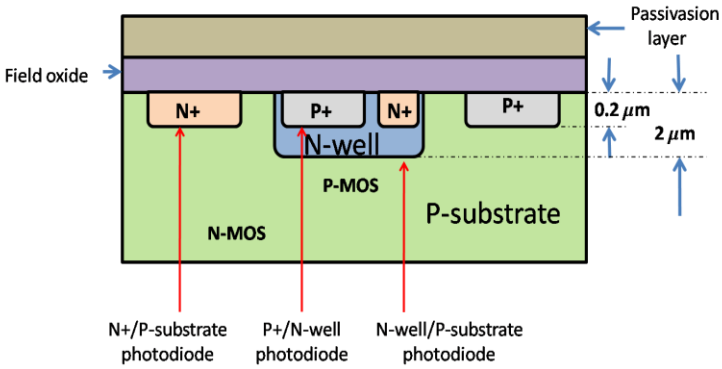

Figure 4: Wafer cross section of 0.35 µm process [4]

The CMOS technology is usually chosen on the merits of low power; high impedance for handling small charge; ability to build high gain voltage amplifiers, capacitors, pass transistors, analog & digital memories; develop photodiode and the readout electronics on the same wafer; high noise immunity; CMOS devices do not produce as much

waste heat as other forms of logic enables chips that are small in size to have features like high operating speeds and efficient usage of energy.

V. LAYOUT DESIGN

Layouts that are carried out automatically using the netlist generated from the schematic design are called schematic driven layouts. The flow diagram of the schematic driven layout is shown in figure 4. Importing the design involves specifying the following setup information. The floorplan defines the actual form, or aspect ratio, the layout will take, the global and detailed routing grids, the rows to host the core cells and the I/O pad cells (if required), and the location of the corner cells (if required). It is a good idea to save the design at this stage to allow restarting here quickly without needing to redo all the previous steps. Powerplan generates the VDD and ground power rings around the core and optionally adds a number of vertical and/or horizontal power stripes across the core. Stripes ensure a proper power distribution in large cores. The Net(s) field defines the number and the kinds of rings from the core. In our case, there will be first a ground ring around the core and a VDD ring around the ground ring. The net names should be consistent with the power net names in the cell LEF file. The rings will be placed in the centre of the channel between the core and the chip boundary. It is possible to extend the ring segments to reach the core boundary. Placement places the cells of the imported Verilog netlist in the rows automatically. CAP cell placement is done to place the termination cells at the beginning as well as end of each row. The so called CAP cells are used to properly bias the P+ and N+ substrates. Then FILLER cells are added to fill the remaining holes in the rows and ensure the continuity of power/ground rails and N+/P+ wells in the row is optional. As the paths that will propagate the clock signal in the design are not necessarily balanced, some registers may receive the active clock edge later than others (clock skew) and may therefore violate the assumed synchronous design operation. Route generates all the wires required to connect the cells according to the imported gate-level netlist. Then design is verified in terms of connectivity as well as geometry to check that the design has been properly placed and routed. The verified layout is then exported outside the design tool for further processing. This is to be done using .gds extension as GDS2 binary format is a standard format for integrating the block in the top-level layout, doing DRC/LVS checking, or delivering the layout to the foundry.

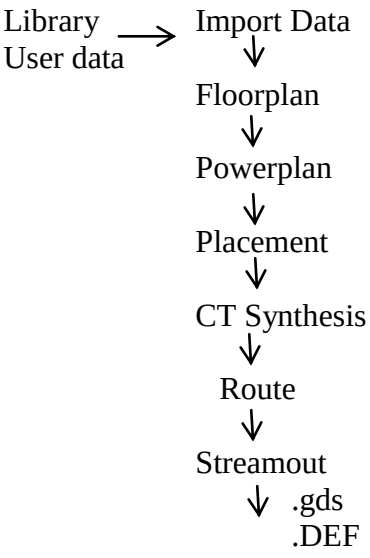

Figure 5: Schematic driven layout flow

VI. RESULTS

The input and output waveforms of Track & Hold circuit is shown in figure 6 & 7. Simulation result of analog multiplexer is shown in figure 8.

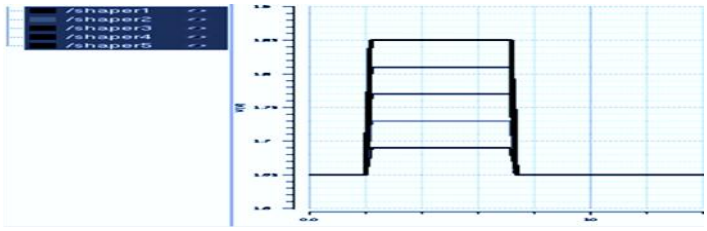

Figure 6: Input to Track & hold

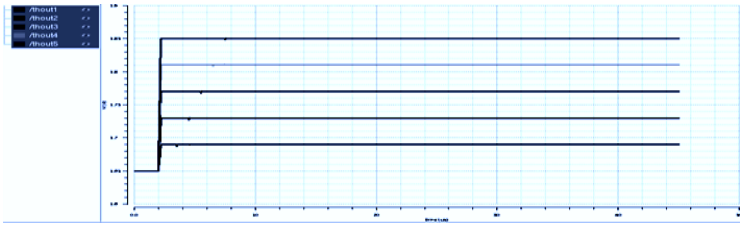

Figure 7: Output from Track & Hold

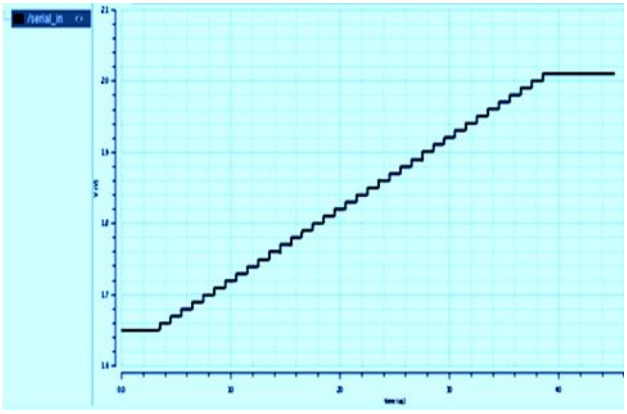

Figure 8: Output from analog multiplexer

VII. CONCLUSION

An analog multiplexer for the serial readout of multichannel system for radiation detector is designed successfully meeting its design considerations. The design is implemented using 0.35 µm CMOS technology and has been optimized for small size, low power and fast response. The schematic design and layout is optimized by comparing pre-simulation and post-simulation results using public domain CAD tool.

VIII. REFERENCES

[1] Jan Kaplon, "Fast, Low power, Analogue Multiplexer for readout of multichannel electronics", CERN CH1211, Geneva 23, Switzerland, CERN/ECP 95-11, 08 June 1995.

[2] Philip E. Allen and Douglas R. Holberg "CMOS Analog Circuit Design", Second Edition, Oxford University Press, 2002.

[3] Ken Martin, "Analog Integrated Circuit Design".

[4] Dr. V. B. Chandratre [S/O H] "Mixed design CMOS design techniques in nuclear instrumentation", Electronics division, BARC, Mumbai, May 29-31, 1995.

[5] Willy M.C. Sansen,"Analog Design Essentials", Catholic University, Leuven, Belgium.

[6] Helmuth Speiler and Lawrence Berkeley, "Front-End Electronics and Signal Processing", National Laboratory, Physics Division, Berkeley, CA 94720, U.S.A.

[7] Philip E. Allen, Douglas R. Holberg, "CMOS Analog Circuit Design" (Holt, Rinehart and Winston, Inc., 1987).

An Improved Approach for Image Splicing Detection: A Research Review

Rachna Mehta and Navneet Aggarwal
College of Technology and Engineering, Udaipur
er.rachnamehta10@gmail.com, navneetctae@gmail.com

***Abstract*—In digital image forensics, it is generally accepted that intentional manipulations of the image content are more critical. Numerous forensic methods focus on the detection of such malicious post processing. In this paper we focus on the prior work for features to detect these specific artifacts and we can introduce some improvements to these features by merging all these spatial, DCT and DWT domains. With these domains we can extract the feature of edges, features for correlation of pixels and multi resolution analysis using Spatial, DCT and DWT domains. We can also improve its complexity and reduce its dimensionality by using a new method for classification i.e. CS RS ensemble based classifier in comparison of SVM classifier, Ensemble Classifier and PCA.**

Keywords—DCT, DWT, Spatial Domain, Ensemble based Clssifiers, PCA, SVM

I. INTRODUCTION

With the rapid diffusion of inexpensive and easy to use devices that enable the acquisition of visual data, almost everybody has today the possibility of recording, storing, and sharing a large amount of digital images. At the same time, the large availability of image editing software tools makes extremely simple to alter the content of the images, or to create new ones, so that the possibility of tampering and counterfeiting visual content is no more restricted to experts. Finally, current software allows to create photorealistic computer graphics that viewers can find indistinguishable from photographic images [1, 2] or also generate hybrid generated visual content.

In summary, today a visual digital object might go during its lifetime, from its acquisition to its fruition, through several processing stages, aimed at enhancing the quality, creating new content by mixing pre existing material, or even tampering with the content. All these issues will get worse as processing tools become more and more sophisticated. While the majority of research work published in image forensics focused on developing robust algorithms for detecting tampering operations, it is sometimes more important to detect which parts of a given image have been manipulated. For this reason, we note here that researchers working in forensics imaging have either adopted the classification perspective or the localization perspective. Fig. 1 shows the work flow for a typical image splicing detection technique. It starts with the pre- processing stage which is usually the color to gray-scale conversion followed by the feature extraction stage. Different types of features are extracted from authentic and tampered images for a given dataset. The feature extraction stage is critical and the classification performance depends on the selection of best features for the problem under investigation [7]. The extracted features are used to train a classifier and the trained model is used to classify the authentic and tampered images. Finally, in the post-processing stage, the tampered regions are localized.

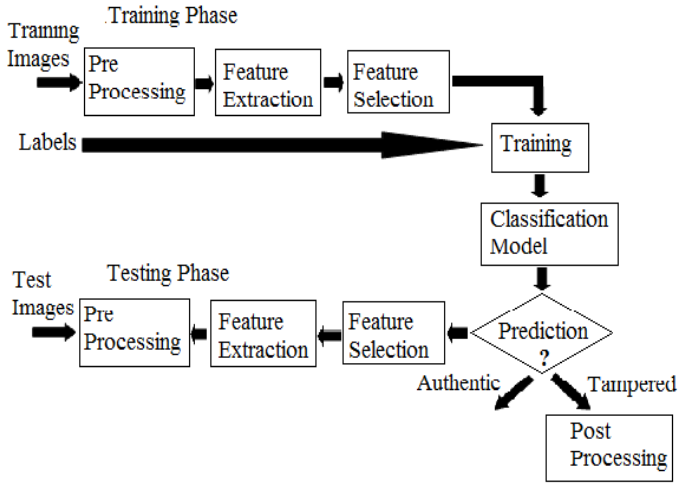

Fig 1. Work Flow for Image Splicing Detection Technique

Classification of high dimensional features [11] poses a serious challenge to image forensics due to several reasons. The required number of labeled samples for supervised learning methods increases exponentially with the dimensionality to achieve high generalization accuracy. The data points become sparse in the higher dimensions, which makes the learning task very difficult if not

impossible. Even though the support vector machine (SVM) seems to be the most popular machine learning tool used in steganalysis, SVMs are quite restrictive due to the complexity of SVM will be increased rapidly with the dimensionality of feature space growing [7]. Traditional approach that tackles classification problems with a high dimensional feature space employs dimensionality reduction or projection techniques like Principal Component Analysis (PCA) or KL-transformation. While such techniques help in reducing dimensionality, one drawback is that the new dimensions can be difficult to interpret, thus making it hard to relate the instances to the original dimensions [8]. A second drawback for the dimension reduction techniques like PCA is the huge computational complexity when calculate the covariance matrix of feature vectors with thousands of dimensions [9].

To address the challenges associated with the curse of dimensionality arising in splicing detection, Kodovsky [10] has designed an ensemble classifier built as random forest with the FLD [11] as a base learner. These ensemble classifier in [10] can provides performance equivalent to that of a Support Vector Machine (SVM) for steganalysis of large databases with large feature vectors. But the features in subspaces used to train the base learners in [10] were selected randomly from the original feature space, this approach is not suitable for high dimensional feature space consisting of thousands of features, thus affecting the classification performance of the base learners. In this suggested work, we can use a new method, called CS-RS which modifies the generation method of feature subspaces in [14] and therefore enhances classification performance over high-dimensional feature space.

The aim of this review paper is to provide a comprehensive overview of the state of the art in the area of blind detection of image splicing based on Markov features and Ensemble based classifiers and also we provide a view for improvement in these features. Unlike earlier work, we can improve these techniques in the terms that, we not only extract features in DCT, DWT and spatial domain but also we merge all these features in one frame work, then we classify these extracted features with a suitable classifier which will helped in the detection technique to achieve better accuracy.

The organization of the paper is as follows. Section 2 gives some preliminary background and reviews work related to different splicing detection methods. Section 3 describes the suggested framework for possibly improvement in the earlier techniques including feature extraction, reduction, and pattern classification. In Sect. 4, describes the comparison of experimental work and simulation results for existing earlier work. Finally, Sect. 5 concludes the paper.

II. Review of some state of art splicing detection methods

In 1999, Farid [15] used bicoherence (normalized bispectrum) based features to catch unnatural high order correlations in speech which was utilized to detect audio tampering. Motivated from his work Ng and Chang [16 - 18] used both magnitude and phase of the bicoherence spectrum. The method was tested on the Columbia Image Splicing Detection Evaluation (CISDE) dataset [20] with a reported detection accuracy of 63%. Then *Ng. et. el.* have shown the difficulties of image splicing detection using bicoherence features [16,17]. In this author uses two methods for improving the capability of the bicoherence features [16,17] in detecting image splicing. In these methods author exploits the dependence of the bicoherence features on the image content such as edge pixel density and offsets the splicing invariant component from bicoherence. Finally, they observe improvements 70.5% and have achieved success detection rates of accuracy [18, 19]. In SVM classification after the derived features are incorporated [12].

Dong et. al.. A 61-D feature set has been generated, which are based on the statistic moments of characteristic function of image run-length histograms. In this the Author utilize a Sobel operator and LoG detector to obtain the local sharp image intensity variations. With these changes author extract, the computation complexity of this approach is very low and their results indicated that these features improve the detection accuracy of 61-D with 76.52% for splicing detection [21,22] without any significant extra costs.

Fu et. el. By considering the high non-linearity and non-stationarity nature of image splicing operation, Hilbert-Huang Transform (HHT) has been utilized to generate features for classification [23]. Furthermore, a statistical natural image model based on moments of characteristic functions (CF) with wavelet decomposition is used to distinguish the spliced images from the authentic images. Support vector machine (SVM) as the classifier has been used [12].

Li et al. [24] combined features from the 1st order histogram of the DWT coefficients with HHT- based features.and this method had tested on the same dataset and classifier with detection accuracy of 86% achieved was higher than previously reported results (72% in [19] and 80% in [23]).

Chen et. el. The authors has pointed out that Fourier phase conveys important information about image structure and features [25]. Phase congruency provides an absolute measure of the significance of such image features and their experiment showed that the combination of moments and phase congruency gave an improved classification performance as compared with the state-of-the-art and have achieved successful detection rates of 120-D with 82% [25]

Zhao et al.used the 3rd order statistical features calculated from Conditional Co-occurrence Probability Matrix (CCPM) to detect image splicing. First, PCA has been used to reduce the feature dimensions, and then, classification was performed using SVM. The overall accuracy of 80.80% [26] has been achieved on CISDE dataset using an SVM classifier.

Zhang et al. applied LBP operator on multi-size DCT coefficients blocks. The discriminative features were extracted from LBP histograms. The feature dimension was reduce during KPCA, classification was performed using SVM, and It achieved detection accuracy of 89.9% on the CISDE dataset [27].

Shi et. al. a new steganalysis scheme has been designed to effectively detect the advanced JPEG steganography. For this purpose, Markov process is applied to modeling these difference JPEG 2-D arrays so as to utilize the second order statistics for steganalysis. In addition to the utilization of difference JPEG 2-D arrays, a thresholding technique has been developed to greatly reduce the dimensionality of transition probability matrices, Due to these features this scheme had achieved accuracy 88.8% for 324-D [28].

Shi et. el. This natural image model is represented by features extracted from a given test image and 2-D arrays produced by applying multi-size block discrete cosine transform to the given test image and they consider the spatial representation of the given test image and extract statistical moments of characteristic functions and Markov transition probabilities from this image pixel 2-D array [29]. With these features this approach has achieved an improved accuracy of 91.87% for 266-D features [30].

Zhang et. al. The author obtained feature set by merging and modifying two previously proposed feature sets with complementary performance (the DCT feature set in that captures inter-block dependencies among DCT coefficients and Markov features in which capture intra-block dependencies) [35]. This approach has achieved an accuracy of 91.5% with a 109-dimensional feature vector.

Zhongwei et. al. The author has combined the two kind of features Markov features in DCT domain and the Markov features in DWT domain. To handle a large number of developed features, feature selection method SVM-RFE has been utilized. At last, the final dimensionality-reduced feature vector has been used for image splicing detection with SVM as the classifier and their Experiment results achieve accuracy rate 93.55% with 100-D [32].

Several forensic techniques, which can be broadly grouped together as statistical classifiers, These forensic techniques use powerful tools from machine learning such as support vector machines (SVMs), neural networks and ensemble based classifiers to identify the specific changes in these features that correspond to manipulation. Before classification can be performed, these techniques must be trained using features extracted from both unaltered and falsified or manipulated image content. But most commonly used classifier is SVM because it is easy to use.

Although there exists a large variety of various machine learning tools, support vector machines (SVMs) seem to be the most popular choice. This is due to the fact that SVMs are backed by a solid mathematical foundation cast within the statistical learning theory [29] because they are resistant to overtraining and perform rather well even when the feature dimensionality is comparable or larger than the size of the training set. Moreover, robust and efficient open-source implementations are available for download and are easy to use, The complexity of SVM training, however, slows down the development cycle even for problems of a moderate size, as the complexity of calculating the Gram matrix representing the kernel is proportional to the square of the product of the feature dimensionality and the training set size. Moreover, the training itself is at least quadratic in the number of training samples. This imposes limits on the size of the problem one can handle in practice and forces the steganalyst to consciously design the features to fit within the complexity constraints defined by available computing resources. Ensemble classifiers give substantially more freedom to the analysts, who can now design the features virtually without constraints on feature dimensionality and the training set size to build detectors through a much faster development cycle

III. SUGGESTED FRAMEWORK

In the prior state of art the authors have not claimed further improvement in the accuracy detection rate and reduction in complexity in terms of dimensionality. In this section we have suggested an improved framework for further improvement in true positive rate, true negative rate and accuracy detection rate and also we have focused on complexity and dimension reduction in one roof. This improved approach with DCT, DWT and spatial domain focuses on markov features to their effectiveness and simple-ness and dumping all the moment based features. The framework of an improved markov features based approach is shown in fig. 2. Given a digital image, we can not only extract markov features in DCT, DWT and Spatial domain , But also we can merge all these features in one framework by taking the advantage of all these three domains.

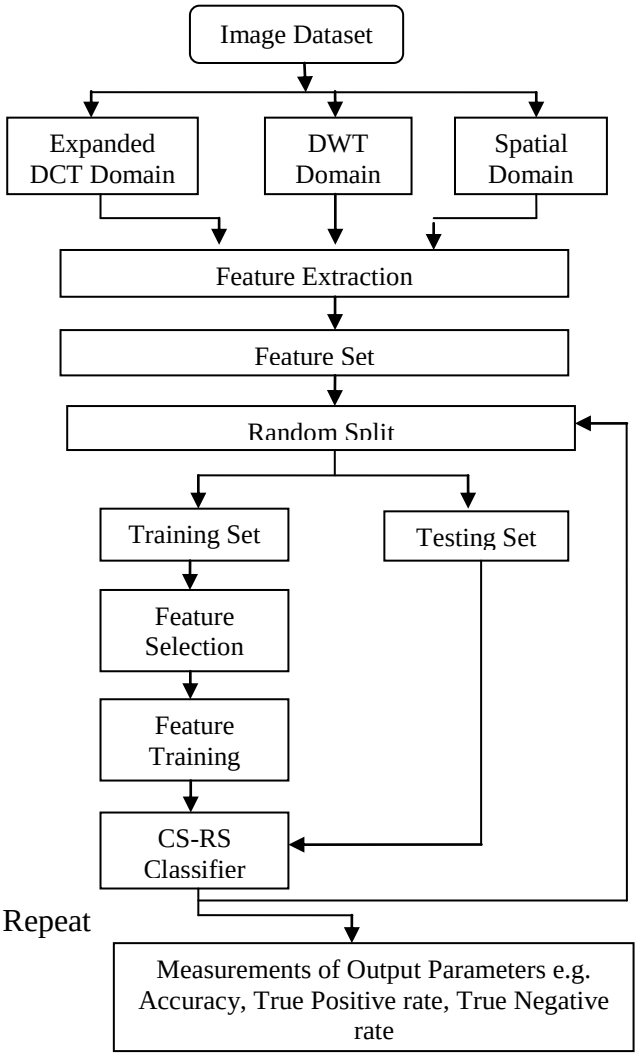

Fig 2. A Framework of Suggested Improved Approach

Furthermore, for feature extraction in DCT domain we can use expanded Markov features extracted in DCT in our approach which is for the purpose of capturing not only the intra-block correlation but also the inter-block correlation between DCT coefficients [35]. The splicing boundaries are normally sharp transitions in nature, for this DWT can be more suitable for image splicing detection with its advantage of multi resolution analysis, This wavelet analysis is good at catching the short-time transient or localized change in signals. Quite a few methods based on DWT have been designed in the past, such as [24]. However, most of the methods deal with all the subbands independently after wavelet decomposition, neglecting the dependency among wavelet coefficients across positions, scales and orientations [23,24].

But here, we can extract the features in DWT domain by using the Markov random process (Transition Probability Matrix) to capture the aforementioned three kinds of dependency among wavelet coefficients, and make the acquired Markov features in DWT domain an important part in the whole image splicing detection [30]. Then we can also extract the features in spatial domain, with this domain the edge images are calculated in horizontal, vertical, major diagonal and minor diagonal directions in spatial domain. For edge detection we can use any suitable edge detection algorithm for better accuracy. After all the related features are generated by all these domain we merge all extracted features in one framework, then a features selection method referred as ensemble based classifier is adopted to reduce the dimensionality of the final feature vector, making the computational complexity more manageable. Finally, the n-D feature vector obtained is used to distinguish authentic and spliced images with ensemble as the classifier.

IV. Comparison of Results for State of Art

The task of image splicing detection among authentic and forged images is an example of binary classification. The detection performance can be evaluated in terms of the detection accuracy (Acc), true positive rate (TPR) and true negative rate (TNR). We can consider the spliced image as positive and authentic image as negative. TPR and TNR are also known as sensitivity and specificity, respectively. The performance metrics are calculated as follows:,

$$Accuracy = \frac{(TP + TN)}{(TP + TN + FP + FN)}$$

$$TPR = \frac{TP}{(TP + FN)}$$

$$TNR = \frac{TN}{(TN + FP)}$$

where TP is number of True Positive, TN is number of True Negative, FP is number of false Positive and FN is number of False Negative. Though there are other metrics like precision, sensitivity and specificity for measuring the performance of classifiers, accuracy seems to be the most important metric as it considers all possibilities of positive and negative outputs of classifiers. We can also use the Receiver Operating Curve (ROC) and the Area Under the Curve (AUC) to plot the changes in TPR and FPR as the decision threshold changes from 0 to 1. The comparison results for state of art are shown in table 1. As we can see in these results in the earlier work the authors focused on the accuracy regardless of the the dimensionality. As the dimensionality increases the accuracy is also increases but increasing dimensionality increases the computational cost and complexity and also it slow down the development cycle even for problem of a moderate size.

Table 1. Comparison of results for state of art

Features	Dimensionality	Accuracy rate
Ng. et.al. [19]	-	63%
Ng. et.al. [18]	768-D	72%
Dong et. al. [21]	61-D	76.5%
Fu et. al. [23]	110-D	80.1%
Chen et. al. [25]	.120-D	82%
Li et. al. [24]	72-D	85%
Shi et. al. [28]	324-D	88.8%
Zhao et. al. [26]	686-D	88.8%
Zhang et. al. [27]	768-D	89.93%
Shi et. al. [30]	266-D	91.8%
Zhang et.al. [31]	109-D	91.5%
Zhangwei et. al.[32]	100-D	93.5%
EI et. al. [33]	50-D	98%

Then the authors start focused on low dimensionality with increasing accuracy and they found fruitful results that as dimensionality reduces complexity reduce and they speed up the development cycle at low computational cost.

V. Conclusion

Our extended overview of image forgery detection techniques shows that this area of research is still in its flourishing stage, and holds a huge potential for future R&D applications. Although many of the techniques discussed here require some

types of assumptions to provide excellent detection results, with more research efforts, we expect some robust methods to become standard tools in the near future.

VI. References

[1] G. W. Meyer, H. E. Rushmeier, M. F. Cohen, D. P.Greenberg, and K. E. Torrance, "An experimental evaluation of computer graphics imagery," *ACM Transactions on Graphics*, vol. 5, no. 1, pp. 30–50, 1986.

[2] "Fake or foto," 2012, http://area.autodesk.com/fakeorfoto.

[3] H. Farid, "Digital doctoring: how to tell the real from the fake,"significance, vol. 3, no. 4, pp. 162–166, 2006.

[4] "Photo tampering throughout history," 2012, http://www .fourandsix.com/photo-tampering-history/.

[5] R. L. Rivest, A. Shamir, and L. Adleman, "A method for obtaining digital signatures and public-key cryptosystems," *Communications of the ACM*, vol. 21, no. 2, pp. 120–126, 1978.

[6] V.M. Potdar, S. Han, E. Chang, A survey of digital image watermarking techniques, in: 3rd IEEE International Conference on Industrial Informatics (INDIN), Perth, Western Australia, 2005, pp. 709–716.

[7] K.Fukunga, Introduction to statistical pattern recognition. MacMillan Publishing Company, San Diego,1990

[8] L.Molina, L.Belanche, A.Nebot, "Feature selection algorithms: A survey and exp. evaluation," in Proc. ICDM, 2002, pp. 306-313.

[9] D.Fradkin, D.Madigan, "Experiments with random projections for machine learning," Proceedings of the ninth ACM SIGKDD international conference on Knowledge discovery and data mining, New York: ACM, 2003, pp. 517-522.

[10] J.Kodovsky, J.Fridrich , V.Holub, "Ensemble classifiers for steganalysis of digital media," Information Forensics and Security, IEEE Transactions on,vol.7,pp. 432-444, June 2012.

[11] R.O.Duda, P.E.Hart, D.G. Stork, Pattern classification, John Wiley & Sons, 2012.

[12] C.Chih-Chung and L.Chih-Jen, "LIBSVM: A library for support vector machines," ACM Transactions on Intelligent Systems and Technology, vol. 2, pp.27:1– 27:27,April 2011.

[13] H.Tao, X.Ma, M.Qiao, "Subspace Selective Ensemble Algorithm Based on Feature Clustering," Journal of Computers,vol.8,pp.509-516, February 2013.

[14] Fengying He Shangping Zhong and Kaizhi Chen, "An Effective Ensemble-based Classification Algorithm for High-Dimensional Steganalysis," Journal of Software, Academic Publisher , Vol 9, No. 27, July 2014, pp 1833-1840

[15] H. Farid, Detecting Digital Forgeries Using Bispectral Analysis, Technical Report AIM-1657, AI Lab, Massachusetts Institute of Technology, 1999.

[16] H. Farid, "Detecting Digital Forgeries Using Bispectral Analysis", Technical Report, AIM-1657, MIT AI Memo, 1999.

[17] Y. C. Kim and E. J. Powers, "Digital Bispectral Analysis and its Applications to Nonlinear Wave Interactions", IEEE Trans. on Plasma Science, vol. PS-7, No.2, pp. 120-131, June 1979

[18] T.-T. Ng, S.-F. Chang, Blind Detection of Digital Photomontage using Higher Order Statistics, Technical Report 201-2004-1, Columbia University, 2004.

[19] T.-T. Ng, S.-F. Chang, A model for image splicing, in: IEEE International Conference on Image Processing, Singapore, 2004, pp. 1169–1172.

[20] T.-T. Ng, S.-F. Chang, A Data Set of Authentic and Spliced Image Blocks, Technical Report 203-2004-3, Columbia University, 2004.

[21] J Dong , W Wang , T Tan , Y Q Shi Run-length and edge statistics based approach for image splicing detection. In: Kim H-J, Katzenbeisser S, Ho ATS (eds) Digital watermarking. Springer, Berlin, pp 76–87,2009

[22] Dong, J., Tan, T.: Blind image steganalysis based on run-length histogram analysis. In: 2008 IEEE International Conference on Image Processing(ICIP08). (2008)

[23] D .Fu, Y.Q .Shi, W. Su ,Detection of image splicing based on Hilbert– Huang transform and moments of characteristic functions with wavelet decomposition ,in: 5th International Workshopon Digital Watermarking, vol.4283, Springer, JejuIsland, Korea, 2006, pp. 177–187.

[24] X.Li, T. Jing, X.Li ,Image splicing detection based on moment features and Hilbert–Huang transform ,in :International Conference on Information Theory and Information Security(ICITIS), IEEE, Beijing, China, 2010, pp.1127–1130.

[25] Chen, W., Shi, Y.Q.: Image splicing detection using 2-d phase congruency and statistical moments of characteristic function. In: Imaging: Security, Steganography, and Watermarking of Multimedia Contents. (January 2007)

[26] X .Zhao, S. Wang, S .Li, J .Li, A comprehensive study on third order statistical features for image splicing detection, in:10th International Workshop on Digital Forensics and Watermarking,vol.7128, Springer, Atlantic City, NY, USA, 2012, pp. 243–256.

[27] Y .Zhang, C. Zhao, Y .Pi ,S .Li ,Revealing image splicing forgery using Local Binary Patterns of DCT coefficients, in: International Conference on Communications, Signal Processing, and Systems, vol. 202, Springer, Gold Coast, Australia, 2012, pp. 181–189

[28] Y. Q. Shi, C. Chen, and W. Chen, "A Markov Process Based Approach to Effective Attacking JPEG Steganography," In Proceedings of Information Hiding Workshop (IH06), Old Town, Alexandria, VA, USA, 2006, pp.249-264.

[29] Shi, Y.Q., Chen, C., Xuan, G.: Steganalysis versus splicing detection. In: Interna- tional Workshop on Digital Watermarking (IWDW07). (December 2007)

[30] Shi, Y.Q., Chen, C., Chen, W.: A natural image model approach to splicing detec- tion. In: ACM Workshop on Multimedia and Security (ACM MMSEC07). (2007).

[31] J. Zhang, Y. Zhao, Y. Su, A new approach merging markov and DCT features for image splicing detection, in: International Conference on Intelligent Computing and Intelligent Systems (ICIS), vol.4, IEEE, Shanghai,China,2009,pp.390–394.

[32] H Zhongwei , Wei Lu W Sun " Digital image splicing detection based on markov features in DCT and DWT domain". Pattern Recogn 45(12):4292–4299, 2012.

[33] E.-S. M. El- Alfy, M. A .Qureshi, Combining spatial and DCT based markov features for enhanced blind detection of image splicing, Pattern Anal.Appl.18(3)(2014)713–723.

[34] C.-C. Chang and C.-J. Lin, LIBSVM: A Library for Support Vector Machines 2001 [Online]. Available: http:// www. csie. ntu. edu.tw/~cjlin/ libsvm.

[35] C. Chen, Y.Q. Shi, JPEG image steganalysis utilizing both intrablock and interblock correlations, in: IEEE International Symposium on Circuits and Systems, Seattle, WA, USA, 2008, pp. 3029–3032.

Path Loss Model based on WiFi RSSI Measurements Using Crowd Sourcing Application

Kartik Bhaiyaji, Jaspreet Singh, Javed Shamim Malik, and M Salim Beg
Department of Electronics Engineering, ZHCET, AMU, Aligarh
kbhaiyaji@gmail.com, jaspreetsngh5488@gmail.com, jmalik.el@amu.ac.in, salim.beg@amu.ac.in

Abstract

Crowd sourcing applications are now being used for performing wireless measurements. These applications measure and log a number of wireless signal parameters/metrics like RSSI, RSRP, throughput, latency to name a few. These can be used in network performance characterization and subsequent optimization. These applications are available as open source and they provide an inexpensive alternative to perform measurements. In this paper authors present and discuss RSSI measurements performed using an open source application installed on an android device. Comparison of measured data and theoretic model shows that the measurements using this open source application are reasonably accurate.

Keywords: Crowdsourcing, RSSI, Path loss, Wi-Fi, open source, android.

I. INTRODUCTION

Traditionally, network performance characterization and subsequent optimizations are done based on drive testing by network infrastructure vendors in coordination with service providers. This involves test teams repeatedly going to the field where network is deployed to perform measurements and collect statistics. This approach has a number of issues:

i. It is a costly affair as it requires a number of expensive equipments.
ii. These results are not available to public and so researchers can hardly contribute to optimize networks.
iii. While this approach is practical in macro cell environment, it is not possible to perform drive test for micro and pico-cell network configurations.

Crowd sourcing is fast emerging as a new method for performing wireless measurements. This technique uses an open source application installed on a smart phone or android device that logs a number of parameters/metrics like received signal strength indicator (RSSI), reference signal received power (RSRP), throughput, and latency [3], [7], [9]. The advantage in using these open source application is that it provides an inexpensive alternative to perform measurements and that dedicated test teams are not required to perform drive tests. A smart phone user can install these applications on their device and enable measurements. The measurements could be uploaded on cloud for further analysis [1], [6]. The research community could benefit from these real life measurements provided by users in live network. The measurements can be analyzed and used to build realistic models for wireless systems and subsequently suggest improvements and optimizations.

Measurements using crowd sourcing is being used in recent years by several researchers. Authors in [6] use this approach for local network topology discovery. It is used in [4], [5] for path loss modeling and [8]

to model LTE Downlink throughput. In [9] authors used crowdsensing approach to find the frequencies used by the different Wi-Fi access points in the city of Edinburgh.

RSSI can be used to estimate the distance between two nodes [5]. It can also be used for indoor positioning and localization [2], [4]. It is also used for occupancy estimation [10] and intrusion detection. In the present paper, the authors limit the studies to Wi-Fi network RSSI measurements. This paper is organized as follows. In section II path loss model is described. Section III describes the measurement setup. Section IV presents the results obtained from the measurements carried out in this work. Finally section V gives the conclusions that can be drawn from this work.

II. PATH LOSS MODEL

Radio signals undergo reflection, refraction, diffraction and scattering when they propagate in free space. Free-space model or Friis formula, ground bidirectional reflectance model and log-normal shadow models are prevalent models that are used to model received signal strength [5]. Given transmit power P_t, transmit antenna gain G_t, receive antenna gain G_r, carrier wavelength λ, at a distance d from transmitter, the received power P_r, according to Friis model is given by eq (1)

$$P_r(d) = \frac{P_t G_t G_r \lambda^2}{(4\pi d)^2} \quad (1)$$

$$PL\ (dB) = 10\ \log\ \frac{P_t}{P_r} = -20\ \log\left(\frac{\lambda}{4\pi d}\right) \quad (2)$$

According to this formula, the received power is inversely proportional to square of the distance between transmitter and receiver. Friis model is used under following assumptions.

i. the transmission distance is much larger than the antenna size and carrier wavelength λ
ii. there are no obstacles between the transmitter and receiver.

Surface bidirectional model is applicable in the following scenarios

i. transmission distance is of the order of a few kilometers.
ii. the height of the transmitter and receiver antenna is more than 50 meters.

Eq (3) gives the expression for received power where h_t and h_r are the heights of transmit and receive antenna respectively.

$$P_r(d) = P_t G_t G_r \frac{h_t^2 h_r^2}{d^4} \quad (3)$$

$$PL\ (dB) = 40\ \log\ d - (10\ \log\ G_t + 10\ \log\ G_r + 20\ \log\ h_t + 20\ \log\ h_r) \quad (4)$$

In this case, the received power in inversely proportional to fourth power of the distance between transmitter and receiver.

Log-normal shadow model is a more general propagation model applicable to both indoor and outdoor environments. This model provides a number of parameters which reflect different kind of environments. The path loss according to this model is given by eq (5).

$$PL\ (dB) = 10\ \eta\ \log\ d + X_\sigma \quad (5)$$

η is a measure of obstacles like door, walls, partitions and X_σ is a normal random variable with standard deviation σ. For free space η= 2 and for indoor environments with walls and obstructions, η= 4 or 5 typically.

III. MEASUREMENT SETUP

In order to understand path loss characteristics, the authors have performed RSSI measurements using OpenSignal application [1] installed on an android based smart phone in this work. The measurements were performed in indoor environment in the Department of Electronics Engineering, AMU, Aligarh. The Wi-Fi access point is operating in 2.4 GHz band and is based on IEEE 802.11g specification. The UE is assumed to be static (no mobility) while the measurements are taken. RSSI is measured at distances of 2, 4, 6, 8 and 10 meters from the access point. At each location 150 RSSI samples were collected which corresponds to a duration of 15 minutes.

IV. RESULTS

Figures 1 and 2 show the variation of RSSI with time and probability distribution and at distances of 2 m and 4 m from the access point (AP) respectively. Looking at one of RSSI distributions as shown in Fig 1(a), it is observed that RSSI varies by about 12dB about its mean value on either side even though the UE is presumably static. This variation in RSSI which appears to have a log-normal distribution is attributed to environment factors such as number of obstacles, noise and interference from other transmitters in this band. Figure 3 shows a plot of mean of the RSSI measured as a function of distance. In this plot it is observed that the RSSI decreases exponentially with distance and is in accordance with the eq. (5).

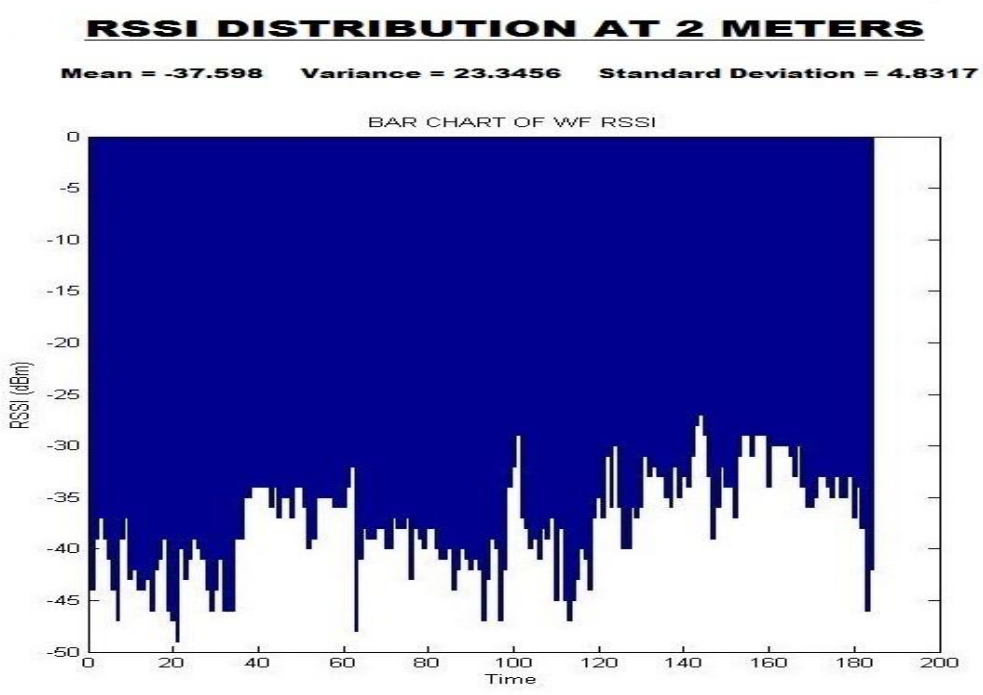

Figure 1(a): RSSI v/s time at 2 meters

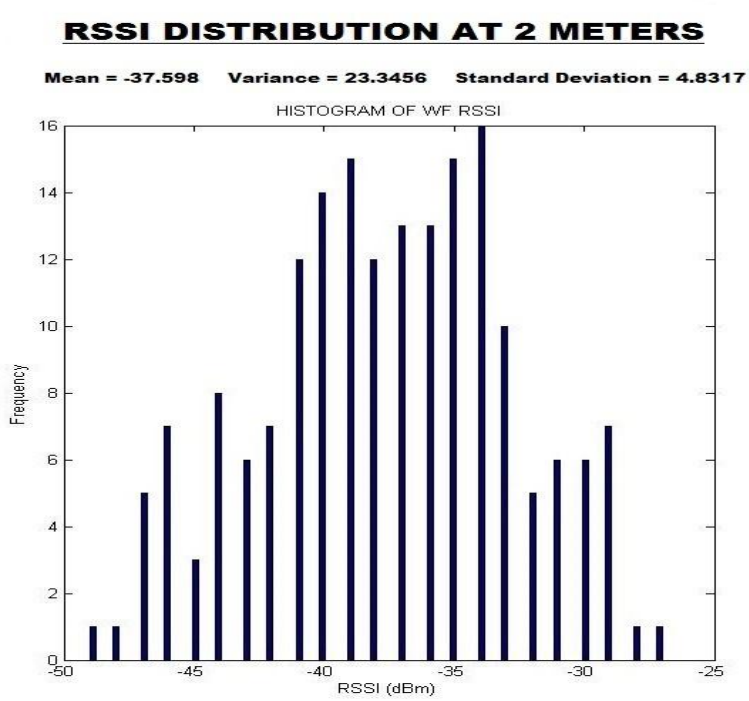

Figure 1 (b): RSSI histogram

.

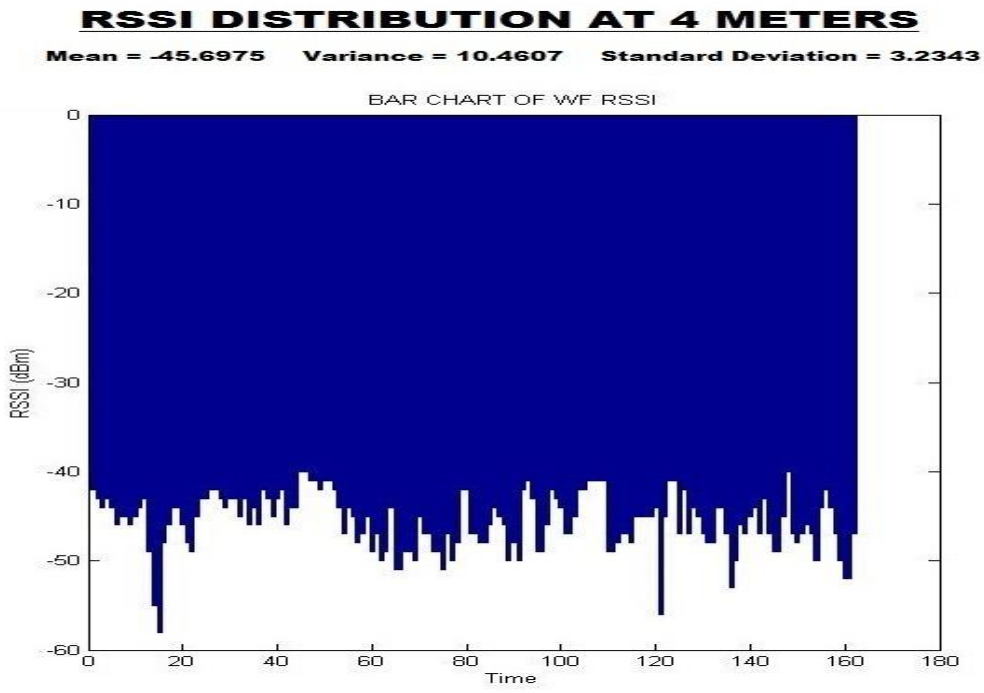

Figure 2(a): RSSI v/s time at 4 meters

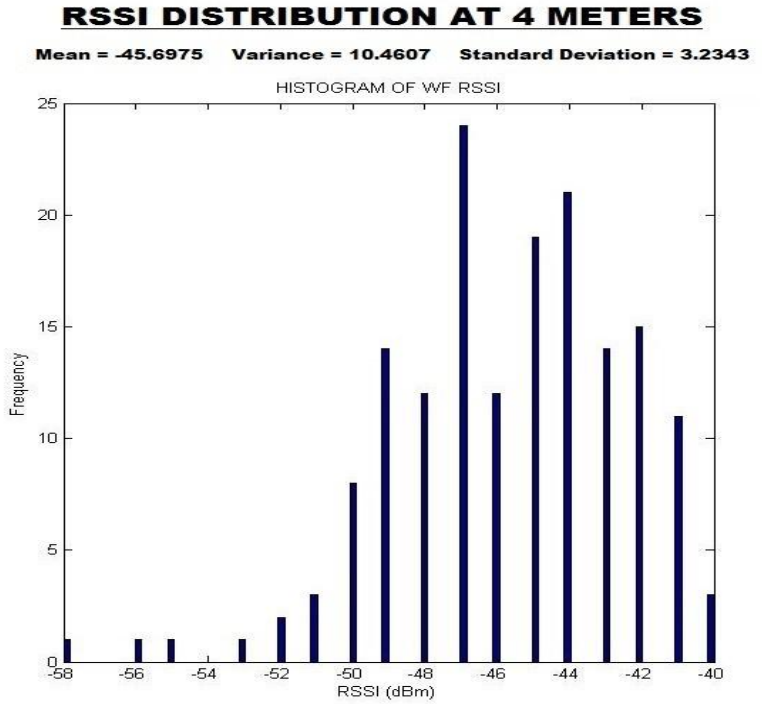

Figure 2(b): RSSI histogram

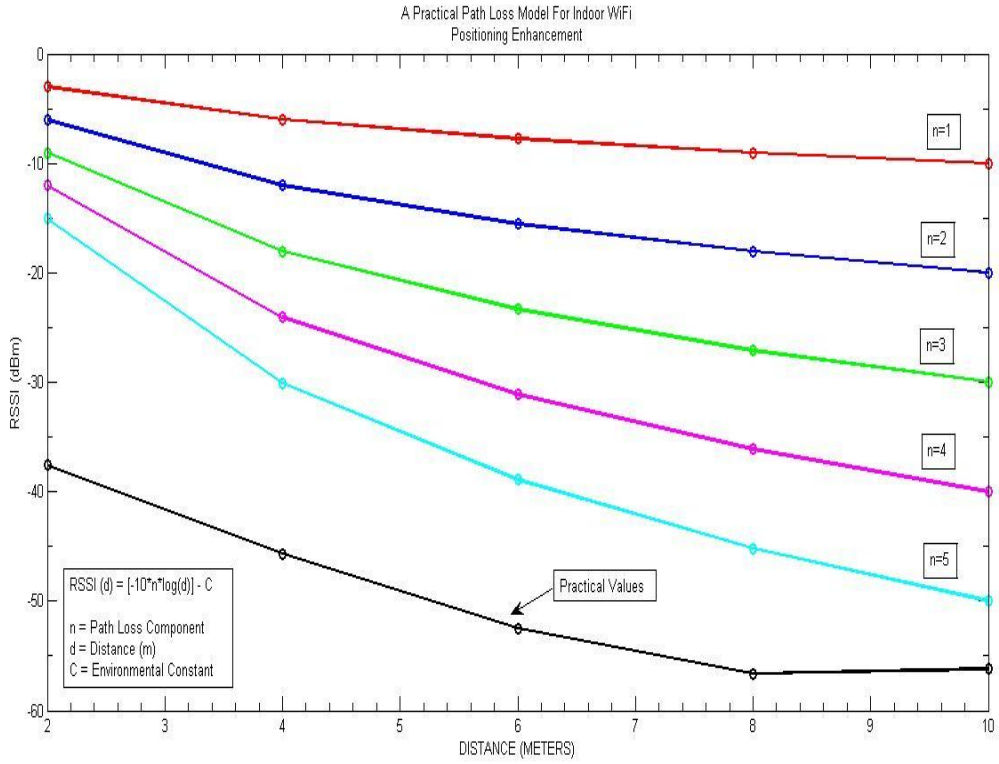

Figure 3: Mean RSSI v/s Distance

V. CONCLUSION

The authors performed RSSI measurements using crowd sourcing application. It is observed that RSSI decreases exponentially as the distance from access point increases. Crowd sourcing applications are economical means which can be used in academics and research community to perform real-time measurement of wireless signal parameters. The measurement studies carried out in this work suggest that the findings are close to theory with some calibration factor applied.

REFERENCES

[1] Open Signal Inc. http://opensignal.com

[2] X. Zhu and Y. Feng, "RSSI-based Algorithm for Indoor Localization," *Communications and Network*, Vol. 5 No. 2B, May 2013, pp. 37-42.

[3] Razvan Musaloiu-E. and Andreas Terzis, "Minimising the effect of WiFi interference in 802.15.4 wireless sensor networks", *International Journal on Sensor Network*, Vol.3, No. 1, December 2008, pp. 43-54.

[4] Atreyi Bose and Chuan Heng Foh, "A practical path loss model for indoor WiFi positioning enhancement," *2007 6th International Conference on Information, Communications & Signal Processing*, Singapore, 2007, pp. 1-5.

[5] J. Xu, W. Liu, F. Lang, Y. Zhang and C. Wang, "Distance Measurement Model Based on RSSI in WSN," *Wireless Sensor Network*, Vol. 2 No. 8, 2010, pp. 606-611.

[6] Checco, A., Lancia, C., & Leith, D. J. (2014). Using crowdsourcing for local topology discovery in wireless networks.CoRR, abs/1401.1551.http://arxiv.org/abs/1401.1551

[7] Mahesh K. Marina, Valentin Radu, and Konstantinos Balampekos. 2015. "Impact of Indoor-Outdoor Context on Crowdsourcing based Mobile Coverage Analysis". In *Proceedings of the 5th Workshop on All Things Cellular: Operations, Applications and Challenges* (All Things Cellular '15). ACM, New York, NY, USA, pp. 45-50.

[8] J. Cainey, B. Gill, S. Johnston, J. Robinson and S. Westwood, "Modelling download throughput of LTE networks," *39th Annual IEEE Conference on Local Computer Networks Workshops*, Edmonton, AB, 2014, pp. 623-628.

[9] A. Farshad, M. K. Marina and F. Garcia, "Urban WiFi characterization via mobile crowdsensing," *2014 IEEE Network Operations and Management Symposium (NOMS)*, Krakow, 2014, pp. 1-9.

[10] S. Depatla, A. Muralidharan and Y. Mostofi, "Occupancy Estimation Using Only WiFi Power Measurements," in *IEEE Journal on Selected Areas in Communications*, vol. 33, no. 7, July 2015, pp. 1381-1393.

On Energy Detection and Matched Filter Detection Techniques for Spectrum Sensing in Cognitive Radio

Hasan Mohsen AlJabali, Raaziyah Shamim and M Salim Beg
Department of Electronics Engineering, ZHCET, AMU, Aligarh
hassanaljabali45@gmail.com, raaziyah2007@gmail.com, salim.beg@amu.ac.in

Abstract

Cognitive radio networks, in interweave mode of operation, use dynamic spectrum access scheme. This approach necessitates sensing the spectrum to reliably determine the spectrum holes available for transmission and detect the existence of primary users. In this paper, energy detection and matched filter based methods are studied through Monte Carlo Simulations for spectrum sensing applications in cognitive radio networks. Statistical analysis for setting optimal detector thresholds and the average probability of detection for a given SNR are done for both techniques. The Receiver Operating Characteristics are plotted for various SNR for the above techniques.

I. INTRODUCTION

Due to high transmission data rate requirements to accommodate various types of multimedia in wireless communication, the pressure on spectrum resources is rising. The concurrent transmissions from high data rate applications are often difficult to achieve due to the inherent limitations of the available spectrum.The reason for spectrum scarcity is not so much because of the physical shortage of the radio channels but more due to the static allocation of spectrum to a particular organization or licensed users. This fixed spectrum assignment to licensed users prevents efficient spectrum utilization as the unused idle channels cannot be utilised by unlicensed secondary users.

Cognitive radio (CR) technology under development is a solution to allow spectrum to be reused more efficiently. The CR is aware of their radio environment and internal state, and can make decisions about their radio operating behaviour based on that information and predefined objectives. The CR automatically adjusts its operation to achieve the desired objectives of providing reliable communication suitable to application and efficient utilization of the radio spectrum[1].

The operating modes of a CR are broadly classified into three types: underlay,overlay and interweave modes.In underlay mode, both the secondary user(SU)and the primary user(PU)transmitdata on the same frequency channel, simultaneously. In this mode, the secondary user adjusts its transmission power such that the interference caused by it to the licensed primary user is below a certain predefined threshold. In practise, more than one secondary user may be transmitting the signal along with the primary user on the same frequency channel. In the overlay mode, the secondary cognitive transmitter is assumed to have aprioriinformation of the primary user's signal. The cognitive transmitter acts as a relay for the primary user by retransmitting the primary user's signal while simultaneously transmitting its own message [2], [3].In interweave mode of operation, the secondary user makes use of spectrum sensing to detect the presence of the primary user and transmits only if the primary user is absent. The interweave mode is also known as dynamic spectrum access mode. In this mode, the primary and secondary transmitters never transmit on the same sub-channel simultaneously and hence, never interfere with each other.

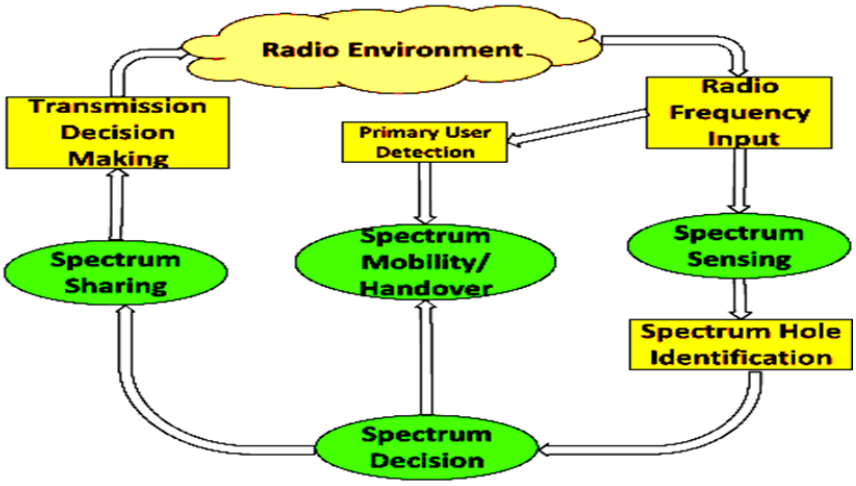

Figure1: Interweave mode in CR

In this paper, energy detection and matched filter based spectrum sensing techniques are studied for cognitive radio applications through Monte Carlo Simulations.The paper is organized as follows. In Section II, we discuss interweave mode of CR operation and spectrum sensing performance metrics.In Section III and Section IV, energy detection and matched filter based spectrum sensing techniques for cognitive radio applications are discussed and simulation results are shown. The paper is concluded in Section V.

II. INTERWEAVE MODE OF CR &SPECTRUM SENSING

In the interweave mode, the operation cycle of a CR comprises four major functions: spectrum sensing, spectrum decision, spectrum sharing and spectrum mobility. These functions are presented in Fig. 1. During spectrum sensing, a CR monitors the available spectrum bands to identify the white spaces. Once the spectrum hole is identified, the spectrum decision phase starts wherein the CR selects the most appropriate band for transmission as per the QoS needs of the application. Since there may be multiple secondary user transmitters trying to access the same frequency band, the transmission and decision making is coordinated among the cognitive radio nodes in the network through efficient resource allocation algorithms. When a primary user is detected to be transmitting on the selected spectrum band, the spectrum mobility function helps the frequency band vacation and handover to a new band with minimum degradation of quality.

In general, there are three signal detection approaches forspectrum sensingto detect the activity of the primary user: energy detection, matched filtering (coherentdetection), and feature detection. Critical factors in the design of thespectrum sensing techniques are selection of the probability of falsealarm threshold and probability of missed detection threshold as per application requirements, sensing duration&data throughput trade-off, abilityto differentiate interference from primary users and noise, computational complexity of spectrum sensing methods[4].

The probability of missed detection and probability of falsealarms are the key performance metrics for spectrum sensing techniques inCR. Sometimes the CR secondary user may wrongly declare that the primary user is absent, and the secondaryuser may transmit the data along with the primary user in the same frequency band, hence causing interference with the primary user. Such cases are called missed detection. The probability of themissed detection should be minimum possible and ideally zero.The failure to detect the primary user may have grave consequences for mission critical radio applications.

In the case of false alarm, the spectrum sensing unit may wrongly classify that theprimary user is present even though the primary user is actually absent.In such cases, the cognitive secondary user does not transmit in the sensed band and remains idle, and it results inreduced throughput for the secondary user. Hence, selectionof the thresholds for the probability of the false alarm is also critical to the overall throughput of the cognitive radio network.

Another major factor in the spectrum sensing is the sensing duration - datathroughputtrade-off. The accuracy of the spectrum sensingdepends on the amount of time or the number of symbols the receiver observes from theenvironment to take a decision. The accuracy of the decisionis proportional to the sensing time. However, with increase in sensingduration or window length, the secondary user's throughput reduces asit does not transmit the data during that time. Finding theright trade-off between the sensing time and throughput is hence required.

III. ENERGY DETECTION BASED SPECTRUM SENSING

In energy detection based spectrum sensing, the signal isdetected by comparing the output of the energy detector witha threshold which depends on the noise floor. The spectrum sensing is formulated by the followingbinary hypothesis testing problem,

$$H0: y(n) = w(n), \quad (1)$$

$$H1: y(n) = s(n) + w(n), \quad (2)$$

where,$w(n)$ is the additivewhite Gaussian noise (AWGN) sample, x(n) is the signal transmitted by PU, h(n) is the LTI channel impulse response, $s(n)$ = x(n)*h(n) is the PU transmitted signal component received by SU, y(n) is the total signal received and processed by SU, and n is the sampleindex. Note that $s(n) = 0$ when there is no transmission byprimary user. Hence, under hypothesisH_0, the PU is absent and y(n) consists only ofw(n). Under hypothesis H_1 the transmittedwireless signal x(n) is also present along with w(n). The decision metric or the test statistic for the energy detector is taken as

$$D(y)=\sum|y(n)|^2, \text{ summed over N samples} \quad (3)$$

The decision metric $D$is compared against a threshold $\lambda_E$to decide the occupancy of frequency band. The white noise is modelled as a zero-mean Gaussianrandom variable with variance σ^2_w, *i.e.* $w(n) = N(0, \sigma^2_w)$.For simplicity, the signal term is also modelled as azero-mean Gaussian variable, *i.e.* $x(n) = N(0, \sigma^2_x)$.Hence, the distribution of the test statistic or decision metric D can be modelled by the chi-square distributionwith $2N$ degrees offreedom $\chi^2_{2N,}$ where N is the length of a signal. To thisend, the following formulation is deduced,

$$D(y)|H_0 = (\sigma^2_w/2)\chi^2_{2N}, \quad (4)$$

$$D(y)|H_1 = [(\sigma^2_w+\sigma^2_x)/2]\chi^2_{2N}, \quad (5)$$

whereσ^2_x and σ^2_wdenote the variance of the transmitted signaland AWGN process, respectively, which are assumed to bestatistically independent. Based on this and given that theinstantaneous SNR is $\gamma = \sigma^2_x/\sigma^2_w$, the corresponding falsealarm probability P_{fa} and detection probability P_d measurescan be expressed as follows:

$$P_d = \text{Prob}\,(D(y)>\lambda_E|H_1) = Q[(\lambda_E - \sigma^2_w(1+\gamma)/(\sigma^2_w(1+\gamma)/\sqrt{N})] \quad (6)$$

$$P_{fa} = \text{Prob}\,(D(y)>\lambda_E|H_0) = Q[(\lambda_E - \sigma^2_w)/(\sigma^2_w/\sqrt{N})] \quad (7)$$

The receiver operating characteristic (ROC) curves areusedto explore the relation betweenthe sensitivity (probability of detection) and specificity (falsealarm rate) of the sensing method for variousthresholds, thus allowing the determination of an optimalthreshold.

Monte-carlo simulations are done for the above specified problem. Fig. 2 shows the ROC simulation curves for different SNRvalues. The number of usedsamples is set to 1000 in this figure, *i.e. N* = 1000 in (3). As thefigure shows, the performance of the threshold detectorimproves at high SNR values.Fig. 3 shows variation of average probability of detection *Pd* with SNR varying from -28dB to -10dBfor different values probability of false alarmPfain energy detector based spectrum sensing. The number of used samples is set to 1000 in this figure, *i.e. N* = 1000 in (3). Fig.4 shows the ROC curves for different values of N with SNR = −13 dB. From simulation results, it is observed that the energy detector performance improves considerably as the sensed signal and hence the sensing duration increases. But in practice, a trade-off needs to be done between the sensing duration and data throughput at the cognitive transmitter as the secondary user remains idle during sensing duration.

In design, P_{fa}should be kept as small as possible to avoid underutilization of transmission opportunities. The decisionthreshold $\lambda_E$should beselected for finding an optimum trade-off between $P_d$and P_{fa}.For optimal decision, prior knowledge of noise variance and detected signal powers is required at the cognitive radio. The signal powerchanges depending on transmission characteristics, transmission channel and the distance between the cognitive radio and primaryuser and hence is difficult to estimate.The performance of energy detector based sensing is limitedwhen the noise may not be stationary or its variance may not be known.In practise, noise level is estimateddynamically by separating the noise and signal subspacesusing algorithms such as multiple signal classification (MUSIC)[6].Noise variance is taken as the smallest eigenvalue of thereceived signal's autocorrelation. Then, the estimated noise variance valueis used to choose the threshold for satisfying a constant falsealarm rate. A smallerror in noise power estimation causes significant performance loss. Hence, a dynamic and reliable noise estimation method needs to be selected.The low computational and implementation complexities of energy detector based method also make it an attractive choice for spectrum sensing.

IV. MATCHED FILTER DETECTION BASED SPECTRUM SENSING

If a deterministic pattern (e.g., pilot, primary user signature sequence, preamble, or trainingsequence) of primary user signals is known at the cognitive radio, then the optimal detector is matched filter detector to maximize the probability of detection[7]. The spectrum sensing isformulated by the following binary hypothesis testing problem,

$$H0: y(n) = w(n), \quad (8)$$

$$H1: y(n) = s(n) + w(n), \quad (9)$$

where where, $w(n)$ is the additivewhite Gaussian noise (AWGN) sample, x(n) is the signal transmitted by PU, h(n) is the LTI channel impulse response, $s(n)$ = x(n)*h(n) is the PU transmitted signal component received by SU, y(n) is the total signal received and processed by SU , and n is the sampleindex.The decision metric or the test statistic for the matched filter detector is taken as

$$D(y)=(1/N)\mathrm{Re}\{\sum y(n)x^*(n)\}, \text{ summed over N samples} \quad (10)$$

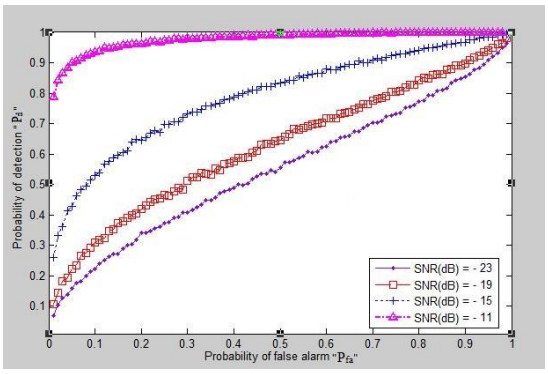

Figure 2: ROCfor energy detector based spectrum sensing for varying SNR

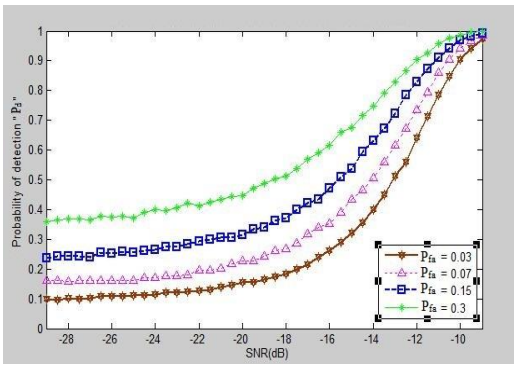

Figure 3:*P*robability of detection $P_d$vs SNR curvefor different values probability of false alarmP_{fa}in energy detector based spectrum sensing

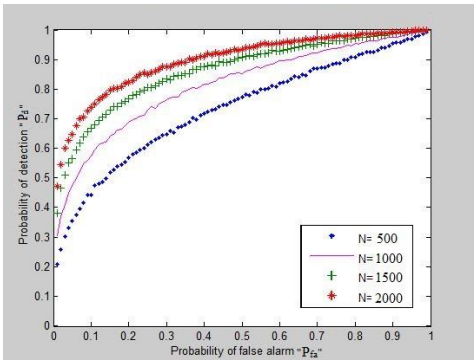

Figure 4:ROC of energy detector based spectrum sensing forvaryingsensing duration N &SNR = −13dB.

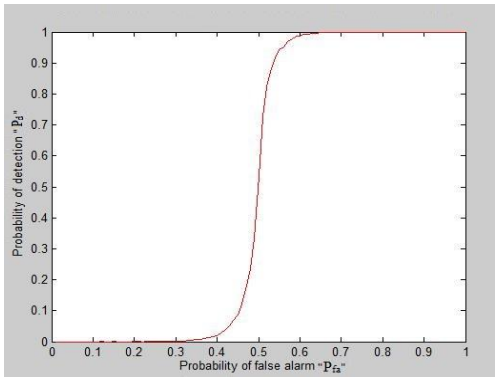

Figure 5:ROC for matched filter based spectrum sensing for SNR= -20dB

where * sign denotes conjugate operation. The decision metric *D*is compared against a threshold $\lambda_E$to decide the occupancy of frequency band . The white noise is modeled as a zero-mean Gaussianrandom variable with variance σ^2_w, *i.e.* $w(n) = N(0, \sigma^2_w)$.The signal sequence termx(n) is known at the receiver.Hence, the distribution of the test statistic or decision metric D can be modeled by linear combination ofgaussiandistributed signals and hence a Gaussian distribution. Based on this and given that the energy of the signal transmitted by primary user is E, by Neyman-Pearson criteria, the corresponding falsealarm probability P_{fa} and detection probability P_d measurescan be expressed as follows:

$$P_d = \text{Prob}\,(D(y) > \lambda_E | H_1) = Q[(\lambda_E - E)/\sqrt{(E\sigma^2_w)}] \quad (11)$$

$$P_{fa} = \text{Prob}\,(D(y) > \lambda_E | H_0) = Q[\lambda_E/\sqrt{(E\sigma^2_w)}] \quad (12)$$

Monte-Carlo simulations are done for the above specified problem. Fig. 5 shows the ROC simulation curves for different SNRvalues. The number of used samples is set to 1000 in this figure, *i.e.* $N = 1000$ in(10).

It is observed that matched filtering needs shorterduration to achieve a certain probability of false alarmor probability of missed detection as compared to energy detection basedmethod. In fact, the requirednumber of samples grows as $O(1/SNR)$ for a targetprobability of false alarm at low SNRs for matchedfiltering[8]. However, matched-filtering requires priorknowledge of the primary users signal features such asbandwidth, modulating frequency, modulation order and type,pulse shape, frame format, andaccurate timing and carrier-frequency synchronization.Moreover, simultaneous existence of primary users following different standards, or signalling schemes in the CR network requires theCR node to

have dedicated receivers for each primary user.Consequently, the implementationcomplexity and power consumption of sensing unit is large.

V. CONCLUSIONS

The performance of energy detector and matched filter based spectrum sensing techniques has been assessed in this paper. The performance of both the detectors improves with increasing SNR and sensing duration. The performance of matched filter is better than energy detector for a given sensing duration and SNR. The implementation complexity and power consumption is larger in matched filter based detection.

REFERENCES

[1] E. Biglieri, A. J. Goldsmith, L. J. Greenstein, N. B. Mandayam, and H. V. Poor, *Principles of cognitive Radio*. Cambridge, U.K.: Cambridge Univ. Press, 2012.

[2] S. Haykin, "Cognitive radio: brain-empowered wireless communications,"IEEE Journal on Selected Areas in Communications, vol. 23,no. 2, pp. 201–220, 2005.

[3] S. Geirhofer, L. Tong, and B. Sadler, "Dynamic spectrum access in thetime domain: modeling and exploiting white space," *IEEE CommunMag.*, vol. 45, no. 5, pp. 66–72, May 2007.

[4] T. Yucek and H. Arslan, "A survey of spectrum sensingalgorithms for cognitive radio applications," IEEECommunications Surveys & Tutorials, vol. 11, no. 1, pp. 116– 130, March 2009.

[5] E. Axell, G. Leus, E. Larsson, and H. Poor, "Spectrum Sensing forCognitive Radio : State-of-the-Art and Recent Advances," IEEE SignalProcessing Magazine, vol. 29, no. 3, pp. 101–116, 2012.

[6] H. Urkowitz, "Energy detection of unknown deterministic signals," *Proc.of the IEEE*, vol. 55, no. 4, pp. 523–531, Apr. 1967.

[7] Alan V. Oppenheim and George C. Verghese,"Class Notes for 6.011: Introduction to Communication, Control, and Signal Processing", Spring 2010 at Massachusetts Institute of Technology, pp. 247–251.

[8] R. Tandra and A. Sahai, "Fundamental limits on detection in low SNRunder noise uncertainty," in *Proc. IEEE Int. Conf. Wireless Networks,Commun. and Mobile Computing*, vol. 1, Maui, Hawaii, June 2005, pp.464–469.

Characterizing Temporal Variations in Wireless Channels

Priyadarshi Mukherjee, Deepak Mishra, and Swades De

***Abstract*—Characterization of the temporally varying wireless channel can lead to energy-efficient dynamic access of the spectrum by exploiting the temporal correlation present in the channel. In this paper, we characterize the temporal variation of the channel using the method of finite mixture of Gaussian distributions. Unlike the classical Gaussian mixture model, the proposed characterization is totally robust and model free; it depends on the current state of the channel and its available statistics. The validation of the proposed characterization has been done through both analysis and extensive Monte Carlo simulations.**

***Index Terms*—Fading channel, Temporal characterization, Rician distribution, Non-central χ^2 distribution, Gaussian mixture model**

I. Introduction and Background

In the recent years, there has been explosive growth of high throughput intensive applications in wireless communication. As estimated by Cisco, global internet traffic will reach 21 GB per capita by 2020 from 7 GB per capita in 2015 [1]. In order to support this massive amount of Internet traffic, efficient characterization and modeling of the wireless channel is very important.

The temporally varying wireless channel, if efficiently characterized, can be used for enhancing the performance of all the communication systems that employ channel state information (CSI). However to the best of our knowledge, the aspect of temporal characterization of wireless channel has not been sufficiently studied yet. Temporal characterization of wireless channel can be used to enhance spectral efficiency as well as energy efficiency. It can be integrated with many modern communication techniques, such as, multiple-input multiple-output (MIMO) and orthogonal frequency-division multiple access (OFDMA), to further enhance spectral efficiency by allowing the heterogeneous users present in the network to access the channel [2]. Hence we propose a novel characterization of the temporally varying wireless channel.

For characterizing the temporal variation of the channel, we use the method of finite mixture of distributions [3] in this paper. The temporal variation of the channel is modeled as a Gaussian Mixture Model (GMM) based on its present state and available statistics. The proposed characterization is of minimal complexity unlike the classical form of GMM that uses the high complexity expectation-minimization (EM) algorithm, coined by Dempster *et al.* [4], for the purpose of parameter estimation. The proposed GMM is more robust, totally model free, and has an analytical closed-form unlike the classical one.

In this context of proposing a new characterization of the wireless channel, the considered fading model of the channel is a very important factor. Though Rayleigh fading model is a reasonable assumption for the fading experienced in most of the wireless scenarios, it does not consider the presence of the line-of-sight (LOS) factor if present. A much more generalized fading model is the Rician model. This Rician model is a more generalized fading model that not only has the Rayleigh model as one of its limiting cases, but it is also able to efficiently model wireless scenarios with a strong LOS component [5]. Hence in this paper, we consider Rician fading for characterizing the wireless channel. It is important to observe that though in this work the Rician fading model has been considered, the proposed model is universal and hence, it can be extended to any underlying fading distribution without any loss of generality.

P. Mukherjee, D. Mishra, and S. De are with the Department of Electrical Engineering and Bharti School of Telecommunication, Indian Institute of Technology Delhi, New Delhi, India (e-mail: {priyadarshi.mukherjee, deepak.mishra, swadesd}@ee.iitd.ac.in).

II. System Model and Temporal Variation of Wireless Channel

A. System Model

We consider communication between a node pair in a mobile environment. The system is assumed slotted, with slot duration T_p sec. Also, the channel remains invariant within a slot duration but may vary from slot to slot [6].

Depending on the received signal quality, the receiver (Rx) sends the useful CSI to the transmitter (Tx) along with the useful channel information, such as Doppler frequency f_D; its estimation from the received signal are known from [7], [8]. We assume the CSI feedback to be error-free and the feedback delay to be negligible.

f_D corresponding to the relative velocity v of the Rx is $f_D \cong \frac{vf_c}{c}$, where f_c is the carrier frequency and c is the velocity of light in vacuum. The product $f_D T_p$ signifies the temporal variation rate of the wireless channel. From [9] we know that small value of $f_D T_p$ (< 0.1) indicates correlated "slow" fading channel, whereas a large value of $f_D T_p$ (> 0.2) implies that the two samples of the channel are almost independent, i.e., "fast" fading.

B. Wireless Channel and its Temporal Variation

If wireless data transmission is taking place in a typical wide-sense stationary (WSS) Rician fading scenario [10] with

signals of constant transmission power P, the received signal y at Rx is:

$$y = \sqrt{P}\, h\, x + n, \tag{1}$$

where x is the signal transmitted, h is the time varying small-scale channel gain, and n is independent Additive White Gaussian Noise (AWGN) at Rx with zero mean and variance σ_o^2. Channel gain h is generally modeled as a complex random variable (RV) and can be written as $h = |h|e^{j\phi}$ with ϕ taking values between $-\pi$ and π depending on the distribution of h.

We further assume that $\mathbb{E}[x] = 0$, $\mathbb{E}[x^2] = 1$, $\mathbb{E}[h] = 0$, and $\mathbb{E}[|h|^2] = 1$, where $\mathbb{E}[\cdot]$ denotes the expectation operator. Assuming non-coherent demodulation at Rx [11], the received signal envelope $\theta = \sqrt{P}|h|$. Moreover, as Rx uses non-coherent demodulation, we are not concerned about the phase ϕ of h [12]. The probability distribution function (PDF) of θ is expressed as [13]

$$f_\theta(\alpha, \mu_\theta, K) = \frac{2(1+K)\alpha e^{-K}}{\mu_\theta} e^{-\frac{(1+K)\alpha^2}{\mu_\theta}} I_o\left[2\alpha\sqrt{\frac{K(1+K)}{\mu_\theta}}\right], \quad \alpha \geq 0. \tag{2}$$

Here $\mu_\theta = \mathbb{E}[\theta]$, K is the Rice factor, and $I_o(\cdot)$ denotes the zero-order modified Bessel function of the first kind. From [14] we know that the time-derivative of θ, i.e., $\dot{\theta} \triangleq \frac{d\theta}{dt}$ is a zero mean Gaussian RV. In other words, we have $\dot{\theta} \sim \mathcal{N}(0, \dot{\sigma}_\theta)$, where

$$\dot{\sigma}_\theta = \frac{\pi f_D}{(K+1)}\sqrt{P(2K+1)}. \tag{3}$$

As θ is Rician in nature, the received signal-to-noise ratio (SNR) $Z = \frac{P|h|^2}{\sigma_o^2}$ is a non-central χ^2 RV with two degrees of freedom. The PDF of Z is [13]:

$$f_Z(z, \mu_Z, K) = \frac{(1+K)e^{-K}}{\mu_Z} e^{-\frac{(1+K)z}{\mu_Z}} I_o\left[2\sqrt{\frac{K(1+K)z}{\mu_Z}}\right], \quad z \geq 0. \tag{4}$$

Here $\mu_Z = \mathbb{E}[Z]$. Just like $\dot{\theta}$, $\dot{Z} \triangleq \frac{dZ}{dt}$ is also a zero mean Gaussian RV, i.e., $\dot{Z} \sim \mathcal{N}(0, \dot{\sigma}_Z)$. The standard deviation of $\dot{Z}$, i.e., $\dot{\sigma}_Z$ can be obtained as follows.

Proposition 1. *The standard deviation of $\dot{Z}$ in a Rician fading scenario is*

$$\dot{\sigma}_Z = \frac{2P}{\sigma_o^2}\frac{\pi f_D}{(K+1)}\sqrt{2K+1} \tag{5}$$

Proof. With $\mathrm{Var}(\cdot)$ as the variance operator, $\mathrm{Var}(\dot{Z})$ is given by:

$$\mathrm{Var}(\dot{Z}) = \mathrm{Var}\left(\frac{d}{dt}\left\{\frac{P|h|^2}{\sigma_o^2}\right\}\right) = \mathrm{Var}\left(\frac{d}{dt}\left\{\frac{\theta^2}{\sigma_o^2}\right\}\right) \tag{6}$$

$$= \mathrm{Var}\left(\frac{2}{\sigma_o^2}\theta\dot{\theta}\right) = \frac{4}{\sigma_o^4}\mathrm{Var}(\theta\dot{\theta}). \tag{7}$$

From [15] we know that $\dot{\theta}$ and θ are independent. Using the definition of variance for product of two independent RV, we get $\mathrm{Var}(\dot{Z}) = \frac{4}{\sigma_o^4}\left\{\mathbb{E}[\theta^2]\mathbb{E}[\dot{\theta}^2] - \mathbb{E}[\theta]^2\mathbb{E}[\dot{\theta}]^2\right\}$. From the definition of $\dot{\theta}$, we have $\mathbb{E}[\dot{\theta}] = 0$. Accordingly the above equation gets reduced as $\mathrm{Var}(\dot{Z}) = \frac{4}{\sigma_o^4}\left\{\mathbb{E}[\theta^2]\mathbb{E}[\dot{\theta}^2]\right\} = \frac{4P^2}{\sigma_o^4}\left(\frac{\pi f_D}{K+1}\right)^2(2K+1)$. Hence we get,

$$\dot{\sigma}_Z = \sqrt{\mathrm{Var}(\dot{Z})} = \frac{2P}{\sigma_o^2}\frac{\pi f_D}{(K+1)}\sqrt{2K+1} \tag{8}$$

□

C. Gaussian Modeling of Received Signal Envelope and SNR

If the received signal envelope θ at time t is denoted by $\theta(t)$, then θ in the next time slot, i.e., after time T_p, is expressed as

$$\theta(t+T_p) = \theta(t) + \dot{\theta}T_p, \quad \text{where} \tag{9}$$

$\dot{\theta}$ is a zero mean Gaussian RV as defined in (3), i.e., $\dot{\theta} \sim \mathcal{N}(0, \sigma_\theta)$. Accordingly we define another RV $\theta_1 (= \dot{\theta} \cdot T_p)$ that signifies temporal variation of the fading envelope in next slot. It is obvious that $\theta_1 \sim \mathcal{N}(0, \dot{\sigma}_{\theta_1})$, where from (3) we get $\dot{\sigma}_{\theta_1} = \dot{\sigma}_\theta \cdot T_p = \frac{\pi f_D T_p}{(K+1)}\sqrt{P(2K+1)}$. Thus for any arbitrary $\theta(t) = \theta_0$, $\theta(t+T_p)$ is a non-zero mean Gaussian RV with mean $= \theta_0$ and variance $= \dot{\sigma}_{\theta_1}^2$, i.e., $\theta(t+T_p) \sim \mathcal{N}(\theta_0, \dot{\sigma}_{\theta_1})$. This implies that $\theta(t+T_p) \in (-\infty, +\infty)$. But as $\theta(t+T_p)$ is the received signal envelope at the Rx, $\theta(t+T_p) \geq 0$ and hence, $\theta(t+T_p) \in [-\theta_0, +\infty)$. In other words, $\theta(t+T_p)$ does not follow a Gaussian distribution but a truncated Gaussian distribution, i.e.,

$$\theta(t+T_p) \sim \frac{1}{1-\Phi\left(-\frac{\theta_0}{\dot{\sigma}_{\theta_1}}\right)}\mathcal{N}(\theta_0, \dot{\sigma}_{\theta_1}), \quad \theta_1 \geq -\theta_0 \tag{10}$$

Here $\Phi(x) = \int_{-\infty}^{x} \frac{1}{\sqrt{2\pi}} e^{-\frac{t^2}{2}}\, dt$ is the cumulative distribution function of standard univariate normal distribution.

We observe that apparently our claim of θ_1 being truncated Gaussian appears contradictory to [16], which is actually not so. [16] and other works use isotropic scattering phenomenon to claim zero mean Gaussian distribution with implicit short tails or very small change over an infinitely small slot duration of investigation. Also to the best of our knowledge, none of the existing works investigated the temporal characterization of $\theta(t)$ and hence the authors did not feel the need for truncated consideration. However as the magnitude of envelope of a signal cannot be negative, truncation is required in this context of temporally characterizing $\theta(t)$; this truncation requirement is generally met implicitly due to very small T_p and short tails due to very small variance $\dot{\sigma}_{\theta_1}$.

Similarly, θ after 2 time slots is $\theta(t+2T_p) = \theta_0 + \theta_2$, where θ_2 is also a zero mean truncated Gaussian random variable like θ_1 with $\dot{\sigma}_{\theta_2} = 2\dot{\sigma}_{\theta_1}$; the difference being that θ_2 resembles the temporal variation of θ over the next two slots, whereas θ_1 denotes temporal variation over next one slot only. Hence,

$$\theta(t+2T_p) \sim \frac{1}{1-\Phi\left(-\frac{\theta_0}{\dot{\sigma}_{\theta_2}}\right)}\mathcal{N}(\theta_0, \dot{\sigma}_{\theta_2}), \quad \theta_2 \geq -\theta_0 \tag{11}$$

Remark 1. *Generalizing this concept over next N slots, we can say that if $\theta(t) = \theta_0$, then*

$$\theta(t + NT_p) \sim \frac{1}{1 - \Phi\left(-\frac{\theta_0}{\dot{\sigma}_{\theta_N}}\right)} \mathcal{N}(\theta_0, \dot{\sigma}_{\theta_N}), \quad \theta_N \geq -\theta_0. \tag{12}$$

Here $\dot{\sigma}_{\theta_N} = N\dot{\sigma}_{\theta_1} = \frac{N\pi f_D T_p}{(K+1)}\sqrt{P(2K+1)}$.

Extending this concept to the received SNR, we can make an analogous statement.

Remark 2. *If the received SNR at time t is $Z(t) = Z_0$, then*

$$Z(t + NT_p) \sim \frac{1}{1 - \Phi\left(-\frac{Z_0}{\dot{\sigma}_{Z_N}}\right)} \mathcal{N}(Z_0, \dot{\sigma}_{Z_N}) \quad Z_N \geq -Z_0. \tag{13}$$

Here $\dot{\sigma}_{Z_N} = N\dot{\sigma}_{Z_1}$, where $\dot{\sigma}_{Z_1} = \dot{\sigma}_Z \cdot T_p$. Thus from (8) we finally get

$$\dot{\sigma}_{Z_N} = \frac{NP}{\sigma_o^2} \frac{2\pi f_D T_p}{(K+1)} \sqrt{2K+1}. \tag{14}$$

III. Proposed Gaussian Mixture Model

From the last section we see that if $\theta(t) = \theta_0$, then the probable received signal envelope after N slots thereafter can be characterized as a truncated Gaussian RV with its mean being θ_0 and variance $\frac{N\pi f_D T_p}{(K+1)}\sqrt{P(2K+1)}$. Thus it can be observed that the mean of $\theta(t + NT_p)$ is a *deterministic* quantity obtained from the CSI sent by Rx to Tx and the variance is obtained from the statistical properties of the channel.

It is important to note here that in general, mean, variance or any moment of a RV are deterministic quantities that define the statistics of the RV. But in this case it is not so; here the variance is obtained from the statistics of the RV while CSI sent by the Rx to Tx acts as the mean. Hence, the proposed characterization of the channel is *hybrid* in nature. We use this very interesting property of θ to model its variation over next ζ slots. Hence, the present state of the channel, i.e., $\theta(t)$ plays a very important role in this characterization.

Since for a given θ_0 the variation of θ in each of the next ζ slots follows a scaled Gaussian distribution, we propose to model the entire variation of θ over the next ζ slots in terms of a Gaussian Mixture Model (GMM).

According to the theory of classical GMM [3], any arbitrary probability distribution $f_A(a)$ can be expressed as a convex combination of finite number of Gaussian distributions $f_{B_i}(b_i)$ in the following form

$$f_A(a) = \sum_{i=1}^{\zeta} \pi_i f_{B_i}(b_i), \tag{15}$$

where $f_{B_i}(b_i)$ is the i^{th} component Gaussian distribution, i.e., $f_{B_i}(b_i) = \frac{1}{\sqrt{2\pi}\sigma_{b_i}} e^{-\frac{(b_i - \mu_{b_i})^2}{2\sigma_{b_i}^2}}$ and π_i is its corresponding weight with the constraints $0 \leq \pi_i \leq 1$ and $\sum_{i=1}^{\zeta} \pi_i = 1$. The optimal values of the unknown parameters, i.e., π_i, μ_{b_i}, and σ_{b_i} $\forall$ $i = 1(1)\zeta$ are generally obtained by the iterative Expectation-Maximization (EM) algorithm [17]. The run time complexity of the EM algorithm is $O(K^2N)$, where K is the number of number of Gaussian components in the GMM and N is the number of size of the data set on which GMM is being implemented to obtain the optimal set of parameters. Accordingly we propose Theorem 1 and 2 that characterize θ and Z respectively in terms of GMM as follows.

Theorem 1. *If Ψ denotes the temporal variation of θ over the next ζ slots from time t, it can be characterized in terms of $\theta(t) = \theta_0$ by a GMM whose PDF is:*

$$f_\Psi(\beta \mid \theta(t) = \theta_0) = \begin{cases} \frac{1}{\zeta} \sum_{i=1}^{\zeta} \frac{1}{1 - \Phi\left(-\frac{\theta_0}{\dot{\sigma}_{\theta_i}}\right)} \mathcal{N}(\theta_0, \dot{\sigma}_{\theta_i}) & \beta \geq -\theta_0 \\ 0 & \textit{elsewhere.} \end{cases} \tag{16}$$

Here $\dot{\sigma}_{\theta_i} = \frac{i.\pi f_D T_p}{(K+1)}\sqrt{P(2K+1)}$.

Proof. In order to prove Theorem 1, we first prove a simpler version of the theorem, i.e., using $\zeta = 1$ and then generalize the proof for any arbitrary ζ. When $\zeta = 1$, (16) gets modified as

$$\theta(t + T_p) = \begin{cases} \theta(t) + \frac{1}{1 - \Phi\left(-\frac{\theta(t)}{\dot{\sigma}_{\theta 1}}\right)} \mathcal{N}(\theta(t), \dot{\sigma}_{\theta 1}) & \theta_1 \geq -\theta(t) \\ 0 & \text{elsewhere.} \end{cases} \tag{17}$$

From Remark 1 we know that if the received signal envelope θ at time t and $t + T_p$ be $\theta(t)$ and $\theta(t + T_p)$ respectively, then

$$\theta(t + T_p) = \theta(t) + \theta_1, \quad \text{where} \tag{18}$$

θ_i follows a truncated Gaussian distribution, i.e.,

$$f_{\theta_1}(\varphi) = \frac{1}{1 - \Phi\left(-\frac{\theta(t)}{\dot{\sigma}_{\theta 1}}\right)} \mathcal{N}(0, \dot{\sigma}_{\theta 1}), \quad \varphi \geq -\theta(t). \tag{19}$$

Here $\dot{\sigma}_{\theta 1} = \frac{\pi f_D T_p}{(K+1)}\sqrt{P(2K+1)}$. As T_p is practically in the order of 10^{-6} secs, this results in $\dot{\sigma}_{\theta 1} \ll 1$.

Thus if we are able to show that the sum of a Rician RV and a Gaussian RV tends to a Rician RV under the $\dot{\sigma}_{\theta 1} \ll 1$ assumption, then the theorem is proved.

We know that the probability distribution of the sum of two independent RVs is obtained by the convolution of their respective probability distributions. As the Rician distribution includes a Bessel function, it is difficult to obtain a closed form expression for the convolution. But it can be seen from Fig. 1 that the theorem holds for Rician fading scenario. In order to have an analytical proof of the same, we consider a special case of Rician fading, i.e., Rayleigh fading scenario. The corresponding probability distribution of $\theta(t)$ is obtained by putting $K = 0$ in (2), i.e.,

$$f_{\theta(t)}(\theta) \triangleq f_\theta(\alpha, \mu_\theta, 0) = \frac{2\theta}{\mu_\theta} e^{-\frac{\theta^2}{\mu_\theta}}, \quad \theta \geq 0. \tag{20}$$

Thus we get $f_{\theta(t+T_p)}(\theta) = (f_{\theta(t)} * f_{\theta_1})(\theta)$. Finally after convolution we get

$$f_{\theta(t+T_p)}(\theta) = A(\theta) + B(\theta), \quad \text{where} \tag{21}$$

$$A(\theta) = \sqrt{\frac{2}{\pi}}\dot{\sigma}_{\theta 1} e^{-\frac{\theta^2}{2\mu_\theta}} \frac{e^{\frac{\theta^2}{2}\left\{\frac{1}{\mu_\theta}-\frac{1}{\dot{\sigma}^2_{\theta 1}}\right\}}-1}{(\mu_\theta+\dot{\sigma}^2_{\theta 1})\left[1-\Phi\left(-\frac{\theta}{\dot{\sigma}_{\theta 1}}\right)\right]} \quad \text{and}$$

$$B(\theta) = \frac{\theta\sqrt{\mu_\theta} e^{-\frac{\theta^2}{2\left(\mu_\theta+\dot{\sigma}^2_{\theta 1}\right)}}}{\left(\mu_\theta+\dot{\sigma}^2_{\theta 1}\right)^{1.5}\left[1-\Phi\left(-\frac{\theta}{\dot{\sigma}_{\theta 1}}\right)\right]}$$

$$\times\left(\text{erf}\left[\frac{\theta\sqrt{\mu_\theta}}{\dot{\sigma}_{\theta 1}\sqrt{2\left(\mu_\theta+\dot{\sigma}^2_{\theta 1}\right)}}\right]+\text{erf}\left[\frac{\theta\dot{\sigma}_{\theta 1}}{\sqrt{2\mu_\theta\left(\mu_\theta+\dot{\sigma}^2_{\theta 1}\right)}}\right]\right).$$

Here $\text{erf}(x) = \frac{2}{\sqrt{\pi}}\int_0^x e^{-t^2}dt$. From the definition of erf function we know that

$$\text{erf}(x) = \begin{cases} -1 & x \le -3 \\ 0 & x = 0 \\ 1 & x \ge 3 \end{cases} \tag{22}$$

As $\dot{\sigma}_{\theta 1} \ll 1$, we can approximate $A(\theta) \approx 0$. For the same reason, the first erf function of $B(\theta)$ has a very high argument while its second erf function has a very small argument. Hence using (22) in $B(\theta)$ we get

$$\lim_{\dot{\sigma}_{\theta 1}\to 0}\text{erf}\left[\frac{\theta\sqrt{\mu_\theta}}{\dot{\sigma}_{\theta 1}\sqrt{2\left(\mu_\theta+\dot{\sigma}^2_{\theta 1}\right)}}\right] = 1 \quad \text{and} \tag{23}$$

$$\lim_{\dot{\sigma}_{\theta 1}\to 0}\text{erf}\left[\frac{\theta\dot{\sigma}_{\theta 1}}{\sqrt{2\mu_\theta\left(\mu_\theta+\dot{\sigma}^2_{\theta 1}\right)}}\right] = 0. \tag{24}$$

Further, $\dot{\sigma}_{\theta 1} \ll 1$ also results in $1-\Phi\left(-\frac{\theta}{\dot{\sigma}_{\theta 1}}\right) \approx 0.5$. Considering all these approximations as stated above, (21) gets simplified as

$$f_{\theta(t+T_p)}(\theta) \approx \frac{2\theta}{\mu_\theta} e^{-\frac{\theta^2}{2\mu_\theta}}. \tag{25}$$

As we can see that this is nothing but the Rayleigh distribution. This proves the theorem for $\zeta = 1$. This proof can be easily extended to the $\zeta > 1$ case under the $\dot{\sigma}_{\theta i} \ll 1$ assumption, as we know that:

1) Sum of multiple independent Gaussian RVs is always a Gaussian RV.
2) Sum of a Gaussian RV and a Rayleigh RV tends to a Rayleigh RV (proved above).

This completes the proof. □

We use the concept of *equal weightage* in Theorem 1, i.e., "$\frac{1}{\zeta}$" in the theorem implies that we are giving equal weightage to all of the next ζ slots. This is because we are interested in characterizing the variation of θ over the next ζ slots without giving any additional priority or being biased to any of these ζ slots. It is important to note that in this proposed modeling of the variation of θ over the next ζ slots, we do not use the high-complexity EM algorithm in order to estimate the parameters of our GMM. The run time complexity of the proposed characterization is $O(1)$, i.e., it always executes in constant time irrespective of the data quantity.

Thus we can see that the proposed characterization is of minimal complexity compared to classical GMM. It is much more robust, model free, and most important of all, has an analytical closed-form that does not require the EM algorithm or rather any other iterative algorithm for its parameter estimation. It solely depends on the current state and statistics of the channel. Similarly, we also characterize the variation of received SNR in next ζ slots in terms of a GMM as follows.

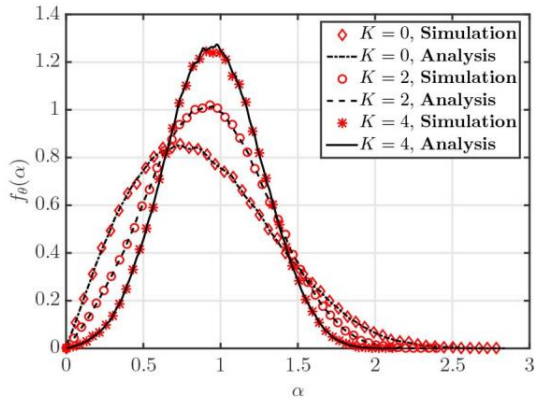

Fig. 1. Theorem 1 verification for various Rice factor K. System parameters: node velocity= 6 kmph, slot duration $T_p = 500$ μs, and $\zeta = 10$.

Theorem 2. *If Ω denotes the temporal variation of Z over the next ζ slots from time t, then it can represented in terms of $Z(t) = Z_0$ by a GMM, whose PDF is:*

$$f_\Omega(\gamma \mid Z(t) = Z_0) = \begin{cases} \frac{1}{\zeta}\sum_{j=1}^{\zeta}\frac{1}{1-\Phi\left(-\frac{Z_0}{\dot{\sigma}_{Z_j}}\right)}\mathcal{N}(Z_0, \dot{\sigma}_{Z_j}) & \gamma \ge -Z_0 \\ 0 & \textit{elsewhere.} \end{cases} \tag{26}$$

Here $\dot{\sigma}_{Z_j} = \frac{jP}{\sigma_o^2}\frac{2\pi f_D T_p}{(K+1)}\sqrt{2K+1}$.

Proof. In order to prove Theorem 2, we follow the same path as in Theorem 1, i.e., first we prove a simpler version of the theorem ($\zeta = 1$) and then generalize the proof for any arbitrary ζ. When $\zeta = 1$, (26) gets modified as

$$Z(t+T_p) = \begin{cases} Z(t) + \frac{1}{1-\Phi\left(-\frac{\theta(t)}{\dot{\sigma}_{Z1}}\right)}\mathcal{N}(\theta(t), \dot{\sigma}_{Z1}) & Z_1 \ge -Z(t) \\ 0 & \text{elsewhere.} \end{cases} \tag{27}$$

From Remark 2 we know that if the received SNR Z at Rx at time t and $t+T_p$ be $Z(t)$ and $Z(t+T_p)$ respectively, then

$$Z(t+T_p) = Z(t) + Z_1, \quad \text{where} \tag{28}$$

Z_1 follows a truncated Gaussian distribution, i.e.,

$$f_{Z_1}(\lambda) = \frac{1}{1-\Phi\left(-\frac{Z(t)}{\dot{\sigma}_{Z1}}\right)}\mathcal{N}(0, \dot{\sigma}_{Z1}), \quad \lambda \ge -Z(t). \tag{29}$$

Here, $\dot{\sigma}_{Z1} = \frac{P}{\sigma_o^2}\frac{2\pi f_D T_p}{(K+1)}\sqrt{2K+1}$. As stated in Theorem 1, T_p is in the order of 10^{-6} secs and hence we have $\dot{\sigma}_{Z1} \ll 1$.

Hence like Theorem 1 if we are able to show that under the $\dot{\sigma}_{Zj} \ll 1$ assumption, the sum of a non-central χ^2 RV and a

Gaussian RV also tends to a non-central χ^2 RV, that proves Theorem 2.

Z being a non-central χ^2 RV, it contains a Bessel function and hence we cannot obtain a closed form expression of its convolution with a Gaussian distribution. But we have obtained the result through numerical computation and that the theorem holds can be seen from Fig. 2. In order to obtain a closed form expression of the convolution, we consider a simple case of non-central χ^2 distribution, i.e., exponential distribution, which is obtained by using $K = 0$ in (4). Hence,

$$f_{Z(t)}(z) \triangleq f_Z(z, \mu_Z, 0) = \frac{1}{\mu_Z} e^{\frac{-z}{\mu_Z}}, \quad z \geq 0. \tag{30}$$

Now we perform $f_{Z(t+T_p)}(z) = (f_{Z(t)} * f_{Z_1})(z)$ to finally obtain

$$f_{Z(t+T_p)}(z) = \frac{e^{-\frac{2z\mu_Z + \dot{\sigma}^2_{Z1}}{2\mu^2_Z}}}{2\mu_Z \left[1 - \Phi\left(-\frac{z}{\dot{\sigma}_{Z1}}\right)\right]} \left(\text{erf}\left[\frac{\dot{\sigma}_{Z1}}{\sqrt{2}\mu_Z}\right] - \text{erf}\left[\frac{-z\mu_Z + \dot{\sigma}^2_{Z1}}{\sqrt{2}\mu_Z \dot{\sigma}_{Z1}}\right]\right). \tag{31}$$

Using (22) and the $\dot{\sigma}_{Z1} \ll 1$ assumption, we get

$$\lim_{\dot{\sigma}_{Z1} \to 0} \text{erf}\left[\frac{\dot{\sigma}_{Z1}}{\sqrt{2}\mu_Z}\right] = 0 \quad \text{and} \tag{32}$$

$$\lim_{\dot{\sigma}_{Z1} \to 0} \text{erf}\left[\frac{-z\mu_Z + \dot{\sigma}^2_{Z1}}{\sqrt{2}\mu_Z \dot{\sigma}_{Z1}}\right] = -1. \tag{33}$$

The $\dot{\sigma}_{Z1} \ll 1$ assumption also results in $1 - \Phi\left(-\frac{z}{\dot{\sigma}_{Z1}}\right) \approx 0.5$. Taking all these constraints into account, (31) is approximated as

$$f_{Z(t+T_p)}(z) \approx \frac{1}{\mu_Z} e^{-\frac{z}{\mu_Z}}, \tag{34}$$

which is nothing but the exponential distribution. This proves the theorem for $\zeta = 1$. However, this proof can be extended to the $\zeta > 1$ case under the $\dot{\sigma}_{Zj} \ll 1$ assumption as:

1) Sum of multiple independent Gaussian RVs is always a Gaussian RV.
2) Sum of a Gaussian RV and an Exponential RV tends to a Exponential RV (proved above).

This completes the proof. □

Results presented in Figs. 1 and 2 validate Theorem 1 and 2. While Fig. 1 also shows the transformation of the Rician distribution to Rayleigh distribution for $K = 0$, Fig. 2 demonstrates the transformation of a non-central χ^2 distribution with two degrees of freedom to the well known exponential distribution for $K = 0$. The root mean square error value in both the cases is in the order of 10^{-4}. Hence, both the theorems are verified via extensive Monte-Carlo simulations.

IV. Conclusion

In this paper we have characterized the temporal variation of the wireless channel. In the proposed model, the temporal variations of the channel have been modeled as a finite GMM. We have validated the proposed model through analysis and extensive Monte Carlo simulations. As the proposed characterization depends on the current state of the channel, it may be used in various applications that aim at increasing the efficiency of the communication system.

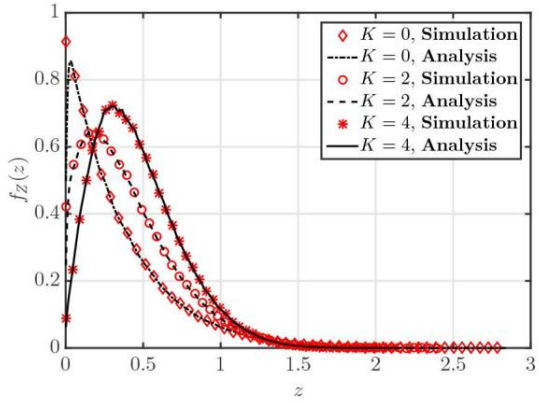

Fig. 2. Theorem 2 verification for various Rice factor K. System parameters: node velocity= 6 kmph, slot duration $T_p = 500$ μs, and $\zeta = 10$

References

[1] Cisco, *Cisco Visual Networking Index: Forecast and Methodology, 2015-2020*. Cisco White Paper, Feb. 2016.

[2] R. Q. Hu and Y. Qian, "An energy efficient and spectrum efficient wireless heterogeneous network framework for 5G systems," *IEEE Commun. Mag.*, vol. 52, no. 5, pp. 94–101, May 2014.

[3] B. S. Everitt, *Finite Mixture Distributions*. Wiley Online Library, 1981.

[4] A. P. Dempster, N. M. Laird, and D. B. Rubin, "Maximum likelihood from incomplete data via the EM algorithm," *J. Royal Statistical Soc.*, vol. 39 (Series B), pp. 1–38, 1977.

[5] G. L. Stüber, *Principles of Mobile Communication (2nd Ed.)*. Norwell, MA, USA: Kluwer Academic Publishers, 2001.

[6] Q. Liu, S. Zhou, and G. Giannakis, "Cross-layer combining of adaptive modulation and coding with truncated ARQ over wireless links," *IEEE Trans. Wireless Commun.*, vol. 3, no. 5, pp. 1746–1755, Sep. 2004.

[7] J. M. Holtzman and A. Sampath, "Adaptive averaging methodology for handoffs in cellular systems," *IEEE Trans. Veh. Technol.*, vol. 44, no. 1, pp. 59–66, Feb. 1995.

[8] C. Tepedelenlioglu, A. Abdi, G. B. Giannakis, and M. Kaveh, "Estimation of doppler spread and signal strength in mobile communications with applications to handoff and adaptive transmission," *Wireless Commun. Mob. Comput.*, vol. 1, no. 2, pp. 221–242, 2001.

[9] M. Zorzi, R. R. Rao, and L. B. Milstein, "ARQ error control for fading mobile radio channels," *IEEE Trans. Veh. Technol.*, vol. 46, no. 2, pp. 445–455, May 1997.

[10] C. Xiao, Y. R. Zheng, and N. C. Beaulieu, "Novel sum-of-sinusoids simulation models for Rayleigh and Rician fading channels," *IEEE Trans. Wireless Commun.*, vol. 5, no. 12, pp. 3667–3679, Dec. 2006.

[11] M. K. Simon and M. Alouini, "A unified approach to the performance analysis of digital communication over generalized fading channels," *Proc. IEEE*, vol. 86, no. 9, pp. 1860–1877, Sep. 1998.

[12] M. Hafez, T. Khattab, and H. M. H. Shalaby, "Blind SNR estimation of Gaussian-Distributed signals in Nakagami fading channels," *IEEE Trans. Wireless Commun.*, vol. 14, no. 7, pp. 3509–3518, July 2015.

[13] M. K. Simon and M.-S. Alouini, *Digital Communication Over Fading Channels*. John Wiley & Sons, 2005.

[14] M. A. Juang and M. B. Pursley, "New results on finite-state Markov models for Nakagami fading channels," in *Proc. IEEE MILCOM*, Nov. 2011, pp. 453–458.

[15] M. D. Yacoub, J. E. V. Bautista, and L. G. de Rezende Guedes, "On higher order statistics of the Nakagami-m distribution," *IEEE Trans. Veh. Technol.*, vol. 48, no. 3, pp. 790–794, May 1999.

[16] N. C. Sagias, D. A. Zogas, G. K. Karagiannidis, and G. S. Tombras, "Channel capacity and second-order statistics in weibull fading," *IEEE Commun. Lett.*, vol. 8, no. 6, pp. 377–379, June 2004.

[17] S. Borman, "The expectation maximization algorithm-a short tutorial," pp. 1–9, 2004, [Online]. Available:http://www.seanborman.com/publications/EM-algorithm.pdf.

CamShare: Real Time Video Streaming over Wi-Fi Direct using Real Time Protocol

Lakshminarayana Potukuchi[1], Gattu Suryateja[2], Devarasetty Anil Saikrishna[3], and Aditya Trivedi[4]
Department of Information and Communication Technology,
ABV-Indian Institute of Information Technology and Management, Gwalior
narayanapot@gmail.com[1], gattusuryateja@gmail.com[2], anildevarasettysk@gmail.com[3], atrivedi@iiitm.ac.in[4]

***Abstract*— This paper utilizes the latent potential of a relatively new technical specification of Wi-Fi Alliance called the "Wi-Fi Peer-to-Peer (P2P) Specification" or Wi-Fi Direct, for video streaming. The video streaming applications presently are limited to the use of the traditional Wi-Fi/internet connection to connect to a third-party video streaming media server. Using Wi-Fi Direct, it is easier to connect the concerned devices directly without the need for a third-party server. Paper discusses the discovery of devices, connection of devices and data transfer among the devices take place in the Wi-Fi Direct specification. Real Time Protocol (RTP) over User Data-gram Protocol (UDP) is implemented in the application to achieve the real-time video streaming between the devices. The advantages of using Wi-Fi Direct and the general restrictions of the technology are also discussed. Furthermore, we calculate various parameters in video streaming over Wi-Fi Direct and draw inferences from them regarding the present state of the network.**

Keywords: Wi-Fi Direct, Real-Time, Video streaming, Android application.

I. INTRODUCTION

In the past two decades, technology has grown by leaps and bounds. The existing technology is being continuously developed and optimized so as to make the systems more efficient. A decade after its initial design, the IEEE 802.11 standard or Wi-Fi has become one of the most common ways to connect to the network and access the internet. With its success, Wi-Fi has had to evolve and adapt to a more diverse set of user cases. Wi-Fi functionality is readily available across various devices. A seemingly possible way for the technology to advance is to target device-to-device connectivity. To do so, without the presence of an Access Point (AP), as traditionally provided by other technologies, has been described in [3]. Wi-Fi Direct technology has been recently developed [10] which allows Wi-Fi client devices to connect to each other directly and form groups, usually one-to-one connections, but sometimes also one-to-many connections and share applications quickly and easily.

The present mechanism for the real-time streaming of videos across various client devices using Wi-Fi is through the use a video streaming media server. The sender client sends the video stream to media server which redirects the video stream to the receiver client. With the release of a new specification in Wi-Fi, we need to discover ways to utilize it so as to improve the system. Using Wi-Fi Direct, the need for a media server is removed since, the client devices connect among themselves and act like an ad-hoc system. Wi-Fi Direct thus creates a situation wherein one of the two client devices acts like a server sending the video data bytes and the other client device acts like a client to receive the video data bytes and streaming the video in real-time.

1) Wi-Fi Direct. 2) Encoding techniques based on hardware specifications. 3) Integrating the modules. The principal concern is major work was on the traditional Wi-Fi. We come up with the new idea of removing the third party server. The main challenge was to change the encoding techniques based on the hardware specifications and also integrating the different modules like Wi-Fi connection and Lib-Streaming. The main motivation for this work on Wi-Fi Direct is to remain up-to-date with the ever evolving technologies and specifications. The direct data route (server device-client device) for the video streaming bits made through the ad-hoc type network of Wi-Fi Direct is more economical than the data route for the traditional Wi-Fi (server device-media server-client device). The cost of maintaining a third party media server is removed and the need for a strong Wi-Fi signal and the requirement for subsequent internet connectivity are also nullified since the data is exchanged directly among the mobile client devices.

So far, a clear understanding about Wi-Fi Direct, the challenges and motivation for the work are discussed. In Section II, a brief description of Wi-Fi Direct and the current real time video streaming mechanisms are given. In section III, the details of the approach are explained. In section IV, diverse experiments are designed and conducted to test different aspects of the application and the quantitative results obtained are shown. In section V, the conclusions are drawn from the results.

II. RELATED WORK

The Wi-Fi Direct is a specification of the Wi-Fi Alliance. It has some minimal requirements like the use of 802.11g, RSN (WPA2) with AES-CCMP encryption, Wi-Fi Protected Setup (WPS), WME (WMM) quality of service, and OFDM data rates for management frames as discussed in [9]. Wi-Fi Direct client devices arrange their roles among themselves in the direct connection made between them, in which one of them assumes the traditional role of AP called Group Owner and the other devices connect to the Group Owner as clients in station mode. Though this is not the ideal

peer-to-peer connection, it is safe to assume it to be one because of its similarities with the P2P network connections as explained in [9].

A comprehensive understanding of Wi-Fi Direct can be made by reading [3], which gives a complete idea of how the discovery and connections are made and also on the architecture of the Wi-Fi Direct network and the process of group formation. Various characteristics of the Wi-Fi Direct network are also discussed including autonomous nature, security, persistent, delay and power saving. The experimental evaluation is conducted and the results are inferred. A further study into the Wi-Fi Direct networks in mobile client devices has been done by [9]. A more scrutinized analysis of the security and the power management of the Wi-Fi Direct networks have been done in [12] and [6] respectively.

The application has been created on the Android Mobile Development Platform. The basic skill of programming in the object oriented programming language, Java is required to write the codes in Android which are given in [8] blog. The fundamental principles and knowledge of Android can be learned from the online developer site [2]. The Libstreaming API is a free, open source API which helps in the implementation of real - time streaming (RTP) using minimal lines of code. The package and the corresponding documentation can be found in [5].

The study of video rendering and real-time streaming in mobile client devices running on Android Platform has been done extensively in [13] and [4] respectively. Both the papers give a clear idea of the present situations in streaming the videos using the traditional Wi-Fi. The security and power management of these real-time video streaming applications have been studied and efficiently recorded in [7] and [11] . A method to reduce the delay and to increase the video quality of the stream based on heuristic technique has been discussed in [1].

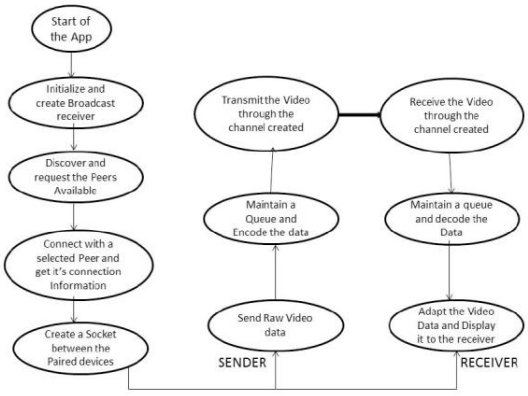

Fig. 1. Design Methodology

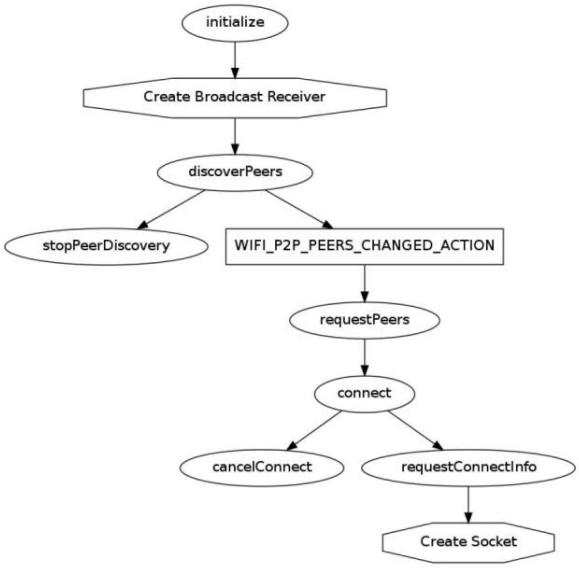

Fig. 2. Flow Diagram of Creating P2P Connections using Wi-Fi Direct

III. SYSTEM DESIGN

The android mobile application has been developed using Android Studio, the official integrated development environment (IDE) for Android platform development. A Design Process for the development of this application has been shown in Fig.1.

Wi-Fi peer-to-peer (P2P) allows Android 4.0 (API level 14) or later devices with the appropriate hardware to connect directly to each other via Wi-Fi without an intermediate access point (Android's Wi-Fi P2P framework complies with the Wi-Fi Alliance's Wi-Fi Direct certification program). Using these APIs, one can discover and connect to other devices when each device supports Wi-Fi P2P, then communicate over a speedy connection across distances much longer than a Bluetooth connection. The complete flow diagram of this API has been shown Fig.2.

The data transfer between the devices is done through the sockets. Creating a Server Socket and it waits for any connection from a client on a specified port and it blocks the whole process until it is going to happen. So it is done in the background Thread. In the meanwhile, Client Socket is created and it uses the IP address and port number of server socket.

For video transmitting between the 2 connected devices, an API, Libstreaming has been used, that allows us, with only a few lines of code, to stream the camera of an android powered device using RTP over UDP. It includes signaling, queuing, and encoding/decoding functionality. Flow chart of this API has been shown in Fig.3.

The application has been programmed, debugged, and run successfully in both LG Nexus 4 and Samsung Galaxy Grand Mobile devices. The Application is build using Android 4.4 Version Android Framework. The Application

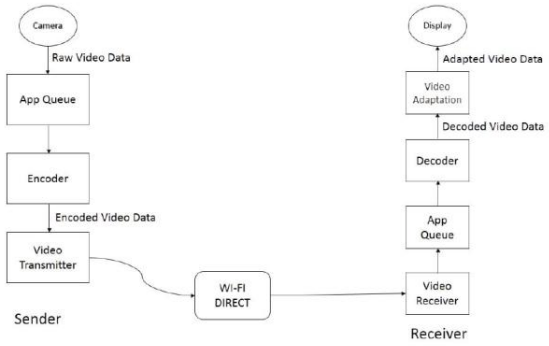

Fig. 3. Flow Diagram of Video Streaming

is based on real time video sharing between two mobile devices connected using Wi-Fi Direct. In Android a screen uses a combination of Layout and Activity and uses Intent to start another Activity. All Activities are declared in Androidmanifest.xml file before using. This Application has been made in 3 parts: First, Connection of 2 Android mobile devices using Wi-Fi Direct, second, Socket Creation between the devices for Data Sharing/Transmission, and third, Real-time Video Streaming between the devices using Libstream API.

IV. RESULTS AND DISCUSSIONS

During the testing of this App, it is simulated on two devices: LG Nexus 4 and Samsung Galaxy Grand mobiles. The installed application named "CamShare" when launched in these devices, is successful in sharing the video from one device to another in real time. The application is tested several times using several pairs of devices and the average of all the results obtained is displayed in the Tables below.

1) CONNECT Wi-Fi DIRECT:

TABLE I
TIME TAKEN TO CONNECT OVER WI-FI DIRECT

User Goal	Obtained Time
Connect using Wi-Fi Direct	30 seconds

In TABLE I, it is observed that the time for connection to be made by the two mobile client devices is around 30 secs. The connection has to be made manually since the Android API's doesn't allow for multiple Main Activities. Future API improvements in Android may make connection within the application feasible.

2) VIDEO STREAM CONNECTION:
After getting connected, Video Stream Connection Time is noted down. We calculate this Time as follows:
   a) One user clicks on "Server Button".
   b) Waits till the Server Launches.
   c) Second user than clicks on the Client button.
   d) Waits until the Video Stream appears.

TABLE II
TIME TAKEN TO STREAM VIDEO OVER WI-FI DIRECT

User Goal	Obtained Time
Video stream connection	50 sec

TABLE II shows how much time is taken by the mobile client devices for forming the video streaming connection. The time to form this connection varies between different client mobile devices and has been averaged to 50 secs. The Libstreaming API makes the video streaming connection plausible but it needs a comparatively large amount of time to build a session and start either streaming or receiving the data bytes based on the role of the mobile client device.

3) DISTANCE TOLERANCE AND RESPONSE TIME: The Threshold Distance is calculated if one user moves away from other user until the video gets dropped.

TABLE III
DISTANCE OVER WHICH A WI-FI DIRECT CONNECTION IS MAINTAINED

User Goal	Obtained Range
Distance Tolerance(in open space)	26 meters
Distance Tolerance(With an obstruction)	7.5 meters

The Time delay between the Server's and Client's Camera Stream is noted down.

TABLE IV
TIME DELAY BETWEEN THE SERVER AND CLIENT CAMERA STREAMS

User Goal	Obtained Time
Response Time	3 sec

Values in TABLE III and IV show that the range and power of the Wi-Fi Direct network is very less. But in reality the range of a Wi-Fi Direct connection is up-to 200 meters as given in and not 26 meters, also the same applies for the response time (delay) should not be existing theoretically as the typical speed of a Wi-Fi Direct connection is about 250 Mbps.

V. CONCLUSION

In this work, the android application is developed with the aid of the Android and Libstreaming API's. The application is successful in connecting and streaming real-time videos across two mobile client devices running on android platform. The various characteristics shown by the application have been systematically tabulated in section IV along with their inferences.
The far-reaching results during the testing of the application can be concluded to the use of low power Wi-Fi Direct hardware used in the mobile client devices. With the help of Enhanced power management for Wi-Fi Direct discussed in [11] , and further improvements of it, we can increase the range of the Wi-Fi Direct network by a notable amount. A substantial increase in the Wi-Fi Direct network can be only

noticed with improved more powerful hardware and further optimization in the Wi-Fi Direct software specifications.

The Wi-Fi Direct technical specification is still new with a lot of latent potential. The current real-time video streaming is promising for near distance live video streaming and can improve in time with the corresponding progress and expansion in the Wi-Fi Direct technology.

The major areas for future development works of the "CamShare" Application are listed below:

1) The application can be modified further to accommodate one-to-many connections and streaming support can be extended across multiple mobile client devices in the Wi-Fi Direct adhoc network. The Group Owner (GO) must be in charge of controlling the flow of the video stream bytes in the network to avoid data congestion.
2) The Wi-Fi Direct connections and video streaming application can be made to support different platforms (IOS and Windows). Inter-platform connections and streaming can also be enabled.
3) Wi-Fi Routers with a large range can be made to act as a fixed GO and the mobile clients can be made to connect to this network to increase the range of the Wi-Fi Direct network. Multiple hops can also be implemented based on the future availability of the hardware in the mobile client devices.
4) The hardware components pertaining to the Wi-Fi Direct can be made more effective with increased powers, so as to increase the data transfer speed and the range of the network availability.
5) Further research in the Wi-Fi Direct security and power management for the increased safety and utilization of the network and making mobile client devices more productive.

REFERENCES

[1] Anand, S. Vijay; Suman, K. S.: 2010, *heuristic buffer management technique on android to enhance video quality on digital handheld audio video terminals, Computers and Communications (ISCC), 2010 IEEE Symposium.*

[2] ANDROID: n.d., `https://developer.android.com/index.html` , ANDROID

[3] Camps-Mur, D.; Garcia-Saavedra, A. S. P.: 2013, Device-to-device communications with wi-fi direct: overview and experimentation, *Wireless Communications, IEEE,.*

[4] Cangzhou, Yuan, C. G.-J. D. W. S.: 2011, An optimizing scheme for wireless video transmission on android platform, *Transportation, Mechanical, and Electrical Engineering (TMEE), 2011 International Conference.*

[5] GitHub:n.d., `https://github.com/fyhertz/libstreaming`, GitHub

[6] Keun-Woo Lim; Woo-Sung Jung; Kim, H.; Han, J. Y.-B. K.: 2013, Enhanced power management for wi-fi direct, *Wireless Communications and Networking Conference (WCNC), 2013 IEEE.*

[7] Massandy, Danang Tri; Munir, I. R.: 2012, Secured video streaming development on smartphones with android platform, *Telecommunication Systems, Services, and Applications (TSSA), 2012 7th International Conference.*

[8] ORACLE: n.d., `http://docs.oracle.com/javase/7/docs/api/` *ORACLE DOCUMENTATION.*

[9] THINKTUBE: n.d., `http://www.thinktube.com/tech/android/wifi-direct` *THINKTUBE.*

[10] WiFi.Org: n.d., `http://www.wi-fi.org/discover-wi-fi/wi-fi-direct` *WiFi.org.*

[11] Yadav, P.K.; Ramasubramanian, N.: 2014, Power consumption of android device using different video codecs: An analysis, *Advance Computing Conference (IACC), 2014 IEEE International.*

[12] Yoo, S. Y. S. P. H. P. H. S.: 2012, Security analysis of vulnerable wi-fi direct, *Computing and Networking Technology (ICCNT), 2012 8th International Conference.*

[13] Zhang, Z. and Yin, C.: 2012, Research on video rendering on android, *Wireless Communications, Networking and Mobile Computing (WiCOM).*

Distributed Fault Tolerance Algorithms for Wireless Sensor Networks

Prasenjit Chanak
ABV-Indian Institute of Information Technology & Management, Gwalior, 474015, MP

***Abstract*— In this paper, we first propose a clustering algorithm in WSNs named Distributed Energy Efficient Heterogeneous Clustering (DEEHC) that select cluster heads according to residual energy and a secondary parameter timer. We then present a *k*-Vertex Disjoint Paths Routing (kVDPR) algorithm where each cluster head finds *k*-vertex disjoint paths to the base station (BS) and relays their aggregate data. The resulting WSNs are tolerant to *k-1* cut in the worst case throughout the monitoring period. We performed extensive experiment on the proposed scheme using various network scenarios and compared it to the existing approaches.**

***Index Terms*— Wireless sensor network, network cut, fault and link failures.**

I. Introduction

In recent years, advance in microelectronic fabrication technology has reduced the manufacturing cost of the portable wireless sensor nodes. Hence, a large numbers of portable low cost smart wireless sensor nodes are deployed in the monitoring field to increase quality of service (QoS) of Wireless Sensor Networks (WSNs) [1- 4]. It also enhances the importance of WSNs as a remarkable technology for monitoring different critical tasks. Therefore, nowadays, WSNs play a vital role in many fields and applicators such as gas detection, habitat surveillance, home automation, military operations, medical treatments, agricultural crops monitoring, environmental and industrial monitoring [5-9]. In such applications, sensor nodes are usually deployed into a field of interest without any preconfigured infrastructure in stochastic manner. After deployment, sensor nodes organize themselves into an adhoc network by nearby nodes discovery process. WSNs suffer by the different types of failures such as energy depletion, internal failures of deployed sensor nodes, communication link errors or adverse environmental conditions like some events that are likely to occur quite frequently in WSNs. Due to these faults, a sub set of nodes which have not suffered any type of failure, become disconnected from the rest, resulting in a "network cut". In network cut condition, sensed information cannot be reached properly to the Base Station (BS). Hence, it will eventually degrade the Quality of Service (QoS) of WSNs [10-12]. The network cut in the deployed WSN is usually difficult to detect and localize due to its improvisational nature and invisibility of internal running status. Therefore, the design of cut tolerance scheme, which can overcome such failures and successfully deliver sensed information to the sink/BS, has drawn significant attention.

In WSN, if a sensor node wants to send data to the BS through an intermediate node that has been cut off from the BS. Without any knowledge of current network condition, sensor node may simply forward the sensing information to the next hop intermediate node, and so on. Then forwarding information cannot be reached to the BS; the network cut prevents the forwarding packet from reaching the BS. Hence, this message passing wastes precious energy of the node. Hence, cut potentially degrades QoS of the network. If the link/node failure can be detected or tolerated, the network cut problem can be reduced and QoS of the WSN can be enhanced. In link/node failures detection strategy, first deployed sensor node status is diagnosed by the node itself or other nodes and then needful topological reconstruction process will repair data routing routes [13-14]. During this time period, non faulty nodes are waiting for the network repairing process for new data transmission. Sometimes network diagnosis and reconstruction process are very time consumed due to large number of nodes deployment.

Hence, link/node failures detection and repairing strategy takes much more time for data routing after a network cut occurs within the network. On the other hand, it also requires much more energy for detection and repairing process. In the critical tasks monitoring application, link/node failures detection and recovery strategy have not got an effective solution after a network cut like problem occurrences; because these applications require current data. Therefore, in critical tasks monitoring applications, a link/node fault tolerance strategy can overcome network cut condition without any detection/recovery time delay and successfully relay data to the BS.

The major contributions of this paper can be summarized as follows.

- We propose a Distributed Energy Efficient Heterogeneous Clustering (DEEHC) algorithm in WSN that selects the Clusters Head (CH) to setup a connected backbone network where sensor nodes make local decisions on whether to join as a CH or non-cluster head in the backbone network. The decision of each sensor is based on its current energy. During the clustering phase, each sensor node also selects *k*-vertex disjoint data routing paths depending on its neighboring nodes energy condition.

- According to the feature of dynamic topology in WSNs, we proposed a *k*- Vertex Disjoint Paths Routing (kVDPR) algorithm in clustered WSNs. Here, kVDPR algorithm selects *k*- number of disjoint routes between the CHs (which are selected by the DEEHC algorithm) and the BS. The kVDPR is a distributed technique, where each CH individually selects *k*-vertex disjoint routing routes according to the residual energy level of their parent CHs and number of existing routes between them.
- We propose a Routes Maintenance Mechanism (RMM) which maintains *k*- vertex disjoint routing paths/routes between the deployed sensor nodes and CH as well as CHs and the BS. RMM is a distributed technique where each sensor node and CHs locally selects new disjoint routing paths/routes in presence of any node/link failure.
- We analyse message and time complexity of the proposed algorithms which are nearly optimal. We derive an expression to estimate the energy consumption of the network considering k-vertex disjoint paths based on data routing.
- We perform extensive experiments on the proposed algorithms and the experimental results are compared with the other existing algorithms to verify effectiveness of our proposed algorithms in terms of various performance metrics.

Rest of the paper is organized as follows. Section 2 describes related works. Section 3 describes the system model. Section 4 presents preliminaries and problem formulation. We discuss the proposed scheme and the complexity of the proposed algorithms in Section 5 and Section 6. Section 7 presents simulation results of the proposed scheme. Finally, the paper is concluded in Section 8 with future work plans.

II. Related Work

A. Clustering in WSNs

Several cluster approaches have been proposed in the recent years to address the energy conservation problem in small as well as large scale WSNs. Distributed clustering approaches are more in large scale WSNs where sensor nodes are deployed in the hostile environment. Low Energy Adaptive Clustering Hierarchy (LEACH) [15] selects CHs based on the predefined probability and it rotates CHs responsibility among the non-cluster head nodes to balance the energy consumption of the deployed sensor nodes. A number of clustering approaches have been presented in the literature that tries to overcome limitation of the LEACH protocol. Hybrid Energy Efficient Distributed (HEED) [16] is another clustering approach where CHs are selected based on the residual energy of sensors and a secondary parameter, such as proximity to its neighbor. An Energy Efficient Heterogeneous Clustering Scheme (EEHC) is introduced for energy efficient data gathering applications in WSNs [17]. It is a LEACH like protocol such that it utilizes node residual energy in the selection of efficient cluster heads. Similarly, in cluster formation phase, load is balanced among cluster heads. It is a distributed clustering approach and experimental results shows that it is 10% more energy efficient than LEACH.

B. Fault Tolerance in WSNs

It has been widely known that the data routing with fault tolerance can cost significant energy expenditure in sensor networks with a heterogeneous topology. To overcome this problem, some two-layered architecture based fault tolerance approaches were studied in [14, 18-20]. These approaches minimize the total power consumption while providing *k*-vertex connectivity between the two deployed nodes. However, majority of these approaches are centralized. Hence, these approaches are mostly of theoretical importance and it is not practical to apply it for large scale WSNs due to the requirement of global topology knowledge. Algorithm for fault tolerant topology in heterogeneous wireless sensor networks is introduced for fault tolerance data routing applications in WSNs [14]. In this approach, authors Cardei et al. deployed some supernodes and established *k*-vertex disjoint paths between the normal deployed sensor nodes and supernodes for fault tolerance data routing. An Inter Cluster Communication (ICC) based energy aware and fault tolerant protocol for wireless sensor network is studied in [21]. It alternates the nodes responsibility for inter-cluster communication inside on cluster. Redundancy Management for Multipath Routing (RMMR) is introduced for intrusion tolerance in heterogeneous WSNs [22]. Here, the query response success probability is maximized while extending the network lifetime.

In the above approaches, cluster heads directly transmit their data to the base station. As a result, the sensors that are far away from the sink drain their energy much more compared to the other nodes. Hence, once these nodes are faulty, existing approaches require multiple rounds to form a clustered WSN. During the cluster formation time far away cluster heads head transmits their data to the base station but these data do not reach the destination. Therefore, a huge amount of energy is lost from the deployed sensor nodes. In addition, multiple rounds introduce extra message overhead over the network. Another drawback of the existing clustering approaches is that they require more than one transmission power level for routing the data to the base station. Therefore, these approaches are not suitable for low-cost sensors which have usually single power level. In [21-22], fault tolerance data routing techniques are suffered by high transmission delay and extra message overhead due to alternative paths selection process. However, existing fault tolerance techniques [14, 18, 21-22] are unable to overcome network cut situation due to random path selection process. Hence, performance of the existing fault tolerance techniques [14, 18, 21-22] is very poor in large scale wireless sensor networks.

III. System Model

A. Energy model

According to first order communication mode that has been adopted from [23], the energy consumption by the nodes to transmit *'β'* bit of data packet to distance *d* is given as follows.

$$E_{Tx}(\beta,d)=\begin{cases}\left(E_{elec}+\varepsilon_{fs}d^2\right)\beta & d<d_0\\ \left(E_{elec}+\varepsilon_{mp}d^4\right)\beta & d\geq d_0\end{cases} \quad (1)$$

where ε_{fs} and ε_{mp} be the energy required by the Radio Frequency (RF) amplifier in free space and multipath respectively. E_{elec} is the energy consumption per bit in the transmitter circuitry. Also the energy consumed in the receiving β bit data by a deployed sensor node is given by

$$E_{Rx}(\beta)=E_{RX-elec}\beta+E_{DA} \quad (2)$$

where $E_{RX-elec}$ is the energy consumption per bit in the receiver circuitry. E_{DA} is the energy consumed in aggregation of data packets.

IV. Preliminaries and Problem Formulation

Here, we represent the initial network topology with an undirected weighted graph $G=(V,E)$ in the *2D* plane, where $V=\{n_1,n_2,\ldots n_i,n_{i+1},\ldots\ldots,n_N\}$ is the set of node and $E=\{(n_i,n_j)\mid dsit(n_i,n_j)\leq R_{max}\}$ is the set of edges, where *dist*(n_i, n_j) depicts the distance between nodes n_i and n_j.

Definition 1: (*k*-vertex disjoint paths). *k-number of independent data routing paths that have common end points but have no other vertices in common is defined as k- vertex disjoint paths.*

A. Problem formulation:

We consider sensor networks (*G= (V, E)*) in *2D* plan where any sensor node $n_i\in V$ senses data periodically from the monitoring area and sends to the BS through multi-hop communication. Due to the different types of environmental hazards like interference and deployed nodes failures, network cut occurs within the network. Therefore, a sub set of nodes $V_j=\{n_1,n_2,\ldots\ldots,n_j\}$, $(V_j\subseteq V)$ become disconnected from the rest. Hence, sensed data packets cannot be reached to the BS. As mentioned earlier, such network crisis can potentially degrade quality of service (QoS) of WSNs. If these cuts can be tolerated during the data routing stage, sensed information can be successfully reached to the BS and quality of services (QoS) of WSN can be improved. On the other hand, due to the node failures or link errors, network structure of the WSNs frequently changes throughout the network lifetime which significantly increases data transmission delay and energy consumption of the deployed sensor nodes. Our main objective is to overcome network cut condition of the WSN in an energy efficient manner and relay data packets from the source nodes to the BS with minimum time consumption. Next we state the problem definition more formally.

Problem Definition: Given an undirected graph $G=(V,E)$, where V is the set of all vertices and E is the set of all edges, selects M number of vertexes (CH node) such as $M\subset V$, $N\subset V$ and $M\cap N=\phi$, where exists at least *k*-vertex disjoint paths from each vertex $n\in N$ to the set of vertices *M*, find the set of edges F such that G (V, E-F) satisfies the following:

1) *There exists at least k-vertex disjoint path from each vertex* $n\in N$ *to the set of vertices M.*
2) $\sum_{i=1}^{N}p_i=\min imum$, *where* p_i *is the weight of the maximum weighted edge* $\in(E-F)$ *of* $n_i\in N$.

V. Proposed Scheme

In the proposed DEEHC algorithm, deployed sensor nodes are organized into different clusters without any central control. Proposed distributed DEEHC algorithm is described as follows.

A. Distributed Energy Efficient Heterogeneous Clustering (DEEHC)

Each deployed sensor node (n_i) checks its current remaining energy (E_{curr}), if it is greater than the $E_{threshold}$, then n_i sets a timer depending on its current energy level and starts advertisement for CH. Let $CH(t_i)$ be the timer of a deployed sensor node n_i which is derived as follows.

$$Ch(t_i)=\frac{E_{max}(n_i)-E_{curr}(n_i)}{E_{max}(n_i)}\times\frac{R_{max}}{E_{curr}(n_i)}\times T_{CH} \quad (3)$$

where T_{CH} is the maximum allotted time for CH advertisement. The $E_{max}(n_i)$ and $E_{curr}(n_i)$ are the maximum energy level and current energy level of the node n_i respectively. During the CH advertisement process, if any other advertisement node n_j within the R_{max} region detects its current residual energy, less than the received advertisement node n_i, node n_j withdraws its nomination for CH by cancelling its timer and it acts as a non- cluster head node. Once CH selection timer expires, node n_i selects itself as a CH and broadcasts a CH selection message "*CH_SELECT*" in the communication range R_{max}. The selection message includes its identification number (*ID*), and location information. Each non-cluster head node also starts keeping track of the sensor nodes from which it receives CH announcement messages by maintaining a neighbor set denoted by NN_{CH} (n_i). Each non-cluster head node computes *k*- vertex disjoint paths depending on average energy of the neighborhood nodes (NN_{CH} (n_i)). For example, a non-cluster head node n_i receives "*CH_SELECT*" message from NN_{CH} (n_i)={n_1, n_2, …n_p} neighbor node set. Therefore, *p* number of disjoint paths may exist between the source node n_i and its neighbor set nodes. If source node n_i transmits its data to the *p* number of disjoint paths, number of network cut tolerance possibility may increase but energy overhead increases highly within the network. Hence, expensive energy of the sensor node is wasted for extra message handling process which potentially reduces lifetime of the network. Therefore, each non-cluster head node selects *k*-vertex disjoint paths according to current energy condition of their neighbor node set and forwarding sense information to the CH through the selected *k*-vertex disjoint paths. The non-cluster head node is calculated average current energy $\vartheta(CH^i_{set})$ of the neighborhood node set NN_{CH} (n_i) as follows

$$\vartheta\left(CH^i_{set}\right)=\frac{\sum_{i=1}^{n}E_{curr}}{n} \quad (4)$$

According to the $\vartheta\left(CH_{set}^{i}\right)$, each non-cluster head node selects k number of neighbor nodes from NN_{CH} (n_i) whose current residual energy is greater than or equal to $\vartheta\left(CH_{set}^{i}\right)$ for k- vertex disjoint data paths. After k number of neighbor nodes selection from the neighborhood node set NN_{CH} (n_i), each non-cluster head node broadcasts join message "*JOIN*" to the CH by the k-vertex disjoint paths. The join message includes its identification number (*ID*), current energy and location information. The detail description about the cluster formation algorithm is summarized in Algorithm 1.

Algorithm 1: Energy Efficient Heterogeneous Clustering

```
/*Cluster head selection strategy*/
for each deployed node n_i
    if E_curr ≥ E_threshold then
        set a time according to eq. 1
        Node n_i broadcasts advertise msg.
        if received advertise node E_curr(n_j) ≥ E_curr (n_i) then
            Stop timer and withdraw advertisement for CH
        end if
    end if
end for
for each node n_i
    if ch(t_i) == 0 then
        n_i broadcasts CH_SELECT msg.
    end if
end for
for each normal node
    Calculated ϑ(CH_set^i) by the eq. (2).
    if requested cluster E_curr(n_i) ≥ ϑ(CH_set^i) then
        node selects cluster head n_i for data transmission
        node tracks CH_SELECT msg. of the cluster head n_i
        selected k vertex disjoint paths from the NP_ch(v_i)
        node broadcasts JOIN msg. to the n_i by the k vertex disjoint paths
        end if
end for
```

B. *k-Vertex Disjoint Paths Routing (kVDPR)*

Here, we present proposed kVDPR algorithm which finds k-vertex disjoint routes between the CHs and BS. Proposed distributed DEEHC algorithm is described as follows. Initial, BS sets its level zero and sends a advertise message *ADVE* to the CH in the range R_{max}. The message contains its *ID*, level (*L*), and location information. When a CH i receives the message then it increments its level to one higher than the sink and sets the sink as its Parent Node (NP_{CH}^{i}) set. Similarly, all CH within the range R_{max} to the BS are designated as level ones. Recursively, node i broadcasts a modified advertise message to the CH in the range $2R_{max}$. The message contains its *ID*, current level value, current energy level (E_{curr}), and location information. If a CH j receives the message and if its level value is less than or equal the level of the CH i, then it simply discords the message. Otherwise, it updates its level to one more than the levels of CH i and sets it as one of the parent nodes. Recursively, all the CHs broadcasts the *ADVE* to complete the data routing routes identification process. During the level detection process, a CH has multiple parents and multiple data routing disjoint routes to the sink. For k-vertex disjoint routes selection, each CH i calculates average current/residual energy of parent CH set (NP_{CH}^{i}) using the following formula.

$$\delta(i) = \frac{\sum_{v=1}^{m} E_{Curr}(n)}{m} \tag{5}$$

Recursively, CH i also calculate average distance of its parent CH set using the following formula.

$$D_P^A(i) = \frac{\sum_{v=1}^{m} D_p(n)}{m} \tag{6}$$

If current energy of a parent node is greater than the $\delta(i)$ within the distance $D_P^A(i)$, CH i selects as an acting parent node for data routing. Similarly, CH i identify k number of acting parent nodes within the distance $D_P^A(i)$ for data routing. Recursively, all CHs selects their k number of acting parent nodes from parent nodes set (NP_{CH}^{i}). Therefore, proposed scheme identifies k-vertex disjoint routes for data routing to the BS. Hence, if any parent node/link between the CH is failed during the data routing phase, aggregated data relay to the BS through other *k-1* disjoint routes. The detailed description about KVDPR is described in algorithm 2.

Algorithm 2: K-Vertex Disjoint Paths Routing

```
/* Fault tolerance data routing rout selection */
1.  Initial, BS sets its level value zero and broadcasts an ADVE msg. in the range r.
2.  for each cluster head i
3.      if Receive ADVE msg. and its level(i) ≤ level(BS) then
4.          Cluster head (i) selects BS as a parent node P(i)
5.          Cluster head (i) sets its level (i) = level (BS)+1
6.          Cluster head (i) broadcasts ROUTE msg. in the range r.
7.          end if
8.  end for
9.  for each cluster head (j)
10.     if Receive ROUT msg. and its level(j) ≤ level(i) then
11.         Cluster head selects BS as a parent node P (j)
12.         Cluster head (j) sets its level (j) = level (i)+1
13.         Cluster head (j) broadcasts ROUTE msg. in the range r.
14.     else
15.         Discord ROUT msg.
16.     end if
17. end for

/* Data routing strategy */
18. for each cluster head i
```

/*sum current energy of its acting parent node set P (*i*) */

19. $sum(e) = sum(e) + E_{Curr}(v_i)$
20. $\delta(i) = sum\ (e) / |P\ (i)|$

/* sum distance of its acting parent node set P(*i*) with respect to single strength */

21. $sum(d) = sem\ (d) + D_p(i)$
22. $D_P^A(i) = sum\ (d) / |P\ (i)|$
23. **if** parent cluster $D_p(i) \le D_P^A(i)$ and $E_{Curr}(v_i) \ge \delta(i)$ **then**
24. Set a timer $T_{routing}$
25. Cluster head start data packets to parent cluster heads.
26. **end if**
27. **end for**

VI. Complexity and Precision

In our proposed scheme, deployed sensor nodes are organized in different clusters and transmit their data through *k*- vertex disjoint paths. Hence, proposed scheme tolerates network cuts problem in an energy efficient manner. In the proposed DEEHC algorithm, non-cluster head nodes reduce extra message overhead and transmission energy loss by the selection of energy efficient data routing paths. Recursively, in the kVDPR algorithm, each CH relays its data to the BS through *k* number of parent CH selection strategy. Since, each CH selects *k*- vertex disjoint data routing routes which overcome network cut within the network. If any failure occurs during the data routing phase within the network, data packets successfully deliver to the BS through other alternative *k-1* routes. However, in the proposed routes maintenance process each cluster head as well as non-cluster head node manages its data routing *k*-vertex disjoint routes according to the T_{out} time interval or parent nodes power condition. On the other hand, proposed route maintenance scheme requires less time to recover any fault. It reduces extra message overhead from the deployed sensor nodes and relays data packets by the tolerance of node and link faults.

Lemma 1: *message and time complexity of the proposed DEEHC clustering algorithm is O(1) per sensor and O(N) for N sensors in the network.*

Proof: In the proposed clustering scheme, a sensor node either selects as a CH or processes a joint message only. Therefore, the message complexity of the proposed clustering strategy is *O (1)*. Each node decides independently whether to become a CH or not. This can be done in constant time. To from clustering, each sensor node needs to process *N-1* in worst case to join a CH. Therefore, the time complexity of the proposed clustering algorithm is *O (N)*.

Lemma 2: *The time complexity of the proposed kVDPR cut tolerance data routing algorithm is O(N) for N sensors in the network.*

Proof: In the proposed cut tolerance data routing strategy, each CH needs to calculate the average energy and distance of the parent nodes of the next hop CHs selection for data routing. Hence, it requires collecting location information from the *N-1* CHs in worst case. Therefore the time complexity of the proposed fault tolerance data routing scheme is *O (N)*.

Lemma 3: *In worst case, proposed cut tolerant scheme tolerates k-1 number of network cuts in energy efficient manner.*

Proof: In the proposed cut tolerance scheme, each deployed sensor selects *k* number of neighbor nodes for data transmission to the CH. Recursively; each CH selects *k* number of acting parent CHs for relaying data packets to the BS. Therefore, any source node transmits its data to the BS by the *k*-vertex disjoint routes. During the data routing phase, if *k-1* numbers of network cut occur within the network due to their internal fault or environment interference, then also proposed scheme successfully delivers data packets to the BS. Hence, proposed scheme is able to tolerate *k-1* number of cut during the data routing phase.

Lemma 4: *Total amount of energy consumption by the proposed cut tolerance data routing kVDPR algorithm* $(E_{routing})$ *is* $E_{routing} = \sum_{n_i \in N_{active}} \left(\sum_{i=1}^{i=k} E_{Tx}^i + \sum_{i=1}^{i=k} E_{Rx}^i \right)$

Proof: In our proposed kVDPR algorithms, each sensor node n_i broadcast its own sensing information over the *k*-vertex disjoint paths for which E_{Tx}^i amount of energy is required. Each deployed sensor node n_i receives data from their *k* number of neighbors for which it requires E_{Rx}^i energy. Therefore, total amount of energy required by the deployed sensor node n_i is $\sum_{i=1}^{i=k} E_{Tx}^i + \sum_{i=1}^{i=k} E_{Rx}^i$. So, total energy consumption of the network is

$$E_{routing} = \sum_{n_i \in N_{active}} \left(\sum_{i=1}^{i=k} E_{Tx}^i + \sum_{i=1}^{i=k} E_{Rx}^i \right) \quad (7)$$

Lemma 5: *Total time requirement to relay sensed data from source node to BS in presence of k-1 number of cut* ($\sigma_{routing}$) *is*

$$\sigma_{routing} = \sum_{n_i \in N_{active}} \left(\left(\sum_{i=1}^{i=level_{max}} \left(T^i(C_i) + T_p \right) \right) + \left(\sum_{i=1}^{p} (T_{n_i} + T_p) \right) \right)$$

Proof: In the proposed cut tolerance scheme, each sensor node n_i broadcasts its own sensed data packets to the nearest CHs for which T_{n_i} time is required. After that, each cluster head C_i receives that data from the *k*-vertex disjoint paths and relays aggregated data to the *k*-vertex disjoint routes for which it required $T(C_i)$ time. During the multi hop data routing process, each sensor node requires T_p for processing the

received data packet. Therefore total time required to reach sensed data packet from the source node to the BS is

$$\sigma_{routing} = \sum_{n_i \in N_{active}} \left(\left(\sum_{i=1}^{i=level_{max}} \left(T^i(C_i) + T_p \right) \right) + \left(\sum_{i=1}^{p} (T_{n_i} + T_p) \right) \right) \quad (8)$$

Lemma 6: *Estimated transmission delay T_{n_i} for sensor node n_i is $\frac{dis(n_i, k_j)}{c} + \tau_i$ where τ_i is the processing time and k_j is the selected parent nodes.*

Proof: Estimated transmission delay is the approximate time required by a sensor node n_i to transmit its sensed data packet to all its parent nodes k which are selected for data transmission. The estimated transmission delay T_{n_i} can be defined as

$$T_{n_i} = \{\max\{T_{n_{i,j}} + \tau_i, \forall k \in NP_{ch}(n_i)$$

where $T_{i,j}$ is the estimated delay time between the sensor node n_i and parent node k_j and τ_i is the processing delay of n. The T_{n_i} can be calculated as given

$$T_{n_{i,j}} = \frac{dis(n_i, k_j)}{c} \quad (9)$$

where c is the speed of light.

VII. Simulation Results

The performance of the proposed scheme (DEEHC-kVDPR-RRM) is evaluated and compared with the existing algorithms EEHC, and ICE in terms of energy depletion ratio, node survival ratio, average success rate, data routing delay. All the algorithms are simulated using MATLAB R2012b and C programming. The number of disjoint multipath from each source node to the nearest CH is k=3. The probabilities of intra-cluster node failure and CH failure are initially set $P_{node\_failure}$ = 0.02 and $P_{CH\_failure}$ = 0.004 [24-25]. To verify the effectiveness, reliability, generality of the proposed algorithms, simulations are conducted into two scenarios: small scale network, and large scale network.

- **Scenario 1:** In scenario 1, sensor nodes are randomly deployed to form a near-uniform distribution in the sensing area of the size 100× 100 meter square and a BS is placed at the coordinates (150, 175) inside the network to collect data from the deployed sensor nodes.
- **Scenario 2:** Sensor nodes are deployed randomly to form a non-uniform distribution in the sensing area of the size 600× 600 meter square and a BS is placed at the coordinates (680, 720) inside the network to collect data from the deployed sensor nodes.

A. Energy Depletion Rate

Fig.1.a and Fig.1.b show details of energy depletion rate in scenario 1 and scenario 2 respectively. In the Fig. 1.a, the number of deployed sensor nodes increases from 10 to 100. We see that the energy depletion rate in the proposed scheme (DEEHC-kVDPR-RRM) is 10% lower than EEHC and 13% lower than ICE algorithm. This is because deployed sensor nodes are arranged into efficient number of cluster and the proposed scheme selects k-vertex disjoint paths depending on the energy level of the deployed sensor nodes.

Fig. 1.b shows the results of our experiments in large scale network scenario. Here, we also see that the energy depletion ratio of our proposed scheme is 15% lower than EEHC and 17% lower than ICE algorithm. So, our proposed scheme shows better performance in terms of energy depletion rate in large size network compared to other existing approaches. In Fig. 1.b, energy depletion rate is increased compared to the Fig. 1.a. This is caused due to the increment of network size. However, in large scale network, rate of energy depletion ratio in the proposed scheme is less compared to EEHC and ICE algorithms due to cluster based data routing strategy and energy efficient multiple data routing paths selection process.

B. Nodes Survival Ratio

In this section, we report our experimental results on node survival ratio in small scale as well as large scale network scenarios. Node survival rate is the measure of ratio between the number of current alive nodes to the total number of deployed nodes. Fig. 2.a shows the node survival rate of the proposed scheme in small scale network (Scenario 1). Here, we observe that node survival rate in the proposed scheme is 12% more as compared to EEHC and 10% ICE respectively. It is due to distributed cluster based data routing process where each deployed node transmits its data to the nearest cluster head by multi hop communication and CHs also relay their aggregated data packets to the BS by multi hop communication. Secondly, proposed scheme reduces the network communication overhead and energy consumption with the efficient RRM, so that deployed sensor nodes would extend their lifetime.

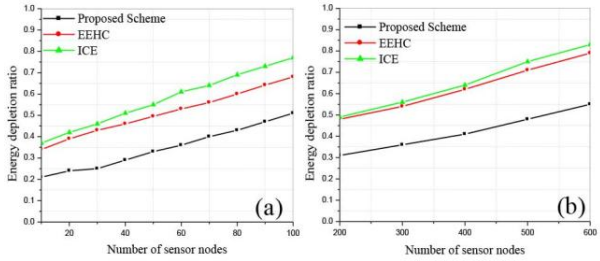

Fig.1. Ratio of energy depletion with different nodes number.

Fig. 2.b shows the comparison of node survival ratio for large scale network topology (Scenario 2). In this figure, we also observe that the proposed scheme has 6% more node survival rate compared to EEHC and 8% compared to ICE. This is because in our proposed scheme each deployed node identifies *k*-vertex disjoint paths using path vector information where path vector information contains nearest neighbor information of each deployed sensor node. However, with the increase of network size, the node survival ratio is decreased. It is due to the fact that the increase of network nodes number would lengthen the average effective length of the path, and thus the probability of path failure is also increased. It speeds up route recover process within the network and hence

increases energy consumption of the deployed sensor nodes. So, the node survival ratio is reduced in large scale network. However, the node survival ratio of the proposed scheme is still the highest compared to EEHC and ICE algorithms.

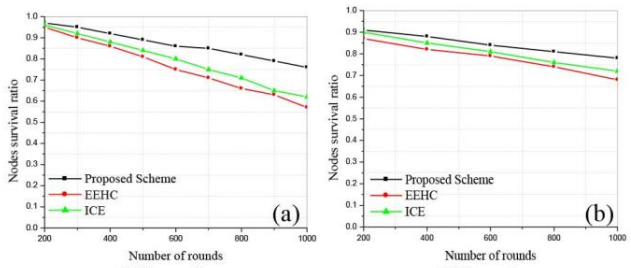

Fig.2. Nodes survival ratio per round with different scale, a) Scenario 1 b) Scenario 2.

C. *Average Success Rate*

Fig. 3.a and Fig 3.b show details of the average success rate in scenario 1 and scenario 2. It is measured as the ratio of message sent from source node to that received by the BS/ sink node. The node failure probabilities are assumed as $P_{node\_failure} = 0.02$ and $P_{CH\_failure} = 0.004$. From Fig. 3.a, we can see that the proposed (DEEHC-kVDPR-RRM) scheme can forward more packets to the BS than EEHC and ICE algorithms to tolerate network cuts. In most cases, the proposed scheme can send 8% more compared to EEHC algorithm and 11% more compared to ICE algorithm. This is because the proposed scheme provides a distributed RRM algorithm for *k*-vertex disjoint paths maintenance process during the data routing which improves the successful delivery rate. Note that average success rate always decreases as the size of the network is extended which indicates that the large network scale will lengthen the routing path from source to sink and increase the packet loss rate (Fig. 3.b). But the average success rate of the proposed scheme is still the highest.

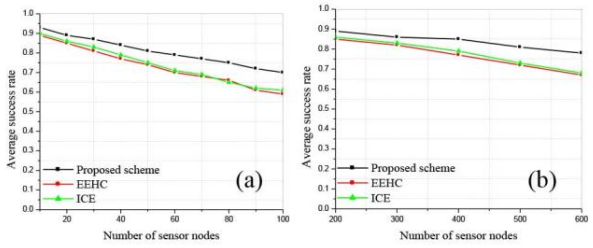

$P_{node\_failure} = 0.02$ and $P_{CH\_failure} = 0.004$

Fig.3.Averge success rate of packet delivery with different failure probability, a) Scenario 1 b) Scenario 2.

D. *Data Routing Delay*

Fig. 4.a and Fig. 4.b show the data routing delay in scenario 1 and scenario 2 respectively. From Fig. 6.a, we can see that the proposed scheme outperforms the ICE and EEHC in terms of data routing delay in scenario 1. A lower delay of packet delivery can be explained by the faster BS communication routing and shorter alternative paths available for data transmission from source node to BS in presence of network cuts condition. On the other hand, during the data routing process, if any sensor node detects any network cut than transmitted packet reaches to the destination node by the shorter alternative data routing path. Fig. 4.b shows data routing delay in scenario 2. With the increase of network size, the data routing delay is increased. This is because of in the large scale network average computational time is increased due to number of nodes increment within the network.

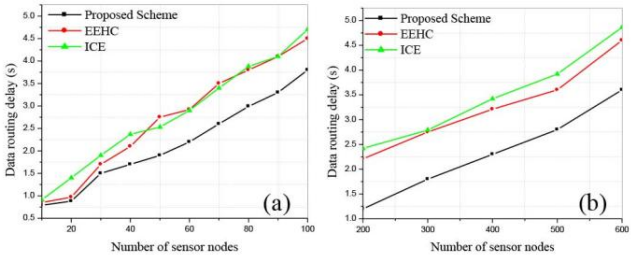

Fig.4. Average data routing delay with different node number, a) Scenario 1 b) Scenario 2.

VIII. CONCLUSION

In this paper, we have proposed a network cut tolerance data routing scheme for wireless sensor networks where each deployed sensor node transmits their data to the based station through the energy efficient *k*-vertex disjoint routes. The proposed clustering scheme (kVDPR) divides entire network into different clusters for better energy management and minimization of transmission energy of the deployed sensor nodes. Each deployed sensor node transmits data to the cluster head by the k-vertex disjoint paths to tolerate *k-1* number of network cut. Cluster head also aggregates all data packets and relay aggregated data packet to the BS through the k-vertex disjoint routs to tolerate of network cuts. In addition, we have also proposed a distributed routes maintenance process where each node and cluster head maintenance its *k*-vertex disjoint paths according to the single hop neighbor node residual energy condition. It has been shown that in worst case proposed scheme tolerates upto *k-1* number of network cuts through the data routing process and improves quality of serves of WSNs. The proposed data routing algorithm has required *O(N)* time complexity. Proposed scheme has been simulated extensively using two different scenarios of WSN and the simulation results have been compared with two existing approaches in terms of energy depletion rate, node survival ratio, average success rate, data routing delay in presence of cuts. Comparison results show that the proposed scheme given better performance compared to the other existing approaches. In the future, this work deserves to some real life-life applications such as agricultural crop management system, Livestock monitoring, road monitoring and home automation system.

REFERENCES

[1] I. Chatzigiannakis, G. Mylonas, S. Nikoletseas, "Modeling and evaluation of the effect of obstacles on the performance of wireless sensor networks," in *Proc. of the 39th Annual Simulation Symposium (ANSS'06)*, 2006, pp. 50-60.

[2] K. Ozaki, K. Watanabe, S. Itaya, N. Hayashibara, T. Enokido, and M. Takizawa, "A fault-tolerant model for wireless sensor-actor system," *in Proc. Of the 20th Int. Conf. Adv. Inform. Netw. Appl.*, Apr. 2006, pp.1-5.

[3] C. Cirstea, M. Cernaianu, and A. Gontean, " Packet loss analysis in wireless sensor networks routing protocols," *in Proc. Of the 5th Int. Conf. Telecommun. Signal Process.*, Jul. 2012, pp. 37-41.

[4] M. Haghpanahi, M. Kalantari, and M. Shayman, "Topology control in large-scale wirless sensor networks: Between information source and sink," *Ad Hoc Netw.*, vol.11, no.3, pp. 975-990, 2012.

[5] Fagen Li and Pan Xiong, "Practical Secure Communication for Integrating Wireless Sensor Networks Into the Internet of Things," *IEEE Sensors Journal*, vol. SEN-13, no. 10, pp. 3677- 3684, Oct. 2013

[6] I. Banerjee, P. Chanak, H. Rahaman, T. Samanta, "Effective fault detection and routing scheme for wireless sensor networks," *Computers and Electrical Engineering*, vol. 40, no. 6, pp. 291–306, 2014.

[7] S. Misra, P. Dias Thromasinous, "A simple, least time, and energy-efficient routing protocol with one-level data aggregation for wireless sensor network," *Journal of Systems and Software*, vol. 83, no. 5, pp. 852-860, 2010.

[8] K. Akkaya, M. Younis, " A Survey of routing protocols in wireless sensor network," *Ad Hoc Networks,* vol. 3, no. 3, pp. 325-349, 2005.

[9] I. F. Akyildiz, W. Su, Y. Sankarasubramaniam, E. Cayirci, "Wireless sensor networks: a survey," *Computer network,* vol. 38, no. 4, pp. 393-422, 2002,.

[10] N. Li and J.C. Hou, "FLSS: Afault-tolerant topology control algorithm for wireless networks," *in Proc. Of the 10th ACM Annu. Int. Conf. Mobile Comput. Netw.*, 2004, pp 275-286.

[11] N.Li and J.C. Hou, "Localized fault tolerance topology control in wireless and ad hoc networks," *IEEE Trans. on Parallel Distrib. Syst.*, vol. PDS-17, no. 4, pp. 307-320, Apr.2006.

[12] L.Wang, H. Jin, J. Dang, and Y. Jin, "A fault tolerant topology control algorithm for large-scal sensor network," in *Pro. 8th Int. Conf. Parallel Distrib. Comput, Appl. Technol.*, 2007, pp. 407-412.

[13] Y. Liu, Q. Zhang, and L. Ni, "Opportunity-Based Topology Control in Wireless Sensor Network," *IEEE Trans. on Parallel and Distrib. Syst.*, vol. PDS-21, no. 3, pp.405-416, May 2010.

[14] M. Cardei, S. Yang, and J. Wu, "Algorithms for fault-tolerant topology in heterogeneous wireless sensor networks," *IEEE Trans. on Parallel Distrib. Syst.*, vol. PDS-19, no.4, pp.545-558, Apr. 2008.

[15] W. Heinzelman, A. Chandrakasan, H. Balakrishnan, "An Application Specific Protocol Architecture for Wireless Microsensor Network," *IEEE Trans. Wireless Comm.*, vol.1, no.4, pp. 660-670, Oct. 2002.

[16] O. Younis and S. Fahmy, "HEED: A hybrid, energy-efficient, distributed clustering approach for ad hoc sensor networks," *IEEE Trans. Mobile Comput.*, vol. MC-3, no. 4, pp. 366-379, Oct./Dec. 2004.

[17] D. Kumar, T.C. Aseri, R. B. Patel, "EEHC: energy efficient heterogeneous clustered scheme for wireless sensor networks," *J. Computer Comm.*, vol. 32, no. 2, pp. 662-667, 2009.

[18] M. Bahramgiri, M.T. Hajiaghayi, and V.S. Mirrokni, "Fault Tolerant and 3-Dimensional Distributed Topology Control Algorithms in Wireless Sensor Network," in *Proc. Of the 11th IEEE Int'l Conf. Computer Comm. And Networks (ICCCN),* 2002.

[19] G.Calinescu and P.-J. Wan, "Rang Assignment for High Connectivity in Wireless Ad Hoc Networks," in *Proc. Of the Second Int'l Conf. Ad Hoc Networks and Wireless (AdHoc-Now)*, 2003.

[20] M. Hajiaghayi, N. Immorlica, and V. S. Mirrokni, "Power Optimization in Fault-Tolerant Topology Control Algorithms for Wireless Multi-Hop Networks," in *Proc. ACM MobiCom*, 2003.

[21] A. Boukerche, A. Martirosyan, "An inter-cluster communication based energy aware and fault tolerance protocol for wireless sensor networks," *Mobile Networks Appl*., vol.13, no. 6, pp. 614-626, 2008.

[22] H. A. Hamadi, C. Ing-Ray, "Redundancy management of multipath routing for intrusion tolerance in heterogeneous wireless sensor networks," *IEEE Trans. Network Service Manage.*, vol. NSM-10, no. 2, pp. 189-203, 2013.

[23] P. Chanak, I. Banerjee, J. Wang, and R.S. Sherratt, "Obstacle avoidance routing scheme through optimal sink movement for home monitoring and mobile robotic consumer devices," *IEEE Trans. Consumer Electronics*, vol. CE-60, no. 4, pp. 596–606, Nov. 2014.

[24] M. Azharuddin, P. Kiula, and P.K. Jana, "A distibuted fault tolerance clustering algorithm for wireless sensor networks," in *Proc. Of the IEEE Int. Conf. Adv. Comput., Commun. Inform.*, 2013, pp. 997-1002.

[25] M. Haghpanahi, M. Kalantari, and M. Shayman, "Topology control in large-scale wirless sensor networks: Between information source and sink," *Ad Hoc Netw.*, vol.11, no.3, pp. 975-990, 2012.

[26] S. Q. Ren, J. Park, Fault-tolerance data aggregation for clustering wireless sensor network, *Wireless Personal Commun.*, vol. 51, no. 1, pp. 179-192, 2009.

Dimensioning of Solar Enabled Base Stations: An Utility Maximization Approach

Suraj Suman and Swades De

***Abstract*—Solar enabled cellular base stations are getting significant attention because it avoid greenhouse gas emission as well as easily available everywhere. The dimensioning of the base station is very important issue where the photovoltaic (PV) panel size and storage capacity are determined to operate the system for a long time with minimum energy black out. Here the hourly harvested energy and traffic dependent hourly consumed energy are considered for analysis. First of all the quantized profile of harvested and consumed energy is obtained. To obtain the outage probability, a discrete-time Markov chain is formed using the different energy level of the battery. The transition probability depends on the harvested and consumed energy profile. It is observed that as the outage constraint becomes more stringent, the harvested energy which is neither utilized nor stored increases significantly. Here we are suggesting the system other than cost optimal where the excess energy is sold to the intelligent smart power grid to generate revenue. Three cities situated at different geographical locations are considered to verify the results.**

***Index Terms*—Solar enabled base station, Energy Harvesting, Discrete-time Markov chain, Outage probability.**

I. Introduction

Today pollution is a very severe issue faced by various countries [1]. It is reported that China, USA and India are three major greenhouse gas emitter across the globe [2]. The adverse effect of pollution on health and environment is very hazardous and may lead to early age death. One of the major source of greenhouse emission is diesel generators used to power the base station. On an average 1500 litres of diesel are consumed by a base station monthly [3]. Apart from pollution, time varying cost as well as transportation is also a difficulty with diesel reliable base stations specially in remote areas.

Now a day renewable sources of energy like solar, wind etc. are found to be promising solution for base station in order to provide the mobile access [4]. Easy availability, environmental friendly, cost effectiveness and less maintenance are some key features which encourage to adopt this solution. The remotely separated regions can also be connected with wireless access using renewable energy sources. These sources are also very helpful in the emergency situation like complete blackout of power and disaster.

Several industry leaders are taking keen interest in installing the solar enabled base station especially in the regions which are not connected like Orange in rural Africa, Eltek in South Africa & Arab Gulf region, Huawei in China & Pakistan, Dialog Telekom in Sri Lanka, Ameresco in United States of America etc. have gained considerable attention. Very recently with help of government of India, Vihaan Network Limited (VNL) has set up nearly 2200 solar powered mobile communication towers in under-developed, inaccessible and heavily forested areas in order to connect more than 1.8 crore citizens with nearly 39 lakh mobile connections [5].

Suraj Suman and Swades De are with the Department of Electrical Engineering, Indian Institute of Technology Delhi, New Delhi, India. (E-mail: {suraj.suman, swadesd}@ee.iitd.ac.in).

The article is organized as follows: in section II the previous reported works are presented followed by outage and excess probability evaluation in section III. Section IV contains result and discussion. The utility optimal dimensioning is presented in section V followed by conclusions in section VI.

II. Related Works

As the solar energy is available during day time only, so the dimensioning of PV panel as well as battery should be done properly such that the energy blackout issue can be minimized. Dimensioning is an important issue as under dimensioning leads to frequent power outage whereas over dimensioning leads to unnecessary increased capital cost.

Days of autonomy criteria is used to dimension the storage capacity for a given photovoltaic panel size [6], [7]. Days of autonomy is the consecutive number of days over which the energy generated is less than threshold [8]. This is not the cost optimal system and threshold strongly depends on the geographical location. Also there are chances of over dimensioning the system. These methods are neither cost optimal nor accurate.

Intensive computation based cost optimal systems are designed in [3], [9]–[13] to meet the required power outage probability. The system is dimensioned using loss of power supply in cost optimal sense [9, 10]. In [11], a multistate Markov model is presented to dimension the system where extensive simulations are used to meet the required outage probability. Zero grid Energy Networking (ZEN) concept is presented in [3] which is based on a networks of BSs that are solely powered with renewable energy sources. Using the Typical Metrological Year (TMY) for a given location is used for dimensioning the system. The system is dimensioned using the battery charge levels obtained from simulation. Hybrid base station is dimensioned which primarily depends on solar but energy is purchased from power grid whenever required [12]. The system is dimensioned aiming to minimize the capital expenditure (CAPEX) which accounts for the cost of PV panel & battery and operational expenditure (OPEX) which accounts for power purchased from grid. In [13], using a Markov model the synthetic radiation data is first generated then storage energy is iteratively evaluated for a given panel size. The iteration runs from either the starting possible values or by initial guess which makes it computationally intensive.

Few methods are reported to compute the outage probability

analytically rather than iteration. Outage probability is the key performance parameter in dimensioning the solar enabled system. In [14], Beta distribution based modelling is done. In [15], using Monte Carlo method the solar radiation data is generated and modelled using exponential distribution. They provide rough estimation because it is difficult to capture the variation of solar data through a well known distribution as it depends on geographic location as well as environmental condition which is changing rapidly. A discrete-time Markov process based model is presented to compute outage probability [16]. This model is based on several threshold parameters and evaluates outage probability for larger size of PV panels only. In [17], a discrete time Markov chain based method is presented where the energy harvested by panel is estimated based on daily solar radiance level. The daily data does not provide a good accuracy and may lead to inaccurate dimensioning.

Here in this work, the solar enabled base station is analysed using the hourly data set of harvested energy and traffic dependent hourly energy consumption profile. The key contributions of our work are as follows:

1) A simple model using discrete-time Markov chain for evaluating the probability of energy outage and excess event is presented. The evaluated outage and excess probability is compared with the simulation result of empirical data to validate the presented model.
2) It is observed that significant amount of excess energy is going to waste which can not be stored. Here the system is dimensioned with same outage constraint which will provide maximum utility when the excess energy is sold back to the intelligent power grid.

III. Outage and Excess Probability Estimation

The statistical solar data of last 14 years (2001-2014) are used. The data available from National Renewable Energy Laboratory (NREL) is fed into System Advisor Model (SAM) to get the hourly and daily energy generated by a panel size of 1 KW rating with default setting [18]. The lead acid batteries are used to store the energy.

The energy generated by the photovoltaic cell of size n_{PV} is given as,

$$E_{n_{PV}} = n_{PV} E_{1KW}, \tag{1}$$

where E_{1KW} denotes the energy generated by a solar panel of rating 1 KW which is considered as reference panel.

In this work the hourly energy harvested is taken into consideration for analysis. Let E_{cons} denotes the hourly energy consumption by base station. First of all the hourly energy harvested by the panel size n_{PV} and the hourly consumed profile data is quantized with quantization step size Δ. Let $\mathbf{E_{nPV}}$ is the hourly energy harvested profile where as $\mathbf{E_C}$ is the hourly consumed profile obtained after quantization.

The system becomes off when required energy is not supplied either by panel or storage. Such an event is called outage. Whereas if the harvested energy which is extra and can not be added to the storage as it is already full then such an event is called excess. In this section we will evaluate the outage and excess probability for a given size of PV panel and number of

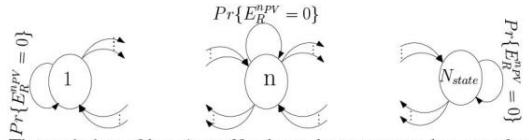

Fig. 1. The variation of hourly traffic dependent consumed energy for a week.

battery. So the residue energy profile $\mathbf{E_R^{nPV}}$ can be given as,

$$\mathbf{E_R^{nPV}} = \mathbf{E_{nPV}} - \mathbf{E_C} \tag{2}$$

The residue energy given in (2) added to the system. The residue energy profile indicates that the energy is drawn from the battery as well as energy is added to the battery. Using this fact a discrete-time Markov chain is formed with different energy levels of battery as shown in Fig.1.

Let N_B batteries are in the system along with PV panel of size n_{PV} having total storage capacity B_{cap} with depth of discharge DoD and assuming that each battery performs with full efficiency. The energy level of first and last energy state of batteries are $(1 - DoD)B_{cap}$ and B_{cap} respectively. The total number of states in the Markov chain is given as,

$$N_{state} = \left\lfloor \frac{B_{cap}}{\Delta} \right\rfloor - \left\lceil \frac{(1 - DoD)B_{cap}}{\Delta} \right\rceil + 1 \tag{3}$$

where $\left\lceil \frac{(1-DoD)B_{cap}}{\Delta} \right\rceil$ and $\left\lfloor \frac{B_{cap}}{\Delta} \right\rfloor$ denotes the quantized energy level of first and last state respectively.

Let $L = [-l_1, l_2], l_1 > 0, l_2 > 0$ is domain of residue energy profile $\mathbf{E_R^{nPV}}$. The elements of the transition matrix which are transition probabilities of Markov chain is calculated in (4) - (5) using residue energy profile. The steady state probability of the different energy states of the battery (say $\mathbf{E_{Bat}}$) can be obtained from the transition matrix. As the residue energy is either added or extracted to the battery which is the stored system energy. The total stored energy in the system is given as,

$$\mathbf{E_{system}^{nPV}} = \mathbf{E_R^{nPV}} + \mathbf{E_{Bat}}, \tag{7}$$

If residue energy is negative then the energy is extracted from the battery upto $(1-DoD)B_{cap}$ whereas if the residue energy is positive then the energy is added to the system maximum upto B_{cap}. If the energy level goes below $(1 - DoD)B_{cap}$ while extracting then the energy outage event happens whereas of the energy level goes above B_{cap} then the excess power event happens. Mathematically the outage and excess probability can be expressed as,

$$P_{out} = \Pr\left\{ \mathbf{E_{system}^{nPV}} \leq \left\lceil \frac{(1 - DoD)B_{cap}}{\Delta} \right\rceil \right\} \tag{8}$$

$$P_{excess} = \Pr\left\{ \mathbf{E_{system}^{nPV}} \geq \left\lfloor \frac{B_{cap}}{\Delta} \right\rfloor \right\} \tag{9}$$

IV. Result And Discussion

In this section three cities of India New Delhi, Ahmedabad and Itanagar situated at different geographical locations are considered for analysis. Ahmedabad has highest potential for solar energy whereas Itanagar has lowest [19]. The energy harvested for each hour of the day is obtained from SAM for

$$P[i,j] = \begin{cases} \Pr\{\mathbf{E_R^{nPV}} = j-i\}, & \text{if } 1 < i < N, 1 < j < N, \;\; j-i \in L \\ 0, & \text{otherwise} \end{cases} \tag{4}$$

$$P[i,1] = \begin{cases} \sum_{z=l_1}^{1-i} \Pr\{\mathbf{E_R^{nPV}} = z\}, & \text{if } 1 \le i \le N, \;\; 1-i \in L \\ 0, & \text{otherwise} \end{cases} \tag{5}$$

$$P[i,N] = \begin{cases} \sum_{z=N-i}^{l_2} \Pr\{\mathbf{E_R^{nPV}} = z\}, & \text{if } 1 \le i \le N, \;\; N-i \in L \\ 0, & \text{otherwise} \end{cases} \tag{6}$$

TABLE I
THE ROOT MEAN SQUARE ERROR (RMSE) FOR OUTAGE PROBABILITY CALCULATED FROM THE PRESENTED MODEL AND EMPIRICAL DATA FOR DIFFERENT PANEL SIZE FOR DIFFERENT CITIES.

	Ahmedabad			New Delhi			Itanagar		
n_{PV} (in KW)	10	11	12	10	11	12	10	11	12
$\Delta = 1$	0.0141	0.0133	0.0127	0.0156	0.0152	0.0142	0.0285	0.0255	0.0230
$\Delta = 1.5$	0.0078	0.0070	0.0068	0.0091	0.0076	0.0072	0.0346	0.0142	0.0097
$\Delta = 2$	0.0094	0.0086	0.0086	0.0097	0.0094	0.0104	0.0195	0.0175	0.0155

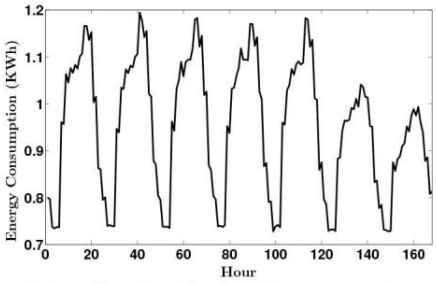

Fig. 2. The variation of hourly traffic dependent consumed energy for a week.

these places using solar data of years 2001 to 2014. The cost of PV panel size of rating 1 KW and cost of a lead acid battery is considered as $ 1000 and $ 280 respectively. The depth of discharge (DoD) is taken as 0.7.

The power consumption profile of a LTE macro base station is given as [20],

$$P_{BS}(t) = N_{TRX}(P_o + \delta_p \rho(t) P_{max}) \tag{10}$$

where N_{TRX} is the number of transceivers. Here 2×2 Multi Input Multi Output (MIMO) configuration with 3 sectors are considered i.e. $N_{TRX} = 6$. The traffic profile $0 \le \rho(t) \le 1$ is generated according to the procedure described in [16]. $P_o = 118.7$ is the circuitry power required to run the amplifiers, $\delta_p = 2.66$ is the slope and $P_{max} = 40$ is the maximum power transmitted. The power consumption profile for one week duration is shown in Fig. 2.

The outage probability obtained from empirical data is calculated using (11). where $B(i)$ is the current battery level at day i, $B(i-1)$ is the battery level on previous day, $E_{BS}[i]$ is the energy consumption by the base station on day i and $E_{n_{PV}}[i]$ is the energy harvested by solar panel on day i. The outage probability is the ratio of the number of times the battery capacity goes below $(1 - DoD)B_{cap}$ to the total number of days.

TABLE II
COMPARISON OF THREE DIFFERENT COMBINATION OF PANEL SIZE AND NUMBER OF BATTERY HAVING OUTAGE PROBABILITY $P_{out} \le 0.001$.

	Case 1	Case 2	Case 3
(n_{PV}, N_B)	(10,25)	(11,17)	(12,14)
$Cost_{system}$	17000	15760	15920
$Cost_{optimal}$		✓	
Excess Energy (yearly in KWh)	7.34 $\times 10^3$	9.00 $\times 10^3$	10.57 $\times 10^3$

The outage probability obtained from the presented model is compared with that obtained from empirical data. They are plotted in Fig. 3 for both the model presented and empirical data with different panel sizes against the number of battery. As the number of battery increases the outage probability decreases. The root mean square error (RMSE) for different quantization step size and different panel size are listed in Table I. The acceptable upper limit of RMSE is 0.07 [21]. The number of battery is ranging from 6 to 40 for RMSE calculation. The listed values shown indicate a good match of outage probability obtained from the presented model and empirical data.

V. COST OPTIMAL SELECTION : MAY NOT BE BEST OPTION

Till now the selection of photovoltaic PV panel size and storage capacity is based on cost optimal for a given performance constraint in terms of outage probability [9]–[13]. But as the performance constraint becomes more stringent,the excess energy significantly increases. This energy is not stored so ultimately useless. Two combination of PV panel are listed in Table II along with the cost optimal system with same

$$B(t) = \begin{cases} B_{cap} & \text{if } B(t) \geq B_{cap} \\ B(t-1) + E(t) - E_{BS}(t), & \text{if } (1-DoD)B_{cap} < B(t) < B_{cap} \\ 0.3B_{cap} & \text{if } B(t) \leq (1-DoD)B_{cap} \end{cases} \tag{11}$$

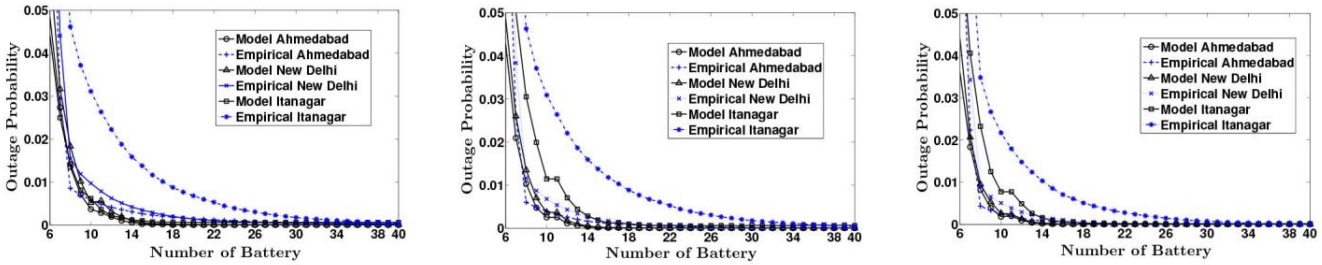

(a) 10 KW (b) 11 KW (c) 12 KW

Fig. 3. The variation of outage probability against the number of battery for three cities with different panel sizes (a) 10 KW, (b) 11 KW and (c) 12 KW.

TABLE III
THE DIMENSIONING OF SYSTEM ACCORDING TO COST OPTIMAL AND UTILITY OPTIMAL CRITERIA WITH DIFFERENT OUTAGE PROBABILITY CONSTRAINT FOR DIFFERENT CITIES.

	Ahmedabad			New Delhi			Itanagar		
	Cost Optimal	Utility Optimal	utility ($)	Cost Optimal	Utility Optimal	Utility ($)	Cost Optimal	Utility Optimal	utility ($)
$P_{out} \leq 0.01$	(8,14)	(12,8)	2076	(8,16)	(12,8)	2329	(13,17)	(16,14)	701
$P_{out} \leq 0.001$	(11,17)	(15,13)	972	(10,23)	(14,13)	1779	(13,24)	(16,17)	1264

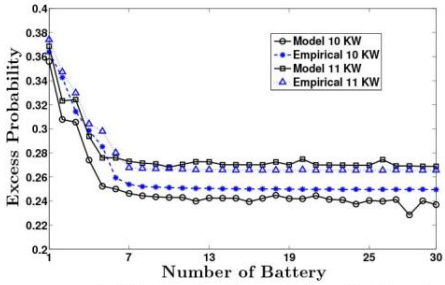

Fig. 4. The excess probability against the number of battery for Ahmedabad city for PV panel size of 10 KW and 11 KW rating.

performance constraint i.e. outage probability $P_{out} \leq 0.001$. One can observe that the excess energy generated yearly is very high and increases with panel size. The variation of excess probability obtained from the presented model and empirical data is shown in Fig. 4 with panel size 9 KW and 10 KW for Ahmedabad city. Nearly more than 25 % of times the excess event occurs.

Significant advancements in power grid technology facilitates the bidirectional energy flow means energy can be purchased as well sold back to the grid also [22]. Assuming that these cities have such facility, we can utilize the excess energy produced to generate revenue. Here we will design a framework where combinations other than the cost optimal may be beneficial without degrading the performance.

The dimensioning is done to operate the system for long period of time up to 20 years. This includes the capital expenditure (CapEx) accounts for initial installment whereas operational expenditure (OpEx) accounts mainly for battery replacement cost. So the cost optimal combination is chosen as,

$$\begin{aligned} \underset{n_{PV}, N_{B_T}}{\text{minimize}} \quad & C_{n_{PV}} n_{PV} + C_B N_{B_T} \\ & P_{out} \leq p. \end{aligned} \tag{12}$$

where n_{PV} is the pannel size. N_{B_T} is the total number of battery used for whole period of operation where as N_B is the number of battery used at any time in the system. $C_{N_{PV}}$ and C_B are the cost of 1 KW PV panel with 1 KW rating and 12 V 205 Ah lead-acid battery. Here the run time of 14 years is considered.

The battery lifetime is limited which depends upon the number of cycles as well as cycle's depth-of-discharge. The variation of lifetime of battery against number of battery is plotted in Fig.5. One can observe that as number of battery increases the lifetime increases. Also higher panel size has longer battery lifetime.

Let C_{opt} is the cost of system $(n_{PV_{opt}}, N_{B_{opt}})$ with cost optimality criteria with given outage probability as discussed in (12). Let $C_{Revenue}(n_{PV}, N_B)$ be the revenue generated by selling the energy back to the grid is given as,

$$C_{Revenue}(n_{PV}, N_B) = \sum_{\text{14 years}} C_{sell}[i] E_{excess}[i] \tag{13}$$

where $C_{sell}[i]$ is the selling price of 1 KWh energy on hour i and $E_{excess}[i]$ is the excess energy generated (in KWh) on hour i with system combination (n_{PV}, N_B). For simulation purpose the cost of selling one unit of electricity i.e. $C_{sell}[i] =$ \$0.05 is considered.

So the total expenditure of system to run over 14 years is with

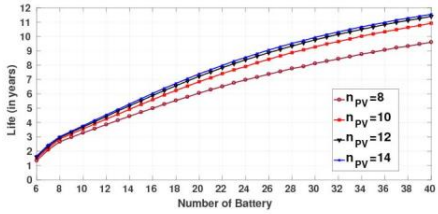

Fig. 5. The excess probability against the number of battery for Ahmedabad city for PV panel size of 10 KW and 11 KW rating.

system dimension (n_{PV}, N_B),

$$C_{Ex}(n_{PV}, N_B) = C_{CapEx}(n_{PV}, N_B) + C_{OpEx}(n_{PV}, N_B) - C_{Revenue}(n_{PV}, N_B) \quad (14)$$

where $C_{Ex}(n_{PV}, N_B)$ is is total expenditure, $C_{CapEx}(n_{PV}, N_B)$ is the CapEx, $C_{OpEx}(n_{PV}, N_B)$ is the OpEx and $C_{Revenue}(n_{PV}, N_B)$ is the revenue generated by selling the energy.
The utility function is defined as,

$$U(n_{PV}, N_B) = C_{Ex}(n_{PV_{opt}}, N_{B_{opt}}) - C_{Ex}(n_{PV}, N_B) \quad (15)$$

This utility function accounts for net profit over cost optimal system dimensioning. Our aim is to choose a combination which generates the maximum revenue as follows:

$$\underset{n_{PV}, N_B}{\text{maximize}} \quad U(n_{PV}, N_B) \qquad P_{out} \leq p. \quad (16)$$

where p is outage probability constraint. So our aim is to choose the system combination with maximum utility without degrading the performance.
The utility optimal and cost optimal selections are listed in Table III for different performance constraints. One can obeserve that significant saving can be done if the system is dimensioned using the utility optimal criteria. Usually the base stations are deployed in bulk in that scenario this will save significant revenue without compromising the performance.
Currently the cost of PV panel and battery is higher but as the technology advances day by day the efficiency will increase and the cost will decrease. Also the selling price vary on country by country. This analysis is done here to motivate the operators so that they can earn in log term without degrading the performance. Along with economical utility such systems have significant social utility which provide energy from renewable sources along with wireless access.

VI. Conclusions

The quantized version of hourly harvested solar energy and consumed energy are used to analyse the system. A discrete-time Markov chain based model is presented to obtain the outage probability. The transition probability depends on the profile of residue energy. A good match between the outage probability obtained from presented model and empirical data validate the accuracy of model. The excess energy produced which is neither utilized nor stored increases significantly with stringent outage constraint. Taking advantage of smart grid technology, the system is over dimensioned and the excess energy is sold back to the grid. A utility function is defined which accounts for net profit and the system is dimensioned aiming to maximize the utility. Simulation results indicate that this simpler non-parametric model can analyse the system efficiently.

References

[1] M. Webb, "Smart 2020: Enabling the low carbon economy in the information age," *Tech. Report*, 2008.
[2] Co2 emissions from fuel combustion highlights. International Energy Agency, 2016. Accessed: Dec. 19, 2016. [Online]. Available: https://www.iea.org/publications
[3] M. A. Marsan, G. Bucalo, A. D. Caro, M. Meo, and Y. Zhang, "Towards zero grid electricity networking: Powering bss with renewable energy sources," in *Proc. IEEE Int. Conf. Commun. Wksp. (ICC)*, June 2013, pp. 596–601.
[4] A. Jhunjhunwala, B. Ramamurthi, S. Narayanamurthy, J. Rangarajan, and S. Raj, "Powering cellular base stations: A quantitative analysis of energy options," *Dept. Telecom Center Excellence (RiTCOE) , Indian Inst. Technol., Chennai, India , Tech. Rep.*, 2012.
[5] S. Nagpal, "The worlds largest green mobile communication network is now live!" *Vihaan Networks Ltd. (VNL), New Delhi, India*, 2016.
[6] H. A. M. Maghraby, M. H. Shwehdi, and G. K. Al-Bassam, "Probabilistic assessment of photovoltaic (pv) generation systems," *IEEE Trans. Power Syst.*, vol. 17, no. 1, pp. 205–208, Feb. 2002.
[7] N. Kakimoto, S. Matsumura, K. Kobayashi, and M. Shoji, "Two-state markov model of solar radiation and consideration on storage size," *IEEE Trans. Sustain. Energy*, vol. 5, no. 1, pp. 171–181, Jan. 2014.
[8] M. Bhuiyan and M. A. Asgar, "Sizing of a stand-alone photovoltaic power system at dhaka," *Renewable Energy*, vol. 28, no. 6, pp. 929–938, May 2003.
[9] E. Ofry and A. Braunstein, "The loss of power supply probability as a technique for designing stand-alone solar electrical (photovoltaic) systems," *IEEE Trans. on Power App. Syst.*, no. 5, pp. 1171–1175, May 1983.
[10] G.B.Shrestha and L. Goel, "A study on optimal sizing of stand-alone photovoltaic stations," *IEEE Trans. Energy Convers.*, vol. 13, no. 4, pp. 373–378, Dec. 1998.
[11] V. Chamola and B. Sikdar, "A multistate markov model for dimensioning solar powered cellular base stations," *IEEE Trans. Sustain. Energy*, vol. 6, no. 4, pp. 1650–1652, Oct. 2015.
[12] M. Meo, Y. Zhang, R. Gerboni, and M. A. Marsan, "Dimensioning the power supply of a lte macro bs connected to a pv panel and the power grid," in *Proc. IEEE Int. Conf. Commun. (ICC)*, June 2015, pp. 178–184.
[13] R. S. Weissbach and J. R. King, "Estimating energy costs using a markov model for a midwest off-grid residence," in *Proc. IEEE Green Technologies Conf.*, Apr. 2013, pp. 430–434.
[14] I. Abouzahr and R. Ramakumar, "Loss of power supply probability of stand-alone photovoltaic systems: a closed form solution approach," *IEEE Trans. Energy Convers.*, vol. 6, no. 1, pp. 1–11, Mar. 1991.
[15] J. Song, V. Krishnamurthy, A. Kwasinski, and R. Sharma, "Development of a markov-chain-based energy storage model for power supply availability assessment of photovoltaic generation plants," *IEEE Trans. Sustain. Energy*, vol. 4, no. 2, pp. 491–500, Apr. 2013.
[16] V. Chamola and B. Sikdar, "Power outage estimation and resource dimensioning for solar powered cellular base stations," *IEEE Trans. Commun.*, vol. 64, no. 12, pp. 5278–5289, Dec. 2016.
[17] G. Leonardi, M. Meo, and M. A. Marsan, "Markovian models of solar power supply for a lte macro bs," in *Proc. IEEE Int. Conf. Commun. (ICC)*, May 2016, pp. 1–7.
[18] N. R. E. Laboratory. System advisor model (sam). National Renewable Energy Laboratory. Accessed: Sep. 15, 2016. [Online]. Available: https://www.sam.nrel.gov
[19] India solar resource map. Ministry of New and Renewable Energy, India. Accessed: Sep. 15, 2016. [Online]. Available: www.mnre.gov.in
[20] G. Auer, V. Giannini, I. Gódor, P. Skillermark, M. Olsson, M. A. Imran, D. Sabella, M. J. Gonzalez, C. Desset, and O. Blume, "Cellular energy efficiency evaluation framework," in *Proc. IEEE Veh. Technol. Conf. (VTC Spring), 2*, May 2011, pp. 1–6.
[21] D. Hooper, J. Coughlan, and M. Mullen, "Structural equation modelling: Guidelines for determining model fit," *Articles*, p. 2, May 2008.
[22] X. Lu, W. Wang, and J. Ma, "An empirical study of communication infrastructures towards the smart grid: Design, implementation, and evaluation," *IEEE Transactions on Smart Grid*, vol. 4, no. 1, pp. 170–183, Mar. 2013.

Impact of Co-Channel and Adjacent Channel Transmissions on DVB-T2 Broadcast

Anshul Thakur and Swades De
Indian Institute of Technology, Delhi
anshul.thakur@ee.iitd.ac.in, swadesd@ee.iitd.ac.in

Abstract
This paper presents a study on the impact of transmitting in the same channel or in the adjacent channel of an ongoing DVB-T2 Broadcast. The power of an interferer, implemented as a bandpass Gaussian waveform was measured for values which resulted in Picture Failure in the ongoing DVB-T2 broadcast with varying levels of channel overlap. Through this study, the maximum tolerable interference from a secondary user on the incumbent broadcaster is evaluated in the form of Protection Ratios. Results for different code rates and guard band settings for the DTT transmission are compared.

I. Introduction

As more countries continue to switch from Analog Broadcasting to its digital counterpart, large amount of spectrum is being freed up.Its use for other technologies is being investigated throughout the world. ITU had ratified the proposal to reallocate the 694-790MHz band to IMT services. It has also scheduled discussions over the future uses of DTT band (470-694MHz) and has requested studies for the same [1].

In India, there is currently only one broadcaster, Doordarshan, holding exclusive transmission rights for terrestrial broadcast and uses DVB-T2. However, opening up this sector to private players has been recommended [2]. Further, GoI'sBharatNet project is underway to provide fiber access till District's Block level, while subsequent distribution is still an open area. We envision TV Whitespace communication to play a significant role in this last mile distribution.

Extensive work has been done to demonstrate the viability of TV Whitespace as a suitable candidate for rural broadband connectivity [3]. CR based approaches are being formalized and IEEE 802.22 WRAN standard has been developed as a result. Further, 802.11af has extended Wi-Fi operation into TVWS. Also, LTE-U has forayed into TV Whitespaces. [4] presented a demonstrator for using LTE offload to DVB-T2 exploiting its Future Extension Frames (FEF) aimed at cooperative spectrum sharing via provider level agreements. In the absence of such agreements, interference issues arise when secondary services operate in the same spectrum as an ongoing TV broadcast. Hence, protection of incumbent services becomes paramount. Studies have tried to quantifythese effects. Popescu et al. [5], [6] have catalogued various configurations in which an interferer may impact the DTT in typical working configurations, and reverse cases where DTT acts as an interferer. [7] have evaluated Protection Ratios required for LTE-A Femtocell operation indoors with varying degree of channel overlap with the primary DTT broadcast. [8] evaluates PRs for LTE-800 transmission in adjacent channels of a DVB-T service. [9] considers coexistence between DVB-T2 Lite services and LTE with focus on LTE as primary. [10] evaluates the effect of using anti-LTE filters for DTT reception considering adjacent channel use of LTE at varying traffic loads, while [11] considers the effect of LTE load, LTE uplink and downlink in adjacent channels only.

This work aims to experimentally quantify the effects of a Gaussian type interferer transmitting in an adjacent channel to the DVB-T2 DTT broadcast. This paper also records the spectral occupancy in Delhi region. The rest of the paper is organized as follows. Section II introduces the system parameters and the setup. Section III outlines the principle of measurement. IV reports the results of the experiments performed and V concludes the paper.

II. System Setup

We seek to quantify the Interference Protection Ratios for DVB-T2 reception. Interference Protection Ratio is the minimum value of wanted-to-unwanted signal ratio that must be maintained in order to achieve a specified reception quality at the receiver. For DVB-T2, this is defined as the onset of picture failure (PF)

using Subjective Point Failure (SPF) method for domestic TV Receivers where no more than one frame error is visible in a time span of 20 seconds [12].
An MPEG-2 Transport stream video was used for DTT Broadcast. SDR implementation of the DVB-T2 transmitter implementing the 1.1.1 version of the specification was used. Various parameters of the Transmitters are given in the table I.
Gaussian interferer was also created using an SDR basedimplementation; FFT plot for the same is shown in figure 1. Transmit antennas used for this purpose were 6dBi Wideband bowtie antennas. A silicon based off-the-shelf DVB-T2 tuner with a whip dipole antenna was used for reception of the DVB-T2 broadcast. FFT measurements were taken using an SDR based receiver placed adjacent to the broadcast receiver.Also, SNR from the TV Receiver was used. The scenario envisioned is shown in figure 2.

Table 1: Transmitter Parameters

DVB-T2 Transmitter Parameters	**Value**
Center Frequency	429MHz
Sample Rate	9.14286Msps
Baseband Gain	0dB
RF Gain	6dB
DTT Bandwidth	8MHz
PAPR correction	None
Mode	SISO
Interferer	**Value**
Sample Rate	9.14286Msps
Baseband Gain	0dB
RF Gain	6dB
Bandwidth	8MHz

Table II: Supported Transmission Parameters

Code Rate	**GI 1/16**	**GI 1/8**
1/2	Yes	Yes
2/3	Yes	Yes
3/4	Yes	No

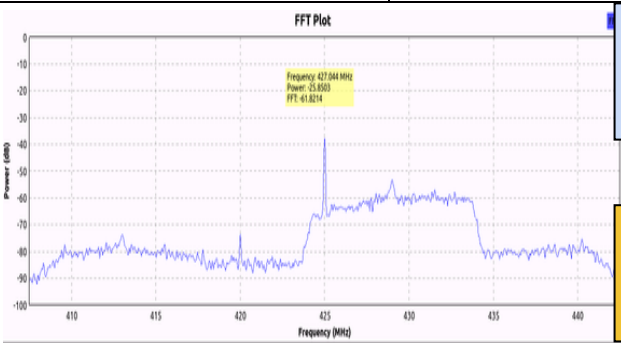

Figure 1: FFT Plot of Interferer

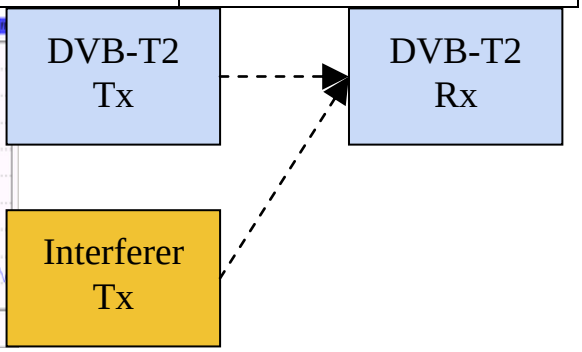

Figure 2: Interference Scenario

For the DVB-T2 transmitter, transmission was done using 64QAM modulation scheme with varying code rates and guard intervals. Due to limitations of the transmitter implementation and the host system, 256QAM and higher FFT schemes could not be transmitted. Various parameter combinations for which the Protection Ratios were measured are listed in table II.

III. Methodology

The following procedure was followed to conduct the experiment:
1. The DVB-T2 Transmitter was set to transmit according to parameters specified in table I and iteratively using a setting from the table II.

2. With this setup, reception was tested at the DTT receiver. The power transmitted was adjusted to a point where the receiver would just start receiving video.
3. Using the value from the previous step as the interference free threshold, the power was increased to have an SNR approximately 3dB above the threshold. The position of the receiver and transmitter and the powertransmitted were then kept static throughout the iteration.
4. The interferer then started transmitting with the parameters listed in table I and at a center frequency matching that of the broadcast. Initially, the power level of the interferer received at the receiver was set to a value lower or approximately equal to the noise floor of the DVB-T2 broadcast and incremented to a point of Picture Failure.
5. Center frequency of the interferer was shifted in 1MHz increments and the above step repeated for each case, thus measuring the acceptable C/I ratios for all offsets.
6. The process was repeated for the next valid DVB-T2 transmit configuration. The choice ofPilot Patterns is restricted for each transmission mode (refer table III) [13].

Table III: Allowed Pilot Patterns (at 4K FFT)

	GI 1/16	**GI 1/8**
Pilot Pattern	PP3	PP1

IV. Results

Based on the spectrum scan, it was found the DD transmits on two frequencies in the Delhi region - at 538MHz and 578MHz respectively. The SNR received at the experiment's location (rooftop) for 538MHz was approximately 5dB less as compared to the reception at 578MHz. The occupancy plots for 578MHz is shown in figure 3. The signals were highly attenuatedindoors, leading to non-detection of signal on the tuner. These readings were taken using SDR and a wideband bowtie dipole antenna aligned for maximum signal reception.

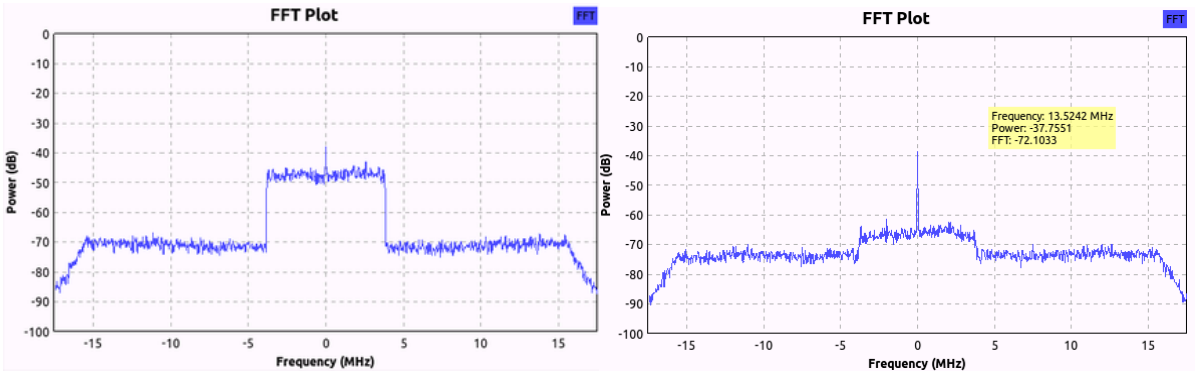

Figure 3: Doordarshan Transmission (578MHz) reception (a) rooftop (b) indoors

The threshold value of SNR (step 2) was found to be 12dB. Thus, the SNR was set to 15dB.

A. Varying code rate for fixed GI

The C/I ratios for different code rates using a GI of 1/16 are shown in figure 4(a). Here, DVB-T2 shows increased susceptibility to interference with increasing degree of overlap. The performance getsworse when code rate is increasedfrom 1/2 to 3/4. Even for complete separation between thetransmissions (437MHz), a C/I of at least 2dB needs to be maintained. This is mostly due to non-conformance to spectral masks by the interferer. On increasing the channel separation further, the C/I is low. Interference power could not be increased beyond a certain level in the SDR and hence, the values at 438MHz could possibly be much higher than observed here. Values with C/I as low as -40dB have been reportedin the literature [5], [7]. Values for co-channel and adjacent channel C/I are listed in table IV.

Table IV: Mesaured C/I values for 64QAM, 1/16 GI, PP3

Code Rate	C/I Cochannel (dB)	C/I Adjacent Channel (dB)
1/2	11.8	-3
2/3	12.2	2.3
3/4	12.3	4

For GI 1/8, C/I ratios for various code rates is shownin figure 4(b). It also follows similar trend except that performance for all code rates is worse than the 1/16 GI case. After complete separation, an SNR difference of morethan 6dB is still required for a code rateof 2/3, when compared to the same case with GI 1/16. It is then imperative that the performance of similar code rates at different Guard Intervals is compared.

B. Varying GI for fixed code rate

The C/I ratios for various cases are shown in the figure 5. For the same code rates, 1/16 GI fraction is seen to perform approximately 2dB better than 1/8 GI fraction. This is ambiguous. Since there is no adjacent channel interferer in the co-channel case, GI should have marginal to no impact on the performance. This has also been noted in [6] and is attributed to the use of different Pilot Patterns with PP3 (GI 1/16) having greater pilot density than PP1 (GI 1/8).

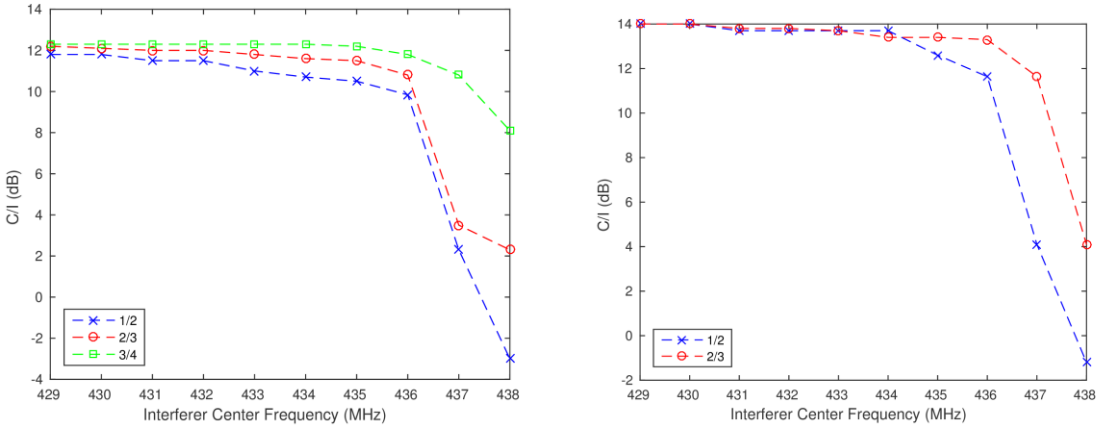

Figure 4: C/I Requirements for varying code rates. (a) 1/16 GIF, PP4 (b) 1/8 GIF, PP1

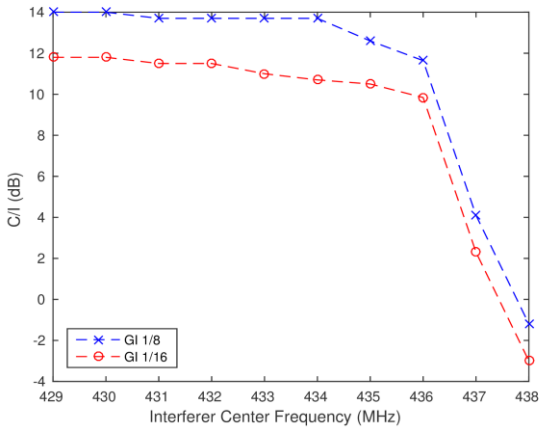

Figure 5: C/I requirement for 64QAM, 1/16 GIF (PP4) and ⅛ GIF (PP1)

V. Conclusion and Future Work

In the co-channel case the amount of interference that can be tolerated from a Gaussian interferer depends on parameters like code rate and pilot pattern (which is governed by the GI fraction). For smaller code rates, slightly higher levels of interference are tolerated. How effective this can be for secondary transmission

depends on the nature of transmission of the secondary. For adjacent channel use, the requirements are relaxed and occupying an adjacent band without disrupting broadcast is feasible with even 25% channel overlap.

Some variants of DVB specify an optional return channel for the receivers to be able to communicate with the transmitter at small data rates. No standardized method of implementation has been specified so far. However, a sibling standard ATSC has made an inband return channel mandatory in its release 3.0.

A scenario is envisioned where the secondary transmitters may use a similar return channel's information for optimizing their performance while avoiding service degradation of the incumbent even when operating within the protection contour (which at present is forbidden).

References

[1] "Provisional final acts world radiocommunication conference (wrc-15)." ITU-R, 2015. [Online]. Available:https://www.itu.int/dmspub/itu-r/opb/act/R-ACT-WRC.11-2015-PDF-E.pdf

[2] (2016, Jun.) Consultation paper on issues related to digital terrestrial broadcasting in India. Telecom Regulatory Authority of India. [Online]. Available:http://www.trai.gov.in/WriteReaddata/ConsultationPaper/Document/ConsultationPaper24june2016.pdf

[3] S. Roberts, P. Garnett, and R. Chandra, "Connecting Africa using theTV white spaces: from research to real world deployments," in*Proc. IEEE International Workshop on Local and Metropolitan Area Networks (LANMAN)*, Japan, Apr. 2015.

[4] D. Rother, S. Ilsen, and F. Juretzek, "A software defined radio basedimplementation of the tower overlay over LTE-A+ system," in*Proc. IEEE International Symposium on Broadband Multimedia Systems and Broadcasting (BMSB)*, China, Jun. 2014.

[5] V.Popescu, M. Fadda, M. Murroni, and D. Giusto, "Coexistence issues for IEEE 802.22 WRAN and DVB-T2 networks," in *Proc. IEEE International Symposium on Broadband Multimedia Systems and Broadcasting*, Japan, Jun. 2016.

[6] V. Popescu and M. F. et al., "Co-channel and adjacent channel interference and protection issues for DVB-T2 and IEEE 802.22 WRAN operation," *IEEE Trans. Broadcast.*, vol. 60, Dec. 2014.

[7] G. Martinez-Pinzon and N. C. et al., "Spectrum sharing for LTE-A and DTT: Field trials of an indoor LTE-A femtocell in DVB-T2 service area," *IEEE Trans. Broadcast.*, vol. 62, Sep. 2016.

[8] D. Denkovski and V. A. et al., "Practical evaluation of LTE-800 and DVB-T coexistence," in*Proc. IEEE International Symposium on Broadband Multimedia Systems and Broadcasting*, Belgium, Jun. 2015.

[9] L. Polak and O. K. et al., "Exploring and measuring the co-existence between LTE and DVB-T2 lite services," in *Proc. IEEE International Conference on Telecommunications and Signal Processing*, Rome, Jul. 2013.

[10] J. Ramirez and e. a. G. Martinez, "Interference analysis between digital terrestrial television (DTT) and 4GLTE mobile networksin the digital dividend bands," *IEEE Trans. Broadcast.*, vol. 62, Mar. 2016.

[11] M. Fuentes and C. P. et al., "Coexistence of digital terrestrial television and next generation cellular networks in the 700 MHz band," *IEEE Wireless Communications*, vol. 21, Dec. 2014.

[12] *Digital Video Broadcasting (DVB); Frame structure channel coding and modulation for a second generation digital terrestrial televisionbroadcasting system (DVB-T2) ETSI EN302 755 V1.4.1*, ETSI Std., 2015.

A Brief Survey on Femtocells and Interference Management Techniques

Kamna Sharma*, Mona Aggarwal†, and Swaran Ahuja‡
Department of Electrical, Electronics and Communication Engineering
The NorthCap University, Gurgaon, Haryana-122001, India
E-mail:kamnasharma93@gmail.com*, ermonagarg24@gmail.com†, swaranahuja@ncuindia.edu‡

***Abstract*—Most of us face the problems of poor coverage while talking on our cell phones in indoor environment. Our cell phone gets very low network signal. For this problem there is a device called femtocell was invented. Femtocell is a very smaller cellular base station which is designed to overcome the problems of poor coverage as well as capacity in indoor environment. Femtocells have the ability to serve indoor users with strong network connectivity at low cost, at the same time decreasing the load of macro cellular system. This paper gives a rundown of the fundamental ideas on femtocell which are explored in the previous researches. Also, the serious threats in femtocell deployment including interference and its management techniques have been discussed.**

Keywords: femtocell, co-tier interference, cross-tier interference, interference management.

I. INTRODUCTION

Femtocell is a combination of two words-femto and cell. Cell stands for smaller subdivision for an area of cellular system. Femtocell is a very smaller cellular base station as compared to standard macrocell base station and is designed for indoor usage to overcome the problem of poor coverage as well as capacity in indoor environment. It provides users with excellent and high quality indoor coverage, higher signal-to-interference-plus-noise-ratio and extends the duration of battery life for handset [1]. Femtocells are low cost, short range, low power base stations. It is basically a self-organizing, self-managing low power access point with full operator management that operates in licensed spectrum and uses mature mobile technology [2]. Femtocell has very low output power, which is less than 0.1 watt. A big reward for wireless operators is that wireless network gets free when mobile calls from homes are directed by operators on the internet. Cellular providers also get benefit, of employing femtocells, such as increasing the spectral efficiency area (total number of active users per Hertz per unit area), data traffic is offloaded from macrocell BSs, benefits in operating cost, base station reliability for macrocell is improved but no extra revenue is provided.

II. ARCHITECTURE

Femtocells are thought to be deployed by home and enterprise users at their premises in large numbers. Femtocell network architecture should meet the following requirements: (i) Scalable to a large number of femtocells with minimum or no impact to the existing infrastructure (ii) Secure and reliable connectivity from femtocell to the operators core network via the Internet (iii) Remotely configurable [3]. Since both macrocells and femtocells are required to operate in same bandwidths causing interference issues to occur. When we

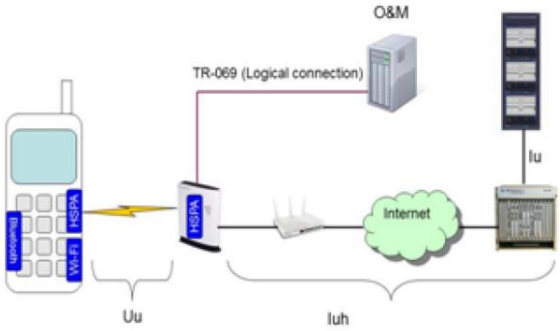

Fig. 1. femtocell connections at present [4]

use our mobile phone (i.e. a standard 3G cellular phone) in outdoor environment, then our femtocell appears as another macrocell and so communication with femtocell goes on as it is some macrocell. We get outstanding call quality because of the short distance between the mobile handset and the femtocell [5]. As the mobile operators telephone switch and

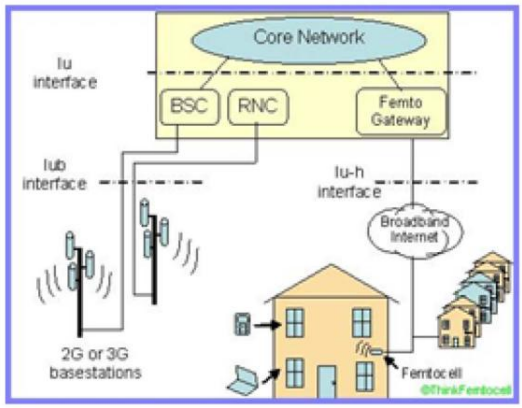

Fig. 2. Femtocell deployment [5]

data switch communicate with other mobile calls, both of these does communication in the same way with the femtocell gateway also. So, all of the services (such as phone numbers, call diversion, voicemail etc.) also operate in the same way and thus, appear the same to the end user. IPSec is used

to encrypt the connection between the femtocell and the femtocell gateway due to the fact that IPSec has the property that prevents these connections from interception. Access point validation is ensured by providing authentication after the installation of femtocell. There is the complete working of a mobile phone basestation inside the femtocell with inclusion of additional functions such as some of the Radio Network Controller (RNC) processing, which would normally located at the mobile switching centre. Certain femtocells include core network element so as to manage data sessions locally without the need of flowing back through the switching centres of operator. Femtocells are expected to have capabilities for self-installation and configuration. For this, there is a need of additional software which allows for reading frequencies (that are available in the environment), power levels and scrambling the codes to be used. This process is continuous in order to meet the requirements of changing radio conditions.

III. TYPES OF FEMTOCELLS

A. Based on access modes

An end user can access a specific femtocell on the basis of access mode in which a femtocell is operating. Generally,

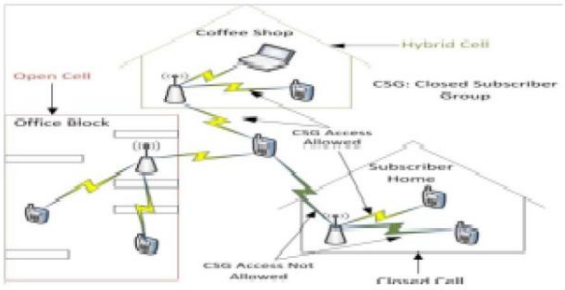

Fig. 3. Different access modes [6]

there are 3 access modes in which femtocell work. These are

1) Open access: mostly used in public places such as airports, shopping malls, different public organizations and not used in homes. Its main objective is to provide excellent coverage to all the public (mobile users) in a specific area in which femtocell is deployed.

2) Closed access: only authorized users can access the femtocell network and its properties.

3) Hybrid access: authorized users can access all the properties of network and unauthorized users have rights of accessing network only upto certain extents.

B. Based on coverage area

1) Domestic femtocell: It can be used for personal use in homes, offices and small business.

2) Enterprise femtocell: It is mainly used in highly populated environment, such as enterprise. It is larger than domestic femtocell.

3) Metro femtocell: It is a new concept in which operators install large no. of femtocells to provide low cost solution and high traffic area saturation.It is mainly for use in 4G LTE Technology.

Fig. 4. Types of femtocells based on coverage area [7]

C. Based on the technologies used

The femtocells can be classified as :

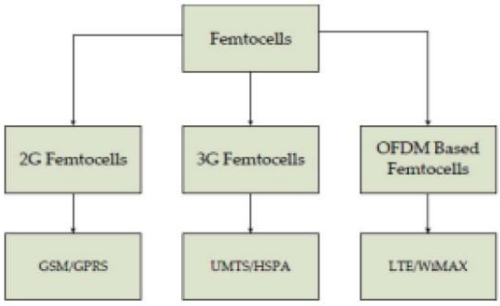

Fig. 5. Types of femtocell based on the technology used [6]

1) 2G Femtocell: When compared to UMTS and LTE, GSM is a very old system but sufficiently tested and supports the large number of subscribers than other technologies which developed after 2G femtocell. 2G femtocell is cheaper to produce than 3G but it cant provide a high quality voice service and is less economical. So, rarely used now a days.

2) 3G Femtocell (UMTS / HSPA): 3GPP network is more independent from accessibility point of view, allows linkage between mobile equipment and core network by other ways instead of going through SGSN. This allows flexibilities to BSs, which are efficient of pairing through IP-based networks. Other aspects, including these above mentioned aspects makes the UMTS technology more advanced than GSM for femtocell deployment.

3) OFDM based Femtocell: Frequency selective fading is one of the major causes of weakening (or impairments) of wireless channels mainly in extreme multipath conditions where performance of channel differs at different frequencies and is especially correct in urban and indoor environments. When wideband signals like CDMA signals are transmitted over such channels, these signals undergo distortion and thus difficult to reconstruct at receiver, hence narrowband signals are employed for their higher counteraction to these channels [8].

IV. FEMTOCELL DEPLOYMENT

A. Operator point-of-view

Planning process and site survey will become very easy if the macrocell sites will be decreased. It means for base station sites usage, little rent will be paid. Rollout of 3G/4G networks particularly in urban areas has a huge challenge for mobile operators, that challenge is site obtainment. In finding base station sites, difficulty has been increased to a greater extent for operators. Femtocells can facilitate operators to achieve a more cost-productive development plan with decreased financial burdens and risks also for increasing network capacity because femtocells are low cost solutions for coverage inside home and users can largely subsidize the operation of femtocell access points (for e.g. operators may also carry out far-off maintenance support) and users will at least share a significant chunk of the installation cost of femtocell access points if operators will subsidize femtocell-open access, it additionally can decrease the requirement of outdoor macrocells. Femtocell will improve QOS, gain customer faith and decrease mixing-up (large-scale issue) and its cost to operator can be some million dollars per day [8].

B. Subscriber-point-of-view

Subscribers who forebear poor or no coverage i.e. weak signal or no signal inside homes, femtocells facilitates them to use there mobile phones at home.

1) Advantages: Multimedia, video and high speed data services, along with voice service, will also become available when we use femtocells. As a lot of improvement can be done in the indoor performance of the network, so the user can try for both data and voice services. Femtocells will provide users a single billing account and one address book for all the three services namely broadband, land line phone and mobile phone. Users can get advantage from packaged services and home zone plans that will be more cost productive. Femtocells may represent itself as the central point for hooking-up all household devices to a home server and for all household devices, it act as the gateway to the Internet. Combined services (voice, video and data services) will be provided by femtocell at home and it facilitate users a flawless user experience across both indoor and outdoor surroundings with individualized gathered services for mobile equipments. Femtocells will save mobile equipment power. The uplink transmitting power can be enough reduced, when the spacing between mobile equipment and femtocell access point is very smaller as compared to the spacing between mobile equipment and macrocell site, which results in power saving of the mobile equipment. In supplying high data sevices to mobile users, battery is the main hinderence. Health troubles by using mobile devices can be decreased, when the transmitting power of mobile equipment can be greatly reduced. This point needs to be noted that if there are any health issues arising due to communication using mobiles, they would primarily due to uplink, because the mobile equipment is very near to the users (particularly near the head) [8].

V. CHALLENGES IN FEMTOCELL DEPLOYMENT

Deployment of femtocell changes macrocellular network in new way. Macrocell layer and femtocell layer are the two different layers that are composed in new network. Hence, it is called a two-layer or a two-tier network architecture. First tier consist of traditional cellular network and second-tier consist of smaller cells as compared to macrocell. These smaller cells are distributed randomly. First-tier and second-tier uses same frequencies. Advantages of using smaller cells, as compared to macrocells, are that it increases capacity and provides excellent coverage inside home where femtocell is employed. There are many confrontations in the network system due to this two-tier architecture.

A. Interference

As macrocell and femtocell layer both are using same frequencies. So, all the signals of a particular area will have same frequency. Due to this, when a transmitter transmits a signal, the intended receiver might be unable to distinguish between this signal and other signals transmitted by other transmitters of that area. Due to this inability to differentiate between accurate signal and signals of other users, there inoccurs interference. Accompanied by interference restricted system such as CDMA (Code Division Multiple Access) and interference nullification approaches such as power controls or time hopping, OFDMA (Orthogonal frequency division multiple access), a capacity-limited system, require acceptance to survive with the interference (caused by femtocell layer) present across subcarriers [6].

B. Self-organisation

1) Self configuration: Self-configuration of femtocells is a crucial function focussing at bettering the network capacity and coverage while reducing interference for current macrocell network together with nearby femtocells. For effective network management, performance and fault management of femtocells is also needed [9].

2) Self optimization: It uses the approaches of revising and accepting parameters of network. It also needs assurance about turning of all parameters to an acceptable level.

3) Self healing: It helps in finding solutions to various problems occurring in femtocell network and restore its default settings [6].

C. Synchronization and timing

Timing and synchronization is a confrontation for femtocell because of the disadvantage of GPS in indoor environment, of suffering significant amount of attenuation.

D. Security

Security is a means of protecting femtocell network from undesired users so that they cannot access the network and use or misuse the resources of network. Because of risk, mobile operators use IP security (IPSec) in between FAP and operator core link. Because of increment in number of femtocells deployed, security will be poor [6].

E. Access modes

There are 3 access modes of femtocells, i.e. open access, closed access, and hybrid access.

F. Mobility

Because of the narrow coverage and density of femtocells, it is possible for the handsets to quickly and repeatedly change in and out of the femtocell coverage area. This gives challenges for both active and idle call handover. In active state, how to identify the target femtocell, is a challenge. In idle state, the handset needs to register so as to authorize effective paging when it moves out of and into a femtocell. A technique is required to identify the availability of the femtocell for the handset on the macrocell frequency because the femtocell may be used on a different frequency than that of the macrocells. There is a disadvantage that frequent registrations (take place if the handset is passing through an area with dense femtocells using open pairing or signalling pairing) influence the battery life of handset [3].

G. Handover

A handover or hand-off is described, for media independent handoff, characterized as a platform independent IEEE standard 802.21. A handover is generally initiated to raise user signal strength when it falls down due to cell switching. If a subscriber move and changes cells, his call need to be handed off from current cell to a new cell with high signal strength. There are two types of handovers. Horizontal handover is the handover in the same network infrastructure. Vertical handover is the handover from one network to the other (e.g. from Wi-Fi to LAN or UMTS). In both cases, an algorithm decides make-before-break and break-before-make.

VI. INTERFERENCE

Here, we are focussing on the interference management which is one of the very important issues in the femtocell network. There are two main types of interference. These are

A. Co-tier interference

In uplink as well as downlink, femtocell can give rise to interference. Consider an example, a femtocell that is installed near a resident window can give rise to notable downlink interference to the macrocell handset that are moving outside the residence and are not served by that FAP. Similarly, during uplink, the handsets that are connected to certain FAP can give rise to significant interference that is uplink interference to the macrocell handset that are moving outside the residence and are not served by that FAP.

B. Cross-tier interference

Random deployment of femtocell cause notable interference to each other. This type of interference is also known as inter-femto interference. Consider an example, FAP set-up in close proximity to a wall which is uncombining two flats on a floor can cause notable interference to neighbouring flat. In this

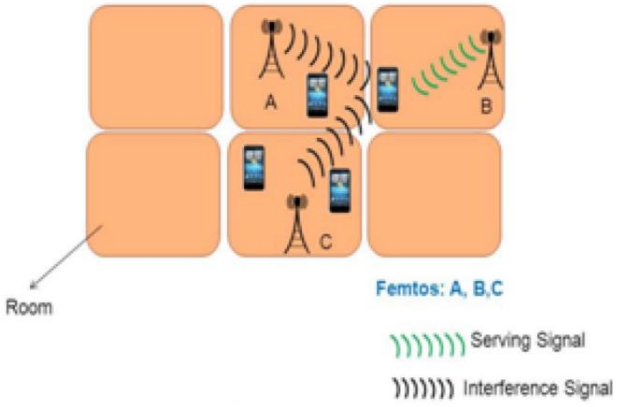

Fig. 6. Example of co-tier interference between femtos deployed indoors [10]

state, the strongest FAP in terms of RF signal strength may not certainly be the serving FAP because of restricted access of FAP in CSG(closed subscriber group) i.e. closed access mode of femtocell as discussed previously.

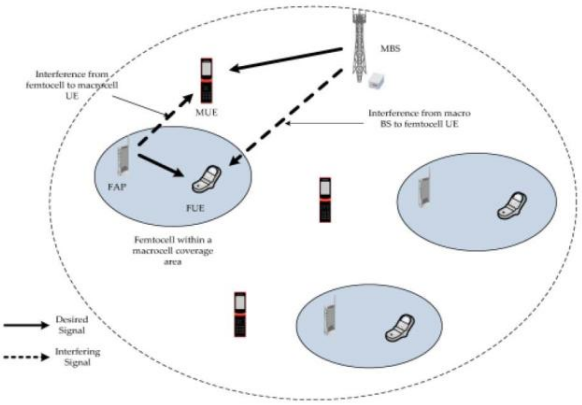

Fig. 7. A scenario showing cross-tier interference between femtocell and macrocell [9]

VII. INTERFERENCE MANAGEMENT METHODS

Following interference management methods are required to be used in femtocell design [11].

A. Interference avoidance

1) SIC: SIC identifies single user in each stage. Out of received signals, firstly the strongest received signal is observed, after that the next strongest, after that the next strongest and so on [12]. Latency and complexity of SIC are proportional to N. If there are many subscribers with real time data, this latency may be unaffordable [13].

2) PIC: PIC identifies all users simultaneously. This is the basic estimation and can be utilized for removing interference in forthcoming time. Parallel detection method is repeated for various stages. Hence, we can also call PIC as multistage interference cancellation [14]. Complexity of PIC is greater, it is proportional to PN because N number of users must be

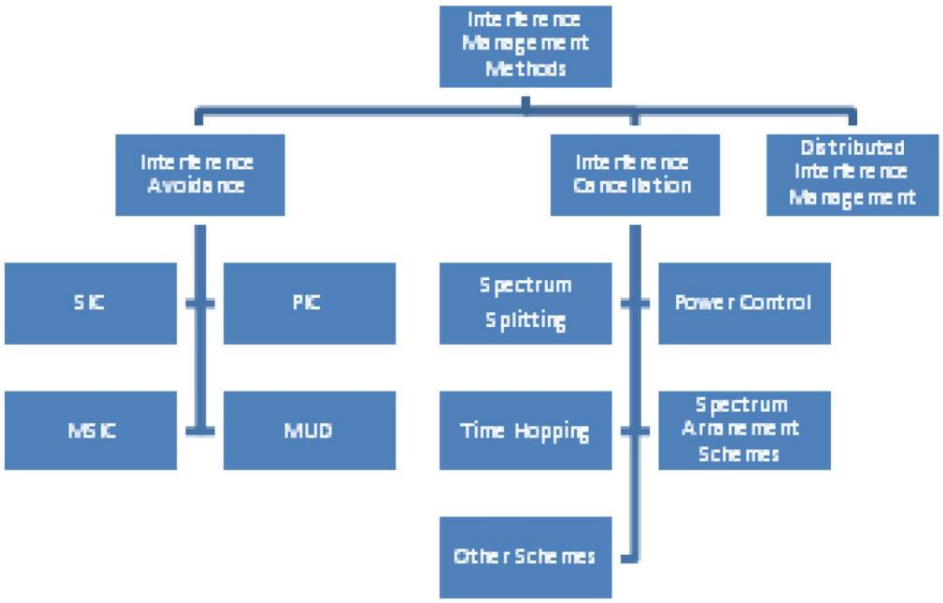

Fig. 8. Interference management techniques [11]

observed side-by-side and there are P stages of cancellation. But latency is reduced. For mobile system, it is proportional to P that implies it is very lesser in value than N.

3) MSIC: MSIC: For having a more efficient action, we use Multistage SIC. It is smoother settlement between the two approaches [15]. In this technique, firstly group of users are observed side-by-side (parallel), and then their combined interference is deducted from the mixed received signal, and then another group is observed side-by-side.

4) MUD: Multiuser detection (MUD) operates on same fundamental and detects the signature of each user. Depending on its channel state information and considerations, it chooses the best feasible signal out of K users. This technique is effectively suitable for CDMA systems, in which near far effect has to be removed for every user having its own spreading code and hence unique waveform. Here, MUD serves to observe various users of CDMA users and all those users can get advantage of joint detection [16].

B. Interference cancellation

Interference cancellation is the technique that is used at receiver for minimizing interference effect. According to the principle, any technique that permits receiver to operate with high-level co-channel interference can be treated as interference cancellation technique.

1) Spectrum splitting: At the beginning spectrum splitting was suggested, to survive with the cross-tier interference [17]. It was suggested that a band of spectrum should be divided into two parts. One part for femtocell operations and the other part for macrocell users. This is the only option to survive with the co-tier interference. However, due to the high price and deficiency of spectrum, this approach will bring on decreased efficiency. It is suggested that where there is very large number of femtocells deployed and it is very difficult to cope with cross-tier interference, spectrum should use different part of spectrum for the operations of femtocell [18]. To reduce the cross-tier interference in OFDMA system, femtocells are allotted with independent sub channels.

2) Power control: Particularly in dense femtocell placement, power control is a fundamental approach in the interference avoidance. If the transmit power of a femtocell is optimised and regulated, the outdoor macrocell mobile equipment can be secured adequately. The two fundamental and generally known schemes for power control in femtocells are closed loop power control and open loop power control [19]. By evaluating the cross tier interference to macrocell base station, mobile equipment of the femtocell evaluate the maximal permissible transmit power in open loop power control. For low macrocell throughput, the closed loop power control performs better. To survive with downlink co-channel interference in femtocell, a channel management, admission control and joint power control algorithm is there [20].

3) Time hopping: One major interference mitigation technique for wireless systems using CDMA, to decrease cross-tier interference in uplink is the time hopping. This scheme in 3G system is called Time Hopped CDMA (TH-CDMA), in which duration for transmission is partitioned into small parts throughout which a user sends or transmits and for other parts it remain quiet [21]. Each network layer independently chooses its duration if both the layers or tiers are not synchronized [22]. We can also put into action a joint hopping approach in which all users of a femtocell transmits in same time duration. In this approach, the femtocell users will not cause interference to each other because of combined interference averaging in systems that are based on CDMA [11].

4) Spectrum arrangement schemes: We can use a dedicated spectrum method in femtocell network so as to survive with the

cross-tier interference [23], [24]. There will be 2 major parts of spectrum, out of which one is for femtocell operation and other for macrocell operation. In close and dense deployment of femtocell, there is problem of inadequacy of orthogonality because of the Multiple Access Interference (MAI) and Inter Carrier Interference (ICI). Both of these interference i.e. MAI and ICI arise due to deficiency of synchronization. We can avoid ICI or MAI by setting-up proper synchronization. For this, every FAP computes the separation between itself and the macrocell Base Station. If this separation is S, then FAP waits for transmission, for S/C time as with respect to the macrocell Base Station transmission time (here C is speed of light) [24]. Generally for better effective usage of valuable spectrum it is preferred by operators to use same spectrum part for both macrocell as well as femtocell.

5) Other schemes: Resource allocation, spectrum sensing functionality, intercell coordination, power allocation, dynamic spectrum access [11].

C. Distributed interference management

Various algorithms are used for distributed interference management in femtocells. One of these algorithms is power control algorithm for interference mitigation in closed access mode. In this algorithm, if we input a set of practical SINR values for femtocell, then it provides a relation that determines the largest practical values of SINR for cellular [25]. Another one is an algorithm that uses fractional frequency reuse (FFR) for varying FFR corresponding to surroundings. It uses interference information along with femtocell location and categorize femtocell into different classes, where sub-channnels are allotted to mitigate interference, then transmit power allocation takes place which is wholly based on RSSI(received signal strength information) in a distributed way [11]. Another approach for decreasing cross-tier interference in femtocell is using a SINR approach based on distributed utility at the FAP. In it, femtocell power generating extreme interference is progressively decreased [26], [27]. Distributed interference management schemes are the fundamental results for the interference mitigation confrontation in femtocells. These approaches are capable to focus on the issues in a manner which is appropriate for femtocells and so we necessitate advance research in this field [11].

VIII. CONCLUSION

Femtocells have the ability to serve indoor users with strong network connectivity at low cost, at the same time decreasing the load of macro cellular system. The paper has analyzed the advantages of using femtocells, the challenges in femtocell deployment, and interference and its mitigation. Due to the inability to differentiate between accurate signal and signals of other users, there inoccurs interference which is a key challenge.

REFERENCES

[1] D.P. Agrawal; Femtocells: Introduction and Research Issues. By. Dharma P. Agrawal. http://www.bmi.yzu.edu.tw/images/seminar/Femtocell.pdf as on 21.02.2016.

[2] A. Germano; The Impact of Femtocells on Next Generation LTE Mobile Networks,www.3gpp.org/Information/presentations/presentations as on 21.02.2016.

[3] J. Chen, P. Rauber, D. Singh, C. Sundarraman, P. Tinnakornsrisuphap, M. Yavuz; Femtocells Architecture Network Aspects, Jan 28, 2010 QUALCOMM

[4] H.P.Narkhede; Femtocells: A Review; International Journal of Advance Research in Computer Science and Management Studies;Volume 2, Issue 9, September 2014 Research Article / Survey Paper / Case Study Available online at: www.ijarcsms.com.

[5] K.Elleithy and V. Rao; Femto Cells: Current Status and Future Directions; International Journal of Next-Generation Networks (IJNGN) Vol.3, No.1, March 2011.

[6] O.A Akinlabi, B.S. Paul, M. Joseph and H.C. Ferreira; A review of femtocells; International MultiConference of Engineers and Computer Scientists 2014 Vol II, IMECS 2014, March 12 - 14, 2014, Hong Kong

[7] http://slideplayer.com/slide/7048281/ as on 26/03/2016

[8] J. Zhang, G. D. L. Roche; femtocells: Technologies and deployment, A john wiley and sons ltd. Publications.

[9] https://www.researchgate.net/figure/268223271fig1Fig3Types of interference in two tier network

[10] http://images.slideplayer.com/25/8018255/slides/slide8.jpg as on 10/04/2016

[11] Talha Zahir, Kamran Arshad, Atsushi Nakata, and Klaus Moessner; Interference Management in Femtocells; IEEE Communications Surveys Tutorials, Volume:15, Issue: 1, pp. 293 311, february 2012

[12] P. Patel and J. Holtzman, Analysis of a simple successive interference cancellation scheme in a ds/cdma system, IEEE J. Sel. Areas Commun., vol. 12, no. 5, pp. 796807, Jun. 1994.

[13] J. G. Andrews, Interference cancellation for cellular systems: A contemporary overview, IEEE Wireless Commun., vol. 2, no. 3, pp. 1929, April. 2005.

[14] P. Frenger, P. Orten, and T. Ottosson, Code spread cdma with interference cancellation, IEEE J. Sel. Areas Commun., vol. 17, no. 12, pp. 20902095, 1999.

[15] F. Wijk, G. Janssen, and R. Prasad, Groupwise successive interference cancellation in a ds/cdma system, Sixth IEEE International Symposium on Personal, Indoor and Mobile Radio Communications, Wireless: Merging onto the Information Superhighway, pp. 742746, 27-29 Sep 1995.

[16] D. Hallen, J. Holtzman, and Z. Zvonar, Multiuser detection for cdma systems, IEEE Personal Commun., pp. 4658, April 1995.

[17] R. S. Karlsson, Radio resource sharing and capacity of some multiple access methods in hierarchical cell structures, in Vehicular Technology Conference, vol. 5, pp. 28252829, Sep. 1999.

[18] M. Fan, M. Yavuz, S. Nanda, Y. Tokgoz, and F.Meshkati, Interference management in femto cell deployment, in 3GPP2 Femto Workshop, Oct. 2007.

[19] J. Han-Shin, M. Cheol, M. June, and Y. Jong-Gwan, Interference mitigation using uplink power control for two tier femtocell networks, IEEE Trans. Wireless Commun., vol. 8, no. 10, pp. 49064910, October 2009.

[20] X. Li, L. Qian, and D. Kataria, Downlink power control in co-channel macrocell femtocell overlay, 43rd Annual Conference on Information Sciences and Systems, pp. 383388, 18-20 Mar. 2009.

[21] A. K. Elhakeem, R. D. Girolamo, I. B. Bdira, and M. Talla, Delay and throughput characteristics of th, cdma, tdma, and hybrid networks for multipath faded data transmission channels, IEEE J. Se. Areas Commun., vol. 12, no. 4, pp. 622637, May 1994.

[22] V. Chandrasekhar and J. G. Andrews, Uplink capacity and interference avoidance for two-tier femtocell networks, IEEE Trans. Wireless Commun., vol. 8, no. 7, pp. 34983509, Jul. 2009.

[23] D. Williams, WiMAX femtocells a technology on demand for cable MSOs, in Femtocells Europe, Jun. 2008.

[24] H. Su, L. Kuang, and J. Lu, Interference avoidance in OFDMA based femtocell network, IEEE Youth Conference on Information, Computing and Telecommunication, pp. 126129, 20-21 Sept. 2009.

[25] V. Chandrasekhar, J. G. Andrews, T. Muharemovic, Z. Shen, and A. Gatherer, Power control in two-tier femtocell networks, IEEE Trans. Wireless Commun., vol. 8, no. 8, pp. 43164328, Aug. 2009.

[26] V. Chandrasekhar, J. G. Andrews, S. Zukang, T. Muharemovic, and A. Gatherer, Distributed power control in femtocell-underlay cellular networks, IEEE Global Telecommunications Conference, pp. 16, Nov. 30-Dec. 4 2009.

[27] H.C. Lee, D.C. Oh, and Y.H. Lee, Mitigation of inter-femtocell interference with adaptive fractional frequency reuse, IEEE International Conference on Communications (ICC), pp. 15, May 2010.

Towards Depth Prediction in Indoor Scenes

Akhil Rana
ABV-IIITM, Gwalior

Aditya Trivedi
ABV-IIITM, Gwalior

***Abstract*—Depth prediction in monocular image is a challenging topic of computer vision. An image taken from camera loses its depth dimension. To recover depth, various techniques are implemented like stereo vision system of human eyes, Microsoft Kinect, etc. But using two cameras are costlier than using single camera. Most algorithms for monocular depth prediction are dependent on the training database. Models are learnt over training database and then applied over semantically similar test database. These give good performance but are not generic algorithm for depth prediction. There are many algorithms which uses super-pixels, semantic labels, pixel wise comparison, SIFT flow to get semantically similar data from training whose depth can be warped over test data. In case, test data is semantically not aligned with any of training data then performance of the depth prediction deteriorates. In this paper, we have tried to make a database independent algorithm for indoor scenes using three steps process. Firstly, predicting room layout, secondly, segmenting the room clutters, and lastly correlating the segmented objects with the depth in database. Results of first and second process are shown in this paper, while third step is under process. The final result will be a generic indoor depth prediction algorithm.**

I. Introduction

Depth estimation is essential component of understanding the scene understanding in geometric relations. Each geometric relation helps us in understanding the location, shape and illumination condition of the objects present in the scene which in turn helps us in recognition task. Thus, enabling many further application in various domains such as 3D modeling, physics and support models, robotics, and potentially reasoning about occlusions. Figure 1 show the depth map of a RGB image which tells us the difference between foreground and background of the scene.

Fig. 1. Image and Corresponding Depth map

Lot of work has been done in the recent years on estimation depth on stereo as well as in monocular images. But compared to stereo case, monocular depth prediction is less traveled due to the complexity present in understanding the scene with only one image as a single image could depicts various structures of a 3D interpretations. There are several reason for increased difficulty in monocular cases than stereo cases but two most prominent are:

- Provided accurate image correspondences
- Depth can be recovered deterministically in the stereo case.

Estimating depth from a single image requires the use of monocular depth cues such as line angles and perspective, object sizes, image position, and atmospheric effects. Furthermore, a global view of the scene may be needed to relate these effectively, whereas local disparity is sufficient for stereo.

Fig. 2. Depth Presumption

Moreover, the task is inherently ambiguous, and a technically ill-posed problem: Given an image, an infinite number of possible world scenes may have produced it. Of course, most of these are physically implausible for real-world spaces, and thus the depth may still be predicted with considerable accuracy.

Recent state of art depth prediction uses various cues like parallax, motion or shading cues but for restricted environment which restrict the prediction model in becoming a generalized model. To address this problem, various databases are built to make it more generalized. These depth databases can be classified in two groups one is outdoor scenes and other is indoor scenes. There are many different features of these databases like in indoor scenes illumination problem is present while outdoor have abundant illumination. Due to there different features it is better to make separate model for each group. Out paper proposes depth prediction in indoor scenes. In our proposed work, I taking help of spatial layout of indoor scenes and the training database in which objects depth distribution is present to get the efficient depth prediction of the images. The result will be semantically independent depth map of arbitrary input image.

II. Literature Survey

The past monocular depth estimation algorithms uses user-annotations such as sparse depth scribbles [19] [2] which assigns manual depth values to the input image. Thus, in order to make process automatic many experiments began. Recent years, many automatic depth prediction algorithm were proposed which need zero user input. These were parallax-based methods [21] and shape-from-shadings [22]. In parallax-based methods [10] camera is given translational motion for a static scene. In few methods, [21] instead of capturing realistic scene depth from the object in motion in the scene, they simply convert an object motion to a scene depth. Shape-from-shading methods [22] typically uses surfaces of an image to have fairly similar distribution of color and texture. In real life situation, it is difficult to exist such requirements.The depth map we have to predict using a single image have various cues other than just one. Therefore, these approaches [21], [22] relying on a single cue only do not scale well for general scenes. Alternatively, data-driven approaches [9], [11] significantly advanced the performance of the single image depth estimation by effectively leveraging the discriminative power of large scale RGB-D databases (consisting of color images and associated ground truth depth maps). The data driven approaches uses scenes with similar semantics to wrap the similar depth distribution.This assumption makes it more unlikely to make them data dependent rather than generalized form which is we trying to remove in this proposed paper.

One of the state of the art algorithm given by, Konrad et al. [11] which proposed to collect K color images with similar histogram of gradient(HoG) features and retrieve depth maps using median depth value of each pixel. The predicted depth map is then refined using a joint bilateral filtering [4] as it is fast and easy to implement. However, the K depth maps are directly fused with no pixel-level dense alignment, and thus local properties of retrieved K depth maps are not considered. Karsch et al. developed the depth transfer algorithm which take into account global depth fusion which automatically recovers scene depth from monocular image. In contrast to [11], the retrieved images are densely warped to the input image by making use of a generic dense scene alignment like SIFT Flow [16]. Due to the implementation of SIFT Flow which provided best matching of the suitable scene the error produced are relatively lower than the HoG based features. But the cost is the increased computation complexity in the operation.

There are many algorithm for monocular depth prediction. The Make3D [17] algorithm results in realistic depth prediction which are sufficient accurate. These uses modeling monocular cues and the relation among multiple regions inside an input image based on a Markov Random Field (MRF). In order to, calculate the depth parameters, they are trained using ground truth RGB-D database. In [15] and [13], labeling of the semantic objects in the scene helps a lot in improving the depth prediction using monocular depth features. Eigen et al. [5] uses multi scale deep neural networks. The methods [6], [20] proposed to incorporate additional geometry information such as surface normal vectors in order to improve an overall performance of depth map prediction.

A. Problem Statement

Data-driven algorithm are largely dependent on the styep of database used for training of the model which required that the database should be huge. They typically attempt to solve a highly ill-posed depth prediction problem by transferring plausible depth labels to an input image from visually similar images retrieved from RGB-D training database. All these methods are running under same assumption that they have training depth images which contain geometric characteristics similar to that of an input color image. Due to highly dependent on database only input images with highly semantic training database produces effcient results, otherwise it will perform poorly.

Th proposed algorithm will be taking help of spatial layout of indoor scenes and the training database in which objects depth distribution is present to get the efficient depth prediction of the images. The result will be semantically independent depth map of arbitrary input image. These indoor scenes are first checked for 3D layout and then segmented. After segmented each objects depth distribution is taken from training database and inscribed on it.

III. Improved Depth Prediction

There are three steps for the proposed improved depth prediction. Firstly, 3D spatial layout of indoor scenes, secondly, Segmentation for objects and last one is Depth warping and smoothing. I have completed the first two steps while the latest one is in progress.

A. 3D Spatial Layout Of Indoor Scene

Our goal is to jointly extract the spatial layout of the room and the configuration of objects in the scene. We model the spatial layout of the room by 3D boxes and we model the objects as solids which occupy 3D volumes in the free space defined by the room walls. Given a set of room hypotheses and object hypotheses, our goal is to search the space of scene configurations and select the configuration that best matches the local surface geometry estimated from image cues and satisfies the volumetric constraints of the physical world. These constraints are:

- Finite volume: Every object in the world should have a non-zero finite volume.
- Spatial exclusion: The objects are assumed to be solid objects which cannot intersect. Therefore, the volumes occupied by different object are mutually exclusive. This implies that the volumetric intersection between two objects should be empty.
- Containment: Every object should be contained in the free space defined by the walls of the room (i.e, none of the objects should be outside the room walls).

We first extract line segments and estimate three mutually orthogonal vanishing points. The vanishing points define the orientation of the major surfaces in the scene [12], [14],

[7] and hence constrain the layout of ceilings, floor and walls of the room. Using the line segments labeled by their orientations, we then generate multiple hypotheses for rooms and objects. A hypothesis of a room is a 3D parametric representation of the layout of major surfaces of the scene, such as floor, left wall, center wall, right wall, and ceiling. A hypothesis of an object is a 3D parametric representation of an object in the scene, approximated as a cuboid. The room and cuboid hypotheses are then combined to form the set of possible configurations of the entire scene. The configuration of the entire scene is represented as one sample of the room hypothesis along with some subset of object hypotheses. The number of possible scene configurations is exponential in the number of object hypotheses 1. However, not all cuboid and room subsets are compatible with each other. We use simple 3D spatial reasoning to enforce the volumetric constraints described above. We therefore test each room-object pair and each object-object pair for their 3D volumetric compatibility, so that we allow only the scene configurations which have no room-object and no object-object volumetric intersection. Finally, we evaluate the scene configurations created by combinations of room hypotheses and object hypotheses to find the scene configuration that best matches the image. As the scene configuration is a structured variable, we use a variant of the structured prediction algorithm [18] to learn the cost function. We use two sources of surface geometry, orientation map [14] and geometric context [8], which serve as features in the cost function. Since it is computationally expensive to test exhaustive combinations of scene configurations in practice, we use beam-search to sample the scene configurations that are volumetrically-compatible.

B. Segmentation

Segmentation of objects in scene helps us in warping of depth of the objects taken from the database. We have used SLIC Superpixel approach [1] in which superpixels are clustered pixels based on their color similarity and proximity in the image plane. It uses a 5 dimensional space $[l, a, b, x, y]$ space, where $[l, a, b]$ is the pixel color vector in CIELAB color space, which is widely considered as perceptually uniform for small color distances, and x, y is the pixel position. While the maximum possible distance between two colors in the CIELAB space (assuming sRGB input images) is limited, the spatial distance in the xy plane depends on the image size. A new distance measure enforces color similarity as well as pixel proximity in this 5D space such that the expected cluster sizes and their spatial extent are approximately equal.

In this algorithm, input a desired number of approximately equally-sized superpixels K (where $K = 3000$). For an image with N pixels, the approximate size of each superpixel is therefore N/K pixels. For roughly equally sized superpixels there would be a superpixel center at every grid interval $S = \sqrt{N/K}$.At the onset of our algorithm, we choose K superpixel cluster centers $C_k = [l_k, a_k, b_k, x_k, y_k]_T$ with $k = [1, K]$ at regular grid intervals S. Since the spatial extent of any superpixel is approximately S^2 (the approximate area of a superpixel), we can safely assume that pixels that are associated with this cluster center lie within a $2S \times 2S$ area around the superpixel center on the xy plane. This becomes the search area for the pixels nearest to each cluster center. Euclidean distances in CIELAB color space are perceptually meaningful for small distances (m in Eq.1). If spatial pixel distances exceed this perceptual color distance limit, then they begin to outweigh pixel color similarities (resulting in superpixels that do not respect region boundaries, only proximity in the image plane). Therefore, instead of using a simple Euclidean norm in the 5D space, we use a distance measure D_s defined as follows:

$$\begin{aligned} d_{lab} &= \sqrt{(l_k - l_i)^2 + (a_k - a_i)^2 + (b_k - b_i)^2} \\ d_{xy} &= \sqrt{(x_k - x_i)^2 + (y_k - y_i)^2} \\ D_s &= d_{lab} + \frac{m}{S} d_{xy} \end{aligned} \tag{1}$$

where D_s is the sum of the lab distance and the xy plane distance normalized by the grid interval S. A variable m is introduced in D_s allowing us to control the compactness of a superpixel. The greater the value of m, the more spatial proximity is emphasized and the more compact the cluster. This value can be in the range $[1, 20]$. We have kept $m = 5$ which provide us the best oversegmentation required for complex cluttered indoor scene.

After oversegmention, we join the neighbors with similar $[L, a, b]$ in order to produce a good segmented objects in the images. Now, currently we have not perfected the segmentation as the indoor scenes are too cluttered and badly illuminated which makes it difficult to segment cluttered objects in the indoor scene we are working on optimum solution for the algorithm.

C. Depth Wraping

Depth of the scene can be assigned using the floor-ground-wall layout from the room layout algorithm. After segmentation of clutters in the indoor scene, we wrap the depth of the objects matched with the objects recorded from the training database. For matching the objects we can use SIFT flow [16] of the cluttered segmented objected with the database of objects. After matching the closest object we wrap the depth of the object in the scene. For further improving, we can smoothen the depth map with the bilateral filter.

IV. Results

The final results of the algorithm is still under process.Thus, we have presented results of the step one, 3D room layout and step two, segmentation of cluttered objects. The results for the room layout using the algorithm proposed in (A) are shown in Figure 3 in which the room layout is predicted correctly. The red lines shows wall lining of the room which shows that 3D room prediction is efficient. The results of Segmentation of the room scenes are in Figure 4 in which most of small cluttered objects like lamp, pillow are segmented while some objects like painting, bed. The problem with the existing used algorithm is weak edges present in or outside

Fig. 3. Room Layout Structure

the objects. Segmentation is not able to take into accounts the weak edges of the scene causing it to perform poorly in indoor cluttered scenes. We are working on improving the segmentation process to extract cluttered objects of the indoor scene efficiently.

Fig. 4. Room Layout Structure

V. Conclusion

Our proposed algorithm will be semantically independent from the training database and out perform some of the state of the art algorithm. The algorithm is however is highly dependent on the efficiency of the 3D layout. We will showed that the 3D layout serves as a better cue for data-driven depth inference for indoor scenes. Our projected depth approach is useful to managing varied training vary pictures involving substantial look and geometric variations. a lot of significantly, our methodology is probably going less obsessed with the looks depth correlation assumption strictly obligatory on previous strategies, and therefore is capable of estimating scene depth from restricted training knowledge in terms of a range of scene semantics

References

[1] R. Achanta, A. Shaji, K. Smith, A. Lucchi, P. Fua, and S. Süsstrunk. Slic superpixels compared to state-of-the-art superpixel methods. *IEEE transactions on pattern analysis and machine intelligence*, 34(11):2274–2282, 2012.

[2] X. Cao, Z. Li, and Q. Dai. Semi-automatic 2d-to-3d conversion using disparity propagation. *IEEE Transactions on Broadcasting*, 57(2):491–499, 2011.

[3] N. Dalal and B. Triggs. Histograms of oriented gradients for human detection. In *2005 IEEE Computer Society Conference on Computer Vision and Pattern Recognition (CVPR'05)*, volume 1, pages 886–893. IEEE, 2005.

[4] F. Durand and J. Dorsey. Fast bilateral filtering for the display of high-dynamic-range images. In *ACM transactions on graphics (TOG)*, volume 21, pages 257–266. ACM, 2002.

[5] D. Eigen, C. Puhrsch, and R. Fergus. Depth map prediction from a single image using a multi-scale deep network. In *Advances in neural information processing systems*, pages 2366–2374, 2014.

[6] D. F. Fouhey, A. Gupta, and M. Hebert. Data-driven 3d primitives for single image understanding. In *Proceedings of the IEEE International Conference on Computer Vision*, pages 3392–3399, 2013.

[7] V. Hedau, D. Hoiem, and D. Forsyth. Recovering the spatial layout of cluttered rooms. In *2009 IEEE 12th international conference on computer vision*, pages 1849–1856. IEEE, 2009.

[8] D. Hoiem, A. A. Efros, and M. Hebert. Recovering surface layout from an image. *International Journal of Computer Vision*, 75(1):151–172, 2007.

[9] K. Karsch, C. Liu, and S. B. Kang. Depth transfer: Depth extraction from video using non-parametric sampling. *IEEE transactions on pattern analysis and machine intelligence*, 36(11):2144–2158, 2014.

[10] D. Kim, D. Min, and K. Sohn. A stereoscopic video generation method using stereoscopic display characterization and motion analysis. *IEEE Transactions on broadcasting*, 54(2):188–197, 2008.

[11] J. Konrad, M. Wang, P. Ishwar, C. Wu, and D. Mukherjee. Learning-based, automatic 2d-to-3d image and video conversion. *IEEE Transactions on Image Processing*, 22(9):3485–3496, 2013.

[12] J. Košecká and W. Zhang. Extraction, matching, and pose recovery based on dominant rectangular structures. *Computer Vision and Image Understanding*, 100(3):274–293, 2005.

[13] L. Ladicky, J. Shi, and M. Pollefeys. Pulling things out of perspective. In *Proceedings of the IEEE Conference on Computer Vision and Pattern Recognition*, pages 89–96, 2014.

[14] D. C. Lee, M. Hebert, and T. Kanade. Geometric reasoning for single image structure recovery. In *Computer Vision and Pattern Recognition, 2009. CVPR 2009. IEEE Conference on*, pages 2136–2143. IEEE, 2009.

[15] B. Liu, S. Gould, and D. Koller. Single image depth estimation from predicted semantic labels. In *Computer Vision and Pattern Recognition (CVPR), 2010 IEEE Conference on*, pages 1253–1260. IEEE, 2010.

[16] C. Liu, J. Yuen, and A. Torralba. Sift flow: Dense correspondence across scenes and its applications. *IEEE transactions on pattern analysis and machine intelligence*, 33(5):978–994, 2011.

[17] A. Saxena, M. Sun, and A. Y. Ng. Make3d: Learning 3d scene structure from a single still image. *IEEE transactions on pattern analysis and machine intelligence*, 31(5):824–840, 2009.

[18] I. Tsochantaridis, T. Joachims, T. Hofmann, and Y. Altun. Large margin methods for structured and interdependent output variables. *Journal of Machine Learning Research*, 6(Sep):1453–1484, 2005.

[19] O. Wang, M. Lang, M. Frei, A. Hornung, A. Smolic, and M. Gross. Stereobrush: interactive 2d to 3d conversion using discontinuous warps. In *Proceedings of the Eighth Eurographics Symposium on Sketch-Based Interfaces and Modeling*, pages 47–54. ACM, 2011.

[20] B. Zeisl, M. Pollefeys, et al. Discriminatively trained dense surface normal estimation. In *European Conference on Computer Vision*, pages 468–484. Springer, 2014.

[21] L. Zhang, C. Vazquez, and S. Knorr. 3d-tv content creation: automatic 2d-to-3d video conversion. *IEEE Transactions on Broadcasting*, 57(2):372–383, 2011.

[22] R. Zhang, P.-S. Tsai, J. E. Cryer, and M. Shah. Shape-from-shading: a survey. *IEEE transactions on pattern analysis and machine intelligence*, 21(8):690–706, 1999.

A Survey on Smart Learning Platforms for Kids

P.Sai Sheela(M-tech), Rashika Joshi(M-Tech), Ms. Jasleen Kaur(PhD Scholar) &
Dr. SRN Reddy(HOD, CSE)
Department of Computer Science & Engineering
Indira Gandhi Delhi Technical University for Women, Kashmere Gate, Delhi
sai19.pidatala@gmail.com
er.rashika@gmail.com
jasleenkochar89@gmail.com
rammallik@yahoo.com

***Abstract*— Smart education, a concept that describes learning in digital age, has gained increased attention. It promotes learners to learn more effectively, efficiently, flexibly and comfortably. Older ways of teaching meant only bookish knowledge which became boring, less fun, less challenging and restricted their area of learning over a period of time. Therefore, as smart, portable and affordable devices became prevalent accompanied with rapid advancement in technology, new avenues of learning emerged. Technology aided learning is inherently engaging, highly interactive, graphically rich and creates a personalized environment for kids. This paper delineates the purpose of various kids learning devices currently available. The authors further present a detailed analysis of the discussed devices to elucidate the design and developmental aspects. Further improvements in this field are contemplated to create a robust, engaging and fun learning device for the kids.**

***Keywords*—Android Applications, Educational tab, Gamification, Smart Education, Technology aided learning.**

I. INTRODUCTION

Education is important for every society. It is the foundation for a better world. India is evolving rapidly and changing times demand innovative ideas and hence the need for **"smart education"**. Till a few years ago, education meant only bookish knowledge and was limited to only chalk and slate. But with the emergence of handheld devices and the advancement of technology, people began realizing how smart devices can be an integral part of our education system and how important it is to make young buds familiar to the emerging technologies.

Children reach for electronic gadgets of all shapes and sizes, particularly the cell phones and computers from the time a child can grasp an object in their hands. When parents start noticing more child-size fingerprints on the iPad than their own, it may be time to consider introducing their child to a handheld wireless device [4]. Tablets are great for keeping children entertained and engaged for hours, but one can't simply hand a new iPad off to junior and hope for the best. If not monitored properly, the little one could accidentally buy a lot of expensive media and apps, or stumble upon a minefield of inappropriate online content [2]. Therefore, **Tablets for kids** are gaining popularity and parents buying a tablet for kids are having a hard time deciding which is the **best tablet for kids** because new products are regularly introduced to the market with more superior specifications than the previous ones[1]. If such an interaction with technology can enable the kid to learn while playing it will lead the kid to absorb information more faster than a sponge, logically at the conscious level and intuitively at the subconscious level. If education is mixed in the perfect proportion with fun of playing games, the kid is in the perfect state of mind to learn; it is in a perfect state of mind to remember that is learned. The kid does not have to sacrifice and sweat; the kid does not need to be forced or disciplined. The kid needs no more motivation than the fun of playing [9

paper]. If the moments and events are ***fun and enjoyable***, the learning is even more at fundamental levels. It can be said, "Fun stimulates and prepares our brain ***mentally*** for **fun**da**mental** learning and thinking" [9].

Technology aided learning has benefits of its own that promotes holistic development of kids. It empowers children to communicate, technology like video-calling on a tablet or phone can support social interaction and communication skills as it makes it easy for children to show people the things they want to talk about or to describe facets of everyday life to family and friends. By doing this they're also learning to take turns, to take account of their conversation partner and to explain things in a way that's understandable for somebody who isn't in the same place. Not all 'educational applications' are suitable for every kid [3]. Choosing an app needs the same kind of thought and care one would put into buying anything else for one's child. It is advised not to rely only on the star rating, but also to read the user reviews and check the privacy policy to know about the personal information that the app might be collecting. A range of games and apps have to be provided to make the child enjoy learning, develop curiosity, and to think about things. Open-ended games/ applications that become progressively more challenging and encourage children to explore and have fun are more likely to establish a love of learning and to lay the foundation for their future development [3]. For school-age children, a smartphone or tablet can give them an additional learning layer, beyond the traditional classroom or book. Smartphones and tablets provide students with multiple opportunities to access content and engage with curriculum. They connect students to the world beyond the four walls of their brick and mortar buildings and give them access to real world experts solving real world problems in real time. Technology makes their learning relevant [4]. At the same time parental guidance is suggested. Experts recommend parents be very involved in their child's experience with electronic devices, especially at a young age. The goal is balanced exposure. It's important to focus on the content and message when making age-appropriate media choices. Distinction between educational and entertainment-based content should be clear. There are many games and interactive activities on mobile devices that are not necessarily about school subjects but still useful for children and beyond purely entertainment. Games and activities that engage children in thinking skills like memory games, puzzles, spatial reasoning activities; nurturing skills such as digital pets; and creative skills - drawing, making music - are also great choices.[4]

The rest of the paper is organized as follows. Section II talks in detail about the present technologies, software and devices for kids' education. Section III presents discussion and conclusion of the literature survey. Section IV outlines the future work and concludes the paper.

II. Literature Survey

Lot of kids tablets claim to be the best tablet for kids. There's no one best tablet for kids. It all depends on what the kids specific needs are. One tablet may be best for some but not for others. The Kurio Smart [5] is a Windows 10-powered slate with a detachable keyboard. It offers a good balance, being as adept at work as it is for play. Design-wise this tablet is distinctive, with bright blue and white plastic featuring heavily. When it comes to features, though, it's basic. Neither the tablet nor the dock include a full-size USB port. On the plus side, there is an HDMI connector, for doing homework on a larger screen. The built-in screen has a 1,280 x 800 pixel resolution, and while this shows itself in a bright panel with responsive touch controls, it is not suitable multi-tasking. It is powered by the quad-core Intel Atom processor that easily handles a few basic games and meet most children's needs. It has excellent Battery life. [5] The Kurio Xtreme 2 [6] has 7 inch capacitive touch screen, 5-point touch android lollipop OS tablet. It is powered by Mediatek MTK8127 Quad-Core processor. Has 16GB Storage expandable up to 32GB and 1GB RAM. It supports multiple languages. Has micro USB –OTG support. It has 0.3 MP in-built camera.

Verizon's GizmoTab [7](fig:1.ii) packs LTE connectivity which allows kids to stream videos or download games on the go. The 8-inch slate comes with a rubber bumper that protects it from falls, so junior can't break it. GizmoTab with a Verizon data plan, grants access to 300 kid-friendly apps that offer educational and entertaining experiences.[2]

Built by Fisher-Price [8] in partnership with Nabi, two leading names in educational toys and tablets, the Fisher-Price Learning Tablet comes complete with 35 apps and games that are designed to help children 3 and up learn. The preloaded content includes Storybook Rhymes volumes 1 to 6, Wings Learning System and a slew of videos that help kids get familiar with shapes, numbers, letters and phonics. The Android-powered, 7-inch slate also includes full access to the Google Play store and 16GB of storage.[2] The 7-inch LeapFrog Epic [10]offers a kids tablet home screen. The Epic runs a proprietary UI on top of Android that offers an interactive virtual world that kids can customize and make their own. Made for children between 3 to 9 years old, this slate comes with a decent set of apps and adequate parental controls, though it weighs more than other kids tablets.[2] on the other hand, the LeapFrog LeapPad Platinum [11] is a tablet from a purely educational standpoint(fig:1.vi). It has lithium ion rechargeable battery. The processor speed is 1GHz. It has access to a library of 1,000+ educator-approved games, apps & more. Targeted for kids aged between 3-9 yrs. Fuhu Nabi's DreamTab[12] is a 8-inch Multi-Touch Capacitive Android 4.4 kitkat OS tablet. While the Dreamworks-themed DreamTab sports the robust parental controls, fast performance and kid-safe design Fuhu is known for, the tablet has a disappointingly short battery life (less than 6 hours). It has 16 GB storage that expandable upto 32GB via microSD card and 2 GB RAM. It is powered by NVIDIA Tegra 4 T40S Quad-Core, 1.6 GHz with burst speed to 1.8 GHz processor.

PraSid English Learner Kid's Laptop [13] with 20 Activities, lets kids learn while they play with it. This English learner laptop encourages creative learning in the child. It enables lots of learning without any stress. The kid learns new words, goes through spelling test and learns to identify the pictures with names. A Laptop shaped English teaching toy with an Inbuilt LCD Screen, Sound Instructions, Key Pad and Mouse Control gives the child an exposure to computers. It has an auto shut-off mechanism which helps save battery. It has three Levels of Difficulty. Step 1 - Learn Alphabets, Alphabets Recognition and Pronunciation, Write capital and Small letters, Find the Letter, (it will speak out the letters- which the child needs to punch in). Step 2 - Learn words, Learn Spelling and Pronunciation, Spelling test. Identification of pictures, find the word. Step 3 - Learn numbers, Learn the Correct Pronunciation and Spelling of Numbers Learn to Write the Numbers, Numbers identification (visual), Number identification (verbal). Step 4 - Learn Musical Notes, Play Melodies, Play Musical Notes. Recognize Musical Notes (visual and verbal). Step 5 - Play games, Catch falling objects, Find the matching pair, Star shooting, Draw a picture. It is easy To Maintain. It is made of durable child-safe plastic that does not break easily. It is also easily cleaned using a damp cloth. [6]

Figure 1: (i) Kurio Smart .(ii) Verizon GizmoTab (iii) Fisher Price Learning Tablet. (iv) LeapFrog Epic (v) FuhuNabi DreamTab (vi) LeapPad Platinum (vii) Kurio Xtreme 2 (viii) PraSid Kids English Learner Laptop

A. Research Gaps

The above delineation brings forth certain points that can be the basis for newer & better educational products.

There is a need for a completely customised product for the kids where the applications are not proprietary, but available in an open environment. This will ensure that the product has a wider reach. This will also help to reduce the cost.

There is a need to explore the kind of applications that are able to move beyond the screen and are able to access the externally interfaced LEDs on the

processor and other such components as these would grab the kids' attention and make them inquisitive and interested. Data services should be provided in a controlled manner under parental supervision.

Such devices should also be used as security devices in disguise to alert the parents if it senses danger in the kids' environment.

Products► Features▼	Kurio Smart	Kurio Xtreme 2	Verizon's GizmoTab	Fisher-Price Learning Tablet	Leap Frog Epic	Leap Frog LeapPad Platinum	Fuhu Nabi's Dream Tab	PraSid English Learner Kid's Laptop
OS	Windows 10	Android lollipop	Android Marshmallow	Android	Android 4.4	-	Android 4.4 kitkat	-
Storage	32 GB	16 GB	16GB	16GB, Expandable via MicroSD (Up to 32GB)	16 GB expandable upto 32 GB	8GB	16 GB	Very minimal storage.
RAM	1 GB	1GB	-	1GB	-	-	2 GB	516KB
Processor	Quadcore Intel® Bay Trail™ - T Z3735G	Mediatek MTK8127 Quad-Core	Qualcomm® Snapdragon™ 617 Octa Core	Quad-Core Processor	1.3 GHz processor.	1GHz clock speed processor	Nviadia 1.6 GHz quad core processor	4 bit CPU
Communication Module	Wi-Fi b/g/n - Bluetooth 4.0	Wi-Fi, 802,11 b/g/n - Bluetooth v4.0 - Micro HDMI	LTE B2, B4, B13 Doubling our 4G LTE bandwidth in cities coast to coast.	Wi-Fi 802.11 b/g/n Bluetooth 4.0	WiFi 802.11 a/b/g/n Bluetooth 4.0	Wifi	Wifi, Bluetooth, NFC, GPS	none
Screen	8.9 inch IPS capacitive touch screen	7 inch capacitive touch screen, 5-point touch	8" IPS TFT LCD display; 1920x1200, 282 PPI	7 inch Capacitive Touch Screen	7 inch capacitive touch screen	7-inch capacitive screen	8 inch multitouch capacitive touch.	LCD screen
Camera	0.3Mpx Front / 2Mpx Rear	0,3 Mpx / Rear: 2,1 Mpx	8MP Rear camera, 5MP Front Camera	2MP Rear, 0.3 Front Camera	2MP front and Back	2MP Front and Back	Front-2MP Rear-5MP	No camera
Additional Features	Supports multi languages CONNECTION: Micro USB - Micro HDMI	Speakers: 1 x 1W mono Languages: Supports multi languages USB Connection: Micro USB 2.0 - OTG support	Battery: 5,100mAh Typical, Non-Removable SAR: 1.23W/kg	Micro USB connector, Built-in micro-phone, 3.5mm Standard audio jack.	20+ apps, 150$ + value. Includes Accelero-meter Parental approval for web access.	access to a library of 1,000+ educator approved games, apps & more	Nabi connector ,MicroSD compatible card slot, built-in micro phone and audio jack.	Built-in music. Uses 3 X AA Batteries

TABLE 1: COMPARISON OF VARIOUS KIDS LEARNING DEVICES.

III. Discussion And Conclusion

It is observed that tablets are **great** gadgets for making **kids** busy in engaging learning activities. A lot of applications are being provisioned with the device which is proprietary. Such applications are educator approved in many cases. Therefore, it is assured that the kids are actually learning while having entertainment. The downside though is if not monitored properly, the little one could accidentally buy a lot of expensive media and apps, or stumble upon a minefield of inappropriate online content. Fortunately, there are tons of kid-friendly tablets on with parental controls, age-appropriate apps and oftentimes a durable rubber frame that will survive the toddler's slippery hands.

IV. Future Scope

A strong, robust device for kids that provides educational content which complements the traditional methods of learning is the need of the hour. The applications should be open source so as to reduce the cost of the device and make it affordable to all kids.

In addition to providing educational apps, the device should be implementing security module that alerts the parents in the event of danger. The device should harness the communication modules to achieve this in addition to implementing the parental controls to monitor the kids activities.

References

[1] Best tablets for kids: The Ultimate Guide.[online] Available URL: http://www.tabletsforkidsguide.com/ [Accessed on 12/1/2017]

[2] Kids tablets to buy.[online] Available URL: http://www.laptopmag.com/articles/kids-tablet-reviews [Accessed on 8/1/2017]

[3] Are Tablets good for Children? [online] Available URL: http://www.bbc.co.uk/guides/z3tsyrd [Accessed on 8/1/2017]

[4] When to introduce your child to smart phone? [online] Available URL: http://www.pbs.org/parents/childrenandmedia/article-when-introduce-child-smartphone-tablet.html [Accessed on 8/1/2017]

[5] Kurio Smart Technical Specs: [online] Available URL: http://www.kurioworld.com/k/us/parents/products/smart/ [Accessed on 6/1/2017]

[6] Kurio Xtreme 2 Technical specs: [online] Available URL: http://www.kurioworld.com/k/us/parents/products/xtreme2/ [Accessed on 6/1/2017]

[7] Verizon GizmoTab Technical Specs [online] Available URL: https://www.verizonwireless.com/tablets/verizon-gizmotab/ [Accessed on 6/1/2017]

[8] Fisher Price Learning Device [Online] Available URL: https://www.nabitablet.com/nabi-fisherprice/specs#overview [Accessed on 6/1/2017]

[9] K. Murthy, "Fun based education for ages from 3 to 100: Lighting the candle of learning passion," *2013 3rd Interdisciplinary Engineering Design Education Conference*, Santa Clara, CA, 2013, pp. 10-18.

[10]LeapFrog LeapPad Epic Technical Specs [Online] Avai;able URL: http://www.leapfrog.com/en-us/products/leapfrog-epic [Accessed on 6/1/2017]

[11]LeapFrog LeapPad Platinum [online] Available URL: http://www.leapfrog.com/en-us/store/p/leappad-platinum/_/A-prod31565 [Accessed on 6/1/2017]

[12] Nabi DreamTab Technical spacs [online] Available URL: https://www.nabitablet.com/dreamtab/specs#overview [Accessed on 6/1/2017]

[13]PraSid kids English Learning Laptop Technical Specs [online] Available URL: https://www.snapdeal.com/product/andalso-kids-english-learner-computer/1404480483 [Accessed on 6/1/2017]

Wearable Healthcare Technologies in India: Review and Survey

Nisha Sharma
Department of Computer Science
IGDTUW
nishabhardwaj611@gmail.com

Zeenat Shareef
Department of Computer Science
IGDTUW
zeenat.taneez@gmail.com

Dr. S.R.N Reddy
Department of Computer Science
IGDTUW
rammalik@yahoo.com

Abstract--: The health of its citizen is the most important concern of any nation. A healthy nation is said to be a wealthy nation. Health care not only deals with medical care but also includes pro preventive care and measures. About 40% of deaths in India occur just because of infection. The government is trying a lot to improve the efficiency of health care system in India, however, several challenges still exists. Due to advancement in engineering and technology, health care system has evolved from dedicated hospital to real time remote health monitoring systems. Nowadays, research and development have made it possible for wearable health monitoring technologies. Medical practices in India are continuously improving but they have failed to meet patients rising expectations. In this paper, review of various wearable health care technologies in India is presented along with contemporary issues and challenges faced by several health care systems. Also, results of survey conducted on need and importance of wearable healthcare devices is highlighted.

Keywords: - Wearable devices, IOT, Zigbee, Obtrusive Sleep Apnea, Hyperthermia

I. INTRODUCTION

It seems today that everyone's life is full of struggle and obligations. People don't have much time for themselves. They are too busy in improving and securing their future life that they forget to pay attention to their present life. People with busy life schedule pay less attention to their health. Tension arising from commercial and business work lead to deterioration of health. Internet of things has led to the introduction of smart wearable technology that has considerably improved the living standard of people and provided them with a safe environment. Wearable computing is the most widespread topic since 2014. Today wearable Technology is paid more attention because of its great prospect. Wearable technology includes small, low power electronic devices, integrated with sensors worn by user or even woven over clothes in order to track his daily activity. In today's era it is found that wearable technology is widely pushed towards health care field and plays a most prominent role in monitoring the health of user. Pedometers, fit bit, wrist band, activity band are some of its examples which are used all over the world. These wearable devices are designed in such a way that user finds them comfortable while wearing 24*7 hours. Functioning of all wearable devices is same. Integrated sensors are deployed in these wearable devices. Real time data is collected by these sensors and is processed by microcontroller. Processed data is further displayed on screen with great accuracy. Many of them are connected to smart phone through wireless technologies like Bluetooth, WI-Fi or zigbee and can be accessed by them. Figure shown below is a basic block diagram of any smart wearable device which can be accessed by smart phone through wireless technology.

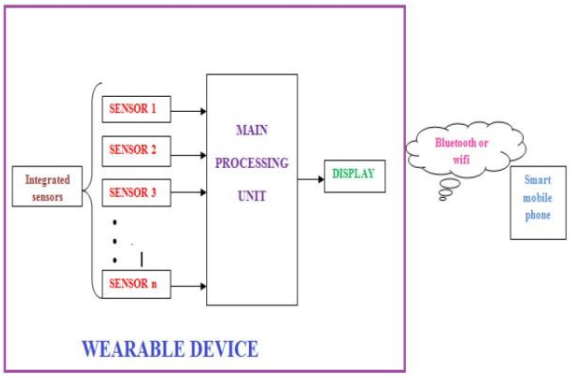

Fig.1 Basic block diagram of any wearable device

This paper is organised as follows. Section II explains the literature review. Review of various wearable health monitoring device is reported in Section III. Section IV depicts various issues and challenges faced by wearable technology. Section V presents the survey report. Section VI describes the proposed solution and paper concludes with section VII.

II. LITERATURE REVIEW

Various health monitoring devices were designed for early detection of disease. Many health care devices such as ECG, PPG are available but they are clinical and are quite expensive. Moreover continuous monitoring is also not possible by such devices as they are not mobile. Several devices has been developed which can be used at home for health monitoring. Various research work carried out in this field is explained below:

Mariam et.al, [1] has designed a system that monitors Obtrusive Sleep Apnea (OSA). Data related to blood oxygen and breathing condition is collected and transmitted to microcontroller for processing. Stored data is further sent to Android based smart phone via Bluetooth.

Vahram et. al, [2] has presented the novel design of a wearable health monitoring device that will monitors the vital body parameters such as heart rate, BP, oxygen saturation level, respiration rate etc. Calculated data is transferred to smart phone through Bluetooth.

Jetendra joshi et. al, [3] has proposed a solution to cope up with the problem of obesity and overweight by integrating WBAN with IoT which help the people to live happy and healthy life.

Subhas Chandra Mukhopadhyay [4] has presented a report on the latest wearable devices in which activity of user is monitored. Various design challenges of wearable sensors are also highlighted.

Sandesh Warbe et. al,[5] has introduced the design of health care monitoring system which measures vital body parameters like heart rate, temperature, humidity and body movement. Data is then passed to home server via Zigbee transmitter or to smart phone via Bluetooth.

Akshay Sugathan et. al, [6] has developed a wearable prototype based on Arduino platform that monitors the body parameters (heart rate, SPO2, body temperature and galvanic skin resistance). Sensors are integrated and woven into the shirt which promotes generic clothing technology.

Thomas Martin et. al, [7] has explained how wearable medical application is different from that of other general purpose wearable applications. A case study on ECG monitoring device is also presented.

K.Hung et. al, [8] has presented an overview of various wearable patient monitoring devices along with the design of tele-home health care system which comprises of wearable sensors and wireless communication technologies. Further a case study on cuffless BP meter, Bluetooth based ECG monitor and ring type heart rate monitoring is also discussed.

Seok-Oh Yun et. al, [9] proposed a small size flexible patch system that monitors the physiological signals such as heart rate and body temperature. These signals are communicated with reader through Bluetooth technology.

M. Scheffler et. al, [10] highlighted various design requirements of wearable devices along with the challenges faced by them. Two Wearable medical devices (WMD) AMON and QBIC are discussed in detail.

Insoo Kim et. al, [11] has discussed various issues and challenges faced by wearable health monitoring devices and has also proposed a algorithm to overcome the problem of motion artifact solutions.

Comparison of various wearable health monitoring device is shown in Table 1.

Paper	Processor	Communication Module	Sensors
Mariam et. al,[1]	Atmega 32A	Bluetooth class 1 v2.0+ EDR	SPO2 measurement sensor
Sandesh warbe et. al,[5]	MSP 430	Zigbee transceiver, Bluetooth	Heart rate, humidity sensor and temperature sensor
AkshaySugathan et. al, [6]	Atmega 328	Nil	Heart rate, SPO2 and temperature sensor
Seok-Oh Yun et. al, [9]	8051 microcontroller	Bluetooth	Temperature sensor
M. Scheffler et. al, [10]	X scale processor	GSM	SPO2,ECG and BP measurement sensors

Table 1: Comparison of wearable health monitoring device

III. WEARABLE HEALTH MONITORING DEVICE (WHMD)

Humans today are getting addicted to life full of ease and comfortable which is the biggest reason of poor health. Wearable Health monitoring devices (WHM) helps user to adapt healthier life style. Table work and lethargy is the main cause of obesity. It is being estimated that an individual should take 1000 steps per day in order to lead fit and healthy life. Pedometer is a step counter device that counts the no. of steps undertaken by user in a day. Heart disease is one of the major big concerns in India that causes threaten to life of million people. In India, there are about 30 million people that are suffering from this disease. Within every 33 seconds a person dies of heart-attack in India. According to a report two million heart attacks are being witnessed currently. Advancement in technology has developed wearable heart monitoring devices which provides user with benefit of early detection and better diagnosis. It is quite difficult for the aged and physically handicapped people to visit regularly to health centre to have their regular check-up. Moreover, it is quite painful for them to stand in a queue and wait for long hours. WHM overcomes such problems. Majority of aged and pregnant women dies because of slipping or falling. Earlier detection of person falling is necessary. Wearable devices for such detection were also introduced which just requires user to push a button and call for help. Pain in neck, back and joints arises because of sitting in a wrong posture. Postures correcting wearable bands are also available now days. Band beeps or vibrates when the user is not in correct posture and notifies him to have correct posture. Many wrist bands employing accelerometer and altimeter are introduced in market which provides the user with information relating to their motion and alternative heights. Activity band which tracks the activity of user is a major application of wearable technology. This band gives a mild shock to user when he is in slack mode. Smart watch is one of the most commonly and widely used application. Since, it comes with multi-functioning features hence popular among common people. Smart watch is most often used as WHM device that monitors the vital body parameters like temperature, Pulse rate, and blood pressure apart from displaying time. It can also be used as step counter. Hypothermia and hyperthermia conditions are also detected. Women, girls often found to have problem with the design and appearances of WHMD. A way to come out of this dilemma was also introduced. Sensors were integrated and stitched into the jewellery. Necklaces track the user activities and keeps on notifying them. Gaudy and fascinating jewellery can also act as wearable health monitoring device. Sleep Apnea is a dreadful disease that can occur at any age. It is generally a sleep disorder where person's breathing is interrupted due to insufficient supply of oxygen to brain and other parts of body. 1-10% of children are affected by Obtrusive Sleep Apnea (OSA). 70% people suffer from this disease within Delhi itself.

IV. ISSUES AND CHALLENGES

Although wearable technology comes with a myriad of benefits but it brings with them certain inevitable security and privacy issues. Wearable technology like fit bit, Google glass, smart watch etc. stores personal information of user like no. of steps undertaken, vital body parameters, activity, location and movement tracking. Due to the absence of right security control, privacy of data is jeopardized and hence can easily be attacked by malicious third party. Since data is transferred wirelessly either through Bluetooth or internet over the air so there is high chance of data being forged or modified by eavesdropper. Privacy is one of the major concerns. No one wants his personal information to be available to other. Since, it belongs to him only so maintaining confidentiality of information is must. According to 2014 report, about 84% of users had expressed their concern about data security. Google glass has been banned in San Francisco just because of privacy issues. Another major challenge faced by wearable technology is its design. Design is a crucial factor that determines the popularity of product in market. Although a large effort has been made to develop a product of small size such that it looks more attractive but still many people find them bulky and have problem while wearing them 24*7. Many of the wearable devices emit heat while working which causes discomfort to user. Apart from this, many of the wearable devices are worn on wrist but wrist is not considered as best place to wear such devices because of motion artifacts. These are the major reason that wearable technology is not socially accepted till now. Research is going on in full swing in order to overcome the above mentioned issues. Various encryption based technologies are being used for maintaining the security and privacy of data.

V. SURVEY REPORT

After seeing so many benefits of wearable devices a survey was conducted among 50 persons. Subjects of all age group and gender (male and female) were asked to fill the feedback form which comprises of 10 questions. These questions are presented below in table 2.

S.No.	Questions	YES	NO
1.	Do you have a sedentary life style?	95%	5%
2.	Do you pay 100% attention to your health?	2%	98%
3.	Do you find your smart phone enough to provide information that you really want?	75%	25%
4.	Do you collect real time data of your daily activity while moving?	20%	80%
5.	Do you want to complete your tedious task within seconds?	100%	0%
6.	Are you a part of rat race life? Is there a need to make your life simple and free from struggles and obligations?	85%	15%
7.	Do you visit health care centre daily for regular check up?	0%	100%
8.	Do you find clinical devices (E.C.G, P.P.G) economical, cost effective and comfortable?	0%	100%
9.	Do you need a wearable health care device?	99%	1%

Table 2: Feedback form

The above report shows that people need a small, economic, user friendly, low power wearable device that can collect real time data about their daily activity. Constant interaction with phone is not possible every time. Moreover, smart phone has much chance of losing. 75% of person finds that their smart phone alone is not enough to provide them with information that they really need. Survey shows that it is not possible for everyone to have regular check up. 100% of people find clinical devices too expensive and discomfortable. 98% of people can't pay attention to their health just because of busy life schedule. More than 98% of people want their tedious task to be completed within seconds. According to this survey report 99% of people need a wearable healthcare device.

VI. PROPOSED SOLUTION

Survey conducted above shows that people are really in need of a smart wearable device. Hence, we have made a genuine effort to propose a device which will cater to the need of people. Our device is basically a health monitoring device which will measure the vital body parameters such as body temperature and movement, pulse-rate. Device consist of LM35 temperature sensor, pulse sensor and inbuilt motion sensors. Data from this device is transmitted to smart phone through Bluetooth technology.

VII. CONCLUSION

Review of wearable health monitoring devices present in market is analyzed in this paper. Various issues and challenges faced by wearable devices is also discussed. A survey highlighting the need and advantage of wearable technology is also conducted. Results shows that people today are seamlessly accepting the new innovations of technology as it will provide incentives for healthy and better life. The day is not far off away when smart watches, shoes will be in common use just like smart phones.

REFERENCES

[1]Mariam Rostami, Amin Janghorbani," Design and Implementation of Telemedicine System for Spo2 Monitoring", *22nd Iranian Conference on Electrical Engineering (ICEE),*Pages: 1945 - 1949,Year 2014,

[2] VahramMouradian Armen Poghosyan and LevonHovhannisyan," Continuous Wearable Health Monitoring using Novel PPG Optical Sensor and Device", *IEEE 10th International Conference on Wireless and Mobile Computing, Networking and Communications (WiMob),* pages 120-123,Year 2014

[3] Jetendra Joshi, Divya Kurian, Satyam BhasinPrakhar Awasthi, Sibeli Mukherjee, Sanya Mittal, and ShribbhaSharma",Health Monitoring Using Wearable Sensor and Cloud Computing",*International Conference on Cybernetics, Robotics and Control,* pages 104-108,Year 2016

[4] Subhas Chandra Mukhopadhyay, "Wearable Sensors for Human Activity Monitoring: A Review", *IEEE SENSORS JOURNAL, VOL. 15, NO. 3,* Pages: 1321 - 1330, Year 2015

[5]Mr.Sandesh Warbhe, Mrs. SwapniliKarmore, "Wearable Healthcare monitoring system: A survey", *IEEE 2nd International Conference On Electronics and Communication System(ICECS),* Pages: 1302 - 1305, Year 2015

[6]AkshaySugathan, Gaurav Gautam Roy, G.J Kirthyvijay, Jeffrey Thomson, " Application of Arduino Based Platform for Wearable Health Monitoring System," *IEEE 1st International Conference on Condition Assessment Techniques in Electrical Systems (CATCON),* pages 1-5,Year 2013

[7] Thomas Martin, Emil Jovanov, Dejan Raskovic , "Issues in Wearable Computing for Medical Monitoring Applications : A Case Study of a Wearable ECG Monitoring Device," *4th International Symposium on*

wearable computer, Pages: 43 - 49, Year 2000

[8] K. Hung, Y.T. Zhang and B. Tai" Wearable Medical Devices for Tele-Home Healthcare", *26th Annual International Conference of the IEEE Engineering in Medicine and Biology Society,Volume: 2,* pages 5384-5387,Year: 2004

[9] Seok-Oh Yun, Moon-Keun Lee, Kyoung G. Lee, Jinsung Yi, Su JeongShin, MinHoYang,Namho Bae, Tae Jae Lee, JinhoKo and Seok Jae Lee,"*An Integrated and Wearable Healthcare-on-a-Patch for Wireless Monitoring System",IEEE Sensors,* Pages: 1 - 4, Year 2015

[10] M. Scheffler1, E. Hirt1, " Wearable devices for emerging healthcare applications ", *26th Annual International Conference of the IEEE Engineering in Medicine and Biology Society,Volume: 2,* pages 5384-5387,Year 2000

[11] Insoo Kim, Po- hsiang Lai, Ryan Lobo and Bruce J.Gluckman,"Challenges in Wearable Personal Health Monitoring System", *36 annual International conference of IEEE Engeeniring in Medicine and Biology Society,* pages 5264-5267, Year 2014.

Speech to Text Application Based Smart Notice Board

Renuka Lakhanpal and Rishibha Yadav
Indira Gandhi Delhi Technical University for Women, Delhi
renukalakhanpal@rocketmail.com, rishbhyadav91@gmail.com

Abstract

This paper emphasizes on an application of smart notice boards which is used to provide information in an innovative and in a smarter way through android application replacing manual work. Wireless notice boards is a technology which saves paper and the user from the tedious tasks of changing and sticking notices on an conventional notice boards every now and then .With the help of the proposed technology , the authenticated and the Authorized user i.e administrator in this case can change or put up the notices from remote place through his android phone which has android application in 3 ways i.e through text (simple message), image and voice. For voice conversion voice to text conversion is used .Here we used raspberrypi3 which has inbuilt wi-fi suitable for our application, lcd to display ,android phone and temperature and humidity sensor when no new notices are there .This saves students at the last time hassle at the exams etc. Android phones are owned and used by large amount of people with the advancement in information & communication Technology (ICT),this can be widely acceptable because of user friendly and low cost applications. This paper deals with such an android application for Academics aid .This kind of application can also comes handy in public places such as colleges , schools, industries, offices, banks, railway stations, bus stands etc.

INTRODUCTION

The main objective of the project is to develop a wireless notice board that displays notices when a message is sent from the user's android application device. Remote operation is achieved by any smart-phone/Tablet etc., with Android OS, upon a GUI (Graphical User Interface) based touch screen operation. While the user sends the message from the Android application device, it is received and retrieved by the raspberry pi at the display unit. The access password will only be known to the admin. It is then sent to the raspberry pi2 that further displays the notice sent from the admin on to the electronic notice board which is equipped with a LCD Monitor display.This study aims to enhance a existing bulletin board using LED/LCD monitor that is capable of display data such as text and image using Raspberry Pi2 a credit card sized single board computer connected to LED/LCD monitor via HDMI to VGA port to make a display output.We can send data such as text and images using your mobile phone or tablet with a network connection of Wi-Fi .We can also send a data to the bulletin board via SMS.The digital board is an enhancement of manual bulletin board in school. A wireless technology applied to transfer data into the raspberry pi interfaced to HDMI to VGA port to make an output display.The Raspberry pi is capable to receive data storing to its SD card.The user can send a data via Wi-Fi connection through SMS.The process of transferring data is required the mobile devices that are capable to connect the Wi-Fi.The raspberry pi receives data from mobile devices.The data which is text /images display into the LCD/LED monitor interfaced to Raspberry pi via HDMI to VGA port.

Who will be the beneficiary

- Student organization
- Offices in school/colleges/industry
- Researchers
- Business.

Purpose of the study

- To post an announcement or advertisement in a digital format.

- To lessen the effort to print some papers and tarpaulin.
- To maximize the usage of mobile devices.

Advantages of the project

- Helps student organization to post an announcement and advertisement without using paper
-Digital visual to the user
- Save money and effort for printing.

RELATED WORK

With the development of cellular networks in the 1970's for increasing the lack of frequencies in the radiotelephone services which in turn lead to introduction of AMPS (Advanced Mobile Phone System) where the transmission was analog based. This was known to be the first generation in cellular networks. The second generation was based on digital transmission and was called with various abbreviations as GSM (Global System for Mobile communications), ERMES (European Radio Messaging System). Various Cordless telephone standards were also introduced during this time only. The third generation has risen with the unification of different technologies; some of them which are popularly known are FPLMTS (Future Public Land Mobile Telecommunications System), UMTS (Universal Mobile Telecommunication System), and IMT-2000 (International Mobile communication). These days, BLUETOOTH technology has become one of the most popular medium for wireless data transfer. It has a wide range and is efficient in its work.

Android is a set of software for mobile devices including Operation System, Middleware and Core Application, and a new Mobile Platform of Google. It is a complete mobile platform based on LINUX 2.6 Kernel that provides universal set of powerful Operation System, Comprehensive Library Set, abundant Multimedia User Interface and Phone Application. Android platform is produced to make new and innovative mobile application program for the developers to make full use of all functions connected to handset internet. The Android platform was developed by Google and later the Open Handset Alliance (OHA).

- Related work in this field includes Notice Board based on 8051 and which uses GSM technology [5]. Another paper shows the work done on 8051 using ZigBee communication. Yet another work has been done based on Arduino platform. Another work shows the use of Raspberry Pi as the platform using the GSM technology [6]. We propose the use of Raspberry Pi2 as the platform and using both GSM and Wi-Fi technologies for communication. The advantage of using these is that apart from text, we can send an image (from an authorized smart phone) which can be in turn shown on the display board.

LITERATURE SURVEY

A. Wireless Electronic Display Board Using GSM Technology [2]

The aim of this paper is to design a SMS based display board which can replace the current programmable electronic display and conventional notice boards. It consists of a display toolkit which can be programmed and be used from an authorized mobile phone. The GSM modem receives a message from the authorized mobile phone .

B. Raspberry Pi based speech recognition system for automation [5]

This paper deals with the implementation of voice-based system by using Bluetooth with the help of android application. It uses a Raspberry pi and for voice recognition an android app is developed. The communication is made possible by using Bluetooth module. At first the smartphone recognizes our voice with the help of Android app and converts it into text and the text is transferred through Bluetooth of phone to external Bluetooth module which is connected to the Raspberry pi board, then the Bluetooth

transfers the message. The Raspberry pi searches the command given. If it finds, then corresponding work will be done.

C. Wireless Electronic Notice Board [1]

This paper introduces a system which will enable people to wirelessly transmit notices on a notice board using Zigbee. Here the authorized people can access the notice board using graphical user interface(GUI).This system consists of two modules.The transmitting module consists of interfacing computer via serial interface to the Zigbee module. The receiver module consists of Zigbee module interfaced with a microcontroller for displaying messages on LCD. Password based authentication is employed on the transmitter side in order to provide access control to only authorized users.

CURRENT THEORY

Currently we rely on putting up notices on the notice boards using papers. This is time consuming since we need time for preparing notices. Also there is wastage of paper. If we need to renew the notice then we have to take a new hardcopy .A separate person is required to take care of this notices display and this becomes a tedious task.

The interfacing of a GSM modem with a normal PC is quite easy with help of the commands sent to it from the HyperTerminal window. But we must take into fact that the modem requires a wired connection at one end and wireless at the other.In view of the above it will be apparent that, there exists a need of electronic notice board that enables efficient way to the user for displaying notice. By considering increasing compactness of electronic systems, there is a need of embedding two or more systems together. This project is an implementation of the idea of wireless communication between a mobile phone and a raspberry pi which is a mini computer.

In this project work, we are supposed to design an embedded system which consists of display unit, printer and audio device using wireless technology. The display unit consists of any type of display that can be interfaced with microcontroller. Wireless printer is used for printing application. Audio device is speaker which is controlled by microcontroller through Speech-To-Text(STS)convertor. GSM technology is specially used for SMS .In order to implement this project, we need to create an Android application that is capable of performing the following:-

Functions:

Convert voice data to text

- Send this text over to Raspberry Pi via Wi-Fi/GSM for displaying on notice board
- Play the message from the audio device .
- Send the message as SMS/Text/Image .

Any type of LCD monitor display can be used as display device. This will be connected to controller via VGA to USB cable.

Proposed Work

Hardware Requirements

A. RASPBERRY PI 3

It is a series of credit card-sized single- board computers developed in the United Kingdom by the Raspberry Pi Foundation. Raspberry Pi is based on the Broadcom BCM2837 system on a chip (SoC), which includes an ARM Cortex A-53, 1.2 GHz processor, Video Core IV GPU with 1GB RAM, Micro-SD card etc. It supports the programming languages such as C, C++, python etc. This has in-built Wi-Fi and Bluetooth.

B. MicroSD CARD

Micro SD Card is flash memory card used for storing information. A minimum of 8 GB memory card is used. It is a non-volatile card developed by SD card association.

1) STEPS FOR PREPARING A Micro SD CARD

- Choose a Micro SD Card of category class 10.
- Download the Raspberry Pi operating system.
- Unzip the file that is just downloaded.
- Download the Win32DiskImager software.
- Writing Raspbian OS to the SD card.
- Insert memory card to the Raspberry pi.

2) BOOTING RASPBERRY PI FOR THE FIRST TIME

- Insert the memory card into the Raspberry pi.
- Perform initial configuration which includes wide range of hardware connectivity options.
- Create a user account to login and develop the programs.

C. HDMI PORT

High Definition Multimedia Interface (HDMI) is an interface used for transferring uncompressed video data and compressed or uncompressed digital audio data from an HDMI devices such as video projector digital television etc.

D. HD DISPLAY

High Definition display is connected to the Raspberry pi the HDMI port to display the notifications.

E. DHT22

Temperature and Humidity Sensor for the time when no notices was displayed.

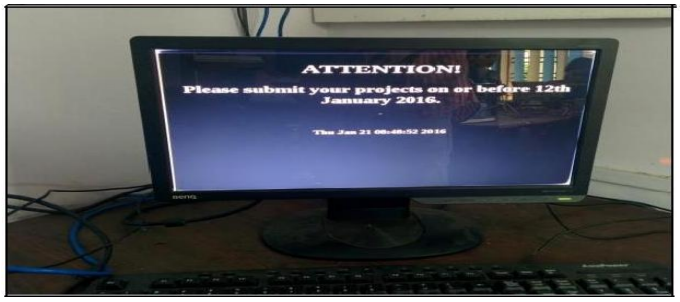

Fig. 1: smart notice board display.

Overview of Proposed System

The proposed system consists of android phone section and a receiver section. Android phone section consists of an android mobile phone in which the announcer speaks through his android mobile which contains speech to text application. To transfer the information, admin need to speak out the message ,send an image or type a text message through an android phone, which is provided with internet facility. A speech to text mobile application is used to convert the spoken voice message into the text message. The converted message is then transferred to the receiver section via Wi-Fi. Thus the text message will be sent to the desired notice board which is predefined. The HD display is connected to the Raspberry pi3 via the High Definition Multimedia Interface (HDMI) port in it. The Raspberry pi3 continuously checks the particular notices and on receiving one, it displays the message and save it as a HTML text file in the Micro SD card provided in the Raspberry pi3. Thus it identifies the new notifications and is displayed on the HD display. The text message can be displayed within 30 seconds. Updating of the new information will be as soon as the arrival of a new message. Thus the notifications are effectively displayed without any delay.Older notices are saved in the database .

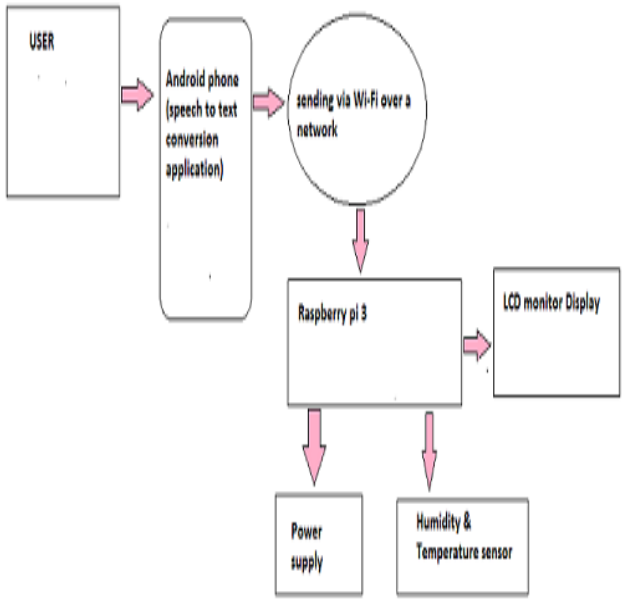

Fig.2 Block diagram of the proposed system

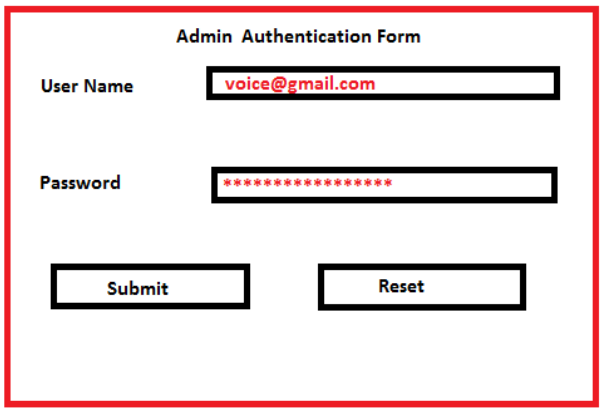

Fig.3 Proposed authentication form

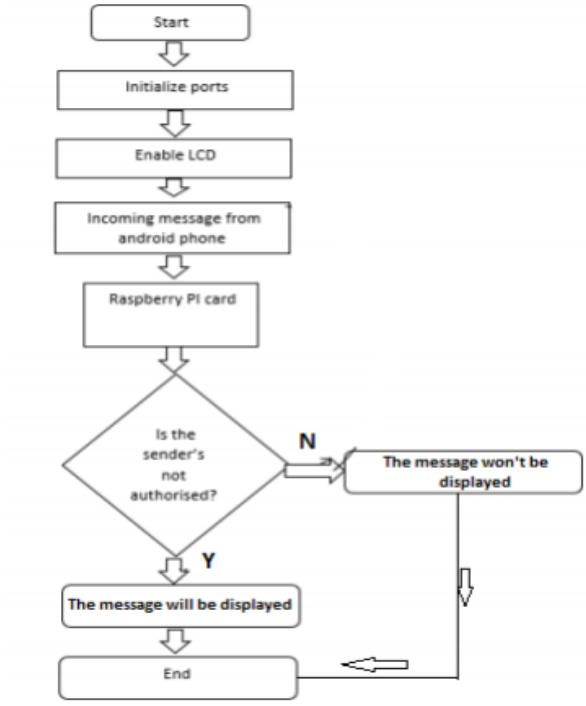

Fig. 4: Block diagram of Raspberry pi based speech to text based smart notice board display.

DEVELOPMENT OF ANDROID SPEECH TO TEXT BASED APPLICATION

Android is software for mobile devices that enables free download of environment for application development. The steps for setting up an Android Studio Development Environment include:

- Installing the Java Development Kit (JDK).
- Download the Android Studio Package.
- Installing the Latest Android SDK Packages.

The steps for creating a Speech to Text Android App in Android Studio include:

- Create a New Android Project.
- Define the Project and SDK Settings.
- Create an Activity.
- Develop the XML and JAVA files for the Speech to Text Application.

FUTURE SCOPE

Hand gestures can be used to control the display. This is achieved by using an image processing. A person doing presentation can do it independently without the help of another person.

At the receiver the text message can be again converted into voice message and message can be delivered through speaker if it is an important message. By commercializing the gmail, the notifications will be able to be displayed for a long time and will be able to refresh the messages. It will be helpful in displaying the timetables and any messages that are to be displayed as rows and columns as notifications.

Cron is used to schedule a job that is executed periodically for example to send out a notice every morning.

Multilingual display can be another added variation in the project, like user can speak in any of the regional languages and that is converted to text [11]

The Bluetooth printing has been implemented successfully with android phone and outputs have been verified. Future work focuses on implementation of Wi-Fi.

REFERENCES

[1] Aniket Pramanik; Rishikesh; Vikash Nagar; Satyam Dwivedi; Biplav Choudhury, "GSM based Smart home and digital notice board", International Conference on Computational Techniques in Information and Communication Technologies (ICCTICT-2016), pp: 41 - 46.

[2] G. P Rajesh; Praveenraj Pattar; M. N Divya; Vara Prasad, "Near field application: NFC smart notice board ", Thirteenth International Conference on Wireless and Optical Communications Networks (WOCN- 2016) ,pp: 1 - 5.

[3] V. C. Osamor, O. S. Aloba, I. P. Osamor, "From wooden to digital notice board (dnb): design and implementation for university administration", International Journal of Electrical & Computer Sciences, vol. 10, no. 2,2010,pp. 79-83.

[4] K. Shruthi, Harsha Chawla, Abhishek Bhaduri, "Smart notice board", Research & Technology in the Coming Decades (CRT 2013) National Conference on Challenges in. IET, 2013.pp: 1-4.

[5] N. Villar, K. Van Laerhoven, H. Gellersen, "A physical notice board with digital logic and display", Proceedings of the 2nd European Union symposium on Ambient intelligence. ACM, 2004.

[6] R. Teymourzadeh, S. Ahmed, K. W. Chan, M. V. Hoong, "Smart gsm based home automation system", Systems Process Control (ICSPC) 2013 IEEE Conference on,Dec 2013, pp. 306-309.

[7] Sayidul Morsalin; Abdur Rahman; Abu Bakar Siddiqe; Prattay Saha; Reduanul Halim," Password protected multiuser wireless electronic noticing system by GSM with robust algorithm",2nd International Conference on Electrical Information and Communication Technologies (EICT)2015, pp:249 - 253.

[8] Sadia Sultana; Md. Al Amin Haque; Md. Shah Alam, "Android academic assistant" ,17th International Conference on Computer and Information Technology (ICCIT),: 2014 ,pp: 65 - 68.

[9] Ying-Wen Bai; Jui-Po Hsu; Hen Teng; Hsing-Eng Lin, "Design and implementation of an embedded surveillance system with video streaming recording triggered by an infrared sensor circuit", International Symposium on Communications and Information Technologies 2007,IEEE Conference on 2007 pp: 335 - 340.

[10] Priyanka P. Patil , Sanjay A. Pardeshi , " Marathi Connected Word Speech Recognition System ", IEEE First InternationalConference on Networks & Soft Computing , Aug. 2014 . pp 314 – 318 .

[11] Yogita H. Ghadage; Sushama D. Shelke, "Speech to text conversion for multilingual languages", International Conference on Communication and Signal Processing (ICCSP-2016) , pp: 0236 – 0240.

Design and Development of 8051 Based Embedded Trainer Kit for Teaching and Project Development Purpose

Manasi Mishra, Rachit Thukral and S R N Reddy
Indira Gandhi Delhi Technical University for Women, Delhi
manasimishra10@gmail.com, rachitthukral@gmail.com, rammallik@yahoo.com

A microcontroller is the heart of an embedded system and plays a foundation steps towards the study of it. Understanding the microcontroller has become necessary not just for engineering but also many other disciplines, such as computer science, electronics and physics. Training session is one approach that helps the students to understand the subject when they are exposed to the hardware and software.
This paper discusses the design, development and use of 8051 based embedded trainer kit for teaching and project development purpose. 8051 [8-bit] microcontroller has been chosen for being widely used for introductory course in Indian universities and colleges because it is affordable simpler and easier to describe than other Microcontrollers. The microcontroller trainer kit has completely been designed and developed in-house which includes 8051 microcontroller, led's, switches, buzzer, LCD, relay and expansion ports so that it can be used not only for teaching in class but also for student's design projects. A series of example-driven programs both in assembly and embedded C language & hands-on tutorials has been developed to guide students to a comprehensive embedded system design flow in a bottom-up fashion. Various workshops and training sessions with this kit were organized for b.tech students in few colleges. The results show that using this platform not only generates excitement and motivation in students, but also enhances their learning and teaches them skills of modern embedded systems design. The motivation behind this paper is to devise a model for learning Microcontroller by developing an 8051 Microcontroller based trainer kit, complete user manual containing the schematic for the board, Programming manual containing experiments in assembly and embedded C language and videos demonstrating simple applications.

Keywords: Microcontroller, Embedded system, trainer kit, Programming

Masquerade Detection Technique based on User Profiling

Md Arquam
Computer Science & Engineering
National Institute of Technology
Delhi, India
arquam@nitdelhi.ac.in

Anurag Singh
Computer Science & Engineering
National Institute of Technology
Delhi, India
anuragsg@nitdelhi.ac.in.

***Abstract*— Data theft is a prime concern of the cybercrime community in the recent years, hence, it gets much more attention to the researchers. Masquerader attacks are a usual information security issue that is result of theft of identity. Such attacks are done by a masquerader who wrongly pretends as actual user. Prevention-focused method such as access control and data loss Prevention tools has failed in protecting these attacks. Therefore detection of data theft is not a mere requirement, but rather a necessity. Previous researches are done aiming on modelling of user command to recognise the uncommon behaviour of impersonation. None of these methods could be packaged into an easily-installable, privacy-preserving, and potent masquerader attack detector. In this paper, a hybrid method is proposed by using the support vector machine and Naïve Bayes classifier techniques to find the masquerader. It works on the basis of probability and frequency of each command respectively. This hybrid method will detect alphanumeric command, while previous researches detect either numerical command or character command.**

***Keywords*— Masquerade Detection, User profiling, Information Security, SVM, NB**

1. INTRODUCTION

The crime watch review states that 35% of the 523 security executives and law enforcement officials experienced illegal access and use of their information, systems, and networks [1]. This type of illegal access of information, called as a masquerader attack. It is second in the list of top five cyber crimes committed by outsiders after virus, worms and other malefic code attacks.

Generally a masquerader gets access to an authorized user's account either by snaffling a sufferer's confidential information via password signing and cracking tools, or by using of a root kit or key logger. Traditional security technologies such as access controls had little effect in preventing masquerader attacks. Passwords can be easily sniffed or cracked by the numerous password crackers readily available through the web such as L0phtcrack. Biometric solutions, whether using fingerprint, iris, or face recognition, can all be easily defeated [2].

2. RELATED WORK

Intensive researches have been shown that lot of methods have been proposed to detect the masquerader based on various parameters.

Data Loss Prevention (DLP) tools [3], which were designed to prevent data theft as their name suggests, are not effective in preventing information leakage.

The first method was proposed by Du Mouchel [4] named as the Bayes one-step Markov approach. Incremental Probabilistic Action Modeling (IPAM), another approach was formulated by Davidson and Hirsch [5] using on one-step command transition probabilities roughly calculated from the trained data, and implemented on the same dataset.

Ju *et al.* [6] proposed a hybrid high order Markov chain model. They proposed signature behaviour of a certain user is identified based on command sequence executed by user. But Markov model is not suitable when the test data consists too many unobserved commands in the trained data set.

Lane *et.al.* [7] proposed an approach based on sequence match. A similarity measurement is calculated for each new coming command

between the latest generated commands and a prior generated command of user's profile. It is slow for large number of commands.

Maxion *et.al*. [8] proposed Naive Bayes classifier for text classification task. It cannot classify numeric data. Yung [9] proposed a self-consistent naive Bayes classifier and deployed on the same dataset by exploiting the property of the naive Bayes classifier and the EM-algorithm. It is not suitable to use self-consistent naïve Bayes classifier to classify newly generated commands block either masquerader or not.

Wang *et.al*. [10] proposed a hybrid model by using binary characteristics of naive Bayes classifier and frequency based characteristics of Support Vector Machine (SVM). It produced better detection rate but high false positive.

Seo and Cha [11] explained sequence base SVM kernels. They show increase in accuracy but higher false positives. Ye *et al.* [12] experimented by taking a small content of data for masquerade detection. This small content of data contained audit phenomenon, system calls, user generated commands, number of consecutive password failures, command execution time of CPU, connection duration of network, phenomenon combination, along with the frequency of incidences, and the sequence or phenomenon transition

Szymanski *et.al*. [13] proposed a model based on recursively mining for the commands sequence. The recurrent sequences of commands are identified, encoded along with novel representations and rewrite the pattern using these new symbols. The process lasted till no new recurrent sequences in the modified input could be identified

To enhance the performance of masquerade detection technique an algorithm is required that detects abnormal commands with high detection rate and low fault rate. In this research an algorithm is designed by considering the low false rate of Navies-Bayes (NB) algorithm and high detection rate of Support Vector Machine (SVM) algorithm [14].

Dataset

In this paper experiment is performed on Schonlau dataset of 20 users of 50 blocks, and each block contains 50 commands.

The Schonlau dataset is provided with map file to check the block, as 0 indicates masquerader block and 1 indicates actual user block. The dataset provides the characteristics of user by repeating frequently used alphanumeric commands [15].

NAIVE BAYES CLASSIFIER

One-Class Naive Bayes (OCNB) in the domain of masquerader detection is based on Bayes Theorem. Naive Bayes (NB) classifiers are a supervised learning technique. They are very simple to implement and understand and more often than not give efficient results [9]. Bayes theorem gives a rule for conditional probability. Conditional probability may be defined as probability of phenomenon A occurring if phenomenon B occurs. In masquerader detection we use Naive Bayes classification to find the probability of a command block belonging to a user. For sample, to estimate that an instance of $w = \{w_1, w_2, w_3, \ldots, w_n\}$ belongs to class z as,

$$p(z \mid w) = \frac{p(z)}{p(w)} p(w \mid z) = \frac{p(z)}{p(w)} \prod_{i=1}^{m} p(w_i \mid z)$$

For Naive Bayes Classifier generally two types of model is used, first is the multi-variate Bernoulli model, and the second is called the multinomial model[16]. To represent a document, multivariate Bernoulli model uses a binary components vector to show a command takes place or not in the particular document. Multinomial model uses number of experienced command to characterize a document that is named as “bag-of-words” approach extracting the information about the number of frequency of word in documents.

According to Mc Callurn’s experiment [17], multi-variants Bernoulli model produces better result for small size vocabulary, while the multinomial model produces better result at larger size vocabulary.

Multi-variate Bernoulli model

Multi-variate Bernoulli Model uses a binary vector to represent command block *e where* $e=(b_1(e),b_2(e),\ldots.b_m(e))$ with $b_i(e)$ set to 1 when the command k_i takes place at least once in a particular block. Here total number of characteristics is represented by *m*, i.e., the number of distinct commands. Calculate the probability of command k_i , for user *U* in the

trained data. Now we can calculate *p(e | U)* of the test block *e* as:

$$p(e \mid U) = \prod_{i=1}^{m} (b_i(e)\, p(k_i \mid U) + (1 - b_i(e))(1 - p(k_i \mid U)))$$

Where $p(k_i \mid U)$ is roughly calculated with a Laplacean prior:

$$p(k_i \mid U) = \frac{1 + N(k_i, U)}{2 + N(U)}$$

N (U) is the number of trained data of user *U*, and $N(k_i, U)$ represents the number of documents comprising number of command k_i generated by user *U*.

Multinomial model

In multinomial model, a characteristic vector *e* is used to represent each command block where $e = (n_1(e), n_2(e), \ldots n_m(e))$ where $n_i(e)$ represents the total frequency of command k_i present in block *e* likewise , probability of the frequency count $p(k_i \mid U)$ is calculated for command k_i of user *U* in the trained data. Now *p(e | U) is* calculated for test block *e*:

$$p(e \mid U) = \prod_{i=1}^{m} (p(k_i / U))^{n_i(e)}$$

Where $p(k_i \mid U)$ is calculated from:

$$p(k_i \mid U) = \frac{\sum_{j=1}^{N(U)} n_i(e_j) + \beta}{\sum_{i=1}^{m} \sum_{j=1}^{N(U)} n_i(e_j) + \beta * m}$$

Here β is used to limits the sensitivity of the past undetectable commands.

SUPPORT VECTOR MACHINE

It has been proved experimentally that Support Vector Machines (SVM) is exceptionally potent to classify the Text data [14]. SVM classify the test data using maximal-margin technique, as compared to Naïve Bayes which is probabilistic. The basic idea of two class statement creation is to calculate the hyper plane that segregates the trained vectors from dissimilar classes by associating of characteristic vectors to a extreme dimensional space, as well as increases this segregation by maximizing the margin as big as feasible.

Scholkopf et al. [18] presented a new method called one-class SVM by modifying the SVM algorithm, in which samples are used from one-class for training in lieu of multiple classes. According to one-class SVM algorithm, input data is mapped to a extreme dimensional characteristic space through a kernel function and acts origin as the only sample from other different classes. Then maximal margin hyper plane is computed iteratively that best segregates the trained data from the origin.

Considering that our trained data set a_1 a_2 a_3 belongs to *A*. *F* is the characteristic associating *A* $\rightarrow F$ to a extreme dimensional space. Kernel function can be defined as:

$$k(a, b) = (F(a) \times F(b))$$

Using kernel functions, if characteristic vectors are not calculated explicitly, then computational efficiency will be improved since the kernel values can be directly calculated and operated. There are different types of kernel as linear and polynomial kernels:

Linear Kernel: $k(a, b) = (a \times b)$

n-th order polynomial kernel:

$$k(a, b) = (a \times b + 1)^n$$

Now, one-class SVM problem is

$$\min_{\alpha} \frac{1}{2} \sum_{i,j} \alpha_i \alpha_j k(a_i, a_j)$$

Subjected to $0 \le \alpha_i \le \frac{1}{v_l}, \sum_i \alpha_i = 1$

Where α_i is a Lagrange multiplier,
a_i is weight on sample
n is a parameter that limits the trade-off between increasing the number of data points and the distance of the hyper plane from the origin.

After solving for a_i , data is classified by solving decision function. The decision function is:

$$f(a) = \text{sgn}\left(\sum_i \alpha_i k(a_i, a) - \rho \right)$$

One-Class SVM

A variant of SVM in which we say whether the data belongs to a particular class or not unlike binary Classifiers like normal SVM and Naïve Bayes which divide the samples into classes based on which class the sample matches closer. So, using one-class SVM, there is no need to train the SVM about the other class. This type of SVM is particularly useful in proposed case because we can say for sure that a particular behaviour belongs a particular user for all possible different behaviours. So, in proposed paper we use one-class SVM.

Performance Criteria

In anomaly-based IDS, first we train a model and set the threshold. Setting this threshold is an essential process, as this threshold is eventually used to find the testing data is malicious or non-malicious.

A false positive (FP) happens when, an IDS classifies actual user data to be attack data. A true negative (TN) is defined as when the IDS predicts non-attack data to non-attack data. Similarly a true positive (TP) occurs when the IDS correctly classifies an masquerader data to be attack data. And lastly, a false negative (FN) is defined when the IDS classifies attack data to non attack data. To determine effectiveness of a masquerader detection technique we calculate detection rate and false positive rate for the technique. The ideal masquerader detector should be able to detect all the true positives and should not have any false positives. To compare two masquerader detectors, their effectiveness is measured by comparing their detection rate and false positive rate.

To empirically analyse and compare the performances of an intrusion detection technique, their accuracy rates (ACR) are considered. Accuracy rate defines the overall accuracy of the IDS. It can be defined as below,

ACR = (TP + TN)/ (P + N)

Detection rate is also known as true positive rate (TPR). Detection rate of IDS defines its correctness.

TPR = TPP=TP / (TP + FN)

Hence we calculate detection rate, accuracy rate for different masquerader detection techniques on the same dataset while comparing and analysing performances of the techniques considered in this paper.

3. PROPOSED METHOD

In this section, the complete detail of the new proposed method is described.

Algorithmic Details

Proposed method of masquerader detection is focused on probability count characteristic of Naïve-Bayes and word count characteristic of SVM. So keeping this in mind multivariate model of Naïve- Bayes and One-Class model of SVM is used. All parameter is choosen based on Schonlau Dataset. Probability p from NBMV is used as deciding factor in masquerader detection. Let a block of k command such that k= {c_1 c_2..... c_m where c_i command} issued by a user u_i. It is assumed that each user has its own characteristics, which will differ from masquerader or other user. This characteristic means some set of command appearing repeatedly in command block, which will define the user behavior. The NB and SVM classifier are trained by command set k_i issued by a user u_i and later after tested by test blocks.

There are different types of command block. We can classify the block as follows:

1. Block having all different command other than what is appearing in training dataset.
2. Block having 25% commands appearing first time and 75% commands belonging to user.
   In this 75% commands belonging to user it can be further classified as:
   i. All commands are unique non repeating
   ii. Commands are repeating more than k times (k refers to sensitivity, which does administrator set)
3. Block having more than 25% commands unique appearing.

Therefore, according to the proposed definition of masquerader first type and third type should be classified as masquerader. Second type should be classified as non masquerader because it is possible that user may issue some new command which he/she has never issued before (that is never seen before command) but that can be only less than or equal to 25% of total command and others having different commands belonging to user.

NB Multivariate model always calculate the probability of commands according to the occurrence of each command in training set and

according to its probability.

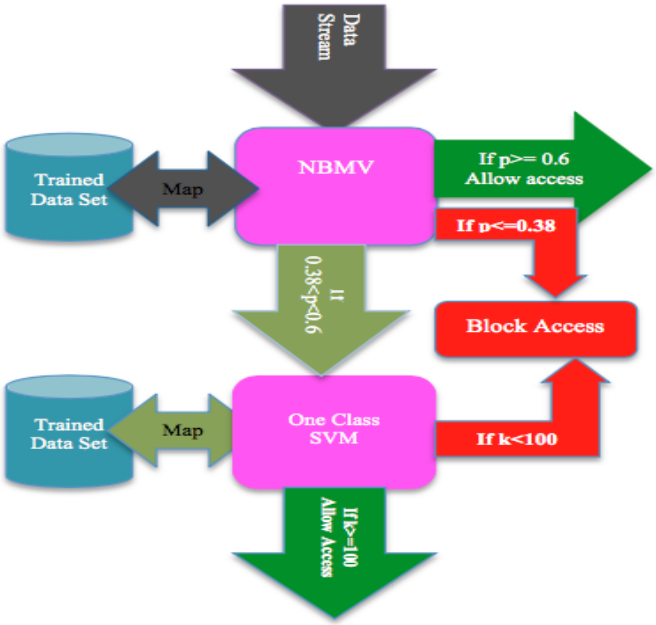

Figure 1: Flow chart of Proposed Method

NB assigns the overall probability of block feed during the testing in following manner as:

1. If $p \geq 0.60$, marked as normal user.
2. If probability p is $(0.38 \leq p \leq 0.59)$, marked ambiguous.
3. If $p < 0.38$ are masquerader

It never focuses on the number of occurrences of commands in testing block. Those commands blocks which are ambiguous and remain undetected due to frequency of occurrences in the test block . That is feed to one class support vector machine that successfully classify the forwarded block in following manner on basis of block size of command as:

1. If $k \geq 100$, marked as actual user, otherwise block the access it will be masquerader.

A flowchart of the working structure of proposed algorithm is shown in figure 1.compared with associating file provided in Schonlau dataset for accuracy.

Table 1: Result of Detection Method.

Method	Detection Rate	False Positive Rate
NBMV	66.78	7.8
One Class SVM	80.1	21.08
Proposed Method	85.04	5.08

Proposed method has better detection rate as compared to NBMV and One class-SVM, while low fault rate as shown in Table 1. Graph is also showing proposed method is better than NBMV and One class SVM in respected of detection rate and false positive rate in figure 2 and figure 3.

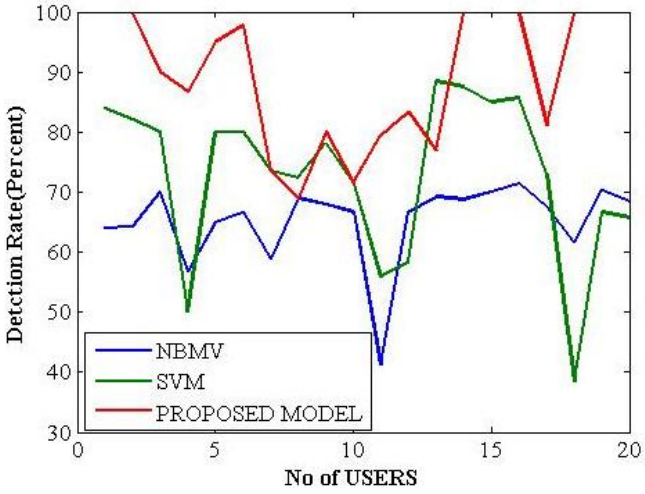

Figure 2. Detection Rate

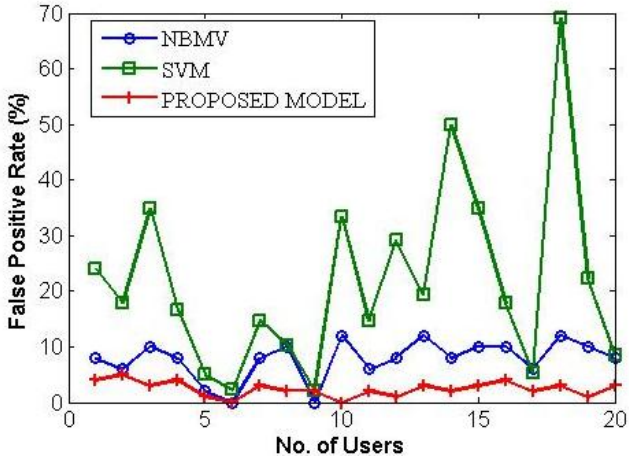

Figure 3. False Positive Rate

4. CONCLUSIONS AND FUTURE WORK

Masquerader detection problem is varying according to various factors. In the proposed method of combining Naïve Bayes and Support vector machine feature masqueraders are detected successfully. Its activity has provided high detection rate and low false positive rate.

Future work of this method could be applied to large data set. Here, we have taken moderate data. By combining Navies Bayes multivariate and Navies Bayes Multinomial with one class SVM could also lead to high detection rate.

REFERENCES

[1] J. CERT. 2010 e-crimes watch survey, 2010.

[2] Mark Lane and Lisa Lordan. Practical techniques for defeating biometric devices. Master's thesis,Dublin City University, 2005.

[3] Vladimir N. Vapnik. The Nature of Statistical Learning Theory (Information Science and Statistics). Springer, 1999.

[4] William Dumouchel. Computer intrusion detection based on bayes factors for comparing command transition probabilities. Technical report, In National Institute of Statistical Sciences, 1999.

[5] B. D. Davison, and H. Hirsh, "Predicting Sequences of User Actions", Working Notes of the Joint Workshop on Predicting the Future: AI Approaches to Time Series Analysis, Fifteenth National Conference on Artificial Intelligence (AAAI98)/Fifteenth International Conference on Machine Learning (ICML98), AAAI Press, 1998.

[6] Wen-Hua Ju and Yehuda Vardi. A hybrid high-order markov chain model for computer intrusion

[7] T. Lane and C. E. Brodley. Sequence matching and learning in anomalydetection for computer security. In In AAAI Workshop: AI Approaches toFraud Detection and Risk Management, pages 43{49. AAAI Press, 1997.

[8] R. A. Maxion and T. N. Townsend. Masqueradere detection using truncatedcommand lines. In DSN '02: Proceedings of the 2002 InternationalConference on Dependable Systems and Networks, pages 219{228. IEEEComputer Society, 2002.

[9] K. H. Yung. Using self-consistent naive bayes to detect masqueraderers. InPAKDD'08: Proceedings of the 8th Paci_c-Asia Conference on KnowledgeDiscovery and Data Mining, pages 329{340, 2004.

[10] K. Wang and S. J. Stolfo. One-class training for masqueradere detection.In Proceedings of the 3rd IEEE Workshop on Data Mining for Computer Security, 2003.

[11] Jeongseok Seo and Sungdeok Cha. Masqueradere detection based on SVM andsequence-based user commands pro_le. In ASIACCS '07: Proceedings ofthe 2nd ACM symposium on Information, computer and communicationssecurity, pages 398{400, 2007.

[12] Nong Ye, Xiangyang Li, Qiang Chen, S.M. Emran, and Mingming Xu.Probabilistic techniques for intrusion detection based on computer auditdata. Systems, Man and Cybernetics, Part A: Systems and Humans, IEEETransactions on, 31(4):266{274, Jul 2001.

[13] Boleslaw K. Szymanski and Yongqiang Zhang. Recursive data mining formasqueradere detection and author identi_cation. In Proceedings of the 13rdAnnual IEEE Information Assurance Workshop. IEEE Computer Society Press, 2004.

[14] Thorsten Joachims, "Text categorization with support vector machines: Learning with many relevant characteristics", In Proc. of the European Conference on Machine Learning (ECML), pp. 137-142, 1998.

[15] Schonlau, M. Masqueradering User Data. In Matthias Schonlau's (Matt Schonlau) Homepage. Retrieved August 30, 2011, from http://schonlau.net/

[16] Lin, D. and Stamp, M. (2011, August 3). Hunting for undetectable metamorphicviruses. Journal in Computer Virology, 7(3), 201- 214

[17] A. McCallurn, K. Nigam, "A Comparison of Phenomenon Models for Naive Bayes Text Classification", AAAI-98 Workshopon Learning for Text Categorization, 1998

[18] B. Scholkopf, J.C. Platt, J. Shawe-Taylor, A.J. Smola, and R.C. Williamson, Estimating thesupport of a highdimensional distribution". Technique report, Microsoft Research, MSR-TR-99-87, 1999.

A Pareto-optimal solution for Data Aggregation in WSN using Fuzzy Logic and Genetic Algorithm

Nonita Sharma and Ajay K Sharma
National Institute of Technology Delhi
nonitasharma@nitdelhi.ac.in, director@nitdelhi.ac.in

This manuscript proposes a creative utilization of Genetic Algorithms (GA) using Fuzzy Logic for solving the problems of data aggregation in heterogeneous Wireless Sensor Network (WSN). The paper is an attempt to demonstrate that the traffic scenarios of WSN could be worked upon accordingly, through parametric fine tuning and algorithm change, particularly when the aggregation node is used to relay the data further to the base station. One of the applications of GA is to construct an optimal data aggregation tree from the sensor nodes to the monitoring station. The proposed algorithm is suitable for applications, where the aggregation node is used to relay data further to the base station in heterogeneous setups. Series of simulation outputs demonstrate a significant improvement in accuracy and efficacy through the proposed algorithm with regard to residual energy, dead nodes, payload, and network lifetime as compared to Classical GA algorithm.

Some Remarks on QoS in WLANs

H M Gupta
ICEIT, Delhi
harimgupta@gmail.com

In the current networking scenario, WLANs form an integral component of data network architecture. These are deployed in residential, commercial and public sites. The application mix is now gravitating towards multimedia data transfer. The limited quality of service (QoS) is a restraint in such deployments. Therefore, it is imperative to alleviate the situation and evolve QoS support mechanisms. Such mechanisms include priority assignment and fair scheduling. These are mapped on to the existing IEEE 802.11 protocols. The end aim is to design MAC protocols by choosing a right set of parameters. We consider some cases of such MAC designs and remark on their effectiveness.

Pareto Optimal Solution for Joint Optimization of Power Assignment and Delay in Wireless ad hoc Networks

Sunita Prasad
Centre for Development of Advanced Computing, Noida
sunitaprasad@cdac.in

In wireless ad hoc networks, energy conservation is of paramount importance because nodes are equipped with batteries of limited lifetime. The minimum energy multicast tree (MEM) problem aims to construct a multicast tree that has the lowest energy consumption. Recently, there has been a phenomenal growth of group communications and real time applications over wireless a network that has focussed the research on QoS-aware multicast routing. However, efficient resource utilization can be achieved when the QoS provisioning technique also conserves energy. In this paper, we extend the classical MEM problem to incorporate end-to-end delay as the QoS parameter between the source and any destination along the tree. We measure the end-to-end delay to a given node in terms of the number of hops the data travels from the source to that node. Clearly, these two objectives are conflicting as the multicast tree with least total transmitted power may have a long delay to the farthest destination. We propose a modified ant colony based algorithm to determine the set of Pareto-optimal solutions that captures the interactions between different objectives. Extensive simulations have been conducted to validate the correctness and efficiency of the protocol. The experimental results demonstrate the ability of the protocol to generate the Pareto optimal solution in a short computational time.

Energy Efficient Approach for a Wireless Sensor Networks using Matrix Completion

Megha Goyal[1] Ridhi[2] Shivangi Jha[3]
Tanvi Surana[4] Vivekanand Jha[5]
[1]meghagoyal_23@yahoo.co.in
[2]ridhi.aqua@gmail.com
[3]tanvisurana20@gmail.com
[4]shivangijha@gmail.com
[5]vivekanandjha@igdtuw.ac.in
Indira Gandhi Delhi Technical University for Women, Delhi

ABSTRACT

A wireless sensor network is a network of autonomous sensor nodes which monitor physical or environmental conditions and send this data to the base station. The wireless sensor network has multiple constraints, which include energy, accuracy, coverage and connectivity. The proposed work in this paper aims to enhance the network lifetime using correlation among sensor nodes and matrix completion technique, under permitted level of accuracy. The proposed work is divided into four stages. In the first stage, nodes are deployed in an optimal manner, in a network having corona-based architecture. In the second stage, correlation among the nodes is exploited to form coalitions in all the coronas. In the third stage, data transmission takes place via multi-hop routing. In the fourth stage, matrix completion technique is applied to the data gathered at the sink, to obtain the data of all nodes. The proposed work reduces the number of messages to be sent to the sink, hence increasing the energy efficiency.

I. INTRODUCTION

A wireless sensor network is a network of autonomoussensors, which monitor physical or environmental conditions, such as temperature, sound, pressure, etc. and cooperatively pass their data through the network to the base station known as the sink. Recent advances in Micro-Electro-Mechanical systems (MEMS) technology have enabled the development of low cost, low power, multifunctional sensor nodes that are small in size and communicate untethered in short distances. These tiny sensor nodes can sense, measure and gather information from the environment, and, based on some local decision process, they can transmit their data to the user.

Smart sensor nodes are devices equipped with one or more sensors, a processor, memory, a power supply, a radio, and an actuator. These nodes are spatially distributed, so they work cooperatively to communicate information gathered from the monitored field through wireless links. Nodes process their gathered data with the help of an on-board processor, to carry out simple computations and transmit only the required and partially processed data. But, due to limited memory constraints, the data needs to be transmitted further to some sink, which either uses the data locally or is connected to some other network, say Internet.

These networks have a wide variety of applications such as military applications and area monitoring applications [1]. These sensor nodes have a limited battery life. Hence, energy efficiency is critically important in design of wireless sensor networks. When the factor of energy consumption is not considered then problem of *energy hole* arises. The sensors in the area near the sink gets drained of energy faster than the rest of the sensors as they have to carry the burden of forwarding more information to the sink due to convergence of data. For improving energy efficiency, many techniques have been proposed. One such technique involves formation of coalitions of nodes, in which only one node from each coalition transmits data on behalf of the other nodes. This leads to an increased network lifetime. But, this scheme can lead to a decrease in accuracy of data obtained as data from all nodes is not considered.

Also the deployment area, 100% covered by the densely deployed sensor nodes, may have *coverage holes*; areas not in range of any node, voids created because of random deployment, obstructions, and, mostly due to, node failures etc. Different techniques exist which can improve the accuracy of data and help in reducing the problem of coverage holes. Matrix Completion is one such technique, in which the incomplete entries of a partially observable matrix are filled. Hence, the whole matrix can then be generated.

The rest of the paper is organized as follows: Section II surveys the related work. Section III explains the proposed work. Finally, Section IV concludes the paper.

II. PAST WORK

Different strategies have been proposed to solve the energy hole and the coverage hole problem. Clustering was one of the earliest approaches to

overcome the non-uniform energy dissipation rate among the nodes of the network. One of the first and most popular clustering protocols proposed for wireless sensor networks was LEACH (Low Energy Adaptive Clustering Hierarchy). It uses homogeneous stationary sensor nodes, which are randomly deployed. It's a hierarchical, probabilistic, distributed, one-hop protocol, with the main objective to improve the lifetime of WSNs by trying to evenly distribute the energy consumption among all the nodes of the network. All nodes have a chance to become CHs to balance the energy spent per round by each sensor node. But, it has the drawback that even a node with low energy can become a Cluster Head, which can lead to the formation of an energy hole. Chen, Li, Ye and Wu proposed an unequal cluster-based algorithm in [2] in which clusters closer to the base station have smaller sizes, while those far away from the base station have larger sizes. It achieves an improved network lifetime as compared to the LEACH algorithm.

Wu and Chen in [3] have proposed a non-uniform node distribution for the network of sensor nodes, in which a corona-based architecture is used. Nodes are deployed in the form of an increasing geometric progression from outermost to innermost coronas, so that maximum number of nodes are present near the sink, which alleviates the energy hole problem.

To solve the coverage hole problem, Ferng et al. has proposed optimal placement of nodes in different coronas in [4], so that all areas of the coronas are covered by at least 1 sensor node. Hence, this ensures that the whole network will be covered by a minimum set of nodes.

But, the clustering algorithms do not factor in the correlation factor present among the nodes of the sensor network. To exploit the spatial correlation among the nodes, coalitions can be formed.

There are various methods that have been used to form coalitions in the most energy efficient manner. Guha, Gunter and Sarkar in [5] have demonstrated that sharing between groups has different properties from sharing between individuals and investigate fair, mutually beneficial sharing between groups. Using these algorithms, it is demonstrated that fair coalition routing allows different groups to mutually beneficially share their resources.

Gao, Zhang, Larish and Shen in [6] have described cluster-based wireless sensor networks where sensor nodes are organized into groups to form coalitions and it is assumed that each coalition head collects data for sensors within that coalition and carries out data compression. Three data transmission schemes are examined. In scheme 1, a node in each coalition is selected randomly by the CH to transmit the data. In scheme 2, the node with the best channel condition in each coalition transmits the data, exploiting multiuser diversity gain. In Scheme 3, all the nodes within a coalition transmit in a cooperative manner, so the cooperative diversity gain could be achieved. Hence, coalition algorithms reduce the energy consumption of nodes in the network. But, they can lead to a decrease in accuracy. This can be avoided using the Matrix Completion technique.

Matrix Completion has been solved by a variety of algorithms. One such algorithm is Singular Value Thresholding (SVT) [7]. It solves the nuclear norm minimization problem by performing a soft-thresholding operation on the singular values of the matrix. The main advantage of this approach is that the algorithm makes use of minimal storage space by exploiting the sparsity of the matrix and has a low computational cost per iteration.

There are a number of problems, which have been solved using Matrix Completion. An efficient data collection approach has been has been proposed for wireless sensor networks [8]. It utilizes spatial and temporal correlation present among the nodes in the network, to save energy, by randomly choosing the node to sample the data and the instance at which the data will be sampled. It samples all nodes, and uses matrix completion to recover the data that is lost during transmission.

It has also been used in network completion, where only a small sample of the network is observed and the unobserved part is inferred from this sample [9]. It makes the assumption that pair wise similarity between nodes has also been provided. First the observed matrix is completed and then transduction of knowledge takes place by exploiting similarity information. This method can be generalized for multiple sources of auxiliary information such as edge attributes of the network.

III. PROPOSED WORK

The objective is to design an algorithm that provides a solution to the *energy hole* and the *coverage hole* problem. This solution should help us to achieve a balanced energy distribution, while at the same time, leave no room for partial coverage.

While these are some mandatory issues that we encounter in Wireless Sensor Networks (WSNs), our focus here will be to maximize:

- Network Lifetime (by forming coalitions), and
- Accuracy (by using Matrix Completion at the sink).

For the same, a corona-based network architecture is considered, where the entire area is divided into a system concentric circles of uniform width. This is the Corona Model I in [4].

In this phase, the proposed solution is divided into four stages: Firstly, nodes are deployed using two Deployment models. The first deployment model is the Pseudo-Random Deployment Model, in which a minimum number of nodes are optimally deployed, and the remaining nodes are randomly deployed. In the second model, all nodes are randomly deployed. After that, coalitions are formed in all coronas, which is followed by data transmission to the sink, using

multi-hop routing via relay nodes. The final stage involves matrix completion, which is performed at the sink, to improve the accuracy of data obtained by regenerating the data of all the nodes.

A. ARCHITECTURE

First of all, a circular area of some radius with a static sink located at the centre of the circular area monitored by sensor nodes is considered. Second, a corona model used to cover the monitored circular area is further considered by dividing the circular area into several coronas, each of width R(Figure 1). Generally speaking, we can use (k+1) tuple $(k,w_1,\ldots,w_k)$ to describe the corona model, where k is the total number of coronas, w1 is the radius of the innermost corona, and w_i , where i = 2, 3…k, denote the width of the i^{th} corona. the sensor node sensing and transmission ranges are s_u and d_u, respectively, where the subscript u is used to explicitly denote the uniform corona width and the width of each corona is set to the node sensing range.

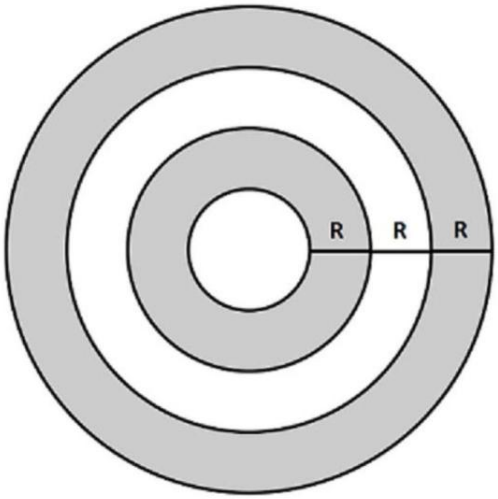

Figure 1: Network Architecture

B. DEPLOYMENT MODELS

Nodes are deployed in **geometric progression** from the outer coronas to the inner ones except C_R randomly [3] in second phase of Pseudo-Random Deployment and in Random Deployment:

Deployment Strategies:

- Pseudo-Random Deployment
- Random Deployment

Analysis for WSNs is done based on 2 deployment models.

Pseudo-Random Deployment

This optimally deploys the minimum number of nodes needed to cover the entire area, corona-wise, and deploys all the other nodes in a random manner using an increasing geometric progression, from the outermost to the innermost corona

Random Deployment

- The basic idea is that the nearer the corona is to the sink, the higher is its node density
- Different numbers of nodes are deployed in different coronas, depending on their distance to the sink
- Let us assume that the nodes in corona Ci are distributed with a density of ρ_i, for 1<=i<=R. The node density increases from the outermost corona C_R to the innermost one C_1. From the viewpoint of the whole network, the nodes are distributed non-uniformly. Therefore $\rho_1>\rho_2>\rho_3>\ldots\rho_R$

Nodes are randomly distributed in the entire Corona model I, according to the Geometric Progression formed in [3].

C. CORRELATION EXTRACTION

Spatial correlation and temporal correlation is exhibited by sensor nodes deployed in a wireless sensor network. Some wireless sensor network applications are developed to track an event. This makes use of temporal correlation as the changes in an event are monitored according to the temporal correlation between different readings of a sensor node.

For satisfactory coverage in a network, a large number of sensor nodes are deployed in an area, leading to high density of nodes in the area. Hence, the data sensed by the sensor nodes is spatially correlated because of the proximity of the nodes to each other. We would use the spatial correlation property of the deployed sensor nodes. Based on the degree of correlation between different nodes, coalitions will be formed in each corona. Each coalition will have a coalition representative which will transmit data, on behalf of all nodes. This reduces the number of messages to be sent to the sink. Hence the ratio of number of nodes in a coalition to the number of messages sent to the sink is n:1, where n is the number of nodes in a coalition. Hence, the energy of the other nodes will be conserved. Coalition representatives in each corona will transmit data to the coalition representatives in the next inner corona as shown in Figure 2. Hence, all data is received at the sink.

D. MATRIX COMPLETION

The matrix obtained at the sink, is an NxT matrix, in which N are the number of nodes and T is the number of samples of each node.

An example of the same is shown in Figure 3. Due to the formation of coalitions, data from all the nodes is not available. The sink receives the data only from the coalition representatives. Hence, data from all non-coalition representatives is not available. In addition to that, coalition representative nodes may also fail or

data from them may be lost in transmission. Hence, the matrix completion technique is applied at the sink to obtain the data of all nodes, as shown in Figure 4. This leads to an increase in accuracy of obtained data, without the sensor nodes expending extra energy.

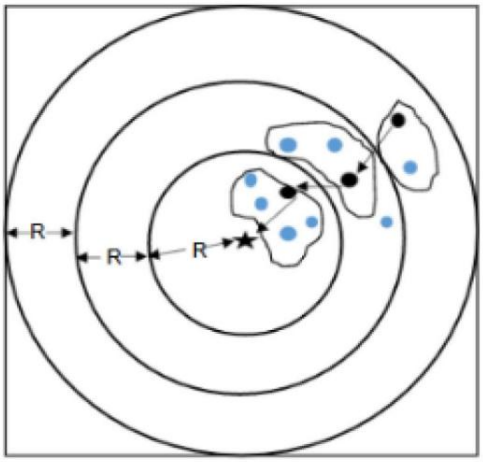

Figure 2 Data transmission by coalition representatives to sink

1	-1	-1	1	1
	1		1	
1				1
	-1	-1		

Figure 3 Matrix obtained at sink

1	-1	-1	1	1
-1	1	1	1	-1
1	1	-1	-1	1
1	-1	-1	1	1

Figure 4 Matrix obtained after applying Matrix Completion

IV. CONCLUSION AND FUTURE

An energy efficient algorithm for wireless sensor networks has been proposed. Firstly, nodes are deployed in such a manner that density of nodes is higher near the sink. After that, coalitions are formed on the basis of correlation between different nodes. Hence, the sink receives data only from the coalition representatives. Data of all nodes of the network is then generated using the matrix completion technique. This will help to obtain accurate data, while saving energy. The paper merely proposes an algorithm. The claims made in the paper will be verified by using a network simulator and the results of the simulation will be compared with other algorithms.

REFERENCES

[1] L. M. Borges, F. J. Velez, and A. S. Lebres, "Survey on the characterization and classification of wireless sensor network applications," *IEEE Commun. Surveys Tuts.*, vol. 16, no. 4, pp. 1860–1890, Nov. 2014.

[2] Chen, Guihai, Chengfa Li, Mao Ye, and Jie Wu. "An unequal cluster-based routing protocol in wireless sensor networks." *Wireless Networks* 15, no. 2 (2009): 193-207.

[3] Xiaobing Wu, Guihai Chen and Sajal K. Das on " Avoiding Energy Holes in Wireless Sensor Networks with Non-uniform Node Distribution" *IEEE Transactions on parallel and distributed systems* vol. 19, no. 5, May 2008.

[4] Huei-Wen Ferng, MardiantoSoebagioHadiputro, and AriefKurniawan on "Design of Novel Node Distribution Strategies in Corona-Based Wireless Sensor Networks" *IEEE Transactions on Mobile Computing* vol. 10, no. 9 (2011): 1297-1311.

[5] Guha, Ratul K., Carl A. Gunter, and Saswati Sarkar. "Fair coalitions for power-aware routing in wireless networks." *IEEE transactions on mobile computing* 6, no. 2 (2007): 206-220.

[6] Gao, Qinghai, Junshan Zhang, B. Larish, and S. Shen. "Coalition-aided data transport in wireless sensor networks: data compression, cooperative transmission and optimal coalition size." In *2006 IEEE Radio and Wireless Symposium*, pp. 83-86. IEEE, 2006.

[7] Cai, Jian-Feng, Emmanuel J. Candès, and ZuoweiShen. "A singular value thresholding algorithm for matrix completion." *SIAM Journal on Optimization* 20, no. 4 (2010): 1956-1982.

[8] Cheng, Jie, Hongbo Jiang, Xiaoqiang Ma, Lanchao Liu, LijunQian, Chen Tian, and Wenyu Liu. "Efficient data collection with sampling in WSNs: making use of matrix completion techniques." In *Global Telecommunications Conference (GLOBECOM 2010), 2010 IEEE*, pp. 1-5. IEEE, 2010.

[9] Masrour, Farzan, ImanBarjesteh, RanaForsati, Abdol-HosseinEsfahanian, and HayderRadha. "Network completion with node similarity: A matrix completion approach with provable guarantees." In *2015 IEEE/ACM International Conference on Advances in Social Networks Analysis and Mining (ASONAM)*, pp. 302-307. IEEE, 2015.

Avoiding Coverage Holes and Energy Holes using Mobile Sink in Wireless Sensor Network

Ayushi Jha[1] Khushboo Goel[2] Megha Agarwal[3]
Vidhi Jindal[4] Vivekanand Jha[5]
[1]jhaayushijha@gmail.com
[2]khushboogoel96@gmail.com
[3]agarwal10megha@gmail.com
[4]vidhijindal1234@gmail.com
[5]vivekanandjha@igdtuw.ac.in
Indira Gandhi Delhi Technical University for Women, Delhi

ABSTRACT

This paper addresses the issues of energy hole and coverage hole in wireless sensor network. The coverage hole refers to areas in a sensor field inaccessible by any of the deployed sensor nodes. A node deployment strategy is proposed so that it is ensured that all points in the network field are covered by at least one sensor and it also targets to provide alpha coverage for the network. The energy hole is created due to load imbalance among sensor nodes as sensors that are closer to the sink dissipate their energy faster due to the additional burden of transmitting data from other sensors collected via multi-hop. Thus, sensor nodes near the sink die faster creating an energy-hole and eventually reducing network lifetime. This paper proposes a sink mobility pattern that ensures load balancing by covering the entire field spending equal time in equal areas of the field and avoids the problem of energy hole by reducing energy consumption and extending network lifetime.

A. INTRODUCTION

Wireless Sensor Networks (WSNs) is an attractive emerging technology because of its usefulness in various areas like military, forests and environment, science, healthcare and industries [1]. A wireless sensor network is composed of several low cost and battery powered devices, called sensor nodes. Every sensor node monitors the situation to obtain real time data from the surroundings like temperature, light or motion. All the gathered data is sent to the central processing element of the network, known as sink, through single-hop communication (direct data transmission to the sink) or multi-hop communication (transmission of data via other intermediate relay nodes to the sink).

Data from multiple sensors reaches the sink through multi-hop communication. Sensor nodes closer to the sink tend to dissipate more energy because of the added burden of transmitting data from additional nodes. Hence the overall traffic carried by nodes nearer the sink is heavier than other nodes. This leads to theproblem of energy hole in the sensor network which in turn reduces the network lifetime. Wireless sensor network can utilise either a static sink or a mobile sink [2], or any combination of both. Static sink has a defined fixed location in the sensor network.

Whereas, mobile sink can move across the wireless sensor network along various trajectories. The path for the movement of the sink can be random, pseudo-random and fixed. Mobile sink moves across the field and collects data from sensor nodes. This reduces the overhead of data transfer from multiple nodes.Therefore, sink mobility also reduces dissipation of energy in the network and prevents energy hole problem.In WSN, the sensor nodes should be deployed to ensure that the entire network field is covered and that the data collected is complete. Hence, coverage in wireless sensor networks can be defined as a metric of how efficiently and fully the sensor nodes can observe the network field. If the deployment of the nodes does not guarantee the total coverage of the field, it causes the problem of the coverage hole. Considering the network field, when each point in the field is sensed by alpha number of sensor nodes or more, the WSN field is known to have alpha-coverage. So, it is required to determine minimum number of sensor nodes required to provide full coverage of the field, that is, every point in area would be sensed by at least one sensor node.

The aim of this paper is to cover maximum area with minimum number of nodes using beehive structure where each sensor node is placed at the center of the hexagonal cell structure, which gives maximum packing efficiency according to honeycomb conjecture. The rest of the paper is organised in multiple sections. Section II discusses the related and past work in this aspect. Section III introduces a node deployment approach on how to deploy nodes in beehive distribution to ensure maximum coverage of the area with minimum number of sensor nodes. Section IV discusses the distribution of the remaining

nodes and the trajectory for sink mobility to prevent energy hole and to balance load across the network so as to increase network lifetime. Lastly section V concludes the paper.

B. RELATED WORK

There is a lot of research done on the node deployment strategies in WSN literature to solve the problem of energy holes and although there exists considerable amount of node deployment schemes, they do not solve the problem of coverage hole in sensor field [3].

Because of the utmost focus on the random sensor node distribution or the controlled node deployment strategy, the entire network field is not completely covered by the sensors. Node density is large enough in network with repetition [3]. Therefore, the collected data from the sensors cannot represent the entire range of the WSN**.**[4] is the study of artificial fish swarm and particle swarm hybrid-based optimization algorithm, used to realize the maximized coverage in monitoring region. But, these algorithms do not ensure 100% coverage of the field. It has also been observed that the nodes near the base station tend to die faster due to the higher energy dissipation than other nodes leading to energy hole problem and reducing network lifetime.

The problem of energy hole was first studied by Olariu and Stojmenovic [5], who proposed a corona selection model. The network region is partitioned in concentric coronas. So, the outer coronas are larger in corona radius than the inner coronas. However, this scheme cannot obtain any energy efficient consumption as most of the nodes in the field don't get an optimal path of transmission to the sink. The energy hole problem can be solved by using mobile sink. Several sink mobility approaches have been studied [6] [7] to improve the network lifetime to prevent the hotspot problem.

Sink mobility can be achieved by several schemes and distinguished on the basis of the selected mobility paths. One of the earliest works in sink mobility [8] suggests the use of multiple mobile base stations (or sinks) for conservation of energy of each sensor node. Further research expanded to the idea of mobile sinks and multiple sinks, together and separately. There are different types of mobility models, such as random or uncontrolled mobility models, controlled mobility models, predictable mobility models etc. Basagni et al. [9] provide a comparison between uncontrolled mobility using the data mules (or collectors) approach where the sink moves on a random path, and controlled sink mobility, where the sink makes an informed decision for its path based on the remaining energy of sensor nodes.

In controlled mobility [10] [11] [12], the speed, direction or other parameters of sink mobility are determined based on the state of the environment. One way of implementing controlled sink mobility is based on the remaining energy levels of sensor nodes. The sink moves in those regions where the energy of the sensor nodes is sufficient or higher than a threshold. This prevents the hot-spot problem where the same sensor nodes would be near the sink, causing them to die sooner than other nodes. In this type of controlled mobility, the lifetime of the network is improved, as energy consumption is balanced across all sensor nodes.

Random sink mobility [13], or uncontrolled sink mobility refers to the mobility schemes where the movement of the mobile sink is non-deterministic, or governed by a random function. Sink mobility schemes also include geometric trajectories of mobile sinks [14]. The path or trajectory of single or multiple mobile sinks is determined by a geometric heuristic, such as the grid, Gaussian or spiral trajectories [15]. Our paper similarly introduces another geometric heuristic with the aim of load balancing among sensor nodes.

Among recent work, Y. Gu et al. [16] proposed a delay bounded sink mobility model wherein the issue of information delay caused by moving the sink is addressed. S. Rahim, et al. [17] propose a circular joint sink mobility scheme in which the cluster heads send data to the nearest mobile sink. Cluster heads are sensor nodes selected from among a group or cluster of nodes to aggregate data from the cluster and send to the sink. N. Ilyas et al. [18] propose a geometric sink mobility scheme to improve the network lifetime of underground wireless sensor networks. The geometrical heuristic for the path of the mobile sink is taken as elliptical, with constant speed of the mobile sink.

III. NETWORK PRELIMINARIES

The wireless sensor network consists of a given number of homogeneous sensor nodes which are to be deployed in the given square field of the size. Transmission range and the sensing range of the sensor nodes can be defined as R_T and R_S respectively. Each sensor is assumed to be stationary with limited battery energy. The sensors are able to communicate with each other via multi-hop communication. Mobile Sink moves on a defined path across the field and aggregates data from nodes and acquires its location through GPS or other location approaches.

IV. PROPOSED WORK

A node deployment strategy based on beehive network structure is discussed in the section A below. Section B illustrates the proposed sink mobility pattern to avoid the energy hole in the network.

A. Beehive Network Structure:

According to Honeycomb Conjecture, a regular hexagonal grid is the best way to divide a square surface into regions of equal area with the least total perimeter. It also states that in densest circle packing of the plane where each circle is tangential to 6 other

circles, which fill just over 90% area of the plane.

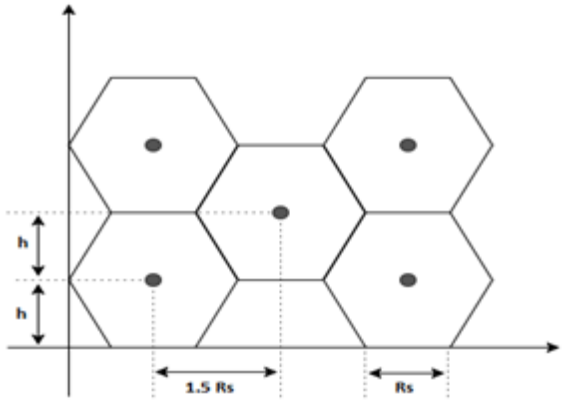

Figure 1: Beehive structured sensor nodes deployment

Hence, we conclude that the least total perimeter implies that the number of hexagons in the area field will be minimum therefore, the number of sensor nodes to be deployed is minimum if placed at the center of each hexagon. Thus, beehive node deployment strategy, as shown in Figure 1, is used to address the coverage hole challenge and provide an alpha-coverage metric in the network and minimize network energy consumption.

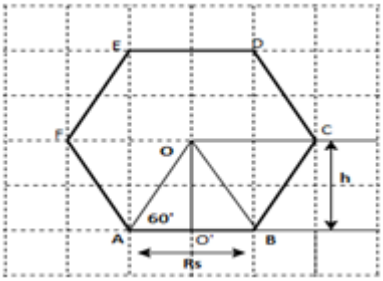

Figure 2: Height calculation in regular hexagon

In Figure 2, a regular hexagon ABCDEF with O as center and R_S as side is shown, h is the height of the equilateral triangle OAO':

$$\sin 60 = \frac{OO'}{OA} \quad (1)$$

$$OA = AB = R_s \quad (2)$$

$$h = \frac{\sqrt{3}}{2} \times R_s \quad (3)$$

Coordinates can be computed for sensor node deployment in order to achieve required structure using proposed BND (Beehive Node Deployment) algorithm shown in Figure 3.

B. Sink Mobility Pattern:

A wide range of possible parameters are considered to determine the optimal trajectory path for the mobility of the sink. And load balancing in the sensor network is selected among all. According to which the sink traverses each zone in the network for a fixed ideal period of time and repeats the cycle after a fixed time.

```
BND(m)
flag =1
centerX = Rs
centerY = h
while centerY<= m:
    while centerX <= m:
        deployNode(centerX, centerY)
        centerX += 3Rs
    flag =!flag
    if (!flag):
        centerX = 1.5Rs
    else :
        centerX= Rs
    centerY += h
```

Figure 3: BND Algorithm

For the proposed mobility scheme, the square field is divided into four square zones which are symmetrical and have equal area. The horizontal and vertical dividing lines are referred to as the axis along which the hyperbola is built. So, four hyperbolic paths are obtained in the four square zones. In each zone, the sink moves along a hyperbolic path and then switches to another zone in the hyperbolic path. In this way, the sink travels across the entire field. As soon as a cycle of the sink movement is completed, the axis along which hyperbola is constructed is rotated counter clockwise by 45 degrees. The hyperbolic path is obtained according to the new axis. This iteration continues after each cycle.

This hyperbolic movement provides a good coverage in the square zone in the center as well as in the outer areas of the network field. Repeated movement of the sink near the center of the network also allows for a large data collection from the concentrated nodes in the center of the field.

V. IMPLEMENTATION AND RESULTS

The beehive deployment structure gives the maximum area coverage among several other possible shapes. Hexagon is the preferred polygon when representing cellular networks. A simulation of the node deployment structure can be used to determine the percentage of area coverage provided by our model. For implementation purpose we have assumed that R_s is 5 units, deployed in a network field of 50 X 50 units squared. The number of sensor nodes is also computed to fill the complete network area so as to provide single full coverage. To determine the percentage of area coverage, the below mentioned formula can be used:

$$Area\ Coverage = \frac{No\ of\ nodes \times Area\ of\ one\ sensor}{Area\ of\ square\ field} \times 100\% \quad (4)$$

Figures from 4 to 8 represent the Matlab implementation of node deployment in triangular,

square, hexagonal, octagonal and circular grid deployment, in order.

Table 1 is evident that hexagonal node deployment provides the most cost efficient way to pack sensor nodes such that the issue of coverage hole is completely resolved. The minimum number of sensor nodes is ensured by circular deployment while the maximum area coverage is given by triangular grid with overlapping. In this regard, any polygon with number of sides greater than that of the hexagon (n > 6) will cause reduced area coverage, even though the sensor nodes required will be less, while any polygon with sides less than that of the hexagon (n < 6) will require more number of sensor nodes, even though they provide maximum to full area coverage. Hence, a hexagon (n = 6) will be the most suitable choice for node deployment, considering area coverage hole and efficient number of sensor nodes.

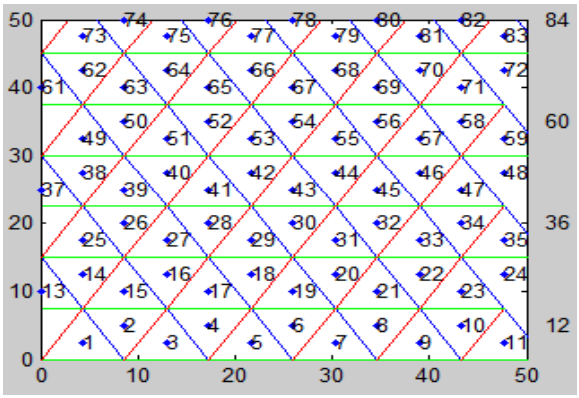

Figure 4: Triangle grid deployment

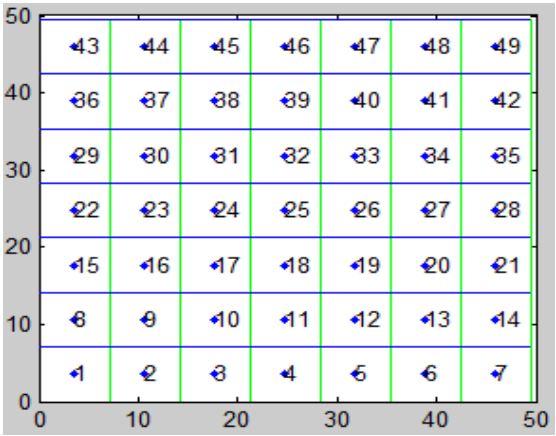

Figure 5: Square grid deployment

VI. CONCLUSION

In this paper, we propose a beehive structured node deployment model, that aims to avoid the coverage hole problem and provide alpha-coverage in the network. The minimum number of sensor nodes required to ensure full coverage in the sensor field is calculated mathematically and implemented in Matlab. An efficient sink mobility trajectory scheme is proposed that avoids the energy hole problem by reducing energy consumption and extending network lifetime by load balancing.

The simulation using Matlab will be used to check the proposed solution for a larger network field in detail and to mathematically calculate the energy levels of the sensor nodes and the network lifetime as the future work.

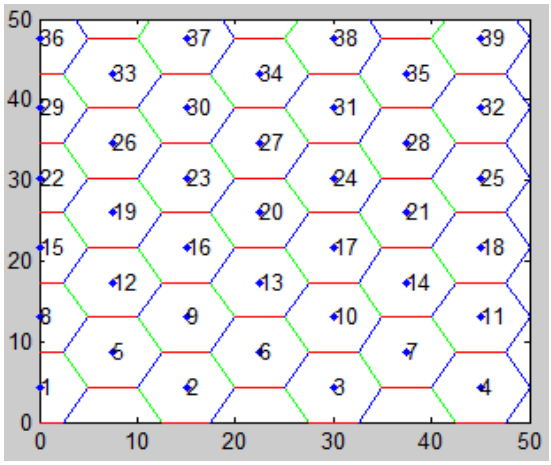

Figure 6:Hexagon grid deployment

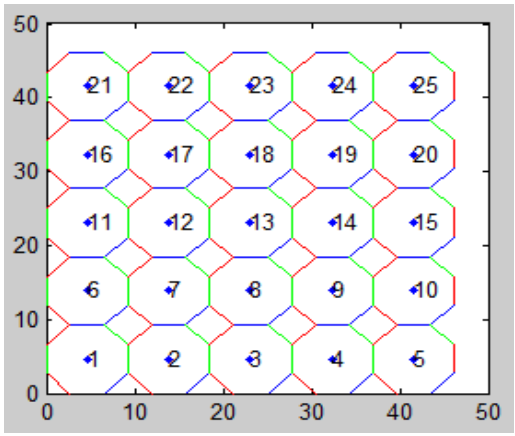

Figure 7: Octagon grid deployment

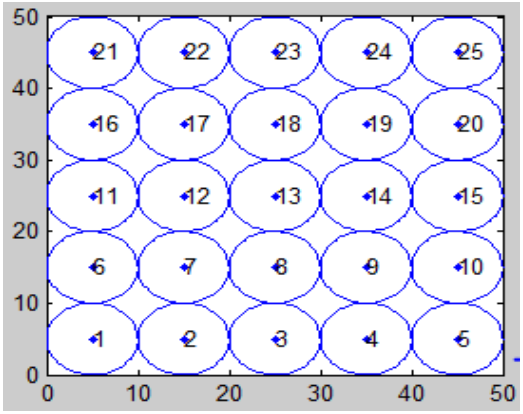

Figure 8: Circular grid deployment

Figure	*Side*	*No. of nodes*	*% Area coverage*	*Ω-coverage*
Triangle	$\sqrt{3}Rs$	84	223%	>=1
Square	$Rs/\sqrt{2}$	49	153.94%	>=1
Hexagon	Rs	39	122.52%	>=1
Octagon	0.924 Rs	25	78.53%	<1
Circle	Rs	25	78.53%	<1

Table 1: Comparative analysis of various structures for node deployment

REFERENCES

[1] I. F. Akyildiz, W. Su, Y. Sankarasubramaniam, and E. Cayirci, "Wireless sensor networks: a survey", *Computer Networks: The International Journal of Computer and Telecommunications Networking*, 2002

[2] Z. Maria Wang, S. Basagni, E. Melachrinoudis and C. Petrioli, "Exploiting sink mobility for maximizing sensor networks lifetime", *Proceedings of the 38th Hawaii International Conference on System Sciences, HICSS-38 2005, Big Island, HI*, 2005

[3] D. Wang, B. Xie and D. P. Agrawal, "Coverage and Lifetime Optimization of Wireless Sensor Networks with Gaussian Distribution," *IEEE Transactions on Mobile Computing, vol. 7, no. 12, pp. 1444-1458*, Dec. 2008

[4] J. Xia, "Coverage Optimization Strategy of Wireless Sensor Network Based on Swarm Intelligence Algorithm," *2016 International Conference on Smart City and Systems Engineering (ICSCSE)*, Hunan, China, 2016

[5] S. Olariu and I. Stojmenovic, "Design Guidelines for Maximizing Lifetime and Avoiding Energy Holes in Sensor Networks with Uniform Distribution and Uniform Reporting," *Proc. IEEE INFOCOM '06, pp. 1- 12*, Apr. 2006.

[6] W. Liu, K. Lu, J. Wang, G. Xing and L. Huang, "Performance Analysis of Wireless Sensor Networks With Mobile Sinks," *IEEE Transactions on Vehicular Technology*, vol. 61, no. 6, pp. 2777-2788, July 2012

[7] Y. Gu, F. Ren, Y. Ji and J. Li, "The Evolution of Sink Mobility Management in Wireless Sensor Networks: A Survey," *IEEE Communications Surveys & Tutorials*, vol. 18, no. 1, pp. 507-524, Firstquarter 2016

[8] Gandham, S. R., Dawande, M., Prakash, R., &Venkatesan, S. "Energy Efficient Schemes for Wireless Sensor Networks with Multiple Mobile Base Stations", *GLOBECOM - IEEE Global Telecommunications Conference*, 2003

[9] S. Basagni, A. Carosi and C. Petrioli, "Controlled Vs. Uncontrolled Mobility in Wireless Sensor Networks: Some Performance Insights," *2007 IEEE 66th Vehicular Technology Conference, Baltimore, MD*, 2007

[10] S. Basagni, A. Carosi, E. Melachrinoudis, C. Petrioli, Z. M. Wang, "Controlled sink mobility for prolonging wireless sensor networks lifetime", *Wireless Sensor Network, vol. 14, no. 6, pp. 831-858*, December 2008.

[11] Natalizio, Enrico, and Valeria Loscrí. "Controlled mobility in mobile sensor networks: advantages, issues and challenges." *Telecommunication Systems*, 2013

[12] F. Tashtarian, M. H. YaghmaeeMoghaddam, K. Sohraby and S. Effati, "On Maximizing the Lifetime of Wireless Sensor Networks in Event-Driven Applications With Mobile Sinks," *IEEE Transactions on Vehicular Technology, vol. 64, no. 7, pp. 3177-3189*, July 2015

[13] Restuccia and S. K. Das, "Lifetime optimization with QoS of sensor networks with uncontrollable mobile sinks," *2015 IEEE 16th International Symposium on A World of Wireless, Mobile and Multimedia Networks (WoWMoM)*, Boston, MA, 2015

[14] W. Y. Poe, M. Beck, J. B. Schmitt, "Planning the Trajectories of Multiple Mobile Sinks in Large-Scale Time-Sensitive WSNs", *Tech. Report 381/11*, February 2011.

[15] O. Cayirpunar, E. Kadioglu-Urtis and B. Tavli, "Optimal Base Station Mobility Patterns for Wireless Sensor Network Lifetime Maximization," in *IEEE Sensors Journal*, vol. 15, no. 11, pp. 6592-6603, Nov. 2015

[16] Y. Gu, Y. Ji, J. Li, B. Han and B. Zhao, "Delay-bounded sink mobility in wireless sensor networks," *2012 IEEE International Conference on Communications (ICC), Ottawa, ON*, 2012

[17] S. Rahim *et al.*, "Circular Joint Sink Mobility Scheme for Wireless Sensor Networks," *2015 IEEE 29th International Conference on Advanced Information Networking and Applications Workshops*, Gwangiu, 2015

[18] N. Ilyas*et al.*, "Extended Lifetime Based Elliptical Sink-Mobility in Depth Based Routing Protocol for UWSNs," *2015 IEEE 29th International Conference on Advanced Information Networking and Applications Workshops*, Gwangiu, 2015

QoS Analysis in Data Network: Stability, Reliability, QoS Invoke Rate Perspectives

P K Mishra, Rameshwar Nath Tripathi and Y N Singh
Indian Institute of Technology, Kanpur
pkmishra@iitk.ac.in , rameshn@iitk.ac.in, ynsingh@iitk.ac.in

Abstract---In a data network, a user demands a service and network offers the service. Every user requires varying degrees of service quality. To fulfil the user demand, network must have service quality support mechanism. Internet offers best effort service, but many users demand some kind of guarantee on theservice. Therefore, there is a need of analysis of QoS in the network. This motivates our work to investigate and analyse QoS from different perspectives. QoS can also be interpreted as measure of service quality that the network offers to the user or application. This analysis can be performed in qualitativeor quantitative fashion. QoS can be analysed from different perspectives. In this paper, we present a qualitative aspect of QoS analysis and we do not assume anything about QoS demand of the user. So, we investigate the situations which demand QoS provisions within the network. We also determine the boundary condition on the packet injection rate which is called QoS Invoke Rate (QIR). Below this QIR, it is safe to operate the network without worrying about QoS provisioning in the network. Above the QIR it is desirable to invoke QoS provisions, because limited resources start playing their role. Our main contribution in this paper includes packet injection rate condition for which a network will be stable and reliable while satisfying the user's QoS demand.We devise the boundary condition on packet injection rate (QIR) forQoS support in the network.

Index Terms---QoS, Stability,Reliability, QoS Invoke Rate

I. Introduction

A packet routing network facilitates end to end delivery of information by breaking it into small pieces called packets. These packets are delivered from source to destination by moving them over the network using store and forward methodology. A user takes benefit of the communication services, information resources and entertainment over internet through various applications. These applications may demand single or combination of various contents like text, voice, video and images. Applications requiring combination of multiple contents are termed multimedia applications. The multimedia applications like HDTV, video conferencing and merchandise have a stringent QoS requirement. QoS is built from essential parameters of Band width, Delay, Jitter (delay variation) and Packet loss that an application desires for its content packets.

Besides, for a packet routing network stability and reliability are functional requirements. A network system is stable when number of packets always remains bounded in the network as system runs for arbitrary long period of timeand it is reliable if every packet is delivered across the network in bounded time. Stability and reliability contribute towards QoS in a overlapping manner. Stability covers bandwidth and delay and reliability deals with delay and packet loss parameters. We can well appreciate that overload conditions cause instability in networks. Because, The overload condition is characterized by higher input rate in a network. A network can also become unstable in under load conditions due to a queuing policy. For last two decades under load instabilities due to queuing policies havebeen shown to exist [1, 2, 3]. Reliability in packet delivery can be lost due to many reasons such as connection break, noise and overload. Unreliability can too occur purely due to starvation of packets in queues. Hence, stability and reliability investigation of a network is essential to determine feasibilityof QoS provisioning.

In a network QoS can be handled at different granularity of routing, admission control, resource reservation and scheduling. One mechanism to assure QoS is packet classification and prioritization for purpose of class based scheduling in time. Packets desiring same QoS make a class. These classes of packets are assigned some priority ordering in a queue dedicated to a forwarding entity called station. A station handling multiple classes of packets is termed multiclass station. In a general network, as packets wait in the queue, a scheduling policy like Nearest To Go (NTG) or First in First Out (FIFO) is chosen to pick and pass packets through the station one by one. For QoS guarantee a QoS scheduling policy like Fair Queuing, Weighted Average Queuing or SP/FIFO policy is used. The QoS Scheduling policy on a priority queue allows control over bandwidth and delay to a class of packets by giving quick service to highest priority class at any time. Eventually, by packet classification and prioritization a multiclass network system is implemented for provisioning of QoS.

A .**Movtivation**

The previous work on multiclass queuing networks by Kelly [5], Kumar and Seidman[6], Lu and Kumar [7], RebkoandStolyar [8] and Bramson [9, 10] are based on stochastic inputtraffic and service times and have used fluid model of networkas a tool of study. Thus the analysis suffers from limitationsof assumptions of traffic modeling and becomes less generalas compared to AQM [1, 2, 3, 4] AQM makes as many fewassumptions about the input traffic and service times in thenetwork as possible which makes it more general and elegant.

Marsanet. al. [4] discussed AQM for multiclass queuingnetworks with SP/FIFO policy but used tools of stochastic andfluid models for their results. Our set up differs in approachfor the analysis being based purely on AQM and uses a simplemulticlass station as network. SP/FIFO as QoS queuing policysignificantly resembles the approaches being considered forQoS provisioning in Differentiated Services [11, 12, 13, 14]for internet. Differentiated services or DiffServ is a computernetworking architecture that specifies a simple mechanism forclassifying and managing network traffic and providing QoSon modern IP networks. DiffServ can, for example, be usedto provide low-latency to critical network traffic such as voiceor streaming media while providing simple best-effort serviceto non-critical services such as web traffic or file transfers.

The SP/FIFO policy on a priority queue allows control overdelay to a class of packets by giving quick service to highestpriority class at any time. This ensures improved band widthand latency to a priority class in accordance with its QoSdemand.We note that little or no effort has been made towards QoSanalysis of a multiclass network under AQM. This motivatesus to analyze stability and reliability at a multiclass stationusing AQM. We investigate network stability and reliabilityunder conditions where network is not overloaded and packetloss is only due to starvation of packets in queues. Under AQMa network system is defined by a triple (G,A, Q). G is theunderlying directed graph of the network, A is a hypotheticaladversary injecting set of packets in network G at some rate rand Q is a queuing policy [1]. We use multiclass single stationas trivial multiclass network and SP/FIFO scheduling policyas it resembles realistic approach in diffserve. The adversaryis characterized by its rate. So, one might be interested inknowing if QoS mechanisms of classification and prioritizationneeds to be invoked for all adversarial injection rates or it canbe relaxed up to some critical rate up to which

QoS guarantee is not affected.

B. Contribution

In this paper we have constructed two class single station and a general multiclass single station as most elementarymulticlass networks. For multiclass packet classification wehave taken case of simplest multiclass i.e two class classificationof packets, for obtaining results. Then we extended theresults over general case of multiclass. Results are presentedin form of theorems and corollaries. We have shown that twoclass Single station network is stable and reliable against alladversaries of rate strictly below one. And an adversary ofrate one can make two class single station networks unreliable,while keeping the network stable. These results have been generalizedfor multiple classes. Then, we provide two resolving issue of unreliability in a stable multiclass station.

Finally we give QoS Invoke Rate for an acyclic network.The paper is organized as follows. In section II we discusssystem model to explain AQM and SP/FIFO and definitions.Section III presents stability and reliability analysis of twoclass and multiclass single station networks. In section IV weprovide two protocols for avoidance of unreliability of a stablemulticlass station. Section V gives the QoS invoke rate. Finally, we have concluded the paper with observations and future research directions for further work.

2.Definitions and Preliminaries

In this section we give out important definitions and conventions used for the study and representation. We formally define Stability and Reliability.

Definition 1.Stable System. A system is said to be stable when total number of packets remains bounded in the system as system runs for arbitrary long period of time.

Definition 2.Reliable System. A system is said to be reliable if every packet in the system experiences bounded delay. The reliable nature of network is called reliability.

Definition 3:Station.A network is a directed graph G(V,E). V is set of vertices or nodes of the network and E is set of directed edges connecting two nodes in the network. Each edge at its tail has a queue-server pair called station

Definition 4.Single class station.A station which is not capable of classification of packets is called single class station.

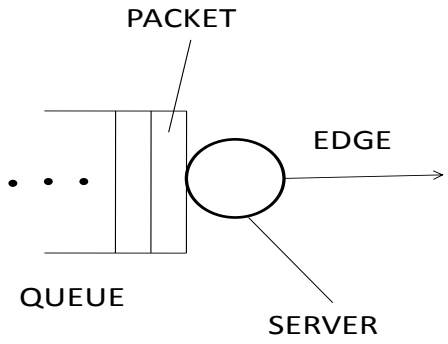

Figure 1. A Single class Station

Definition 5.*Multiclass station.*A station which is capable of classification of packet is called multiclass station.

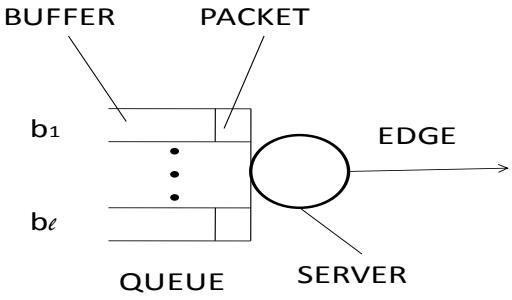

Figure 2. A Multiclass Station

3 .QOS INVOKE RATE

It has been discussed that to meet the stringent QoS demand of various services over packet routing network, the packetsentering the network from a source are classified into different classes at the entry node. This classification is done based onQoS demand. The packets of a class are treated in preferential manner by allocation of priority over the classes. Each priorityclass is assigned a buffer at a queue and a single server servers the queue. This is the basic description of a multiclass scheduling. Conclusively, a multiclass scheduling policy supports QoS by Classification and prioritization mechanism.

Our network system is (G, A, Q) that supports QoS . Where adversary A injects set of packets during any time step with injection rate r _ [0; 1) into the network G. Various packet classes demand different QoS. So, a multiclass queuing policy support the demanded QoS by classification and prioritization of packets. We use SP/FIFO multiclass queuing policy.The QoS mechanisms of classification and prioritization are resource consuming in terms of processing, time and energy.

At this juncture an intuitive question arises that does the system (G, A, Q) have to provide QoSsupport at all rates of adversarial injections or the QoS support mechanisms are to be invoked only above a certain adversarial injection rate?

If the critical rate of adversarial injection up to which QoS support mechanisms are not required to be activated is foundthen one can save on the committed resources. This critical rate is termed QoS Invoke Rate (QIR).

A**. Main Idea**

Parameters like bandwidth, delay, jitter, and packet loss constitute a QoS. Besides bandwidth, delay is another desirableparameter of QoS that comes before jitter and packet loss. As many packets contest for one edge, packets have to wait and delay becomes inadvertent. Thus delay is natural indication of congestion build up or backlog. Congestion in turn demands classification and prioritization of packets for priority treatment. Hence, for the purpose of determining QIR in a stable and reliable network system we choose singleparameter of delay. The delays experienced by a packet in a network are of two types. One is propagation delay thatis equal to time taken to traverse the path. The second is waiting delay that is the total time spent by a packet waiting in queues for servicing. Propagation delay is unavoidable unlike waiting delay. Waiting delay is function of backlog and prioritytreatment in a queue. Delay of a packet is the sum total of thepropagation and waiting delays. QoS is provided to packets byclassification and then offering different delays as per functionof backlog and priority. Hence, total delay of a packet too isa function of backlog and priority.

To evaluate QIR there is a need to develop two basic conceptsof Bottle neck topology and edge stress. These two help in determining maximum packet arrival at an edge in a timestep. Firstly we introduce bottleneck topology by reviewingconcepts of tree, directed tree, rooted tree and defining reverserooted tree. Secondly, we conceptualize edge stress of an edgein a network. Finally we determine QIR of an acyclic packetrouting network by determining maximum congestion at anyedge in the network and give out observations based on QIR.

B. Bottleneck Topology

Network topology is arrangement of network elements like vertices and edges. It essentially gives how data flows in a network. Two or more networks with different physical layouts can be topologically identical. A topology that limits the network performance by bottleneck formation is calledbottleneck topology.

Lemma 1 . There is a unique path from a node to the root in a reverse rooted tree.

Proof: A tree has a unique path from a node toanother node. The underlying graph of a reverse rooted tree is a tree. All edges are implicitly

directed towards root node.Therefore, there exists a unique path from a node to the root node.

Bottleneck Network: A bottleneck network is a reverse tree where the root node is connected by only one edge. The single edge incident to the root is called bottleneck edge. Possible bottleneck topologies are given in figure 3.

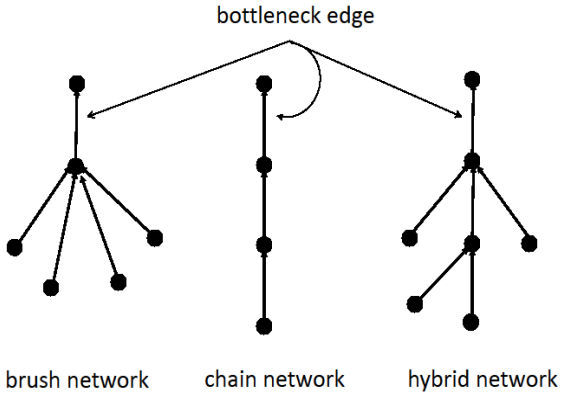

Figure 3: Three possible Bottleneck topologies

Lemma 2: Bottleneck edge is shared by exactly (n-1) paths in a bottleneck network of n nodes.

Proof: In a n node bottleneck network there are exactly (n-1) nodes reaching the root node. Any bottleneck network is a reverse tree, so each node reaches through a unique path to the root as per lemma 11. Besides, there is only one edge called bottleneck edge incident to the root, therefore exactly (n - 1) paths share this edge.

C. Edge stress

In a network packets arrive is at the tail of an edge. These packets are forwarded over the edge one by one per time slot. The packets have predetermined path. Path is sequence of edges from source to destination. So, many packets following different paths can arrive at the tail of an edge in a time slot and contest for the edge. These packets are forwarded over the edge one by one per time slot. One packet out of contestingpackets is selected by the queuing policy for forwarding over the edge and rests of the packets have to wait in queue at the tail of the edge. More the number of paths sharing an edge more is the congestion at the tail of the edge. A notion of stress at an edge at any given time can be developed based on paths sharing the edge. We describe edge stress of an edge for an acyclic network now.

Edge Stress: Edge stress of an edge in any acyclic packet routing network is the maximum number of paths that share the edge at any point of time.

Theorem 1. In a n node acyclic network maximum edge stress of an edge is (n-1).

Proof: To obtain maximum edge stress on an edge in a node acyclic network we need to maximize number of paths through an edge. Each source reaches a destination by single path in the network. Therefore, we need to maximize number of sources to maximize number of paths that claim an edge. Besides, at least one destination is mandatory. Therefore in nnode acyclic directed network there can be at most (n - 1) distinct paths originating from (n-1) distinct sources to one destination. Now, for maximizing edge stress these paths have to do maximum sharing of edges. Hence, these paths reach the common destination by converging on a single edge incident to the destination node. This edge becomes the bottleneck edge in the bottleneck topology created by (n -1) sources and one destination. The destination node becomes the root node.The bottle neck edge experiences the maximum edge stress of (n -1). This is verified by lemma 1 that edge stress of bottleneck edge is exactly (n - 1).

Lemma 3. The maximum number of packets that can arrive at bottleneck edge in n node bottleneck network over a roundof k time steps when adversary injects at rate r is knr .

Proof: When adversary injects at rate r in a network, eachpath receives packets at most rate r. Bottleneck edge in a n node bottleneck network is shared by (n-1) paths. Therefore, over a round of k time steps bottleneck edge receives at most k(n - 1)r packets from the sharing paths. Besides, uptokr packets can be directly injected by the adversary at the tailof bottleneck edge in the same round. Hence, bottleneck edge receives total of knr packets over round of k rounds.under AQM to model QoS environment. Next we discuss SP/FIFO.

D. QoS Invoke Rate

Many packets arriving in a time slot at an edge create congestion. Bottleneck topology creates the worst case of congestion. This worst case of congestion occurs precisely at the bottleneck edge. The condition satisfying avoidance of congestion at bottleneck edge will also hold for any other edge in the network and any other topology. One way to avoid congestion is to restrict the adversary. Determination of peak adversarial rate up to which no congestion occurs at the bottleneck edge will give the QIR. We now formally define QIR.

Definition 6.QoS Invoke Rate. It is the threshold adversarial injection rate above which QoS policies need to be invoked in a network to guarantee QoS requirements of a traffic class.

To obtain QIR we state and prove condition of equivalence between single class and multiclass scheduling.

Theorem 2. Single class and multiclass packet scheduling are indistinguishable in terms of QoS up to QoS Invoke Rate.

Proof: We prove the theorem by considering single class traffic and multiclass traffic one by one and then establishing equivalence in delay suffered by a packet in both cases of scheduling.

Single Class Packet Routing Network: Consider a n node single class bottleneck network with all queues empty initially. If adversary injects at rate r in the network then during any time slot maximum nr packets can simultaneously arrive atthe tail of bottleneck edge. However, only one packet can be forwarded in a time slot. For a round of k time steps at most knr packets will arrive at the tail of bottleneck edge. Hence, for all packets to get transmitted to the root in the same round leaving no packets to wait beyond the round duration, the condition is knr ≤ k, hence r ≤1=n. No packet of around waits in any subsequent round.

Multiclass Bottleneck Network: Consider a*l* class *n* node bottleneck network with adversarial injection rate *r*. The initial condition of network is zero. Any edge has buffers b_1 to $b_l$in its queue. For all packets arriving in a round of k timesteps to get transmitted living no packets to wait at the tailof bottle neck edge is$k|\sum_1^l bi|$=knr≤r i.e. r≤ 1/n .

For r > 1=n the packets have to experience delay more thanthe backlog delay created in the same round and congestionoccurs at bottleneck edge and then QoS traffic needs priorityin treatment and we need to invoke QoS policies. We also realize from theorem 1 that bottleneck topology is worst casefor congestion to occur and hencer = 1/n is the critical rateabove which congestion starts to build up. So, we define $rater_q$ = 1/n of adversary to be QoS Invoke Rate.

E. Interpretation of QIR

QIR depends on network size and edge capacity in thenetwork. We assume all edges in network to be of samecapacity. As number of nodes increase, QIR decreases. Whenedge capacity increases, QIR also increases. For a packetrouting network of n nodes and Z bps,rq = Z=n bps. Asexample,200 nodes and 40 Mbps link capacity network hasQIR of 200 Kbps. QIR is more significant for high bandwidthsmall networks and starts to loose significance for low bandwidth large networks.

F. Observation

We note some important some important observations from QIR. Firstly, QoS network resources are non-effectively usedbelow QIR. Secondly, as a outcome of first observation single class and multiclass traffic have equivalence in treatment by the network below QIR. Thirdly, QIR gives the minimum threshold rate above which only effectiveness of QoS measures in a network can be verified by process like simulation. Energy can be saved in a network that runs below QIR by idling QoS routing resources.

This section has formally introduced the sense of QIR. Irrespective of any bound on QIR, occurrence of such a parameter is established by this section. QIR depends up on the network size inversely edge band width directly. We have also noted its use.

7. Conclusion

The paper explores stability and reliability in realistic QoS environment under adversarial queuing model. Our analysisprovides meaningful insight of the multiclass traffic behavior based on priority treatment in a network. In stable networks nonempty initial conditions and bursty injections of packets are root cause of unreliability. We also obtain two protocols to offset unreliability in stable but unreliable multiclass single station network. We also analyzed QIR for an acyclic network with delay as QoS parameter.

An important open issue for study is stability-reliability analysis for more complex multiclass networks like and trees, meshes and cycles. Stability-reliability study of other multiclass queuing policies like Fair queuing and Earliest-Deadline-First is also an interesting open area

References

[1] A. Borodin, J. Kleinberg, P. Raghavan, A. Sudan, and D. Williamson, Adversarial queueing theory, In Symposium on Computer Science, 1996.

[2] M. Andrews, B. Awerbuch, A. Fernandez, J. Kleinberg, T. Leighton, and Z. Liu, Universal stability results for greedy contention-resolution protocols, 37th IEEE Symposium on Foundations of Computer Science, 1996, pp. 380–389.

[3] A. Goyel. Stability of Networks and Protocols in the Adversarial Queuing Model for Packet Routing Networks, 37(2001) 219-224.

[4] M.AjmoneMarsan, M.Franceschinis,E.Leonardi, F.Neri, A.Tarello,InstabilityPhenomena in Underloaded Packet Networkswith QoS Schedulers,TechnicalReport,http://www.tlcnetworks.polito.it/emilio/netrep/instability-tec-rep.pdf, 2003.

[5.]F. P. Kelly. Networks of queues with customers of different types.J.Applied Probability.12:542–554, 1975

[6] P. R. Kumar and T. I. Seidman. Dynamic instabilities and stabilization methods in distributed real-time scheduling of manufacturing systems.

[7] S. H. Lu and P. R. Kumar. Distributed scheduling based on duedates and buffer priorities. IEEE Transactions on Automatic Control,36:1406–1416, 1991

[8] A. N. Rybko and A. L. Stolyar.Ergodicity of stochastic processes describing the operation of open queueing networks. Problems of Information Transmission, 28:199–220, 1992.

[9] M. Bramson. Instability of FIFO queueing networks. Annals of AppliedProbability, 4:414–693-718, 1994.

[10] M. Bramson. Instability of FIFO queueing networks. Annals of AppliedProbability, 4:414–431, 1994.

[11] S. Blake et.al..al. An Architecture of of Differentiated Services .RFC2475,1998.

[12] K. Nicholaset.al. Definition of Differentiated Services Field (DS Field) in the IPv4 and IPv6 Header. RFC2474,1998.

[13]V.Jacobson, K.Nichols, K.Poduri, An Expedited Forwarding PHB, RFC 2598, June 1999.

[14] J.Heinanen, F.Baker, W.Weiss, J.Wroclawski, Assured Forwarding PHB Group, RFC 2597, June 1999.

[15] A. Ros´en, A note on models for non-probabilistic analysis of packet switching networks, Information Processing Letters, 84 (2002) 237 -240.

Reputation System and Incentive Mechanism to Handle The Malicious Peers and Free-riders in Peer-to-Peer Networks

Sateesh Kumar Awasthi and Yatindra Nath Singh
Indian Institute of Technology, Kanpur
sateesh@iitk.ac.in,ynsingh@iitk.ac.in

Abstract **- The open and anonymous environment of peer-to-peer (P2P) networks gives an opportunity to everyone to interact with the others; at the same time it brings new security threats. The malicious peers or the peers having conflict of interest can easily put inauthentic contents in the network. This can easily sabotage the system. Further, lack of central control leads to the problem of free-riding, i.e., peers download the resources without contributing anything back to the network. This leads the large difference between amount of upload and download of resources in the peers. In such a situation, downloading speed for non-free-riders becomes very slow. The implementation of reputation system and incentive mechanism have been proposed by many authors in past to resolve this problem. In this paper we will discuss some popular reputation systems and incentive mechanisms.**

Index Terms - P2P networks, trust, reputation, DHT.

I. INTRODUCTION

The peer-to-peer (P2P) networks attract a significant amount of traffic on Internet due to its inherent advantages over traditional client-server networks, e.g., scalability, robustness and diversity of data. Every peer in P2P network can initiate the communication and each peer can act both like client as well as server, and has equal responsibility. But due to lack of functionality of central control, some peers can easily sabotage the network by putting inauthentic contents in the network. Such peers are called malicious peers. Furthermore, rational behavior of peers encourages them only to draw the resources from network without sharing anything. These types of peer are called free-riders. In such a situation, P2P network functions like a poor client-server system where only few peers act as server with much less upload bandwidth and storage capacity. The success of P2P networks largely depends on the policy by which these two issues can be handled.

II EXPERIMENTAL STUDIES

Adar *et al.* [1] conducted a survey on Gnutella network in 2000. They observed that, 70% users did not share any file, 70% of files are shared by 5% of the peers. Top 1% peers shared 25% and top 25% shared 98% files. Free-riders were distributed uniformly through the network.

Another study was conducted on Gnutella and Napster network by Saroiu *et al.* [2] in 2002, which shows that 25% users in Gnutella did not share any file, 75% of users in Gnutella shared 100 or less number of files and 7% of peers shares majority of files, 40% - 60% users shared 5% - 20% of total files in Napster.

Cuevas *et al.* [3] conducted another study on popular file sharing P2P network BitTorrent in 2013. Which conclude that 3% of publishers are responsible for 67% of the contents and 75% of download session. Antipiracy agencies or malicious users are responsible for 30% of contents and 25% of download session.

These experimental studies show that malicious peers and free-riders are major problems in P2P networks. It attracted the attention of many researchers in the recent past and many solutions have been proposed for it. The implementation of reputation system and incentive mechanism has been suggested by many authors. In this paper, we will critically analyze the some of the reputation system and incentive mechanism.

III. BACKGROUND

Let us define some definitions which will be used throughout the paper

Definition 1. A numerical value, which models the past behavior of peers in the network, is defined as trust.

Definition 2. The value of trust, evaluated by any peer based on the direct interaction it has had with evaluated peer, is defined as a local trust.

Definition 3. The value of trust, system as a whole keeps on any peer, is defined as a global trust.

IV REPUTATION SYSTEM

A. EigenTrust Algorithm

The EigenTrust, algorithm was proposed by Sepandar *et al*., [4] of Stanford university in 2003. The basic idea of EigenTrust is taken from Google's PageRank [28] algorithm.

In EigenTrust [4] algorithm, each peer *i* keeps the record of all transactions it has had with peer *j*. Then it calculates the local trust, T_{ij}, of peer *j* as follows:

$$T_{ij} = sat(i,j) - unsat(i,j)$$

Where, *sat(i, j)* and *unsat(i, j)* are the number of satisfactory and unsatisfactory transactions of peer *i*, which has had with peer *j*, respectively. For the purpose of aggregation, they used normalized local trust instead of local trust, which is defined as follows:

$$T_{ij}^{norm} = \frac{\max(T_{ij},0)}{\sum_{j=1}^{N}\max(T_{ij},0)} \quad (1)$$

Here, *N* is the number of peers in the network. This normalization process makes the trust matrix, T_{norm}, as a row stochastic matrix. Global trust vector, t, is calculated as a left principal eigenvector of transpose of normalized trust matrix.

$$t=(T^{norm})^{tr}.t \quad (2)$$

It can also be interpreted as the weighted average of normalized local trust of peers where weight factor is given by the global trust of local trust assigning peer. If there is no interaction of peers they give zero local trust to each other. Some pre-trusted peers are assumed to be in the network and they are trusted by all the peers in the network. To include the impact of pre-trusted peers' global trust is modified as:

$$t=(1- a)(T^{norm})^{tr}.t + ap \quad (3)$$

Where p is some distribution over pre-trusted peers. By normalizing the trust matrix, global trust can be calculated by iterative method and it converge at left principal eigenvector of transpose of normalize trust matrix. The major limitation of EigenTrust [4] algorithm is that it gives only ranking of peers without any absolute interpretation of their past.

B. Power Trust

PowerTrust was proposed by Zhou *et al*., [5] in 2007. The basic idea of aggregation of local trust in this algorithm is same as in EigenTrust [4], i.e., using normalized trust matrix. It used some higher reputable nodes known as power nodes in place of pre-trusted nodes. These power nodes are searched and elected dynamically in the whole network. Thus, pre-trusted nodes are free to leave the network unlike in EigenTrust [4]. This method used the enhanced trust matrix for the purpose of aggregation of local trust. Enhance trust matrix is the square of trust matrix. Speed of convergence of PowerTrust [5] is higher than EigenTrust [4]. In both, EigenTrust [4] and PowerTrust [5] distributed hash table (DHT) is used to locate the peer who is calculating and managing the global trust.

C. Flow Based reputation

Flow-Based Reputation was proposed by Simone *et al.,* [6] in 2012. They identified the problems with normalization and used basic trust matrix without normalization, for aggregation of local trust. For this purpose, they redefined the local trust of a peer by mapping a function from positive (+1), neutral (0) and negative (-1) rating to a value into the range [0,1]. Global trust vector was taken as the left principal eigenvector of trust matrix. It was calculated using power method [7]. Main drawback of this method is that it cannot be implemented in a distributed system.

D. Absolute Trust Algorithm

We Proposed Absolute Trust algorithm [8] in 2016. In this algorithm, the global trust of peers is estimated using weighted average of the local trust. The weight factor for individual peer is given by the global trust of a peer. In order to compare the global trust of any two peers, the global trust of individual peer is biased by the global trust of trust assigning set, S_i . The global trust of any peer *i* is given as:

$$t_i = \left\lceil \left(\frac{\sum_{j \in S_i} T_{ji} t_j}{\sum_{j \in S_i} t_j} \right)^p \cdot \left(\frac{\sum_{j \in S_i} t^2{}_j}{\sum_{j \in S_i} t_j} \right)^q \right\rceil^{\frac{1}{(p+q)}} \quad (4)$$

Here T_{ji} is local trust of peer *i* estimated by peer *j*. The t_i is global trust of peer *i* and *p*, *q* are some suitable chosen constants. The global trust of peers depends on the global trust of the other peer. It can be calculated by iterative method thus, can be implemented in a distribution fashion.

TABLE 1: Comparison of Reputation Systems

S. N.	Reputation System	Normalization	Distributed Implimentation
1	EigenTrust	Needed	Possible
2	PowerTrust	Needed	Possible
3	Flow Based	Not Needed	Not Possible
4	Absolute Trust	Not Needed	Possible

V INCENTIVE MECHANISM

A. Tit-for-Tat

The tit-for-tat (TFT) approach is used by a most popular file sharing system named BitTorrent [9], to prevent the free-riding. In this approach, a peer cooperates with other peers in the same proportion as they have cooperated with him in the previous round. In each round, every peer updates the contributions of peers in the previous round.

To improve the performance, many variants of TFT have been proposed. Garbacki *et al.*, [10], proposed ATFT in which bandwidth is used rather than content to decide the incentives. Dave *et al.*,[11], proposed auction based model to improve the TFT. In this model, peers reward one another with proportional shares, [12], of bandwidth. Sherman *et al.*, [13], proposed FairTorrent. It is a deficit based distributed algorithm in which a peer uploads the next data block to the peer, whom it owes the most data as measured by a deficit counter. These approaches consider the peers shared history with limited number of peers.

B. Global Contribution Approach

A Global Contribution Approach (GC) for Fairness was proposed by Nishida *et al.,* [14] in 2010. This approach was used to prevent the free-riding in the network and to balance the upload and download amount in each peer. Global contribution, x_i, of any peer *i* is calculated as following:

$$x_i = \alpha \frac{\beta e_i.S.x + (1-\beta)e_i.S.e - e_i.S^{tr}.x}{e_i.(S+S^{tr}).x} + (1-\alpha) \quad (5)$$

If no transaction happened at node i then

$$x_i = \frac{2-\alpha(1+\beta)}{2+\alpha(1-\beta)} \quad (6)$$

Where, x is global contribution vector. The S is share matrix in the network with its *ij* element as the amount shared by peer *i* to peer *j*. The e_i is a row vector with its i^{th} entry as '1' and e is a column vector with each entry as '1'. The parameter α and β are some scalars decide the initial value of global contribution vector and guaranteed the convergence of it.

Any peer is only allowed to take the resources from the network if its global contribution is higher than the threshold value. Thus, peer wants to earn more global contribution. They can earn more global contribution if they upload to high contributing peer and download from low contributing peer. This method can balance the upload and download amount in the network and thus can prevent the free-riding. But this is complex to implement in real system due to its slow speed of convergence.

C. Biased Contribution Approach

We proposed a light-weight algorithm named Biased Contribution Index (BCI), [15], in 2016. This algorithm is able to balance the upload and download amount in each peer. It can be implemented in a distributed system with faster convergence speed. The BCI of any peer *i* is expressed as:

$$x_i = \alpha \frac{e_i.S.x}{e_i.(S+S^{tr}).x} + (1-\alpha) \quad (7)$$

If no transaction happened at node i then

$$x_i = (1 - \alpha/2) \quad (8)$$

The value of BCI of any peer remains in between (1 - α) to 1.

TABLE 2: Comparison of Incentive Mechanisms

S.N	Incentive Mechanism	Approach	Convergence Speed
1	Tit-for-tat	Local	-
2	ATFT	Local	-
3	FairTorrent	Local	-
4	GC	Global	Slow
5	BCI	Global	Fast

VI CONCLUSION

In this paper, we presented the problems with peer-to-peer networks with some experimental survey. We focused that the malicious peers and free-riders are two major problems with these networks. Further, we summarized the popular reputation systems and incentive mechanisms, which are proposed to handle the malicious peers and free-riders. We explained the metrics, which are used in these different approaches with their shortcomings.

REFERENCES

[1] E. Adar and B. A. Huberman, "Free-riding on Gnutella," *First Monday* vol. 5, no.10, Octbor 2000.

[2] S. Saroiu, P. K. Gummadi, and S. D. Gribble. "A Measurement Study of Peer-to-Peer File Sharing Systems." *In Proceedings of Multimedia Computing and Network-ing 2002 (MMCN '02)*, San Jose, CA, USA, January 2002.

[3] R. Cuevas, M. Kryczka, A. Cuevas, S. Kaune, C. Guerrero, and R. Rejaie, "Un-veiling the Incentives for Content Publishing in Popular BitTorrent Portals," *IEEE/ACM Trans. Networking*, vol. 21, no. 5, pp.1421-1435, October 2013.

[4] S. D. Kamvar, M. T. Schlosser and H. Garcia-Molina, "The EigenTrust Algorithm for Reputation Management in P2P Networks," *Proc. of the 12th international conference on World Wide Web, ser. WWW'03*. New York, USA: ACM, pp. 640-651, 2003, .

[5] R. Zhou and K. Hwang, "PowerTrust: A Robust and Scalable Reputation System for Trusted Peer-to-Peer Computing," *IEEE Trans. Parallel and Distributed Systems*, vol. 18, no. 4, pp. 460-473, April 2007.

[6] A. Simone, B. Skoric and N. Zannone, "Flow-Based Reputation: More than Just Ranking," *International Journal of Information Technology and Decision Making*, vol. 11, no. 3, pp. 551-578, December 2012.

[7] Denis Serre, Matrices Theory and Applications, Springer-Verlag New York, Inc., 2002.

[8] S. K. Awasthi and Y. N. Singh, "Absolute Trust:Algorithm for Aggregation of Trust in Peer to Peer Network", *http://arxiv.org/abs/1601.01419*

[9] B. Cohen, "Incentives build robustness in BitTorrent," *presented at the 1st Workshop Econ. Peer-to-Peer Syst.*, Jun. 2003.

[10] P. Garbacki and D. H. J. Epema, "An Amortized Tit-For-Tat Protocol for Exchanging Bandwidth Instead of Content in P2P Networks," *First Int'l Conf. Self Adaptive and Self-Organizing Systems*, pp. 119-228, 2007.

[11] D. Levin, K. LaCurts, N. Spring, and B. Bhattacharjee, "BitTorrent is an auction: Analyzing and improving BitTorrent's incentives," *in Proceedings of the ACM SIGCOMM*, pp. 243-254, August 2008.

[12] F. Wu and L. Zhang. Proportional response dynamics leads to market equilibrium. *In ACM STOC*, 2007.

[13] A. Sherman, J. Nieh, and C. Stein, "FairTorrent: A Deficit-Based Distributed Algorithm to Ensure Fairness in Peer-to-Peer Systems" *IEEE/ACM Trans. Networking*, vol. 20, no. 5, pp.1361-1374, October 2012.

[14] H. Nishida and T. Nguyen, "A Global Contribution Approach to Maintain Fairness in P2P networks" *IEEE Trans. Parallel and Distributed Systems*, vol.21, No.6, pp. 812-826, June 2010.

[15] S. K. Awasthi and Y. N. Singh, "Biased Contribution Index: A Simpler Mechanism to Maintain Fairness in Peer-to- Peer Networks," *https://arxiv.org/pdf/1606.00717.pdf*, June 2016.

Configuration of Offset Time in Optical Burst Switching Networks for Delay Sensitive Traffic

Anupam Soni and Yatindra Nath Singh
Indian Institute of Technology, Kanpur
anusoni@iitk.ac.in,ynsingh@iitk.ac.in.

Abstract— **In Optical Burst Switching (OBS), the Burst Header Packet (BHP) is sent prior to the burst payload. The time gap between the BHP and payload is referred as offset time. The initial offset value is set by the ingress node and depends upon the processing time of BHP at core node and number of hops between ingress and egress pair. As the BHP propagates through the intermediate nodes, the offset value reduces at each hop by the amount the BHP spends at each node. This offset value is kept sufficiently large in order to allow the intermediate nodes to configure themselves before the burst arrival. The decision for the optimum offset value is not trivial and is important parameter for delay sensitive traffic. The small offset values result in burst loss due to insufficient remaining time between BHP and burst arrival to configure the switch while large offset values reduces the burst loss but increases the average packet delay. In this paper we study the effect of offset value on burst loss probability. The input and output queuing delay for BHP at core nodes effects the burst loss probability and is crucial factor for computing the offset value at an ingress node as these values vary with traffic intensity.**

Index Terms—**Optical burst switching; Burst header packet; Fiber delay lines;**

I. INTRODUCTION

An enormous growth in internet traffic in recent years has been the reason for increased network capacity. The need for large bandwidth demanded new high speed transmission and switching technologies. WDM has emerged as a most viable transmission technology to cater to the demand of increasing network capacity. WDM supports large number of high speed channels on a single fiber, thereby offering enormous bandwidth at the physical layer. The large mismatch in electronic switching technologies and optical transmission has been the bottleneck in effectively utilizing the advantages of WDM. To overcome this bottleneck optical switching technologies like optical circuit switching, optical packet switching and optical burst switching were proposed.

A. Optical Circuit Switching

This is implemented by establishing all-optical lightpaths between the pair of ingress and egress nodes using wavelength routing capability of the optical layer [1]. The establishment of lightpath involves several tasks like topology and resource discovery, routing wavelength assignment, and signaling and resource reservation. However, it gives efficient utilization of bandwidth only if transfer of data happens for longer time duration than the set-up time of lightpath.

B. Optical Packet Switching

Packets are switched and routed independently throughout the network without O/E/O conversion [2]. At intermediate nodes, packets are kept in optical domain alongwith the conversion of tapped copy of header to electronic domain to take appropriate routing decisions. Optical packet switching offers greater degree of statistical

multiplexing gain than optical circuit switching (OCS) and is better suited for bursty traffic. Unfortunately there are certain crucial limitations to its implementation. One major challenge is the non availability of optical RAMs. The payload needs to be buffered for the time taken by the header processing and switch configuration. The only way to achieve optical buffering is fiber delay lines (FDLs) which can only provide limited delay because large lengths of fiber are needed for more delay. This degrades the signal quality and also requires more space to house the fiber. Another major challenge is the synchronization which is difficult to achieve. Also the increase in traffic increases the processing overhead as more headers need to be processed per unit time.

C. Optical Burst Switching

To cope up with the electronic bottleneck and implement all-optical switching Optical Burst Switching (OBS) which combines OCS and OPS was proposed. OBS avoids buffering and packet processing in the optical domain and reserves bandwidth on demand [3].

Optical Switching Paradigm	Bandwidth utilization	Setup Latency	Switching Time	Processing/ Synchronization Overhead	Traffic Adaptivity
OCS	Low	High	Slow	Low	Low
OPS	High	Low	Fast	High	High
OBS	High	Low	Medium	Low	High

II. OBS NETWORK ARCHITECTURE

The OBS network consists of core network and client network as shown in figure 1. The edge routers lie on the boundary of core network and act as an interface between core network and client network. The main tasks of edge routers are packet aggregation, burst assembly, formation of burst header packet (BHP) and scheduling of bursts [4]. The nodes in the core network are known as core routers and are responsible for switching of burst in all-optical domain and handling contentions.

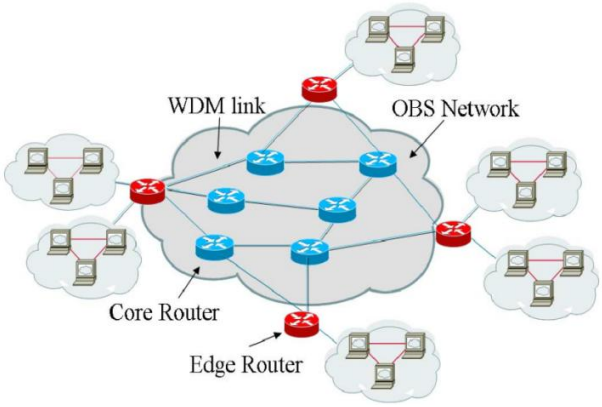

Figure 1. OBS Network Architecture

In an OBS network, at the *ingress* node, the packets arrive from different traffic sources. The packets which are destined to the same *egress* node are aggregated into a single data burst which is transmitted entirely in optical domain. To avoid buffering and processing of optical data bursts at the intermediate *core nodes*, a Burst Header Packet (BHP) with the information about the corresponding data burst is sent in advance. At the egress node, the received data bursts are disassembled into IP packets and are forwarded to their respective destination client networks.

The implementation of OBS network infrastructure involves following major tasks.

- Burst Assembly
- Burst Scheduling
- Contention Resolution
- Signaling Scheme

BURST ASSEMBLY

Burst assembly determines when and how to assemble the incoming data packets into burst. The assembly schemes can be broadly classified into timer based scheme and size based scheme [5]. In timer based scheme data bursts are created after the assembly timer value of the ingress node expires. The BHP's are sent into the network at periodic intervals. The burst length depends upon the timer value and traffic load. In size based schemes the bursts are formed when burst length reaches the particular threshold set by the ingress node. The BHP's are sent at non-periodic intervals and the bursts from an ingress node are of fixed length.

BURST SCHEDULING

Burst scheduling occurs at ingress node as well as core node. Scheduling involves assignment of data wavelength to the burst on an outgoing link. The scheduling algorithm searches the suitable channel and allocates it for the burst. The scheduling algorithms are mainly classified as void filling such as HORIZON and non void filling algorithms such as LAUC-VF [6].

BURST CONTENTION

Contention occurs when more than one burst are destined to the same output port on same wavelength channel at the same time. There are various policies to resolve the contention [7].

A) *Optical Buffering*
The incoming burst is buffered using fiber delay lines (FDL's) until the channel is available for the burst.

B) *Wavelength Conversion*
The contending bursts are scheduled on different data wavelengths. All optical wavelength conversion is assumed at nodes.

C) *Deflection routing*
The contending bursts are routed to different output ports following different routes.

SIGNALING SCHEMES

The reservation of resources and configuration of switches for a burst depends upon signaling scheme implemented. Signaling scheme can be broadly classified into one-way and two-way signaling. In one-way signaling bursts are sent following the BHP without waiting for acknowledgment. In two-way signaling the ingress node sends the burst after receiving the positive acknowledgment from the egress node. The BHP informs the intermediate node along the route, about the bursts arrival and request for resource reservation. In TAG the resources are reserved as soon as the BHP arrives and bursts are buffered at each node for the processing of BHP. In TAW BHP reserves the resources along the route and if the reservations are successful at each intermediate node then a positive acknowledgment is sent back to ingress node. The ingress node sends the burst after receiving the acknowledgment otherwise it attempts for retransmission. Depending upon the time when the reservation is made for the burst the signaling is classified as immediate reservation or delayed reservation. In immediate reservation such as JIT resources are reserved immediately after the arrival of BHP [8]. In delayed reservation scheme such as JET reservation is made just before the burst arrival [9]. In JET there is time gap between BHP and burst sending known as offset time as shown in Fig 2.

Figure 2 Offset Time in JET signaling Scheme

The offset time is set in such a way that processing of BHP is complete at all the nodes and connection between the desired input and output port is established before the arrival of corresponding burst. Thus bursts are transmitted without buffering them at intermediate nodes [10].

In this paper, the study of impact of offset time is carried out.

III. CONFIGURATION OF OFFSET TIME

The offset time depends upon number of hops between ingress and egress nodes, processing time at each core node and switch configuration time.

$$T_{offset} \geq (N_{hops} * T_{PROC}) + T_{OXC}$$

The processing time of BHP (T_{PROC}) comprises of O/E/O conversion time, burst scheduling time and queuing time at input and output of the switch. The queuing time of BHP varies with traffic intensity. Thus T_{PROC} time also varies with traffic load at each node.

The average packet delay in case of timer based assembly scheme is $D_{TA} = (T/2) + T_o$ where T is assembly time and T_o is offset time. For size based scheme the average packet delay is $D_{SA} = (S/2\lambda) + T_o$.

The average packet delay depends upon offset time. For delay sensitive traffic such as video traffic, VOIP etc. the average packet delay should be kept as minimum as possible.

The large offset time increases the packet delay while short offset time results in burst losses due to insufficient offset time as shown in Fig. 3.

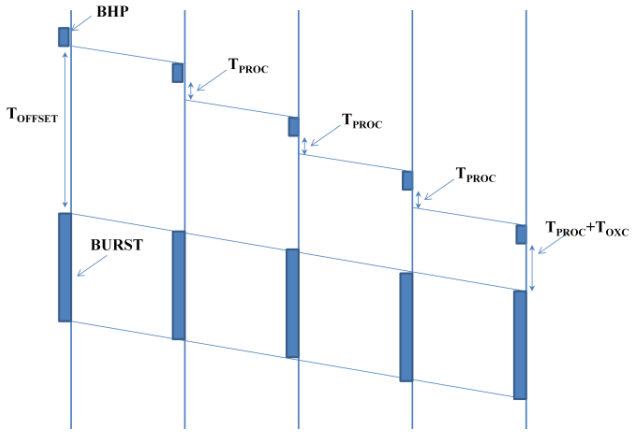

Figure 3 Offset value for successful Burst Transmission

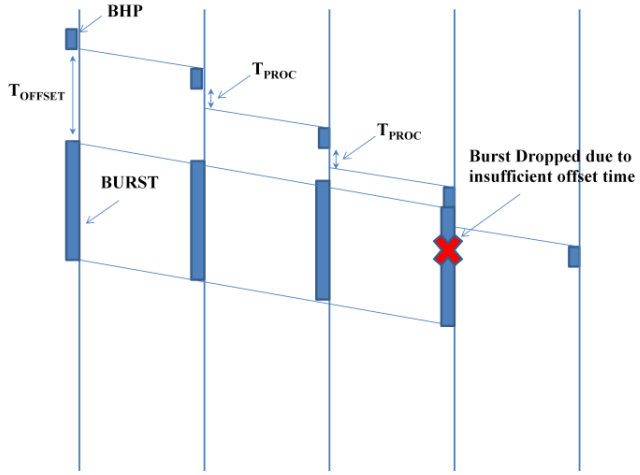

Figure 3 Burst Dropping due to Insufficient Offset time

For delay sensitive traffic large packet delays are not desirable thus there is a tradeoff between burst losses and average packet delay if fixed value of offset value is applied in all traffic scenarios.

IV. Results And Discussion

In this section the simulation results are presented that shows the burst loss probability for different offset time values. NFSNET topology of 14 nodes was used for the simulation. Our simulation model assumes that 4 data wavelengths are available at each node having 2X2 ports and each port has a 1Gbps transmission rate. Three different values of offset times were used having queuing delays of 2, 4 and 6 time slots. Fig 3 shows the blocking probability versus offered load. It is seen that blocking of bursts due to insufficient remaining offset time at higher load is reduced by increasing the offset time.

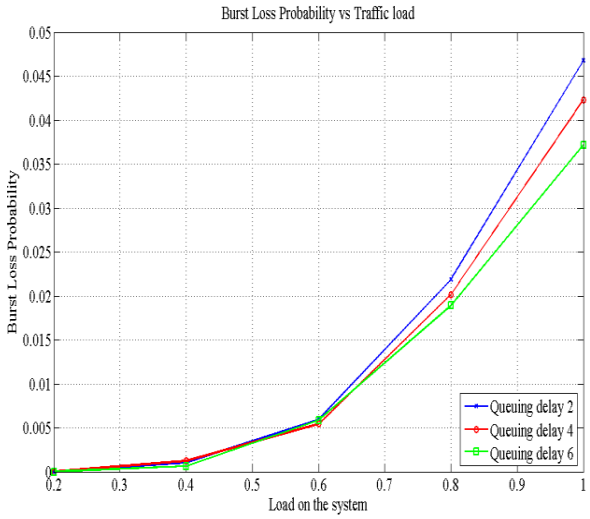

V. Conclusion

In this paper the study carried out shows the effect of offset time configuration on burst blocking probability. The burst blocking probability decreases at higher load values if offset values are large. The offset values need to be increased at ingress node due to increase in queuing delay at higher load values. Instead of fixed value, dynamic offset time values for various traffic scenarios need to be considered which will result in different average packet delays for different traffic scenario. A study on various other factors that influence the burst blocking probability and average packet delays such as assembly time, scheduling time will be considered in our future research work.

REFERENCES

[1] N. Ghani, S. Dixit, and T. S.Wang, "On IP-over-WDM integration," *IEEECommun. Mag.*, pp. 72–84, Mar. 2000.

[2] M. J. O'Mahony, D. Simeonidou, D. K. Hunter, and A. Tzanakaki, "The application of optical packet switching in future communication networks,"*IEEE Commun. Mag.*, vol. 39, pp. 128–135, Mar. 2001.

[3] C. Qiao and M. Yoo, "Optical burst switching (OBS)–a new paradigm for an optical Internet," *J. High Speed Networks*, vol. 8, no. 1, pp. 68–84,1999.

[4] J. S. Turner, "Terabit Burst Switching", J. High Speed Networks, Vol. 8, No. 1, pp. 3-16, Jan.1999.

[5] Xiaojun Cao "Assembling TCP/IP Packets in Optical Burst Switched Networks It, GLOBECOM 2002 no. 1, November 2002 pp. *2815*-2819.

[6] J. Xu, C. Qiao, J. Li, G. Xu, Efficient channel scheduling algorithms in optical burst switched networks, in: IEEE Infocom, 2003.

[7] M Yoo, C. Qiao, and S. Dixit "QoS Performance of Optical Burst Switching in IP-over- WDM Networks," IEEE JSAC, vol. 18, no.10, Oct.2000, pp.2062-71.

[8] J.Y.Wei, R.I. MacFarland, "Just-In-Time Signaling for WDM Optical Burst Switching Networks" J.Light- wave Tech., vol.18, no.12 , Dec, 2000, pp2019-37.

[9] M.Yoo, M.Jeong, C.Qiao, "Just-Enough-Time (JET) :A High Speed Protocol for Bursty Traffic Optical Networks" Proc. IEEE/LEOS Conf. on Technologies for a Global Information Infrastructure, Aug. 1997, pp26-27.

[10] Y. Xiong, M. Vandenhoute, H.C. Cankaya, Control architecture in optical burst-switched WDM networks, IEEE Journal on Selected Areas in Communications 18 (10) (2000) 1838–1851.

Wireless Systems with Optical and RF Signals

Parul Garg
Netaji Subas Institute of Technology, Dwarka, Delhi
parulsaini@yahoo.co.in

This presentation deals with the current scenario of the wireless communication. It starts with an introduction about the conventional radio frequency (RF) wireless communication system. Although RF communication is the most popular frequency band mainly due to little interference and good coverage. For future communication systems, more spectral resources are mandatory. Of the many popular solutions, free-space optical (FSO) communication systems have gained significant research attention as a cost effective and wide bandwidth solution operating at the unlicensed optical spectrum, relative to the traditional radio frequency (RF) transmission. Contrary to RF links, the major severe limiting factor in FSO communications is its high vulnerability to the atmospheric turbulence conditions. To tackle these problems hybrid systems involving RF as a parallel link has been discussed in the presentation.

After discussing pros and cons of hybrid relayed system a new contemporary communication technique that combine illumination with communication is being introduced. Visible light communication (VLC) provides ubiquitous communication while addressing the shortfalls and limitations of RF communication. VLC is compared with existing RF systems and the necessity for using this beneficial technology in communication systems is justified. Different modulation schemes and dimming techniques for indoor VLC are discussed. After that VLC system model is presented and system performance analysis is being depicted on varying various parameters. Finally, the limitations of VLC as well as the probable future directions are presented.

Outage Analysis of Variable-Gain Amplify and Forward Relayed Hybrid FSO/VLC Communication System

Kamna Sharma*, Anshul Vats†, and Mona Aggarwal‡
Department of Electrical, Electronics and Communication Engineering
The NorthCap University, Gurgaon, Haryana-122001, India
E-mail:*kamnasharma93@gmail.com**, *nalurajput2@gmail.com*†, *ermonagarg24@gmail.com*‡

***Abstract*—In this paper, we consider a three node hybrid free space optical communication/visible light communication (FSO/VLC) system, where source node communicates with the destination node via an amplify and forward relay. The source to relay is an FSO link modelled by gamma-gamma fading distributions whereas the relay to destination is considered as VLC link. We derive the statistical characteristics of end-to-end signal to noise ratio at the destination in terms of moment generating function and derive the closed form expression of end to end Outage Probability of the hybrid system. Furthermore, we analyzed the impact on outage probability of hybrid FSO/VLC link by varying different parameters of both the links.**

Amplify and forward relay, Gamma-Gamma distribution, hybrid FSO/VLC system, outage probability.

I. INTRODUCTION

In recent years, Free Space Optical (FSO) communication, a type of optical wireless communication (OWC), has gained extensive study as well as research activity due to various benefits provided, out of which some are unlicensed spectrum, high data rates, very low installation cost, easy deployment, and less costly as compared to its optical fibre and radio frequency (RF) counterparts [1].FSO is a OWC technology that uses wireless transmission of light in free space. FSO communication technology is familiar and employed at various places for different services such as Outdoor wireless access, storage Area Network (SAN), last-mile access, enterprise connectivity, Fiber backup, backhaul, point-to-point links and point-to-multipoint links communication, for example, two buildings, two ships, and, from aircraft to ground or satellite to ground, for short and long reach communication respectively, and military access. Using FSO system, large areas can be securely linked in minimum devising and arrangement time [2].

One more type of optical wireless communication is Visible Light Communication (VLC). This technology has many features also it has many advantages over Radio Frequency (RF). VLC has wide unregulated spectrum, typically from 428 to 750 THz. This gives large communication bandwidth for communication to provide license free extremely high data rate services. VLC offers hundreds of terahertz of license free bandwidth, which is ten thousand times more than that of RF. It has high spatial reuse, high security, and it is high energy efficient [3]. In literature, multihop routing has been extensively used in optical wireless systems when the direct source to destination communication is not possible due to unsatisfied line of sight communication condition or large distance and in this approach, relays, which act as intermediate nodes, are placed in between source and destination nodes to reduce the misalignment fading and scintillation effect [4]. There are 2 types of relays i.e. Amplify and Forward relay and Decode and Forward relay. Decode and forward (DF) relay decodes the signal coming from previous node, then re-modulates this signal, and send this decoded and re-modulated signal towards the destination node whereas the amplify and forward (AF) relay amplify the signal coming from previous node and then forwards this signal, without any decoding process, to the next node, towards destination [5], [6]. DF relay is more complex as compared to AF relay because it has full processing capacity. Throughout, a DF relay has complexity like a base station [5]. AF relay is used due to less complexity and simple implementation [4]. There are two types of AF relays, fixed gain and variable gain.

In this paper, we analyze the outage probability of a variable gain AF relayed hybrid system where both the links are optical wireless links and the first link, that is free space optical communication link, is used for outdoor communication and is assumed to follow gamma-gamma distribution which is independent but no necessarily identically distributed (i.n.i.d). The second link is visible light communication link, is used for indoor communication. Firstly, we find the moment generating function(MGF) of end to end signal to noise ratio of the system in (13). Then, we have used this MGF to find out the outage probability of the entire system as in (29).

II. SYSTEM MODEL

We consider a three node mixed free space optical communication / visible light communication (FSO/VLC) system, where source node (S) communicates with the destination node (D) via an intermediate node i.e. amplify and forward relay (R) as shown in figure 1.

Fig. 1. System model showing hybrid FSO/VLC system

The S-R link is a free space optical communication (FSO) link, whereas R-D link is a visible light communication (VLC) link. All the channels are assumed to be quasi-static. Also, the S-R link is assumed to have flat fading. The communication is assumed as half duplex so as to maintain the low cost of the system. The FSO link (S-R) as well as the VLC link (R-D) are assumed to be ergodic and memoryless with independent but not particularly identically distributed (i.n.i.d.) fading statistics.

A. FSO link

The FSO link is assumed to follow gamma-gamma fading distribution having impairments of atmospheric turbulence, pointing errors and path loss. The probability density function of Signal to Noise Ratio of the link is given in [4] can be expressed as

$$f_{\gamma_{(FSO)}}(\gamma) = \frac{\xi_o^2}{2\gamma\Gamma(\alpha_{(FSO)})\Gamma(\beta_{(FSO)})} \times G_{1,3}^{3,0}\left(\alpha_{(FSO)}\beta_{(FSO)}\sqrt{\frac{\gamma}{\Omega_{FSO}}}\,\middle|\, \begin{matrix}\xi_o^2+1 \\ \xi_o^2, \alpha_{(FSO)}, \beta_{(FSO)}\end{matrix}\right) \tag{1}$$

where ξ_o is the pointing error, Ω_{FSO} is the average electrical SNR of the link , and is defined as $\Omega_{FSO} = (\eta\mathbb{E}[h])^2/N_0$ with $\mathbb{E}$ denoting the expectation operator, η being the optical to electrical conversion ratio, and N_0 is the variance of additive white Gaussian noise (AWGN). Also, $\alpha_{(FSO)}$ is the effective number of small scale scattering environment eddies, and $\beta_{(FSO)}$ is the effective number of large scale scattering environment eddies, and are defined as

$$\alpha_{(FSO)} = \left[\exp\left(\frac{0.49\chi^2}{(1+0.18d^2+0.56\chi^{12/5})^{7/6}}\right)-1\right]^{-1} \tag{2}$$

and

$$\beta_{(FSO)} = \left[\exp\left(\frac{0.51\chi^2}{(1+0.9d^2+0.62d^2\chi^{12/5})^{5/6}}\right)-1\right]^{-1} \tag{3}$$

where χ^2 is the Rytov variance given as $\chi^2 = 1.23C_n^2\kappa^{7/6}L^{11/6}$, $d = \left(\kappa\mathscr{D}^2/4L\right)^{1/2}$ with $\mathscr{D}$ being the receiver aperture diameter, $\kappa = 2\pi/\lambda$ is the optical wave number, and C_n^2 is the index of refraction structure parameter.

B. VLC link

The VLC link is assumed to be modelled with uniform distribution of N users. The probability density function of Signal to Noise Ratio of VLC link is given by

$$f_{\gamma_{(VLC)}}(\gamma) = \frac{[E(n+1)L^{(n+1)}]^{(\frac{2}{n+3})}}{r^2(n+3)} \times \gamma^{-(\frac{n+4}{n+3})} \tag{4}$$

where the LED radiation pattern is given by $n = \frac{-1}{log_2(x)}$, in which x is the semi-angle of the LED. Also,

$$E = \frac{1}{2.pi} gR_{p'}wL(\psi)Q(\psi) \tag{5}$$

is a system constant, where g is area of photodetector, w is the optical concentrator refractive index, $L(\psi)$ is the gain of optical filter, $Q(\psi)$ is the optical concentrator gain [7].

III. MGF OF THE END TO END SNR

The equivalent end to end signal to noise ratio (SNR) of the system is given by

$$\frac{1}{\gamma_{(AF)}} = \frac{1}{\gamma_{(VLC)}} + \frac{1}{\gamma_{(FSO)}} \tag{6}$$

or

$$\gamma_{(AF)} = \frac{\gamma_{(VLC)}\cdot\gamma_{(FSO)}}{\gamma_{(VLC)}+\gamma_{(FSO)}} \tag{7}$$

For simplicity, we obtain $\gamma_{(AF)}$ in terms of MGF by using (8)

$$M_{\gamma_{(AF)}^{-1}}(s) = \left[M_{\gamma_{(FSO)}^{-1}}(s)\right] \times \left[M_{\gamma_{(VLC)}^{-1}}\right] \tag{8}$$

In this section,the pdf of SNR of both the links is utilized for evaluating the inverse MGF of γ_{AF}, then using this inverse MGF, we find the closed form expression for MGF of end to end SNR. Now finding the

$$M_{\gamma_{(FSO)}^{-1}}(s) = \int_0^\infty e^{\frac{-s}{\gamma}}.f(\gamma)\,d\gamma \tag{9}$$

Substituting equation (1) in equation (9), we obtain

$$\begin{aligned} M_{\gamma_{(FSO)}^{-1}}(s) &= \int_0^\infty e^{\frac{-s}{\gamma}}.\frac{\xi_o^2}{2\gamma\Gamma(\alpha_{(FSO)(FSO)})\Gamma(\beta_{(FSO)})} \\ &\quad\times G_{1,3}^{3,0}\left(\alpha_{(FSO)}\beta_{(FSO)}\sqrt{\frac{\gamma}{\Omega}}\,\middle|\, \begin{matrix}\xi_o^2+1 \\ \xi_o^2, \alpha_{(FSO)}, \beta_{(FSO)}\end{matrix}\right)d\gamma \\ &= \int_0^\infty e^{\frac{-s}{\gamma}}.\gamma^{-1}\frac{\xi_o^2}{2\Gamma(\alpha_{(FSO)})\Gamma(\beta_{(FSO)})} \\ &\quad\times G_{1,3}^{3,0}\left(\alpha_{(FSO)}\beta_{(FSO)}\sqrt{\frac{\gamma}{\Omega}}\,\middle|\, \begin{matrix}\xi_o^2+1 \\ \xi_o^2, \alpha_{(FSO)}, \beta_{(FSO)}\end{matrix}\right)d\gamma \end{aligned} \tag{10}$$

We know that

$$e^{\frac{-s}{\gamma}} = G_{1,0}^{0,1}\left(\frac{\gamma}{s}\,\middle|\, \begin{matrix}1 \\ -\end{matrix}\right)d\gamma \tag{11}$$

$$\begin{aligned} M_{\gamma_{(FSO)}^{-1}}(s) &= \frac{\xi_o^2}{2\Gamma(\alpha_{(FSO)})\Gamma(\beta_{(FSO)})}\int_0^\infty \gamma^{-1}G_{1,0}^{0,1}\left(\frac{\gamma}{s}\,\middle|\, \begin{matrix}1 \\ -\end{matrix}\right) \\ &\quad\times G_{1,3}^{3,0}\left(\alpha\beta_{(FSO)}\sqrt{\frac{\gamma}{\Omega}}\,\middle|\, \begin{matrix}\xi_o^2+1 \\ \xi_o^2, \alpha_{(FSO)}, \beta_{(FSO)}\end{matrix}\right)d\gamma \end{aligned} \tag{12}$$

By using the property(2.24.1.1, [8]), we obtain

$$\begin{aligned} M_{\gamma^{-1}}(s) &= \frac{2^{\alpha_{(FSO)}+\beta_{(FSO)}-1}.\xi_o^2}{4\pi\Gamma(\alpha_{(FSO)})\Gamma(\beta_{(FSO)})} \\ &\quad\times G_{2,7}^{7,0}\left(\frac{\alpha_{(FSO)}^2\beta_{(FSO)}^2.s}{16\Omega}\,\middle|\, \begin{matrix}c_1 \\ c_2\end{matrix}\right) \end{aligned} \tag{13}$$

where

$$c_1 = \frac{{\xi_o}^2+1}{2}, \frac{{\xi_o}^2+2}{2}$$

and

$$c_2 = \frac{{\xi_o}^2}{2}, \frac{{\xi_o}^2+1}{2}, \frac{\alpha_{(FSO)}}{2}, \frac{\alpha_{(FSO)}+1}{2}, \frac{\beta_{(FSO)}}{2}, \frac{\beta_{(FSO)}+1}{2}, 0$$

Similarly, calculating MGF of inverse of SNR of VLC channel as shown below

$$M_{\gamma^{-1}_{(VLC)}}(s) = \int_0^\infty e^{\frac{-s}{\gamma}}.f_{VLC}(\gamma)d\gamma \tag{14}$$

Substituting equation (4) in equation (14), we get $M_{\gamma^{-1}_{(VLC)}}(s)$ as

$$M_{\gamma^{-1}_{(VLC)}}(s) = \int_0^\infty e^{\frac{-s}{\gamma}}.\frac{[E(n+1)L^{(n+1)}]^{\left(\frac{2}{n+3}\right)}}{r^2(n+3)} \times \gamma^{-\left(\frac{n+4}{n+3}\right)}d\gamma \tag{15}$$

Now using property, given by equation (11), in (15), we get

$$M_{\gamma^{-1}_{(VLC)}}(s) = \frac{[E(n+1)L^{(n+1)}]^{\left(\frac{2}{n+3}\right)}}{r^2(n+3)} \times \int_0^\infty G^{0,1}_{1,0}\left(\frac{\gamma}{s}\middle| \begin{matrix}1\\-\end{matrix}\right) \times\gamma^{-\left(\frac{1}{n+3}\right)-1}d\gamma \tag{16}$$

Also using identity (2.24.2.1, [8]), we obtain

$$\begin{aligned} M_{\gamma^{-1}_{(VLC)}}(s) =& \left(\frac{1}{s}\right)^{\left(-\left(\frac{-1}{n+3}\right)\right)} \times \Gamma\left(1-1-\left(\frac{-1}{n+3}\right)\right) \\ =& s^{\left(\frac{-1}{n+3}\right)}\Gamma\left(\frac{1}{n+3}\right) \end{aligned} \tag{17}$$

To obtain the expression of $M_{\gamma^{-1}_{(AF)}}(s)$, substitute (13) and (17) in (8) as given below

$$\begin{aligned} M_{\gamma^{-1}_{(AF)}}(s) &= \left[M_{\gamma^{-1}_{(FSO)}}(s)\right] \times \left[M_{\gamma^{-1}_{(VLC)}}\right] \\ M_{\gamma^{-1}_{(AF)}}(s) &= \left[\frac{2^{\alpha_{(FSO)}+\beta_{(FSO)}-1}\xi_0^2}{4\pi\Gamma(\alpha_{(FSO)})\Gamma(\beta_{(FSO)})}G^{7,0}_{2,7}\left(\Phi s \middle| \begin{matrix}c_1\\c_2\end{matrix}\right)\right] \\ &\times \left[s^{\left(\frac{-1}{n+3}\right)}\Gamma\left(\frac{1}{n+3}\right)\right] \end{aligned} \tag{18}$$

To obtain $M_{\gamma_{(AF)}}(s)$ from $M_{\gamma^{-1}_{(AF)}}(s)$, we use the identity given by [4] as

$$\begin{aligned} M_{\gamma_{(AF)}}(s) =& 1-\sqrt{s}\int_0^{\frac{\pi}{2}} \frac{\sec^2(\phi)}{\sqrt{\tan(\phi)}}J_1\left(2\sqrt{s\tan(\phi)}\right) \\ &\times M_{\gamma^{-1}_{AF}}(\tan(\phi))\,d\phi, \end{aligned} \tag{19}$$

where J_v is the bessel function of order v=1. Using a change of variable method, put $tan(\phi) = p$, $sec^2(\phi)d\phi = dp$, this gives

$$\begin{aligned} M_{\gamma_{(AF)}}(s) =& 1-\sqrt{s}\int_0^\infty \frac{1}{\sqrt{p}}J_1(2\sqrt{sp}) \\ &\times M_{\gamma^{-1}_{AF}}(p)\,dp \end{aligned} \tag{20}$$

Now substituting value of $M_{\gamma^{-1}_{(AF)}}(s)$ from (18) in (20), gives

$$\begin{aligned} M_{\gamma_{(AF)}}(s) = 1-\sqrt{s}\int_0^\infty \frac{1}{\sqrt{p}}J_1(2\sqrt{sp}) \times \frac{2^{\alpha_{(FSO)}+\beta_{(FSO)}-1}\xi_0^2}{4\pi\Gamma(\alpha_{(FSO)})\Gamma(\beta_{(FSO)})} \\ \times G^{7,0}_{2,7}\left(\frac{\alpha^2_{(FSO)}\beta^2_{(FSO)}}{16\Omega_{FSO}}.s \middle| \begin{matrix}c_1\\c_2\end{matrix}\right) \times s^{\left(\frac{-1}{n+3}\right)}\Gamma\left(\frac{1}{n+3}\right)dp \end{aligned} \tag{21}$$

Taking the constant part of above equation out of the integral and using identity

$$J_v(x) = G^{1,0}_{0,2}\left(\frac{x^2}{4}\middle| \begin{matrix}-\\ \frac{v}{2}, \frac{-v}{2}\end{matrix}\right) \tag{22}$$

we get

$$\begin{aligned} M_{\gamma_{(AF)}}(s) &= 1-\sqrt{s}.\frac{2^{\alpha_{(FSO)}+\beta_{(FSO)}-1}\xi_0^2}{4\pi\Gamma(\alpha_{(FSO)})\Gamma(\beta_{(FSO)})}.\Gamma\left(\frac{1}{n+3}\right) \\ &\times\int_0^\infty \frac{1}{\sqrt{p}}.p^{\left(\frac{-1}{n+3}\right)} \times G^{1,0}_{0,2}\left(sp \middle| \begin{matrix}-\\ \frac{1}{2}, \frac{-1}{2}\end{matrix}\right) \\ &\times G^{7,0}_{2,7}\left(\frac{\alpha^2_{(FSO)}\beta^2_{(FSO)}}{16\Omega_{FSO}}.p \middle| \begin{matrix}c_1\\c_2\end{matrix}\right)dp \\ &= 1-\sqrt{s}.\frac{2^{\alpha_{(FSO)}+\beta_{(FSO)}-1}\xi_0^2}{4\pi\Gamma(\alpha_{(FSO)})\Gamma(\beta_{(FSO)})}.\Gamma\left(\frac{1}{n+3}\right).\int_0^\infty \frac{p^{\left(\frac{-1}{n+3}\right)}}{\sqrt{p}} \\ &\times G^{1,0}_{0,2}\left(sp \middle| \begin{matrix}-\\ \frac{1}{2}, \frac{-1}{2}\end{matrix}\right) \times G^{7,0}_{2,7}\left(\frac{\alpha^2_{(FSO)}\beta^2_{(FSO)}}{16\Omega_{FSO}}.p \middle| \begin{matrix}c_1\\c_2\end{matrix}\right)dp \\ &= 1-\sqrt{s}.\frac{2^{\alpha_{(FSO)}+\beta_{(FSO)}-1}\xi_0^2}{4\pi\Gamma(\alpha_{(FSO)})\Gamma(\beta_{(FSO)})}.\Gamma\left(\frac{1}{n+3}\right).\int_0^\infty p^{\left(\frac{m+1}{2(m+3)}\right)-1} \\ &\times G^{1,0}_{0,2}\left(sp \middle| \begin{matrix}-\\ \frac{1}{2}, \frac{-1}{2}\end{matrix}\right) \times G^{7,0}_{2,7}\left(\frac{\alpha^2_{(FSO)}\beta^2_{(FSO)}}{16\Omega_{FSO}}.p \middle| \begin{matrix}c_1\\c_2\end{matrix}\right)dp \end{aligned} \tag{23}$$

Using identity(2.24.1.1, [8])and substituting (III) and (III), we get

$$\begin{aligned} M_{\gamma_{(AF)}}(s) &= 1-\sqrt{s}.\frac{2^{\alpha_{(FSO)}+\beta_{(FSO)}-1}\xi_0^2}{4\pi\Gamma(\alpha_{(FSO)})\Gamma(\beta_{(FSO)})}.\Gamma\left(\frac{1}{n+3}\right). \\ &s^{\left(\frac{m+1}{2(m+3)}\right)-1} \times G^{7,1}_{4,7}\left(\frac{\frac{\alpha^2_{(FSO)}\beta^2_{(FSO)}}{16\Omega_{FSO}}}{s} \middle| \begin{matrix}\frac{1}{n+3}, \frac{n+4}{n+3}, c_1\\ c_2\end{matrix}\right) \\ &= 1-\frac{s^{\left(\frac{-1}{n+3}\right)}\Gamma\left(\frac{1}{n+3}\right)2^{\alpha_{(FSO)}+\beta_{(FSO)}-1}{\xi_0}^2}{4\pi\Gamma(\alpha_{(FSO)})\Gamma(\beta_{(FSO)})} \\ &\times G^{7,1}_{4,7}\left(\frac{\frac{\alpha^2_{(FSO)}\beta^2_{(FSO)}}{16\Omega_{FSO}}}{s} \middle| \begin{matrix}\frac{1}{n+3}, \frac{n+4}{n+3}, c_1\\ c_2\end{matrix}\right) \end{aligned} \tag{24}$$

IV. Outage Analysis

In this section, the closed form expression of end to end outage probability of the hybrid system is evaluated. Outage probability tells the quality of the channel. It can be calculated by finding the probability that a particular transmission rate is not supported. For calculating the outage probability, first we need to calculate the CDF of end to end SNR which can be find out by the MGF of end to end SNR, evaluated in (24). The expression for finding the CDF of end to end SNR of the system,$F_{\gamma_{AF}}(\gamma)$, is obtained by applying the inverse Laplace transformation to (24), as follows

$$F_{\gamma_{eqAF}}(\gamma) = \mathscr{L}^{-1}\left[\frac{1}{s}M_{\gamma(AF)}\right] \tag{25}$$

where $\mathscr{L}^{-1}(.)$ denotes the inverse Laplace transform operator. By substituting (24) in (25) and using (3.40.1.1, [9]), we get

$$F_{\gamma_{eqAF}}(\gamma) = \mathscr{L}^{-1}\left[\frac{1}{s}\right] - \mathscr{L}^{-1}\left[\frac{\Gamma\left(\frac{1}{n+3}\right) 2^{\alpha_{(FSO)}+\beta_{(FSO)}-1}\xi_0{}^2}{4\pi\Gamma(\alpha_{(FSO)})\Gamma(\beta_{(FSO)})}\right.$$
$$\left.\times\frac{1}{p^{1-\frac{1}{n+3}}}\times G_{4,7}^{7,1}\left(\frac{\frac{\alpha^2_{(FSO)}\beta^2_{(FSO)}}{16\Omega_{FSO}}}{s}\;\middle|\;\begin{matrix}\frac{1}{n+3},\frac{n+4}{n+3},c_1\\ c_2\end{matrix}\right)\right] \tag{26}$$

Taking the constant out of the bracket, we get

$$F_{\gamma_{eqAF}}(\gamma) = \mathscr{L}^{-1}\left[\frac{1}{s}\right] - \frac{2^{\alpha_{(FSO)}+\beta_{(FSO)}-1}\xi_0^2}{4\pi\Gamma(\alpha_{(FSO)})\Gamma(\beta_{(FSO)})}.\Gamma\left(\frac{1}{n+3}\right).$$
$$\mathscr{L}^{-1}\left[\frac{1}{p^{1-\frac{1}{n+3}}}\times G_{4,7}^{7,1}\left(\frac{\frac{\alpha^2_{(FSO)}\beta^2_{(FSO)}}{16\Omega_{FSO}}}{s}\;\middle|\;\begin{matrix}\frac{1}{n+3},\frac{n+4}{n+3},c_1\\ c_2\end{matrix}\right)\right] \tag{27}$$

So, the CDF of end to end SNR of the proposed system is

$$F_{\gamma_{eqAF}}(\gamma) = 1 - \frac{\Gamma\left(\frac{1}{n+3}\right).2^{\alpha_{(FSO)}+\beta_{(FSO)}-1}\xi_0^2}{4\pi\Gamma(\alpha_{(FSO)})\Gamma(\beta_{(FSO)})}\gamma^{\left(\frac{-1}{n+3}\right)}$$
$$\times G_{3,7}^{7,0}\left(\frac{\alpha^2_{(FSO)}\beta^2_{(FSO)}}{16\Omega_{FSO}}\gamma\;\middle|\;\begin{matrix}\frac{n+4}{n+3},c_1\\ c_2\end{matrix}\right) \tag{28}$$

Now, the closed form expression of end to end outage probability of the proposed hybrid FSO/VLC system can be obtained by putting $\gamma = \gamma_{th}$ in (28),

$$F_{\gamma_{eqAF}}(\gamma_{th}) = 1 - \frac{\Gamma\left(\frac{1}{n+3}\right).2^{\alpha_{(FSO)}+\beta_{(FSO)}-1}\xi_0^2}{4\pi\Gamma(\alpha_{(FSO)})\Gamma(\beta_{(FSO)})}\gamma_{th}^{\left(\frac{-1}{n+3}\right)}$$
$$\times G_{3,7}^{7,0}\left(\frac{\alpha^2_{(FSO)}\beta^2_{(FSO)}}{16\Omega_{FSO}}\gamma_{th}\;\middle|\;\begin{matrix}\frac{n+4}{n+3},c_1\\ c_2\end{matrix}\right) \tag{29}$$

V. NUMERICAL ANALYSIS

In this paper, the hybrid FSO/VLC system model is studied and analyzed. The system is analyzed in terms of outage probability with different parameters. Figure 2 and figure 3 shows the graph for outage probability versus average electrical SNR of the system. In figure 2, the graph is obtained for different values of pointing errors from 1 to 5. It is observed that as the pointing errors are increasing, we get the good result in terms of decreasing outage probability. And at pointing error value ξ =5 we get the best result.

In figure 3, the graph is obtained for different values combination of small scale and large scale scattering environment eddies. Here, the large scale scattering environment eddies(β) value is kept constant at 1.5 and the values of small scale scattering environment eddies(α) are varied from 0.5 to 5. At α=5,β=1.5, we get the good results in terms of decreasing outage probability.

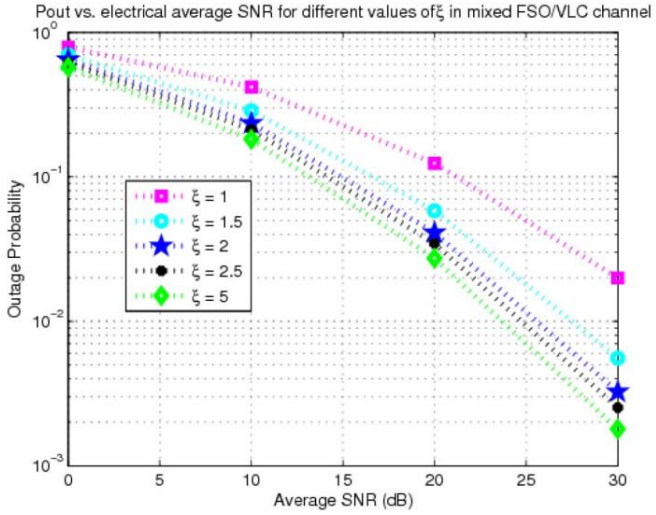

Fig. 2. Outage Probability (Pout) versus average electrical SNR for different values of ξ_0 in FSO hop in mixed FSO/VLC system

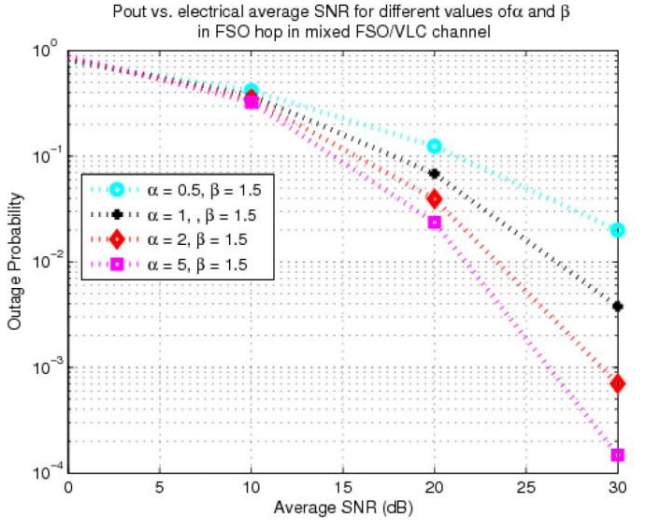

Fig. 3. Outage Probability (Pout) versus average electrical SNR for different values of α and β in FSO hop in mixed FSO/VLC system

VI. CONCLUSIONS

We described a hybrid FSO-VLC system in which the FSO link is for outdoor communication and the VLC linnk is for indoor communication. In this paper, we analysed the system performance on the basis of its outage probability. We firstly derived the MGF of SNR of both the links then utilised them for finding the equivalent end to end MGF of the system. This MGF is used to find the equivalent end to end outage probability of the system. After this, The numerical analysis is carried out to check the system outage at different values of pointing errors. In this, the outage probability versus average electrical SNR is plotted by varying pointing errors, small and large scale scattering environment eddies. As the pointing errors are increasing, we are able to get the better results in terms of decreasing outage probability. As the small scale

scattering environment eddies are increasing, we are getting the better results in terms of decreasing outage probability.

REFERENCES

[1] M. Aggarwal, P. Garg, and P. Puri, Analysis of subcarrier intensity modulation-based optical wireless DF relaying over turbulence channels with path loss and pointing error impairments, IET Commun., vol. 8, no. 17, pp. 31703178, 2014.

[2] A. Malik and P. Singh, "Free Space Optics: Current Applications and Future Challenges," International Journal of Optics, vol. 2015 (2015), article ID 945483, 7 pages, 2015.

[3] S. Wu, H. Wang, and C.H. Youn, "Visible Light Communications for 5G Wireless Networking Systems:From Fixed to Mobile Communications," IEEE Network, vol.28,no.6, pp.41-45, Nov.-Dec. 2014.

[4] M. Aggarwal, P. Garg, and P. Puri, "Exact MGF-based performance analysis of AF-Relayed Optical Wireless Communication Systems," Journal of lightwave technology, vol. 33,no. 9, May 2015.

[5] G. Levin and S. Loyka, "Amplify-and-Forward Versus Decode-and-Forward Relaying: Which is Better?," Int. Zurich Seminar on Communications (IZS), February 29 March 2, 2012

[6] M. Aggarwal, P. Garg, and P. Puri, "Ergodic Capacity of SIM-Based DF Relayed Optical Wireless Communication Systems," IEEE Photonics Technology letters , vol. 27,no. 10, May 2015.

[7] A. Papoulis and S. U. Pillai, Probability, Random Variables and Stochastic Processes, Tata McGraw-Hill Education, January 2002.

[8] Direct laplace transform, volume 3.

[9] Direct laplace transform, volume 4.

[10] http://mms.businesswire.com/media/20130409/en/FranhofrHHIVLC.jpg

A Brief Survey on Underwater Wireless Optical Communication System

Gaurav Pandey, Mona Aggarwal and Swaran Ahuja
The NorthCap University, Gurgaon
Gauravpandey524@gmail.com, monaaggarwal@ncuindia.edu, swaranahuja@ncuindia.edu

Theunderwater wireless optical communication (UWOC) system gives very high rate of underwater data transmission over several meters. It utilizes the visible band in the spectral range of 390-750nm of the electromagnetic spectrum.In this paper, westudy various types of link configurations depending upon the circumstances in water environment. We also study the effect of various water types on the system performance. We find that theUWOC system is affected especially by inherent optical properties such as absorption and scattering and the effect of these properties is different in various water types. We also present that misalignment in UOWC system adversely affects its functioning and reliability.Finally, we present that hybrid system design for a proper systematic UOWC system.

Keywords-Autonomous underwater vehicles (AUV),link misalignment, remotely operated underwater vehicles (ROV), Underwater Wireless optical communication (UWOC).

Impact Zone Analysis of P-cycles

Pallavi Athe and YN Singh
Indian Institute of Technology, Kanpur
apallavi@iitk.ac.in, ynsingh@iitk.ac.in

P-cycle method has been extensively studied for optical network protection. A large p-cycle has high capacity efficiency and can protect large number of nodes against single link failure. For such a p-cycle, all the links protected by it, lose protection when the p-cycle is consumed to protect a failure. As the probability of multiple link failure is high for large network, it also means that with higher probability, on second failure, protection may not be there for the failed link. If the number of links protected by a p-cycle is large it makes the network unprotected on the occurrence of second failure. In this paper, we study the impact zone due to first link failure in various configurations of p-cycles. The study gives insight into how to choose from the p-cycle configurations to reduce the impact zone while using minimum spare capacity.

Mobilty Management for Indoor VLC System

Akash Gupta[1], Parul Garg[2], Shashikant[3]
Division of Electronics and Communication Engineering
Netaji Subas Institute of Technology
Dwarka, New Delhi- 110078
Email: *akashgemini@gmail.com*[1]
parul_saini@yahoo.co.in[2]
kantshashilu91@gmail.com[3]

***Abstract*—In this paper we have analysed received signal strength (RSS) based horizontal handover scheme for indoor visible light communication (VLC) system. Two separate mobility management techniques are discussed for two different VLC node arrangements: spotlighting and uniform lighting arrangement. The proposed handover scheme will assist mobile user to have uninterrupted communication services while traversing across the room. Numerical results are conducted to corroborate the superiority in performance of the proposed system over existing system.**

I. Introduction

The increase in wireless data consumption has created pressure on dwindling radio frequency spectrum. This has motivated researchers to search for unconventional communication technologies. Visible light communication (VLC) has gained notable attention as an alternative to existing indoor communication technologies [1], [2]. VLC system not only serves illumination with communication but also provides qualities like no health hazards, no electromagnetic interference, high bandwidth unlicensed spectrum and highly secured network. The bottleneck in VLC is mainly the mobility management as multiple light emitting diode is installed on ceiling with limited cell coverage. In [3], authors have investigated mobility in VLC devices and proposed handover handover management for small cells and directional characteristics. In [4], method of receiving signal power (RSP) handover between the moving vehicle and multiple LED streetlights transmitters was studied by the authors. For providing uninterrupted services to the mobile terminals fast horizontal handover mechanism must be incorporated in the VLC system. The handover delay must be shortened as the overlapping area in VLC system are quite small. The main contributions of the paper are: 1) A novel variable timer based horizontal handover mechanism for mobile devices in uniform lighting indoor VLC systems. 2) Mobility management schemes for spotlighting scenarios. 3) Received power analysis at user terminal with and without handover mechanism.

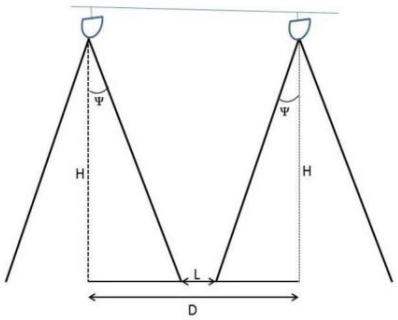

Fig. 1. Spotlighting arrangement of LED luminaries.

II. System Model

In this paper we have considered two scenarios: spotlighting and uniform lighting arrangement of VLC node arrangement. In spotlighting arrangement light emitting diodes (LEDs)

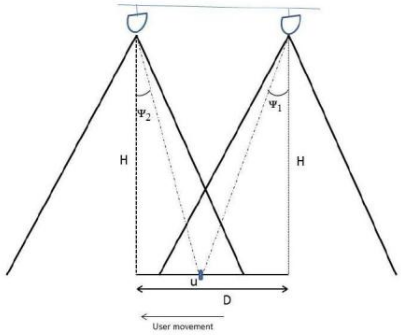

Fig. 2. Uniform lighting arrangement of LED luminaries.

with small semiangles are deployed that produce intense and focussed light as shown in Fig. 1. In Fig. 2 uniform lighting scenario is depicted, in which wider semiangle LEDs are used that results in uniform distribution of light throughout the room. While uniform lighting suffers from intercell interference, there exist dark spots with no VLC coverage in spotlighting arrangement that lead to interruption in communication. The VLC system is mounted in a room of dimensions $8m \times 8m \times 3m$ and system specifications as given in table 1. We have considered a mobile user with an average velocity of v m/s. The LED luminaries are uniformly arranged with a distance (D) of $4m$ between two adjacent VLC nodes.

TABLE I
VLC SYSTEM PARAMETERS

Parameters	Values
Effective aperture of PD	$10^{-4}m^2$
Field of view of photodiode	60^o
Transmitted Power (per LED)	20 mW
Number of LEDs per array	60×60
Centre luminous Intensity	300-910 lx
Area of VLC cell	12.56 m^2
Modulation bandwidth of LED	40 MHz
Optical Filter Gain	1
Refractive index	1.5
Optical to electrical conversion efficiency	0.81 A/W
Noise Power Spectral Density	$10^{-21}A^2/Hz$

III. CHANNEL MODEL

VLC channels incorporate both LOS and diffuse components, however it is observed, that energy of reflected signal is much lower than the energy of LOS. Thus, it is assumed that each user is served by a single VLC access point which has the strongest channel gain for that user. In VLC since the carrier is in the order of terahertz (THz), Doppler frequency of fading is higher than the data rate. Moreover, the dimensions of the photo-detector are in the order of thousands of wavelengths, having efficient spatial diversity, that prevents multipath fading. For the above mentioned reasons multipath fading can be neglected in our proposed indoor broadcasting system.

The LED lamp is placed at height H from the user terminal. The maximum radius covered by an LED cell is $r_e = Htan(\phi_{1/2})$, where $\phi_{1/2}$ is the semiangle (transmit power half width) of the LED. The user terminal's photo-detector is more commonly encapsulated in a hemispherical plastic lens that concentrate the received optical energy and also maintain a wide field-of-view (FOV) which is denoted by ψ_c. It is observed in [5], that the LED follows a Lambertian radiation pattern with order $m = -1/\log_2(\cos(\phi_{1/2}))$. As seen from Fig. 3 angle of incidence and angle of angle of irradiance are denoted by ψ and ϕ respectively. The DC channel gain h_t of the LOS link between LED and user is given as in [6] as,

$$h_t = \frac{A(m+1)R_p}{2\pi D^2}\cos^m(\phi)T(\psi)G(\psi)\cos(\psi) \quad , \tag{1}$$

where A is the area of detector, R_p represents responsivity of photo-detector, D is the distance between LED and the user, $T(\Psi)$ defines the gain of optical filter and $G(\Psi)$ is the gain of optical concentrator given as

$$G(\Psi) = \begin{cases} \frac{n^2}{\sin^2(\Psi_c)}, & 0 \le \psi_t \le \Psi_c \\ 0, & \psi_t > \Psi_c \end{cases} \tag{2}$$

where n denotes the reflective index of the optical concentrator.

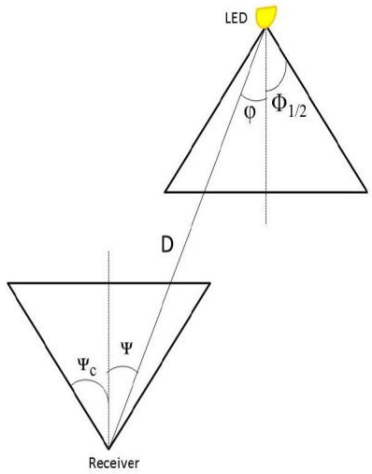

Fig. 3. Line of sight channel of VLC node.

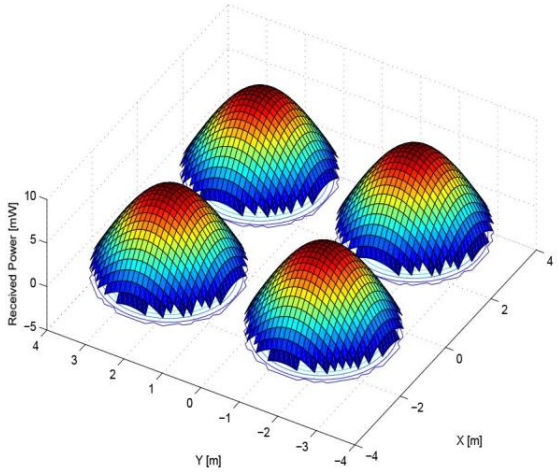

Fig. 4. Received power distribution for spotlighting arrangement.

IV. The Mobility Management

In this section different schemes are proposed for individual scenarios.

A. Spotlighting Arrangement

It is clearly seen from Fig. 1 that there is no coverage between two LEDs for distance L. In this case, when a mobile user is exiting the coverage of base node, the dark spot will cause an interrupt in communication. If the user is moving with v velocity then the time spent in dark spot will be $t = L/v$ where $L = D - 2Htan(\psi)$. To get uninterrupted communication at user end we have to provide the user terminal with enough buffer space. For an average data rate R_s the buffer space can be given as $B_s = R_s \times t$.

B. Uniform lighting Arrangement

It is seen from Fig. 2 that there is a power overlap area between the base node and neighbouring nodes. The mobile user moving away from the base node will start receiving links from multiple neighbouring nodes. The user device will select the signal based on the received signal strength (RSS). If RSS of base node P_{base} goes low than the RSS of neighbouring node $P_{neighbour}$ then the terminal will wait for dwell time T_{dwell} before switching to the neighboring link. In the proposed scheme we have used the variable T_{dwell} to protect the system from false handovers. the dell time is given as $T_{dwell} = (Htan(\phi_{1/2}) - D/2)/v$. From the Fig. 2 the power received at user u from base node is given as

$$P_{base} = P_t \frac{(m+1)A(cos(\psi_1))^{m+1}}{2\pi H^2 tan^2(\psi_1)}, \quad (3)$$

where P_t is the transmitted power and ψ_1 is angle of incidence at user from base node. The power received by user from neighbouring node is given as

$$P_{neighbour} = P_t \frac{(m+1)AH^{m+1}}{2\pi(H^2 + (D - Htan(\psi_1))^2)^{\frac{m+3}{2}}} \quad (4)$$

V. Result Analysis

The Fig. 4 depicts the received power distribution for a four LEDs spotlighting placement with each LED having a semiangle of 30^o. It is seen that there are spaces left in the room where the received power is zero, hence no communication. In Fig. 5 variation of received power is shown with varying user position. It is seen that due to dark spot the user did not receive any VLC link for almost a metre. when the user moves in neighbouring node coverage it gets connected to VLC network.

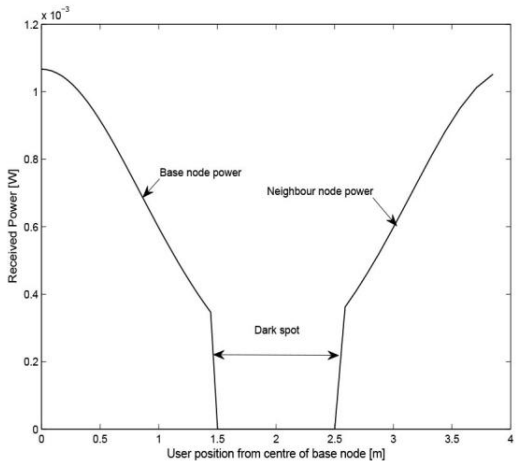

Fig. 5. Received power vs. user position variation .

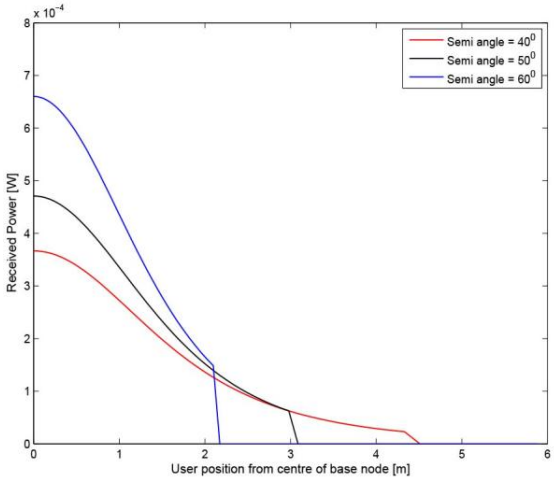

Fig. 7. Variation of received power at user terminal without handover.

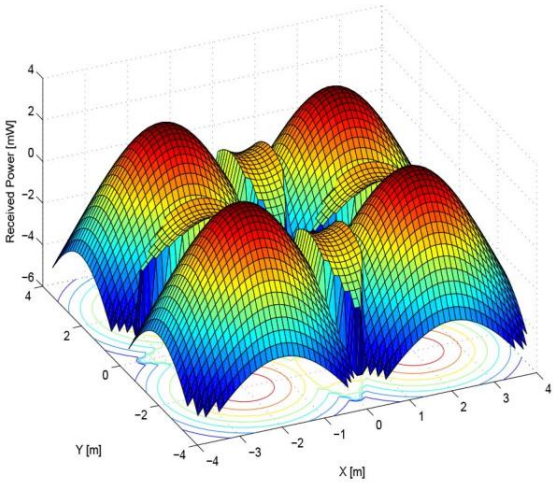

Fig. 6. Received power distribution for uniform lighting arrangement.

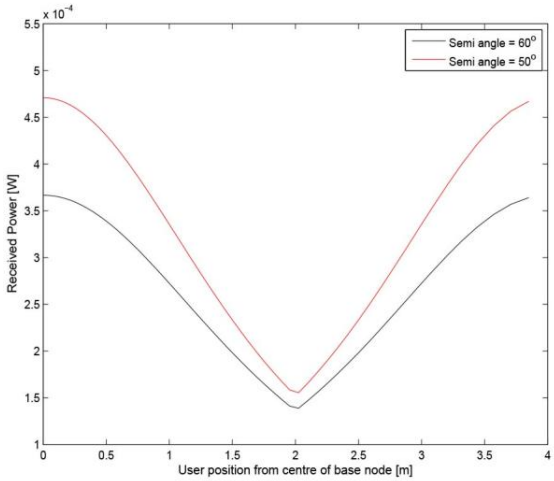

Fig. 8. Variation of received power at user terminal with handover.

Fig. 6 shows the received power distribution for four LED uniform lighting placement with each LED having a semiangle of 60^o. The complete room is illuminated with no dark spots available. Fig. 7 depicts the range of mobility for various semiangles. It can be seen that as the semiangle decreases the strength of signal is increased but the cell coverage area is reduced.

Fig. 8 depicts the received power variation with changing user position for the proposed system. It can be clearly seen that as the user moves out of the base cell coverage, the power starts increasing due to successful handover and establishment of connection with neighboring cell.

VI. Conclusion

We have proposed a mobility management scheme for both type of scenarios. In spot-lighting while buffer size can be varied for uninterrupted communication and a RSS based handover with dwell timer is proposed for uniform lighting. We validate our proposed scheme with results showing an improvement in received power for a mobile user.

REFERENCES

[1] J. Grubor, O.C.G. Jamett, J.W. Walewski, S. Randel and K.D. Langer, “High-speed wireless indoor communication via visible light,” in proc. ITG Fachbericht, Mar. 2007.

[2] D. O’Brien, H.L. Minh, L. Zeng, G. Faulkner, K. Lee, D. Jung, Y. Oh and E.T. Won, ”Indoor visible light communications: challenges and prospects,” Proc. SPIE Free-Space Laser Communications VIII, 709106, Aug. 19, 2008.

[3] A. M. Vegni and T. D. C. Little, ”Handover in VLC systems with cooperating mobile devices,” 2012 International Conference on Computing, Networking and Communications (ICNC), Maui, HI, 2012, pp. 126-130.

[4] Na Zhu, Zhe Xu, Yuxiang Wang, Hendan Zhuge, Jibin Li, ”Handover method in visible light communication between the moving vehicle and multiple LED streetlights”, Optik - International Journal for Light and Electron Optics, vol.125,Issue 14, July 2014, pp. 3540-3544.

[5] H. Cuiwei, T.Q. Wang, M. Abdullah Masum and J. Armstrong, “Performance of optical receivers using photodetectors with different fields of view in an indoor cellular communication system,’ in proc. of International Telecommunication Networks and Applications Conference (ITNAC), 2015 , pp.77-82, 18-20 Nov. 2015.

[6] J.M. Kahn and J.R. Barry, “Wireless infrared communications,” in Proceedings of the IEEE , vol.85, no.2, pp.265-298, Feb 1997.

MIGRATION TO NEXT GENERATION OPTICAL NETWORK
OFDM based ElASTIC OPTICAL NETWORK

Varsha Lohani
Ph.D Scholar
Electrical Engineering
Indian Institute of Technology
Kanpur, Uttar Pradesh-208016
Email: lohani@iitk.ac.in

Y.N.Singh
Professor
Electrical Engineering
Indian Institute of Technology
Kanpur, Uttar Pradesh-208016
Email: ynsingh@iitk.ac.in

***Abstract*—The rapid growth in the data traffic lead to the need of optical network that operates beyond 100 Gbps and one of the network that we are going to discuss in this paper is Elastic Optical Network (EON). The multiplexing technique efficient for EON is Optical Orthogonal Frequency Division Multiplexing because of its high spectral efficiency, robustness against inter-carrier and inter-symbol interference. In this paper, we are going to present a survey on O-OFDM based EON, Routing and spectrum assignment and Survivability in EON.**

I. INTRODUCTION

The data traffic growth in worldwide is increasing day by day so there is a requirement of optical network which can support high bandwidth, high speed data transmission, and is cost effective. To accommodate high capacity demand i.e., beyond 400 Gbps, elastic optical networks can be used. OFDM based EON is very efficient technology as it focuses on OFDM technology, and its flexible properties. OFDM based EON has various advantages as compared to previous optical networks vig., segmentation of Bandwidth, aggregation of Bandwidth, accommodation of multiple data rates, energy efficiency and virtualization.
Fig.1 shows comparison between conventional and elastic optical paths [1, 2].

II. ELASTIC OPTICAL NETWORK (EON) ARCHITECTURE

The elastic optical network is very useful in order to fulfill the need of increasing bandwidth demands because of its flexible data rate and spectrum allocation, low signal attenuation, low signal distortion, low power requirement as some subcarriers can be switched off when not required, low use of material, small space requirement and low cost. In this section we are going to discuss about architecture of elastic optical network as shown in Fig.2 [3] and its various components (sliceable bandwidth variable transponder and bandwidth variable wavelength cross-connect).

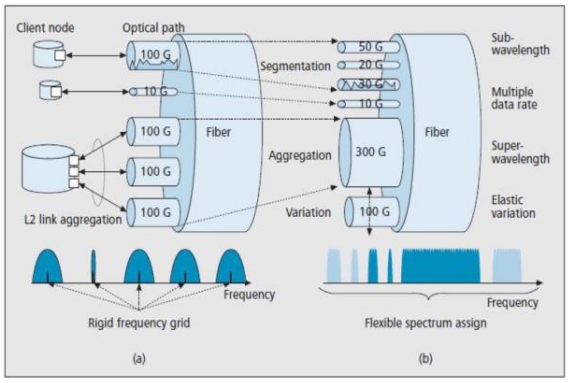

Fig. 1. Comparison between conventional and elastic optical paths reproduce from [1, 2].

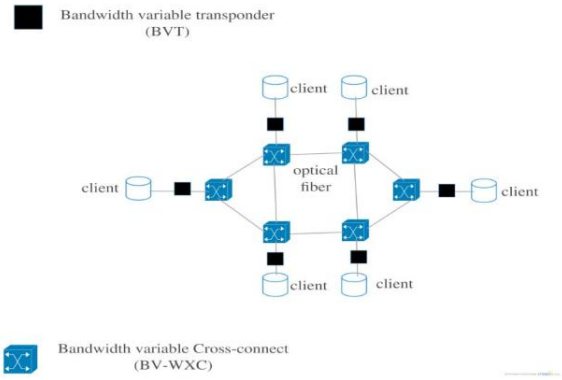

Fig. 2. Architecture of Elastic Optical network.

A. Components of EON

The two main components of EON are (i) Sliceable Bandwidth Variable Transponder (ii) Bandwidth Variable- Cross Connects.

1) Sliceable Bandwidth Variable Transponder(S-BVT): SBVT can tune optical bandwidth and transmission reach by

adjusting certain parameters such as bit rate, forward error correction, modulation format, and shaping of optical spectrum [4].

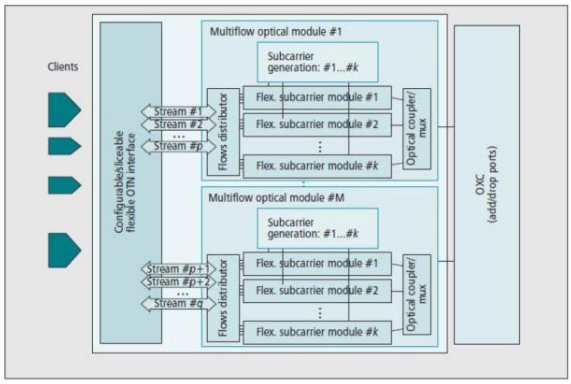

Fig. 3. S-BVT Architecture reproduce from [4].

In this bandwidth is sliced so as to serve several traffic demands to one or more destinations. Fig.3 shows architecture of S-BVT.

Configurable/Sliceable flexible Optical Transport Network (OTN) interface is used to slice high data rates to lower data rates for example as shown in Fig.4 1 Tbps is sliced into 600 Gbps and 400 Gbps [4].

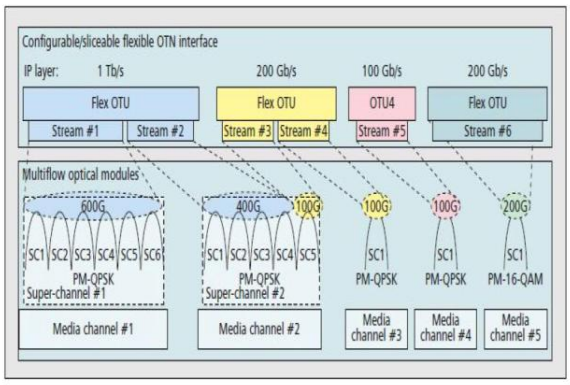

Fig. 4. OTN frames and flexible association with media channels reproduce from [4].

Each multi flow optical module is used to generate multiple sub-carriers. The p-stream from the OTN layer are used to modulate k non modulated sub-carriers where k is greater than equal to p. The modulated traffic is multiplexed via optical mux/coupler and output goes to the fiber.

2) Bandwidth Variable- Cross Connects(BV-WXC): BV-WXC is used to allocate appropriate sized cross connection with the corresponding spectrum bandwidth for elastic optical network. Fig. 5 shows architecture of BV-WXC [3]. Here BVT is Bandwidth Variable Transponder and BV-SSS is Bandwidth Variable Spectrum Selective Switch.

Whenever there is increase in traffic, the transmission capacity of transmitter increases and therefore switching window of every WXC on the route expands in a flexible way according

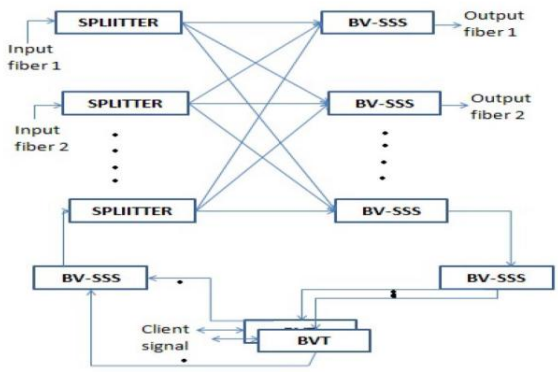

Fig. 5. BV-WXC Architecture.

to the spectral width of the input signal. BV-SSS performs multiplexing/De-multiplexing of spectrum. BV-SSS can be designed using either Liquid crystal on Silicon (LcoS) [5] or Micro-Electro-Mechanical System (MEMS) [6] that can be employed as switching element to realize an optical cross connect with flexible bandwidth and center frequency.

III. ROUTING AND SPECTRUM ASSIGNMENT(RSA) IN EON

A. Basic concept of RSA

RSA is used to find route between nodes and allocate spectrum slots to the desired demand. For RSA two constraints must be satisfied:

1. Spectrum Contiguity: contiguous sets of spectrum must be allocated for a connection.
2. Spectrum Continuity: same set of spectrum must be allocated on each link along the route of the demand [3].

The above both constraints are shown in Fig. 6

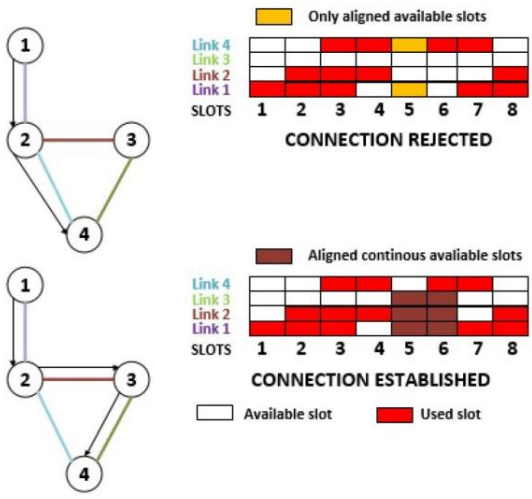

Fig. 6. Spectrum contiguity and continuity constraints.

First we are going to discuss about routing and after that about spectrum allocation.

B. Routing

There are two types of routing i.e., without elastic characteristics and with elastic characteristics. Since we are discussing about elastic optical network, we will focus on routing with elastic characteristics.

Routing with elastic characteristics: In this approach, when a connection request arrives, a group of frequency slots for a connection are allocated. In this multipath routing is used instead of single path routing because of spectrum fragmentation in single path [3].

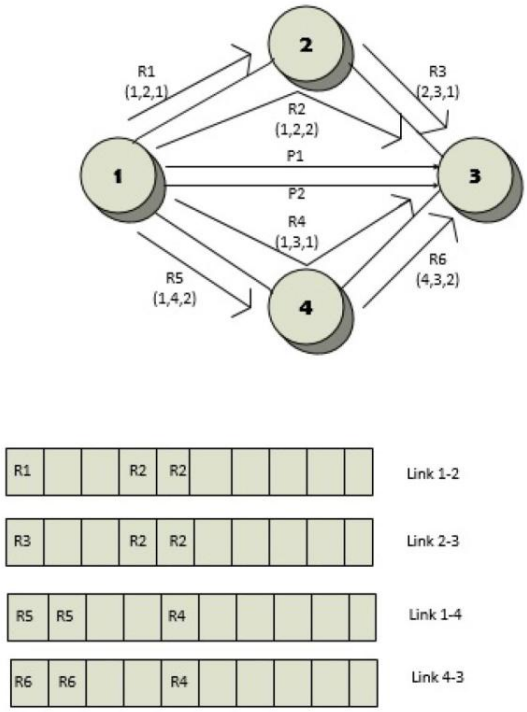

Fig. 7. Multi-path Routing in EON.

In Fig.7, R(S,D,F) is a connection request between node pairs (S: source, D: destination) with F: number of contiguous spectrum slots. In this, two slots are reserved for guard band. Let us explain this with an example as shown in Fig.7, R7 connection request arrives from node 1 to node 3 with a demand of four frequency slots. As it is unavailable the demand will be blocked. But with the help of multipath routing, two paths P1 and P2 can be generated through which connection request can be fulfilled.

C. Spectrum Allocation

In this spectrum allocation is categorized based on the spectrum range for connection groups and spectrum slot for individual connection request [3].

1) Spectrum range for connection groups: This is further categorized in three parts:

a) Fixed spectrum allocation: Central frequency and assigned spectrum width remain static as shown in Fig.8 [7, 8] Demands either utilize the whole of it or only a part of it.

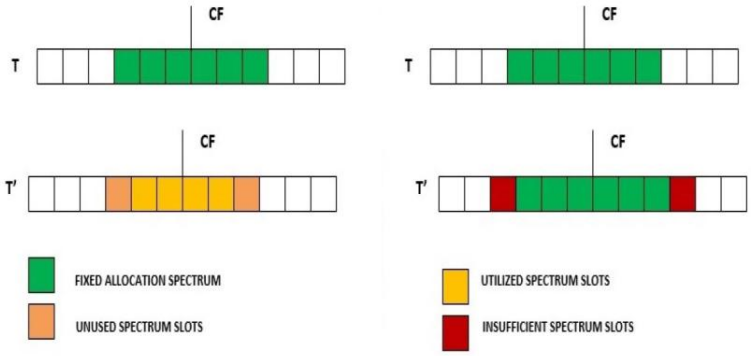

Fig. 8. Fixed Spectrum Allocation (a) underused spectrum condition, and (b) insufficient spectrum condition.

b) Semi-elastic spectrum allocation: In this central frequency is fixed but we can vary the spectrum dynamically width according to our requirement as shown in Fig.9 [7, 8].

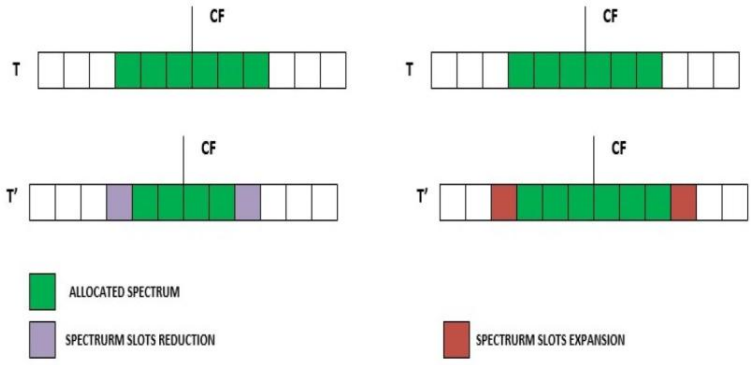

Fig. 9. Semi-elastic spectrum allocation policy with (a) spectrum slot reduction, and (b) spectrum slot expansion.

c) Elastic Spectrum allocation: The central frequency (CF) and spectrum width both can be dynamically varied. Two cases of elastic spectrum allocation are:

i) CF movement within a range

ii) Elastic spectrum reallocation.

Both the above cases are shown in Fig.10 [7, 8].

2) Spectrum slot for individual connection request: There are 7 allocation policies for individual connection request:

a) First Fit : In this spectrum slots are indexed. Whenever a connection request arrives, the lowest indexed slots from the list of available slots are allocated [3, 9, 10].

b) Random Fit : In this, a list of free or available spectrum slots is maintained. Whenever connection request arrives, from the list, any slot that available and suitable for connection, is randomly chosen [3, 9].

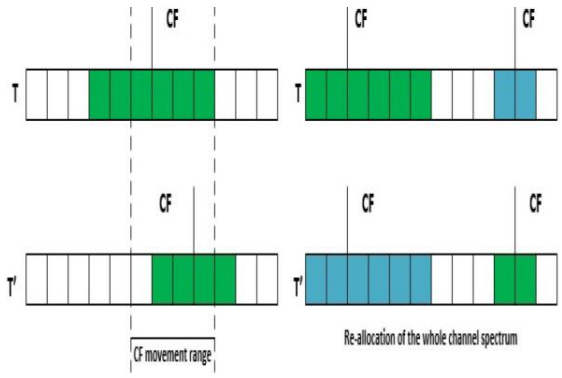

Fig. 10. Elastic spectrum allocation policy with (a) CF movement within a range, and (b) elastic spectrum reallocation.

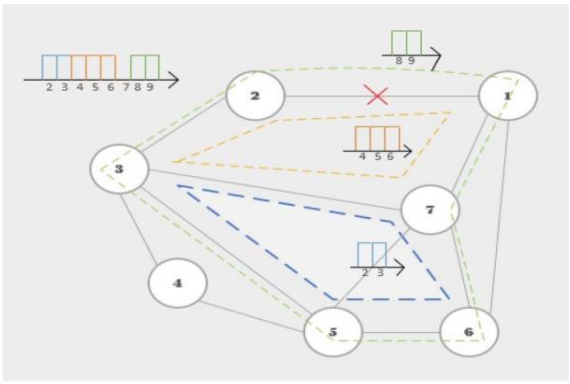

Fig. 11. Ring Cover technique.

c) Last Fit : In this, from the indexed spectrum slots, highest indexed slot is chosen for a connection [3, 11].
d) First-Last Fit: In this, all spectrum slots of each link is partitioned into odd and even numbered slots. The lowest indexed slot is chosen from from odd number of partition from the list of available slots. The highest indexed slot is chosen from even number of partition from the list of available slots [3, 10].
e) Least Used : In this, from the list of available spectrum slots least used slot is allocated to the demand. Otherwise, first fit method is used [3].
f) Most Used : In this, from the list of available spectrum slots most used slot is allocated to the demand. Otherwise, first fit method is used [3].
g) Exact Fit : In this, exact slots are allocated for a demand so that there is no wastage of slots. If not, the first fit method is used [3, 9].

IV. SURVIVABILITY IN EON

Various protection and restoration mechanisms are used for the survivability of elastic optical network. We will discuss only ring cover protection, p-cycle protection and bandwidth squeezed restoration.

A. Ring Cover Protection

Ring cover provides protection only on on-cycle span. In this whenever a link fails that is traversed through by pre-deployed rings, ring cover technique is used to find the eligible ring to provide protection to the failed link. Spectrum constraints must be considered in this scheme [12].

As shown in Fig.11 three pre-deployed rings for protection are (3-2-1-7-3), (3-7-6-5-3) and (3-2-1-7-6-5-3). If (2-1) link fails, this failure affects the two pairs of working nodes i.e., (3-1) and (2-7). So, the two pre-deployed rings i.e., (3-2-1-7-3) and (3-2-1-7-6-5-3) are used to recover the working flows. Two pair of fibers are used for working and protection.

B. P-Cycle

P-Cycle is considered significant technique for an optical network because it provides ring like restoration speed and mesh like spare capacity efficiency. P-Cycle provides protection on on-cycle as well as straddling span [13].

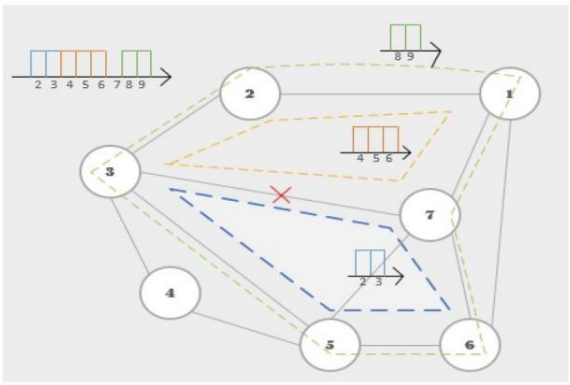

Fig. 12. P-cycle technique.

The concept of p-cycle used in elastic optical network, is shown in Fig.12. In this there are three p-cycles i.e., (3-2-1-7-3), (3-7-6-5-3) and (3-2-1-7-6-5-3) on which there are three working flows i.e., FS (2-3), FS (4-6) and FS (8-9). Let us consider span (3-7) is affected, so (3-7) is on-cycle span for (3-2-1-7-3) and (3-7-6-5-3) and straddling span for (3-2-1-7-6-5-3). In (3-2-1-7-6-5-3), there are two protection paths but due to the requirement of specturm contiguousness constraint only upper half of the cycle is used for protection. Two pair of fibers are used for working and protection in this scheme also.

C. Bandwidth Squeezed Restoration

The BSR scheme is a type of recovery scheme in which when working path is affected the bandwidth of backup path is reduced to the required minimum amount considering the client requirement when working path is switched over to backup path. This enables cost-effective restoration in terms

of spectral resource utilization Fig.13. shows an example of the BSR scheme in which there are two optical paths in the network.

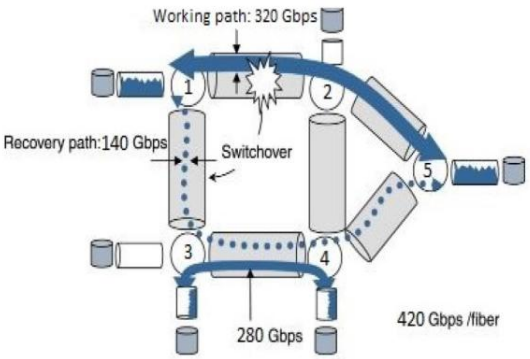

Fig. 13. Bandwidth Squeezed Restoration Technique reproduce from [14].

Two working flows one is from Node 1 to Node 5 which has a bandwidth of 320 Gbps and other is from Node 3 to Node 4 which has a bandwidth of 280 Gbps. Let us assume that each fiber has a bandwidth of capacity 420 Gbps and so the available bandwidth between Node 3 and Node 4 has 140 Gbps. As shown in Fig.13, the failure occurs in the link between Node 1 and Node 2, the optical path can be switched over to the Node 1, Node 3, Node 4, Node 5 route [14]. The path bandwidth is reduced by changing the bit rate of a bandwidth-variable transponder (BVT) from 320 Gbps to less than 140 Gbps. The recovery route can be calculated either in advance or after the failure occurs. Restoration must be done as fast as possible so as to avoid traffic loss.

V. CONCLUSION AND FUTURE WORK

The elastic optical network is a significant optical network technology for high speed transmission because of its flexible properties. In this paper different elements and aspects of EON has been discussed. We started with basic concept of EON, its architecture, and finally we covered different RSA and survivability issues in EON. Future work that can be done is instead of using optical OFDM we can use Orthogonal Wavelength Division Multiplexing(OWDM) so as to make it cost effective as there is no requirement of optical-electrical-optical converters (O-E-O) and all process will be in optical form.

REFERENCES

[1] M. Jinno *et al.*, "Distance-Adaptive Spectrum Resource Allocation in spectrum-Sliced Elastic Optical Path Net- work ," *IEEE Commun. Mag.*, vol. 48, no. 8, pp.138 145, Aug. 2010.

[2] O. Gerstel *et al.*, "Elastic optical networking: A new dawn for the optical layer?,"*IEEE Commun. Mag.*, vol. 50, no. 2, pp. 12 20, Feb. 2012.

[3] N. Sambo *et al.*, "Next Generation Sliceable Bandwidth Variable Transponders "*IEEE Communications Magazine*,vol. 53, no. 2, pp. 163 - 171, February 2015.

[4] B.C. Chatterjee *et al.*, "Routing and Spectrum Allocation in Elastic Optical Networks: A Tutorial ," *IEEE communication surveys and tutorials*, vol. 17, no. 3, third quarter 2015.

[5] S. Frisken *et al.*, "Flexible and grid-less wavelength selective switch using LCOS technology," *Optical Fiber Communication Conf.*, Los Angeles, CA, USA, Paper OTuM3, 2011.

[6] R. Ryf *et al.*, "Wavelength blocking filter with flexible data rates and channel spacing,"*J. Lightw. Technol.*, vol. 23, no. 1, pp. 54 - 61, Jan. 2005.

[7] M. Klinkowski *et al.*, "Elastic spectrum allocation for time-varying traffic in flexgrid optical networks ,"*IEEE J. Sel. Areas Commun.*, vol. 31, no. 1, pp. 26 38, Jan. 2013.

[8] A. A. Garcia*et al.*, *"Elastic spectrum allocation in flexgrid optical networks ,"* Univ. Politcnica Catalunya, Catalunya, Spain, Tech. Rep., 2012.

[9] A. Rosa *et al.*, "Spectrum allocation policy modeling for elastic optical networks," *Proc. 9th Int. Conf. HONET*, pp. 242 246, 2012.

[10] R. Wang *et al.*, "Spectrum management in heterogeneous bandwidth optical networks ," *Opt. Switching Netw.*, vol. 11, pp. 83 91, Jan. 2014.

[11] W. Fadini *et al.*, *"A subcarrier-slot partition scheme for wavelength assignment in elastic optical networks,"* n Proc. IEEE Int. Conf. HPSR, pp.7 12, 2014 .

[12] Y. Wei *et al.*, "Applying Ring Cover Technique to Elastic Optical Networks," *Proc. ACP*, 2013.

[13] Y. Wei *et al.*, "Applying p-Cycle Technique to Elastic Optical Networks," *IEEE ONDM, Stockholm, Sweden*, 19 - 22 May 2014.

[14] Y. Sone *et al.*, "Bandwidth Squeezed Restoration in Spectrum-Sliced Elastic Optical Path Networks (SLICE),"*Journal of Optical Communication and Network*, vol. 3, no. 3, pp. 223 - 233, March 2011.

Institution of Communication Engineers and Information Technologists

About ICEIT

Institution of Communication Engineers and Information Technologists (ICEIT) is a non-profit professional society established under the Societies Registration Act 1860 for advancement of Information and Communication Technology (ICT). It aims to provide a strong knowledge network to facilitate exchange of ideas and promote the role of ICT in all walks of life.The Institution functions with and among the industrial affiliates, academics, engineers, scientists, management experts, economists, social scientists and government agencies; who are active contributors to and users of ICT. It provides an array of technical and professional interactive spaces for industries, academia and ICT communities. The Institution is committed to providing best possible service to its members for knowledge development, skill acquisition, support and development advice for career enhancement. The Institution promotes individual and organizational excellence through well designed recognition processes.

List of Organizational Members

- ABV-Indian Institute of Information Technology and Management (ABV-IIITM), Gwalior
- Devi Ahilya Vishwa vidyalaya, Indore
- Maulana Azad National Institute of Technology, Bhopal
- Jawaharlal Nehru University, Delhi
- Mahamaya Technical University, Noida
- University of Allahabad, Allahabad
- Baddi University of Emerging Sciences & Technology, Solan
- Indira Gandhi Institute of Technology, Delhi
- Ambedkar Institute of Technology, Delhi
- Birla Institute of Technology, Mesra Ranchi
- Birla Institute of Technology and Science, Pilani
- PDPM Indian Institute of Information Technology, Design & Manufacturing, Jabalpur
- Guru Nanak Dev University, Amritsar
- National Institute of Technology, Karnataka
- National Institute of Technology, Patna
- GLA University, Mathura
- Shobhit University, Meerut
- Sharda University, Greater Noida
- DOEACC Society, Ministry of Communication and Information Technology
- Power Grid Corporation Limited, New Delhi
- G Telecom Research Data Center & Info Services Pvt Ltd, New Delhi
- Radha Govind Engineering College, Meerut
- Raj Kumar Goel Institute of Technology (RKGIT), Ghaziabad
- G L Bajaj Institute of Technology & Management, Greater Noida
- Panipat Institute of Engineering & Technology, Panipat
- Inderprastha Engineering College, Ghaziabad
- ABES Engineering College, Ghaziabad
- I M S Engineering College, Ghaziabad
- Babu Banarasi Das Institute of Technology, Ghaziabad
- Vishwakarma Institute of Information Technology, Pune
- I T S Engineering College, Greater Noida
- IIMT Engineering College, Meerut
- Maharaja Agarsain Institute of Technology, Ghaziabad
- Ajay Kumar Garg Engineering College, Ghaziabad
- Baddi University, Himachal
- H M R Institute of Technology and Management, Hamidpur
- Maharana Pratap University of Agriculture & Technology, Udaipur
- Asia Pacific Institute of Management, Jasola, Delhi
- Centre For Development of Advanced Computing, Noida
- Manipal University, Jaipur
- Malaviya National Institute of Technology, Jaipur
- Jaypee University of Information Technology, Waknaghat
- IMS Unison University, Dehradun
- Dr K N Modi University, Tonk
- School of Engineering, G D Goenka University, Gurgaon
- DIT University, Dehradun
- Amity University, Madhya Pradesh

The Institution of Communication Engineers and Information Technologists (ICEIT)

301, V4 Mayur Plaza IV, Mayur Vihar, Phase I
Delhi-110091, India.
Tel: 09313440370 Email: iceit01@gmail.com, iceitoffice@gmail.com
Website: www.iceit.org.in

Application form for Corporate Individual Membership

1. Name in full (Block letters):_____
2. Father's/Husband's Name:_____
3. Designation:_____
4. Address:_____

_____

_____

State_____ PIN Code_____

Tel. No._____Office:_____Res.:_____
Mobile:_____Email:_____

5. Date of Birth_____ Age on date of Application_____
6. Highest Qualification:_____
7. Experience:_____Y_____M_____
8. Educational Qualifications (degree granting programme for students)

S.No.	Examination Passed	Degree with discipline	College	University/Institution	Year
1.	Bachelor's				
2.	Master's				
3.	Doctoral				
4.	Any Other				

9. Details of Experience:

S.No.	Position Held	Name & Address of the Employer	From (Date)	To (Date)

10. Details of the membership of other Institutions/Professional Societies:

S.No.	Grade of Membership & Number	Name of Institution/Society

Fee structure

Member (MICEIT)/Senior Member(SMICEIT) : **First Installment -** Rs 100 (Entrance fee) + Rs **600** Annual Subscription; **Total Rs 700** . Subsequent annual subscription: Rs **600**

Life Member/Senior Member: Rs 100 (Entrance fee) + Rs 6,000 (Life Time Subscription); **Total Rs 6,100 in single installment.**

Student Member (AICEIT): **First Installment -** Rs 100 (Entrance fee) + Rs 250 Annual Subscription; **Total Rs 350** . Subsequent annual subscription: Rs 250

11. Details of Fee Paid:

Rs.:_____(Rupees:_____)

Vide DD No.:_____Dated:_____in favour of **"ICEIT"** drawn on_____.

(Name of the Bank and Branch)

Note:

(i) DD to be drawn in favour of "**ICEIT**" and payable at New Delhi (ii) Please write your name, address and contact phone at the back of DD (iii) Please send a passport size photo for office use (iv) You may send any additional professional information.

Undertaking

1. I here by apply for admission as a SMICEIT/MICEIT/AICEIT in accordance with the rules and regulations and the Bye-laws as they stand now or maybe amended from time to time. 2. The particulars contained in the application form are true as I understand that the validity of my admission depends upon the accuracy of these particulars. 3. I undertake to abide by professional conduct rules and/or code of conduct that the institution may frame from time to time. 4. The decisions of the institution in granting me the membership shall be final and binding on me. 5. I shall promote the objectives of the institution as far as may be in my power. 6. In the event of invalidity of my membership for any reason I shall forthwith cease to describe myself as SMICEIT/MICEIT/AICEIT. 9. If I withdraw my membership from the institution I shall do so after payment of any arrears that may be due from me to be free from this obligation.

Date: Signature:

(FOR OFFICE USE)

Received with thanks duly filled application form for SMICEIT/MICEIT/AICEIT from …… along with DD No…….. for Rs…… towards Entrance Fee and/or Subscription Fee (Annual/Life)

Approval of the membership

Membership No:_____ Grade of Membership_____

President/Secretary ICEIT

The Institution of Communication Engineers and Information Technologists (ICEIT)

301, V4 Mayur Plaza IV, Mayur Vihar, Phase I
Delhi-110091, India.
Tel: 09313440370 Email: iceit01@gmail.com, iceitoffice@gmail.com
Website: www.iceit.org.in

Application form for Organizational Membership

Information about the organization

Name of the organization .....

Name of the Head of the Organization.....

Name of the contact person .....

Address.....

.....

Contact Nos.....; Email.....

Website.....Year of foundation ....

Area of activity ..... Legal status .....

Membership of other professional societies/ institutions

Please state the names and address of such societies/institutions, if any
(1).....

(2).....

(3).....

Fees structure:

Entrance Fee	Five Year Block Subscription (Industry)	Five Year Block Subscription(Educational & Research)	**Total fee payable in *single* installment**
Rs. 2,500	Rs. 22,500	Rs. 12,500	**Rs 25,000 (Industry)** **Rs 15,000(Edu. &Res.)**

Details of Fee Paid:

Rs.:_____(Rupees:_____)
Vide DD No.:_____Dated:_____in favour of **"ICEIT"** drawn on_____.

(Name of the Bank and Branch)

Note: Please write name, address and contact phone number at the back of DD

Privileges of organizational members

1. Organizational members can work as a local industrial /educational chapter and establish students' chapter of ICEIT to facilitate technical advancements for the students/employees.
2. Organizational member will receive all publications of ICEIT at reduced rate.
3. Invitations to conferences, symposia, seminars etc. throughout India arranged by ICEIT.
4. Render Technical advice as and when necessary.
5. Concessional rates are offered to regular members for participation in seminars, conferences, workshops etc. Also, concessional advertising rates are offered in ICEIT publications.

Undertaking

1. I here by apply for admission as an organizational member of the ICEIT in accordance with the rules and regulations and the Bye-laws as they stand now or maybe amended from time to time. 2. The particulars contained in the application form are true as I understand that the validity of the admission depends upon the accuracy of these particulars. 3. I undertake to abide by professional conduct rules and / or code of conduct that the institution may frame from time to time. 4. The decisions of the institution in granting the organizational membership shall be final and binding on me. 5. I shall promote the objectives of the institution as far as may be in my power. 6. In the event of invalidity of membership for any reason the organization shall forthwith cease to describe as an organizational member of ICEIT. 7. The withdrawal of membership from the institution for any reason will be done after payment of any arrears that may be due to be free the organization from this obligation.

Date: ……
Signature: ……

Signature of the Head of the organization with seal

(FOR OFFICE USE)

Received with thanks duly filled application form for organizational membership from……along with DD No……for Rs……in favour of "**Institution of Communication Engineers and Information Technologists (ICEIT)**" payable at New Delhi towards entrance fee and/or subscription fee (for five year block) beginning …… … (month and year)

Authorized Signature for ICEIT

Approval of the membership

Membership No:_____

President/Secretary ICEIT

Join ICEIT for Professional Development

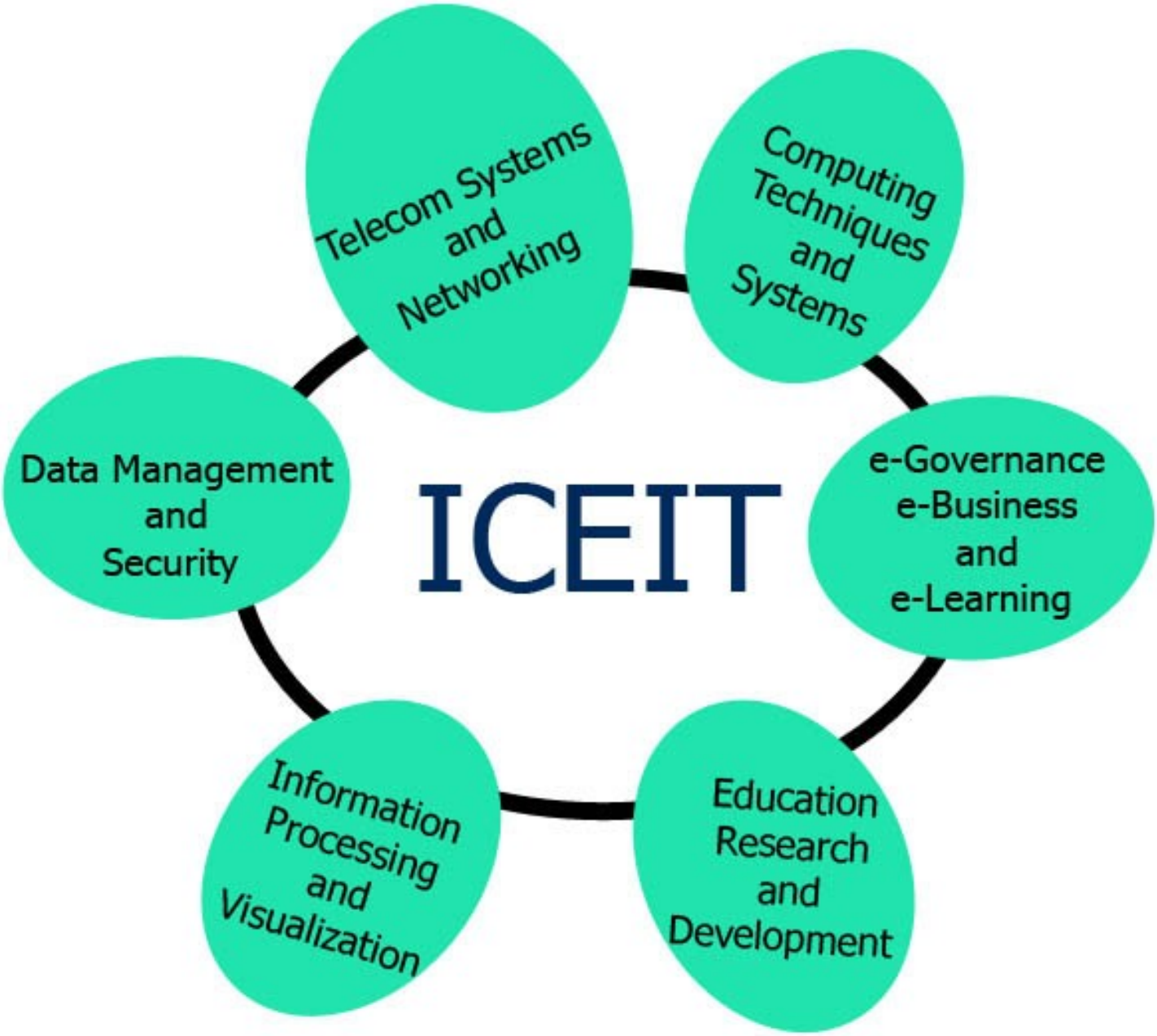

www.iceit.org.in